Universität Potsdam
Institut für Erd- und Umweltwissenschaften
und
Helmholtz-Zentrum Potsdam – Deutsches GeoForschungsZentrum GFZ
Sektion 5.2 – Klimadynamik und Landschaftsentwicklung

---

# Lateglacial to Holocene climatic and environmental changes in Europe – multi-proxy studies on lake sediments along a transect from northern Italy to northeastern Poland

**Kumulative Dissertation**

zur Erlangung des akademischen Grades
"doctor rerum naturalium" (Dr. rer. nat.)
in der Wissenschaftsdisziplin Geologie – Paläoklimatologie

eingereicht an der
Mathematisch-Naturwissenschaftlichen Fakultät
der Universität Potsdam

von
Stefan Lauterbach

Potsdam, Januar 2011

Published online at the
Institutional Repository of the University of Potsdam:
URL http://opus.kobv.de/ubp/volltexte/2012/5815/
URN urn:nbn:de:kobv:517-opus-58157
http://nbn-resolving.de/urn:nbn:de:kobv:517-opus-58157

*„The world is the geologist's great puzzle-box; he stands before it like the child to whom the separate pieces of his puzzle remain a mystery till he detects their relation and sees where they fit, and then the fragments grow at once into a connected picture beneath his hand.“*

Louis Agassiz

# Table of contents

# List of figures

## List of tables

# Abstract

As a part of the project DecLakes (*Decadal Holocene and Lateglacial variability of the oxygen isotopic composition in precipitation over Europe reconstructed from deep-lake sediments*), which has been funded within the frame of the European Science Foundation EuroCLIMATE programme, the sediment records of three lakes from different climatic regimes – Lake Hańcza in northeastern Poland, Lake Mondsee in Upper Austria and Lake Iseo in northern Italy – were investigated. The main objective of the project was the high-resolution reconstruction of past temperature variability at the respective sites in order to gain a better understanding of the regional peculiarities of climate variability in Europe during the past 15 000 years. For this purpose, the oxygen isotope composition of the calcareous valves of benthic ostracods from the lake sediments, which is mainly controlled by the isotopic composition of past precipitation and thus air temperature variability, was analyzed. Within this context, this thesis mainly aimed, by utilizing sediment microfacies analyses on large-scale thin sections and high-resolution geochemical and geophysical analyses and combining these with pollen data and the results of stable isotope measurements, at reconstructing the Lateglacial and Holocene climate development at the respective sites, investigating the response of local sedimentary regimes and ecosystems to climatic fluctuations and relating the identified regional peculiarities of past climate development to climatic changes on a larger, extraregional to hemispheric, scale.

Work on the Lake Hańcza sediment record focused on reconstructing the regional climate development during the early Holocene and identifying possible differences to Western Europe. Following mainly clastic-detrital deposition during the Lateglacial, climatic improvement at the onset of the Holocene is indicated by the onset of biochemical calcite precipitation and the replacement of Lateglacial shrub vegetation by boreal forests. A further period of environmental and climatic improvement occurred between 10 000 and 9000 cal. a BP, mainly reflected by the spread of deciduous forests and a pronounced $\delta^{18}O$ rise, probably reflecting increasing temperatures. Based on these findings, it is supposed that relatively cold and dry climate conditions persisted in northeastern Poland during the first ca. 1500 years of the Holocene, most likely due to a specific regional atmospheric circulation pattern. Prevailing anticyclonic circulation linked to a high-pressure cell above the remainder of the Scandinavian Ice Sheet might have blocked the eastward propagation of warm and moist Westerlies and thus attenuated the early Holocene climatic amelioration in the eastern Baltic region until the final decay of the ice sheet. These results confirm previous studies from northwestern Russia and reveal that large areas southeast of the retreating Scandinavian Ice Sheet might have undergone an early Holocene climate development different from that in Central and Western Europe.

The Lateglacial sediment record of Lake Mondsee was investigated in order to study both the regional climate development and the response of different environmental parameters to rapid climatic fluctuations. While the temperature rise, the recovery of local pine forests, the decrease of detrital matter flux and the intensification of biochemical calcite precipitation at the onset of the Holocene

took place quasi-synchronously, the onset of the Lateglacial Interstadial was characterized by major leads and lags in proxy responses. In particular, the spread of coniferous woodlands and the reduction of detrital flux lagged the initial Lateglacial warming by ca. 500–750 years. Major cooling at the onset of the Younger Dryas is reflected by the simultaneous reaction of $\delta^{18}O$, i.e. temperature, and vegetation, while the reduction of biochemical calcite precipitation and the increase of detrital matter flux were delayed by about 150–300 years. Complex proxy responses are also detected for three short-term climatic fluctuations during the Lateglacial Interstadial, corresponding to Greenland isotope substages GI-1d, GI-1c2 and GI-1b. In summary, periods of major warming at the onset of the Lateglacial Interstadial and the Holocene and major cooling at the onset of the Younger Dryas as well as short-term coolings during the Lateglacial Interstadial are characterized by complex and temporally variable proxy responses to climatic forcing, mainly controlled by ecosystem inertia and the environmental preconditions, i.e. the long-term evolution of the lake and its catchment.

A study on the Holocene Lake Mondsee sediment record focused on two small-scale climate deteriorations around 8200 and 9100 cal. a BP, which have been triggered by freshwater discharges to the North Atlantic, causing a shutdown of the Atlantic meridional overturning circulation (MOC). Combining microscopic varve counting and AMS $^{14}C$ dating of terrestrial plant macrofossils yielded a precise duration estimate (ca. 150 years) and absolute dating of the so-called 8.2 ka cold event in the oxygen isotope record, both being in good agreement with results from the Greenland ice cores and other varved lake sediment records. Moreover, a sudden ca. 100-year-long temperature overshoot after the 8.2 ka cold period was identified, which is also seen in other proxy records around the North Atlantic. This was most likely caused by enhanced resumption of the MOC, which also initiated substantial shifts of oceanic and atmospheric front systems, particularly the Arctic Front and the Intertropical Convergence Zone. Although there is also evidence for a pronounced recovery of the MOC and atmospheric circulation changes after the 9.1 ka cold period from other proxy records, no temperature overshoot is seen in the Lake Mondsee record, indicating the complex behaviour of the global climate system.

The Holocene sediment record of Lake Iseo was studied to shed light on past earthquake activity in the region and the influence of climate variability and anthropogenic impact on catchment erosion and detrital flux into the lake. Frequent small-scale detrital layers within the sediments reflect allochthonous sediment supply by extreme surface runoff events. During the early to mid-Holocene, intervals of increased detrital flux coincide with regional lake-level highstands and minima in solar activity, i.e. cold and wet climate conditions, and thus are apparently mainly controlled by climate variability. In contrast, intervals of high detrital flux during the late Holocene partly also correlate with phases of increased human impact, reflecting the complex influences on catchment erosion processes. Five large-scale event layers within the sediments, which are composed of basal mass-wasting deposits and overlying turbidites, are supposed to have been triggered by local earthquakes with magnitudes in the order of $M_w$=5.0–6.5. While the uppermost of these event layers is assigned to a

documented adjacent earthquake in AD 1222, the four other layers are supposed to be related to previously undocumented prehistorical earthquakes around 350 BC, 570 BC, 2540 BC and 6210 BC.

In summary, all studies reveal an unexpected high sensitivity of the sedimentary regimes and ecosystems of comparatively large lake systems to climatic and environmental changes. Besides the imprint of hemispheric-scale climate processes, also local to regional climate signals can be detected by using high-resolution proxy analyses. However, the reflection of climate variability by changes in the sedimentary regime and the ecosystem is largely determined by the local boundary conditions such as glaciation history, topography, vegetation cover and soil development and furthermore might be modified by anthropogenic impact. Only the sound knowledge of these and other possible influencing factors as well as the use of multi-proxy analyses allows the reliable interpretation of such lake sediment records in terms of past climatic and environmental changes.

# Kurzfassung

Im Rahmen des Projekts DecLakes (*Decadal Holocene and Lateglacial variability of the oxygen isotopic composition in precipitation over Europe reconstructed from deep-lake sediments*), welches Teil des Forschungsprogramms EuroCLIMATE der European Science Foundation war, wurden Sedimentbohrkerne aus drei europäischen Seen, dem Jezioro Hańcza (Nordostpolen), dem Mondsee (Oberösterreich) und dem Lago d'Iseo (Norditalien), untersucht, die unter anderem anhand ihrer Lokation in unterschiedlichen Klimaregionen Europas ausgewählt wurden. Ziel des Projekts war dabei, über die Analyse des Sauerstoffisotopenverhältnisses der Kalkschalen benthischer Ostrakoden, welches hauptsächlich das temperaturabhängige Sauerstoffisotopenverhältnis des Niederschlags widerspiegelt, hochauflösende Temperaturrekonstruktionen für die letzten etwa 15 000 Jahre zu erhalten um regionale Aspekte der Klimavariabilität in Europa besser zu verstehen. Im Rahmen dieser Dissertation sollte dabei versucht werden, durch die Untersuchung der Sediment-Mikrofazies und hochauflösende geochemische und geophysikalische Analysen, welche unter anderem mit Pollenanalysen und den Messungen von Sauerstoff- und Kohlenstoffisotopenverhältnissen an Ostrakoden kombiniert wurden, die spätglaziale und holozäne Klimaentwicklung im Bereich der drei Lokalitäten und die Reaktion der jeweiligen Sedimentationsregime und Ökosysteme auf Klimaschwankungen zu rekonstruieren sowie die regionalen Besonderheiten der spätquartären Klima- und Umweltveränderungen in einen überregionalen Kontext zu setzen.

Ziel der Untersuchungen an den Sedimenten des Jezioro Hańcza war die Rekonstruktion der regionalen Klimaentwicklung während des Frühholozäns und die Identifikation möglicher Unterschiede gegenüber Westeuropa. Im Anschluss an das hauptsächlich durch klastisch-detritische Sedimentation geprägte Spätglazial war die Erwärmung zu Beginn des Holozäns vor allem durch das Einsetzen biochemischer Kalkfällung und das Verschwinden der spätglazialen Strauchvegetation zugunsten borealer Nadelwälder gekennzeichnet. Eine weitere Verbesserung der Klima- und Umweltbedingungen, die vor allem durch die Ausbreitung von Laubwäldern und einen deutlichen Anstieg im Sauerstoffisotopenverhältnis von endogenem Kalzit und Ostrakodenschalen charakterisiert ist, war zwischen 10 000 und 9000 Jahren vor heute zu verzeichnen. Zusammenfassend lässt sich sagen, dass in Nordostpolen offensichtlich auch noch während der ersten 1500 Jahre des Holozäns relative kalte und trockene Klimabedingungen vorherrschten. Dies war höchstwahrscheinlich das Resultat besonderer regionaler atmosphärischer Zirkulationsverhältnisse zu dieser Zeit. Eine antizyklonale Zirkulationszelle als Resultat eines Hochdruckgebiets über dem verbleibenden Rest des Skandinavischen Eisschilds verhinderte wahrscheinlich das Vordringen von Westen kommender warmer und feuchter Luftmassen und verursachte damit eine Abschwächung der frühholozänen Klimaverbesserung im östlichen Baltikum bis zum endgültigen Zerfall des Skandinavischen Eisschilds. Diese Ergebnisse bestätigen frühere Studien aus Nordwestrussland und zeigen, dass weite

Gebiete südöstlich des abschmelzenden Eisschilds durch eine frühholozäne Klimaentwicklung gekennzeichnet waren, die grundsätzlich anders als in West- und Mitteleuropa verlief.

Die spätglazialen Sedimentablagerungen des Mondsees wurden sowohl im Hinblick auf die regionale Klimaentwicklung als auch auf das Reaktionsverhalten verschiedener Umweltparameter während abrupter Klimaschwankungen untersucht. Der Beginn des Holozäns war durch einen abrupten Temperaturanstieg und die dazu zeitlich nahezu parallele Ausbreitung von Kiefernwäldern, den Rückgang des erosionsbedingten klastisch-detritischen Eintrags und die Intensivierung der biochemischen Kalkfällung gekennzeichnet. Im Gegensatz dazu war die Reaktion des Ökosystems auf die initiale Erwärmung zu Beginn des Spätglazials deutlich verzögert. Insbesondere die Ausbreitung von Nadelwäldern und die Reduktion des klastisch-detritischen Eintrags folgten der Erwärmung erst mit einer Verzögerung von etwa 500–750 Jahren. Die deutliche Abkühlung zu Beginn der Jüngeren Dryas war wiederum durch eine deutliche Synchronizität zwischen Temperaturabfall und Vegetationsänderung gekennzeichnet, wohingegen der Rückgang der biochemischen Kalkfällung und der Anstieg des klastisch-detritischen Eintrags dem Temperaturrückgang erst mit einer deutlichen Verzögerung von 150–300 Jahren folgten. Ein komplexes Reaktionsmuster der verschiedenen Umweltparameter zeigt sich auch während kurzfristigen Klimaschwankungen innerhalb des spätglazialen Interstadials, die mit den Sauerstoffisotopen-Substadien GI-1d, GI-1c2 und GI-1b in den grönländischen Eisbohrkernen korrelieren. Zusammenfassen lässt sich sagen, dass die abrupten Erwärmungen zu Beginn des Spätglazials und des Holozäns sowie die Abkühlung zu Beginn der Jüngeren Dryas und kürzere Abkühlungsphasen während des Spätglazials durch komplexe und zeitlich variable Reaktionsmuster der untersuchten Umweltparameter gekennzeichnet waren. Änderungen im Ökosystem sind dabei in hohem Maße von dessen interner Klimasensitivität und den ökologischen Ausgangsbedingungen, d.h. der langfristigen Entwicklung des Sees und seines Einzugsgebiets, abhängig.

Eine Studie an den holozänen Sedimentablagerungen des Mondsees konzentrierte sich vorrangig auf zwei kleinere Klimaschwankungen vor etwa 8200 und 9100 Jahren. Als Ursache für diese beiden Abkühlungsereignisse wird gemeinhin Schmelzwassereintrag in den Nordatlantik und ein damit verbundenes Zusammenbrechen der thermohalinen Zirkulation angesehen. Durch die Kombination von Warvenzählungen an Dünnschliffen und $^{14}$C-Datierungen an terrestrischen Pflanzenresten konnten sowohl die Dauer der Kältephase vor etwa 8200 Jahren (ca. 150 Jahre) als auch deren absolutes Alter (8225–8075 Jahre vor heute) zuverlässig bestimmt werden. Diese Ergebnisse zeigen eine gute Übereinstimmung mit früheren Studien an grönländischen Eisbohrkernen und anderen warvierten Seesedimentprofilen. Darüber hinaus konnte eine etwa 100 Jahre andauernde Warmphase direkt im Anschluss an das Abkühlungsereignis identifiziert werden, die auch in anderen Klimaarchiven im nordatlantischen Raum nachweisbar ist. Diese plötzliche Erwärmung wurde wahrscheinlich durch ein plötzliches deutliches Wiedererstarken der atlantischen thermohalinen Zirkulation verursacht, welches darüber hinaus auch eine Verschiebung ozeanischer (Arktische Front) und atmosphärischer Frontsysteme (Intertropische Konvergenzzone) und somit deutliche Auswirkungen auf das globale

Klimasystem zur Folge hatte. Obwohl Daten aus dem Nordatlantik auch nach dem Abkühlungsereignis vor etwa 9100 Jahren auf ein, wenn auch schwächeres, Wiedererstarken der thermohalinen Zirkulation hindeuten, finden sich in den Sedimenten des Mondsees keine Anzeichen für eine korrespondierende Wärmeperiode. Dies verdeutlicht anschaulich die Komplexität des globalen Klimasystems.

Die holozänen Sedimentablagerungen des Lago d'Iseo wurden im Hinblick auf die regionale Erdbebenaktivität in der Vergangenheit und die Auswirkungen von Klimaveränderungen und menschlichem Einfluss auf Erosionsprozesse im Einzugsgebiet und den Eintrag klastisch-detritischen Materials in den See untersucht. Zahlreiche kleinere detritische Lagen in den Sedimenten spiegeln Sedimenteintrag durch extreme Oberflächenabflussereignisse wieder. Während des Früh- und Mittelholozäns zeigt sich dabei eine deutliche Übereinstimmung zwischen Phasen erhöhten detritischen Eintrags, Phasen erhöhter Seespiegelstände im Alpenraum und niedriger Sonnenaktivität, welches gemeinhin als Anzeichen für kühlere und feuchtere Klimaverhältnisse angesehen wird. Somit scheint der klastisch-detritische Eintrag während dieses Zeitraums hauptsächlich durch die natürliche Klimavariabilität gesteuert zu sein. Im Gegensatz dazu zeigen Phasen erhöhten klastischen Eintrags während des Spätholozäns teilweise auch eine Korrelation mit erhöhter Siedlungsaktivität, was die Komplexität der Einflüsse auf Erosionsprozesse im Einzugsgebiet verdeutlicht. Neben den kleineren klastisch-detritischen Eintragslagen konnten im Sedimentprofil auch fünf größere Ereignislagen nachgewiesen werden, welche durch basale Rutschmassen und darüberliegende Turbidite gekennzeichnet sind. Für diese Ereignislagen werden lokale Erdbeben mit Magnituden von $M_w$=5.0–6.5 als Ursache vermutet. Insbesondere die jüngste dieser Ereignislagen kann mit einem historisch dokumentierten proximalen Erdbeben im Jahr AD 1222 korreliert werden. Für die anderen vier Ereignislagen werden entsprechend ihren Datierungen bisher undokumentierte prähistorische Erdbeben um 350 BC, 570 BC, 2540 BC und 6210 BC als Ursache vermutet.

Zusammenfassend lässt sich sagen, dass alle vier Studien auf eine relativ hohe Klimasensitivität vergleichsweise großer Seesysteme gegenüber Klima- und Umweltveränderungen hindeuten. Neben großräumigen Klimaveränderungen können vor allem unter Anwendung hochauflösender Analysemethoden auch kurzfristige und vergleichsweise schwach ausgeprägte regionale Klimaveränderungen nachgewiesen werden. Allerdings wird der Einfluss dieser Klimaveränderungen auf die jeweiligen Ökosysteme und Sedimentationsregime in großem Maße von den jeweiligen klimatischen Ausgangsbedingungen, der Vereisungsgeschichte, der Topographie, der Vegetationsentwicklung und darüber hinaus auch vom menschlichen Einfluss bestimmt. Nur die Kenntnis und das Verständnis dieser und anderer möglicher Einflussfaktoren sowie die Analyse zahlreicher, möglichst komplementärer Umweltparameter erlaubt die verlässliche Interpretation solcher Seesedimentprofile im Hinblick auf Klima- und Umweltveränderungen in der Vergangenheit.

# Acknowledgements

First of all, I want to thank my supervisor Achim Brauer, head of Section 5.2 “Climate Dynamics and Landscape Evolution” at the GFZ German Research Centre for Geosciences, for his constant encouragement during the last years. I greatly benefited from our inspiring discussions as well as your guidance and constructive criticism! I also wish to thank the external examiners for their critical review of my thesis. Furthermore, I am grateful to the Deutsche Forschungsgemeinschaft (DFG) for funding my PhD student position as a part of the research grant BR2208/2-2 to Achim Brauer.

I am deeply indebt to the DecLakes project members – particularly to the project leader Uli von Grafenstein (LSCE, Gif-sur-Yvette), but also to Nils Andersen, Matthias Hüls and Helmut Erlenkeuser (Leibniz Laboratory, Kiel), Dan L. Danielopol (Institute for Limnology, Mondsee; presently Austrian Academy of Sciences, Commission for the Stratigraphical & Palaeontological Research of Austria, Graz), Tadeusz Namiotko (University of Gdańsk) and Ángel Baltanás (Universidad Autónoma de Madrid) – for making available all the data that significantly contributed to the manuscripts presented in this thesis and the fruitful and stimulating discussions at any stage of my work. It was a pleasure to work with you!

I am also grateful to the scientific partners not directly involved in the DecLakes project. Krystyna Milecka and Milena Obremska (Adam Mickiewicz University, Poznań) carried out the pollen analyses for Lake Hańcza and Lake Mondsee and provided valuable information concerning data interpretation. Roland Schmidt (Institute for Limnology, Mondsee) provided useful information on Lake Mondsee and Soumaya Belmecheri (LSCE, Gif-sur-Yvette), Andrea Piccin (Regione Lombardia, Direzione Generale Territorio e Urbanistica, Milan), Jérôme Nomade (LGCA, Grenoble) and Marc Desmet (ISTO, Tours), who was also involved in the project proposal, greatly contributed to the success of the field work. Special thanks go to Fabien Arnaud (Laboratoire EDYTEM, Le Bourget-du-Lac) and Emmanuel Chapron (ISTO, Orléans) for their great hospitality and help during my stays in France and also for the stimulating and fruitful discussions concerning the interpretation of the Lake Iseo record.

This thesis would have not been possible without the support of the technical and scientific staff at the GFZ: Michael Köhler (presently MKfactory), Gabriele Arnold and Dieter Berger prepared the innumerable thin sections, but also had a solution for any technical problem which arose during the past years; Birgit Plessen, Petra Meier and Katarzyna Zamelczyk (presently University of Tromsø) provided the carbon and stable isotope analyses for Lake Hańcza; Peter Dulski and Brigitte Richert ran the μ-XRF measurements; Rudolf Naumann provided XRD measurements; Georg Schettler and Ursula Kegel helped with the Lake Mondsee carbon analyses; Juliane Herwig assisted during the SEM sessions – many thanks for your invaluable help with all the analyses and your useful comments concerning the interpretation of the data! I also wish to thank the other people working at the GFZ for the stimulating atmosphere and, last but not least, the non-scientific backbone of Section 5.2 at the

GFZ: Christine Gerschke managed all the administrative and bureaucratic stuff, Andreas Hendrich and Manuela Dziggel provided solutions for any graphical problem and Marcus Günzel kept the computer running – your help made life much easier!

Very special thanks go to my former room mates Clara Mangili, Susanne Stefer, Olga Kwiecien – I will miss the coffee breaks, open windows during winter, endless telephone calls and this very special atmosphere, sharing the office with three women ;-) – and my other present and former PhD student colleagues Sebastian Breitenbach, Christian Wolff, Hans von Suchodoletz, Markus Czymczik, Gordon Schlolaut and especially Tina Swierczynski, with whom I shared working on the Lake Mondsee record. I really enjoyed the time with all of you…

Last but not least, I would like to thank my friends and especially my whole family for their patience and never-ending support whenever work and family life had to be managed. This work would not have been possible without you!

# 1 Introduction

## 1.1 General introduction

As highlighted by the Fourth Assessment Report of the Intergovernmental Panel on Climate Change (IPCC AR4; Solomon *et al.* 2007), global climate change since about AD 1750 and particularly the warming during the past four decades are largely attributable to human activities. However, the exact quantification of the contributions of anthropogenic impact and natural climate variability, e.g. variations in solar and volcanic activity, to the observed rise of global average air and ocean temperatures is still matter of debate (e.g. Mann *et al.* 1998; Crowley 2000; Krivova & Solanki 2004). Within this context, improved understanding of past natural climate variability, which might vary regionally due to different boundary conditions, may serve as the basis for the reliable assessment of future climate change and the anthropogenic influence on the climate system. Furthermore, gaining enhanced knowledge about the response of local ecosystems to climatic changes is of particular importance as the environmental response is considered as the link between climate change and its impact on the socio-economic system (Ammann *et al.* 2000). Because of their high population density and importance for global economy, but also because of the close connection to the global climate system via ocean and atmospheric circulation processes (e.g. North Atlantic Current, North Atlantic Oscillation), the circum-North Atlantic region and particularly Europe are key areas to be investigated concerning the understanding of past, present and future climate dynamics and their environmental impact. Although numerous studies during the past decades have addressed different aspects of the palaeoclimatic evolution during the Late Quaternary in this region, a full understanding of natural climate variability and its regional peculiarities can only be gained by combining different types of palaeoclimate proxies and by establishing a dense spatial coverage of palaeoclimate records.

Previous palaeoclimate studies in the North Atlantic realm have utilized a multitude of archives, among whose the Greenland ice cores (e.g. Johnsen *et al.* 1992; Grootes *et al.* 1993; NGRIP Members 2004) and marine sediments (e.g. Haflidason *et al.* 1995; Hughen *et al.* 2000; Ebbesen & Hald 2004) are the most well-established. However, these palaeoclimate records are often dominated by climatic changes on a global or at least hemispheric scale, as for example changes in ocean or atmospheric circulation. In contrast, terrestrial palaeoclimate archives such as speleothems (e.g. Wurth *et al.* 2004; Boch *et al.* 2009; Spötl *et al.* 2010) or lake sediments (e.g. Birks & Ammann 2000; Brauer *et al.* 2000; Litt *et al.* 2001; Marshall *et al.* 2002; Yu 2007) are also recording climatic changes on a more regional scale. Although these types of archives are often influenced by site-specific effects like altitudinal position, local topography, vegetation history or soil development, which may modify the imprint of global climatic changes, they provide the unique opportunity to study past climate variability at high temporal resolution and furthermore to directly associate climatic changes at a global/hemispheric scale with the environmental response in the human habitat.

Within this context, lake sediments are of particular value as they offer, instead of speleothems, tree rings or ice cores, the possibility to study the response and sensitivity of a multitude of chemical, physical and biological proxy parameters to climatic changes in one archive and thus enable exploring possible relationships as well as leads and lags between the responses of different proxy data under changing climate conditions. Understanding these often fairly complex relationships may provide essential insights into past, present and future climate dynamics.

## 1.2 The DecLakes project

Stable oxygen ($\delta^{18}O$) and carbon ($\delta^{13}C$) isotope ratios are among the most frequently used proxies in palaeoclimate studies, allowing for instance the reconstruction of past changes in temperature, hydrology or vegetation cover (cf. McKenzie 1985; Schwalb 2003; Leng & Marshall 2004). Besides several studies on ice cores (e.g. Johnsen *et al.* 1992; Grootes *et al.* 1993; NGRIP Members 2004) and marine sediments (e.g. McManus *et al.* 1999; Ebbesen & Hald 2004), which have utilized oxygen isotopes to reconstruct climate variability in the Atlantic sector of the Northern Hemi-sphere since the Last Glacial Maximum and beyond, also numerous lake sediment records in temperate climate regions of North America (e.g. Yu 2007; Zhao *et al.* 2010) and Europe (e.g. Lotter *et al.* 1992; Marshall *et al.* 2002; Schwalb 2003) have been investigated in order to obtain high-resolution oxygen isotope data from lacustrine carbonates. Results of these studies strengthened the knowledge about past climate development in the North Atlantic realm, but in most cases provided $\delta^{18}O$ records that could only be interpreted qualitatively in terms of past climate variability. In contrast, oxygen isotope records obtained from benthic ostracods like that from Lake Ammersee in southern Germany (von Grafenstein *et al.* 1999a) revealed, when secondary effects influencing the oxygen isotope composition of the lake water ($\delta^{18}O_L$) and consequently also that of the ostracod valves can be quantified (see below), a high potential for long-term quantitative reconstructions of the oxygen isotope composition of precipitation ($\delta^{18}O_P$) in Europe. As $\delta^{18}O_P$ in Central Europe is largely controlled by temperature variability (Różański *et al.* 1992; Baldini *et al.* 2008), such records could be used for the quantitative reconstruction of past variations of mean atmospheric temperature. In the particular case of Lake Ammersee, the potential for precise palaeoclimate reconstructions has been shown by the validation against a 200-year-long instrumental record of meteorological data (von Grafenstein *et al.* 1996).

However, the spatial coverage of long quantitative high-resolution oxygen isotope records in Europe is still scarce; up to present, only the sediments of Lake Ammersee provided a decadally to sub-decadally resolved $\delta^{18}O_P$ record for almost the entire last 15 000 years. To overcome this deficit, the DecLakes project (*Decadal Holocene and Lateglacial variability of the oxygen isotopic composition in precipitation over Europe reconstructed from deep-lake sediments*), funded within the frame of the European Science Foundation EuroCLIMATE programme, has been initiated. Its main objective was to provide new decadally resolved oxygen isotope records obtained from the calcitic

valves of benthic ostracods in order to gain a spatial view of variations in $\delta^{18}O_P$ in Europe during the past ca. 15 000 years and thus an understanding of the regional characteristics of past climate variability. Furthermore, using the same proxy parameter as in the Greenland ice core studies should allow a direct comparison between these archives and thus could provide useful insights into climatic teleconnections on a hemispheric scale. For this purpose, the already existing $\delta^{18}O$ records from Lake Ammersee in southern Germany (von Grafenstein *et al.* 1999a) and Lake Annecy in southeastern France (Nomade 2005) should be extended and refined and in addition be supplemented by new high-resolution oxygen isotope records obtained from the sediments of three other deep European lakes (Fig. 1.1, Table 1.1): Lake Hańcza (northeastern Poland), Lake Mondsee (Upper Austria) and Lake Iseo (northern Italy).


**Figure 1.1** Geographic overview map of Europe with the location of the five lakes, which were subject of the DecLakes project. Orange points mark the two already existing lake sediment records of Lake Ammersee and Lake Annecy, while red points mark the three lakes, whose sediment records were investigated within this thesis.

**Table 1.1** Location and general characteristics of the three new lakes studied within the DecLakes project, whose sediments have been subject of this thesis.

| | Lake Hańcza | Lake Mondsee | Lake Iseo |
|---|---|---|---|
| **Location** | Suwałki-Augustów Lake District, northeastern Poland | Salzkammergut Lake District, Upper Austrian pre-Alps | Lombardian Southern Alps, northern Italy |
| **Coordinates** | 54°16'N, 22°49'E | 47°49'N, 13°24'E | 45°43'N, 10°05'E, |
| **Elevation** | 229 m a.s.l. | 481 m a.s.l. | 185 m a.s.l. |
| **Surface area** | 3.1 km² | 14.2 km² | 60.9 km² |
| **Catchment area** | ~40 km² | ~247 km² | ~1842 km² |
| **Maximum depth** | 108.5 m | 68.0 m | 256.0 m |
| **Depth coring site** | 60, 80 and 100 m | 62 m | 100 m |

Combining the latter two records with those from Lake Ammersee and Lake Annecy should provide new information on the spatial variability of $\delta^{18}O_P$ in Central Europe by providing transects across the Alps as well as along their northern margin. This would be of special interest as the Alps represent a major climatic divide in Europe, separating the Atlantic climate domain, where $\delta^{18}O$ records mainly reflect temperature variability (e.g. Eicher & Siegenthaler 1976; Lotter *et al.* 1992; von Grafenstein *et al.* 1999a), from the Mediterranean climate domain, where $\delta^{18}O$ records are mainly controlled by hydrological or moisture source changes (e.g. Baroni *et al.* 2006; Zanchetta *et al.* 2007; Finsinger *et al.* 2008). Furthermore, adding the Lake Hańcza record could be used to address past variations in continentality and their influence on temperature development.

In order to (1) obtain sediment cores with a robust chronology and consequently well-dated high-resolution oxygen isotope records from the valves of benthic ostracods and (2) allow the quantification of secondary isotopic effects influencing $\delta^{18}O_L$ and consequently also the $\delta^{18}O$ of the ostracod valves, which is essential for the reliable reconstruction of $\delta^{18}O_P$, the studied lakes have been chosen based on the following criteria:

- high sedimentation rates (>0.5 mm $a^{-1}$), allowing at least decadal data resolution for the stable isotope measurements (0.5 cm sampling resolution)
- sufficient terrestrial organic material within the sediments for accelerator mass spectrometry (AMS) $^{14}C$ dating and preferably annually laminated sediments, allowing varve counting and thus a precise age control for the palaeoclimatic reconstructions

- dimictic or monomictic mixing behaviour and relatively high calcium concentrations in both lake and interstitial water, favouring the development and preservation of an *in-situ* benthic ostracod fauna
- a large catchment/surface area ratio, resulting in minimized evaporation effects in the water balance and consequently a very small, almost constant offset between $\delta^{18}O_L$ and $\delta^{18}O_P$
- a maximum water depth of more than 60 m, ensuring a nearly constant bottom water temperature of about 4°C and thus the quasi-absence of a water temperature-dependent bias on the $\delta^{18}O_L$ reconstruction from benthic ostracod calcite
- presence of ostracods with a well-known isotopic offset from the $\delta^{18}O$ composition of the ambient lake water (cf. von Grafenstein *et al.* 1999b)
- a short theoretical water residence time (preferably <5 years) in order to assure a fast response of $\delta^{18}O_L$ to changes in $\delta^{18}O_P$

The DecLakes project initially focused on three time intervals (Fig. 1.2), characterized by large- and small-scale climatic changes, whose detailed understanding and spatial reconstruction could yield important insights into past climate dynamics in Europe. For these time intervals, sub-decadally to decadally resolved continuous analyses of the $\delta^{18}O$ composition of benthic ostracod valves were planned for each of the three sediment records, while the remaining sections were intended to be analyzed discontinuously at ca. 50-year intervals.

For the youngest of the three time intervals, the last millennium, investigations were intended to focus on identifying the prevailing forcing mechanisms of decadal- to centennial-scale natural climate variability in Europe during this period. In particular, the possible response of $\delta^{18}O_P$ in Europe to changes in solar activity (cf. Stuiver *et al.* 1995; Grootes & Stuiver 1997) as well as to variations in the strength of the North Atlantic thermohaline circulation and decadal variability of the North Atlantic Oscillation (cf. Baldini *et al.* 2008; Mangili *et al.* 2010b) should be addressed. Furthermore, the data should be used contribute to the present discussion about human impact on global warming (e.g. Ruddiman 2003) by adding information from an archive, that is located within the human habitat, but whose proxy record is not biased by direct anthropogenic influence or complex internal feedbacks as most biotic proxy data.

The period around the prominent mid-Holocene climate perturbation at ca. 8200 cal. a BP was chosen as the second time window under investigation. Although the so-called 8.2 ka event is relatively well reflected in various proxy records worldwide (cf. Rohling & Pälike 2005) and also in many European oxygen isotope records (e.g. von Grafenstein *et al.* 1998; Veski *et al.* 2004; Hammarlund *et al.* 2005; Marshall *et al.* 2007; Boch *et al.* 2009), its regional significance has been questioned by results from other proxy records (Seppä *et al.* 2007). These indicate a strong spatial variability of the 8.2 ka cold event across Europe.

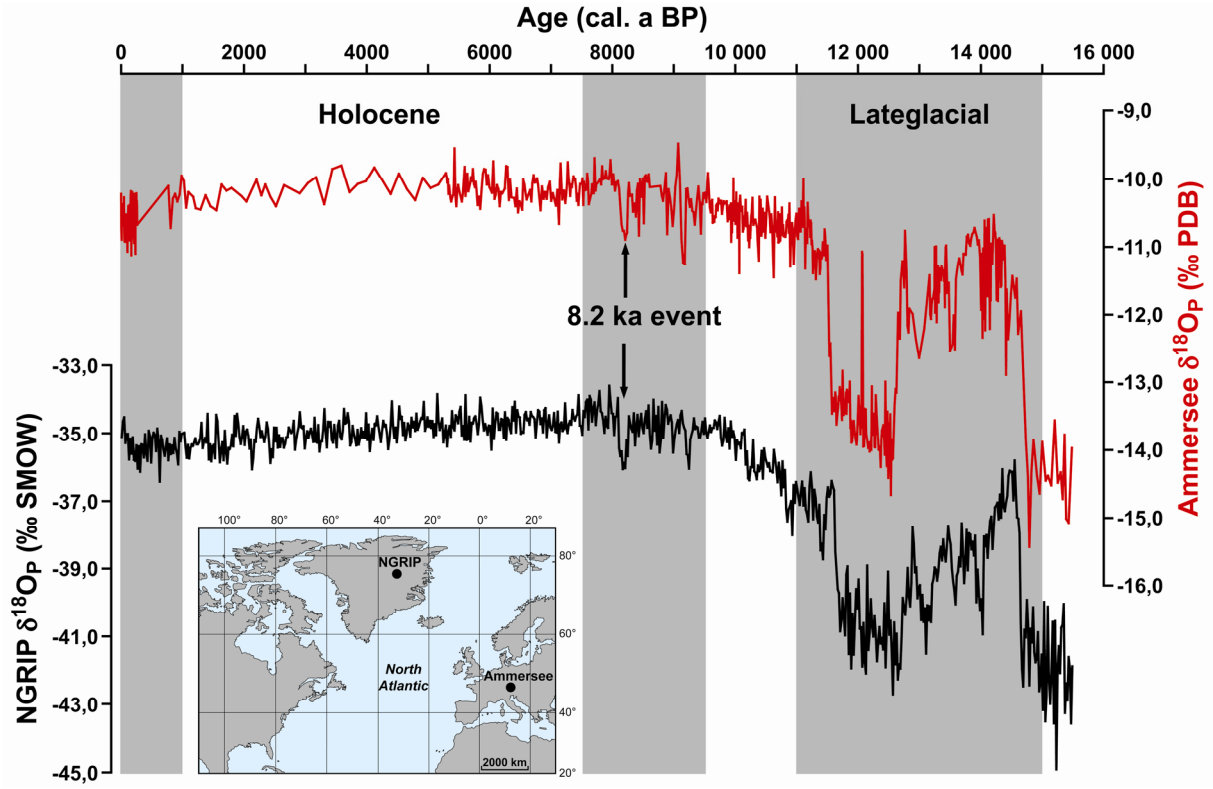


**Figure 1.2** Comparison of the oxygen isotope records from Lake Ammersee (von Grafenstein *et al.* 1999a) and the NGRIP ice core (NGRIP Members 2004; Andersen *et al.* 2006; Rasmussen *et al.* 2006; Svensson *et al.* 2006; Vinther *et al.* 2006). Grey shaded areas highlight the time intervals under investigation in the DecLakes project – the last millennium, the period around the 8.2 ka cold event and the transition from the Last Glacial to the Holocene.

New $\delta^{18}O_P$ records obtained within the DecLakes project could therefore improve knowledge about the spatial extent and regional peculiarities of the 8.2 ka cold event in Europe and also provide quantitative data sets for testing the performance of fully coupled ocean-atmosphere general circulation models in reproducing the respective regional expression of the 8.2 ka cold event.

The period between the onset of the Weichselian Lateglacial and the early Holocene was chosen as the third time interval to be studied in detail within the DecLakes project. This interval is characterized by numerous, apparently closely corresponding decadal- to centennial-scale temperature variations in Central Europe and Greenland (Fig. 1.2; von Grafenstein *et al.* 1999a). However, although even small-scale climatic fluctuations during the Lateglacial Interstadial have been identified in several European lake sediment oxygen isotope records (e.g. Eicher *et al.* 1981; Lotter *et al.* 1992), their significance and synchronicity in the circum-Atlantic region and even across the European continent is still matter of debate (Björck *et al.* 1998; Lowe & Hoek 2001). In addition, although some studies addressed the temporal relationships between atmospheric climate forcing, reflected by changes in $\delta^{18}O$, and the environmental response (e.g. Goslar *et al.* 1993; Goslar *et al.* 1999; Ammann *et al.* 2000; Ralska-Jasiewiczowa *et al.* 2003), particularly the exact timing between temperature-driven changes in oxygen isotope and pollen records, the latter being frequently used for the

biostratigraphic subdivision of the Lateglacial (e.g. Ammann & Lotter 1989; Litt & Stebich 1999), and thus the comparability of such records is still subject of discussion. Moreover, although the climatic signal seen in the $\delta^{18}O$ records from the Greenland ice cores (e.g. Johnsen *et al.* 1992; Grootes *et al.* 1993; NGRIP Members 2004) is commonly considered to be valid on a large spatial scale, e.g. for the entire circum-North Atlantic region, comparison of the Greenland and Lake Ammersee $\delta^{18}O$ records revealed significant quantitative differences in the millennial-scale trend of climate evolution during the Lateglacial Interstadial. These have been attributed to the complex interplay between changes in atmospheric and ocean circulation and sea ice extent (von Grafenstein *et al.* 1999a), but, nevertheless, the driving mechanisms of this climate asymmetry are still not fully understood. New high-resolution $\delta^{18}O_P$ records achieved within the DecLakes project could help investigating the synchronicity of Lateglacial climate fluctuations and quantifying inner-European climate gradients, but could also aid the understanding of teleconnections between the climate development in Greenland and Europe and possible driving mechanisms of hemispheric-scale climate variability.

## 1.3 Objectives of this thesis

Oxygen isotope studies on lake sediments (e.g. Lotter *et al.* 1992; von Grafenstein *et al.* 1999a; Marshall *et al.* 2002; Schwalb 2003; Yu 2007; Zhao *et al.* 2010) have provided substantial information on past climate development in the North Atlantic realm since the Last Glacial Maximum. In addition, many other studies on lakes from this region addressed the environmental response to changing climate conditions by combining oxygen isotopes with biotic proxy data (e.g. Ammann *et al.* 2000; Ralska-Jasiewiczowa *et al.* 2003). However, a thorough understanding of past climate dynamics and the full assessment of its influence on local ecosystems requires not only a dense spatial coverage of palaeoclimate records to understand the regional aspects of climate variability but also information from sedimentological proxy parameters, allowing to estimate the influence of climate changes on, for instance, erosion processes or lake productivity. Such comprehensive information can only be gained from multi-proxy studies, combining directly climate-related proxy data like oxygen isotopes with sedimentological, geochemical and pollen data, which rather reflect the environmental response (e.g. vegetation development, erosion processes, lake productivity).

Arising from the main goal of the DecLakes project, which was the identification of regional peculiarities of Lateglacial and Holocene climate variability in Europe, and my responsibility within the project, the sedimentological characterization of the three new lake sediment records and the establishment of robust chronologies, I decided to use the sediments themselves to track climate variability. I partly also tried to put the regional or even local aspects of climate variability recorded in the three individual lake sediment records into a larger, extraregional to hemispheric-scale context in order to contribute to a better understanding of large-scale climate dynamics.

As large lake systems, like those investigated within the DecLakes project, are generally considered to have only a limited sensitivity to climatic and environmental changes as well as to human impact because of the inertia of these systems, the sedimentological response to climatic changes might be, particularly in the case of small-scale climatic perturbations, rather subtle. Furthermore, the high temporal resolution, which is necessary for the reliable reconstruction of rapid climate fluctuations, is often hampered by the relatively low sedimentation rates in large lakes. Hence, I decided to utilize a combination of different high-resolution methods in order to detect these changes but also to achieve the most comprehensive picture of the environmental response. First of all, I focused on the detailed investigation of sediment microfacies changes by microscopic inspection of large-scale petrographic thin sections, an approach whose potential for palaeoclimate studies has previously been shown (e.g. Brauer *et al.* 1999a). The obtained qualitative data were further supplemented by high-resolution geochemical and geophysical methods such as micro-X-ray fluorescence (µ-XRF) scanning, magnetic susceptibility and spectrophotometry measurements, X-ray diffractometry (XRD) and measurements of carbon contents (total carbon, total organic carbon, total inorganic carbon). In addition the sedimentological and geochemical data were combined with the results of stable isotope measurements and pollen and ostracod analyses, carried out by the co-authors of the respective manuscripts, in order to provide a comprehensive insight into the nature of climatic changes (temperature and/or precipitation) and the related response of each individual sedimentary regime and ecosystem.

Having the sediments of the three new DecLakes sites and in addition a robust chronological framework and high-resolution stable isotope data as a kind of quantitative measure of past climate variability at my disposal, I decided to focus on investigating the following issues, being of overall importance for the understanding of climatic changes in Central Europe during the past ca. 15 000 years and their influence on the sedimentary regime and ecosystem of comparatively large lakes:

- How did the climate change at the respective sites during the intervals under investigation and in which way and how fast did the local sedimentary regimes and ecosystems respond to climate variability?
- To which extent are regional peculiarities of past climate development preserved in the individual lake sediment records and how are these regional aspects of climatic variability related to global-scale climate dynamics?
- How sensitive are depositional processes in rather large lake systems to rapid, large- and small-scale climatic changes and how are climatic changes reflected in the sediments?
- How important are site characteristics and environmental preconditions for the reflection of climatic changes in lake sediments?
- Is it possible to discern between the influences of natural climate variability and human impact on depositional processes in large lake systems and what is the major control?

## 1.4 Overview of manuscripts

This thesis is based on three already accepted manuscripts, which are or will soon be published in peer-reviewed international journals, and one manuscript still to be submitted.

The first manuscript, entitled **"Multi-proxy evidence for early to mid-Holocene environmental and climatic changes in northeastern Poland"** (S. Lauterbach, A. Brauer, N. Andersen, D. L. Danielopol, P. Dulski, M. Hüls, K. Milecka, T. Namiotko, B. Plessen, U. von Grafenstein and DecLakes participants (2011), *Boreas 40*, 57–72), addresses the issue of regional peculiarities in climate development in Europe during the transition from the Last Glacial to the Holocene by applying a multi-proxy approach to the sediment record of Lake Hańcza. For this study, I developed the chronology of the record, performed the sediment microfacies analysis and evaluated and interpreted all proxy data, benefiting from discussions with the co-authors. I drew eight of the ten figures and wrote the manuscript almost independently with only minor contributions from the co-authors (mainly from Achim Brauer).

The second manuscript **"Environmental responses to Lateglacial climatic fluctuations recorded in the sediments of pre-Alpine Lake Mondsee (northeastern Alps)"** (S. Lauterbach, A. Brauer, N. Andersen, D. L. Danielopol, P. Dulski, M. Hüls, K. Milecka, T. Namiotko, M. Obremska, U. von Grafenstein and DecLakes participants, *Journal of Quaternary Science*, in press), focuses on the question, whether the sediments of comparatively large lakes are sensitive recorders of rapid climatic shifts during the Lateglacial. In addition, this study explores in detail temporal relationships between the responses of different environmental parameters (i.e. vegetation, lake productivity, catchment erosion) and climatic changes by applying a multi-proxy approach to the sediment record of Lake Mondsee. Within this study, I aided in thin section preparation, analyzed 232 thin sections for the sediment microfacies, carried out the varve counting, constructed the age model for the Lateglacial part of the record and performed the analyses for inorganic and organic carbon. In addition, I conducted the evaluation and interpretation of the other proxy data, aided by discussions with the co-authors. I drew eight of the nine figures and wrote the manuscript almost independently with only minor contributions from the co-authors (mainly from Achim Brauer).

The third manuscript, which is entitled **"Were there overshooting warm temperatures in Central Europe after the abrupt 8.2 ka and 9.1 ka cold events?"** (N. Andersen, S. Lauterbach, D. L. Danielopol, T. Namiotko, M. Hüls, H. Erlenkeuser, A. Brauer, U. von Grafenstein and DecLakes participants, to be submitted to *Geology*) addresses the reflection of two prominent cold phases during the early Holocene, the so-called 8.2 ka and 9.1 ka events, and possible subsequent temperature overshoots in the oxygen isotope record of Lake Mondsee. Moreover, this study draws conclusions about climatic teleconnections in the North Atlantic realm, driven by changes in ocean and atmospheric circulation. For this study, I provided the chronological framework by conducting the varve counting and developing the supplementary radiocarbon-based age model. In addition, I drew

three of the figures and contributed to the discussion of the presented data. Moreover, I wrote the manuscript jointly with N. Andersen with only minor contributions from the other co-authors.

The fourth manuscript **"A sedimentary record of Holocene surface runoff events and earthquake activity from Lake Iseo (Southern Alps, Italy)"** (S. Lauterbach, E. Chapron, A. Brauer, M. Hüls, A. Gilli, F. Arnaud, A. Piccin, J. Nomade, M. Desmet, U. von Grafenstein and DecLakes participants, *The Holocene*, accepted pending minor revisions) explores the sediment record of Lake Iseo as an archive of climate- and human-induced catchment erosion processes as well as of earthquake activity during the Holocene by using a combined approach of high-resolution seismic surveying, detailed sediment microfacies analysis and non-destructive core scanning techniques. I participated in the field campaign and assisted in thin section preparation. Furthermore, I analyzed 319 thin sections for the sediment microfacies, performed about the half of the spectrophotometry measurements and developed the age model. I evaluated and interpreted the proxy records, drew most of the figures and wrote about 80% of the manuscript, with a major contribution by E. Chapron (seismic data) and only very minor contributions from the other co-authors.

In order to achieve a uniform appearance of the individual chapters of this work, the original layout of the already accepted manuscripts has been slightly modified. However, this does not affect the scientific data and their interpretation. All data obtained from the three lake sediment records, which appear in the respective chapters of this thesis, as well as a digital version of this thesis can be found on the accompanying CD-ROM in the back cover.

# 2 Multi-proxy evidence for early to mid-Holocene environmental and climatic changes in northeastern Poland

Stefan Lauterbach[1], Achim Brauer[1], Nils Andersen[2], Dan L. Danielopol[3], Peter Dulski[1], Matthias Hüls[2], Krystyna Milecka[4], Tadeusz Namiotko[5], Birgit Plessen[1], Ulrich von Grafenstein[6] and DecLakes participants[7]

[1] GFZ German Research Centre for Geosciences, Section 5.2 – Climate Dynamics and Landscape Evolution, D-14473 Potsdam, Germany

[2] Christian-Albrechts-University, Leibniz Laboratory for Radiometric Dating and Stable Isotope Research, D-24118 Kiel, Germany

[3] Austrian Academy of Sciences, Institute for Limnology, A-5310 Mondsee, Austria; present address: Austrian Academy of Sciences, Commission for the Stratigraphical & Palaeontological Research of Austria, c/o Institute of Earth Sciences, Geology and Palaeontology, University of Graz, A-8010 Graz, Austria

[4] Adam Mickiewicz University, Faculty of Geographical and Geological Science, Department of Biogeography and Palaeoecology, PL-61-680 Poznań, Poland

[5] University of Gdańsk, Department of Genetics, Laboratory of Limnozoology, PL-80-822 Gdańsk, Poland

[6] Laboratoire des Sciences du Climat et de l'Environnement, UMR CEA-CNRS, F-91191 Gif-sur-Yvette, France

[7] Soumaya Belmecheri (LSCE, Gif-sur-Yvette), Marc Desmet (ACCES-INRP, Lyon), Helmut Erlenkeuser (Leibniz Laboratory, Kiel), Jérôme Nomade (LGCA, Grenoble)

**published in *Boreas* (Volume 40, Pages 57–72, DOI: 10.1111/j.1502-3885.2010.00159.x)**

***ABSTRACT*** *We investigated the sedimentary record of Lake Hańcza (northeastern Poland) using a multi-proxy approach, focusing on early to mid-Holocene climatic and environmental changes. Accelerator mass spectrometry (AMS) $^{14}C$ dating of terrestrial macrofossils and sedimentation rate estimates from occasional varve thick-ness measurements were used to establish a chronology. The onset of the Holocene at ca. 11 600 cal. a BP is marked by the decline of Lateglacial shrub vegetation and a shift from clastic-detrital deposition to an autochthonous sedimentation dominated by biochemical calcite precipitation. Between 10 000 and 9000 cal. a BP, a further environmental and climatic improvement is indicated by the spread of deciduous forests, an increase in lake organic matter and a 1.7‰ rise in the oxygen isotope ratios of both endogenic calcite and ostracod valves. Rising $\delta^{18}O$ values were probably caused by a combination of hydrological and climatic factors. The persistence of relatively cold and dry climate conditions in northeastern Poland during the first one and a half millennia of the Holocene could be related to a regional eastern European atmospheric circulation pattern. Prevailing anticyclonic circulation linked to a high-pressure cell above the retreating Scandinavian Ice Sheet might have blocked the influence of warm and moist Westerlies and attenuated the early Holocene climatic amelioration in the Lake Hańcza region until the final decay of the ice sheet.*

## 2.1 Introduction

Detailed information about the regional characteristics of past climate variability is key for the assessment of possible regional environmental responses to future global climate change. Previous studies have shown that major climate oscillations across the Lateglacial-Holocene transition were synchronous within dating uncertainties in lacustrine (e.g. Björck *et al.* 1996; Gulliksen *et al.* 1998; von Grafenstein *et al.* 1999a; Brauer *et al.* 2000; Brauer & Casanova 2001; Litt *et al.* 2001; Yu 2007), marine (e.g. Koç Karpuz & Jansen 1992; Haflidason *et al.* 1995; Hughen *et al.* 2000; Ebbesen & Hald 2004) and ice core (Johnsen *et al.* 1992; NGRIP Members 2004; Rasmussen *et al.* 2006) archives in the North Atlantic realm. In contrast, early Holocene warming and the associated environmental response in northeastern Europe have been suggested to be delayed (Subetto *et al.* 2002; Wohlfarth *et al.* 2002; Wohlfarth *et al.* 2007; Stančikaitė *et al.* 2008). However, multi-proxy palaeoclimate studies for the southeastern Baltic region, which could aid in gaining an understanding of the regional climate evolution, are still limited to only a few sites and focus mainly on the Lateglacial (Goslar *et al.* 1993; Ralska-Jasiewiczowa *et al.* 1998; Goslar *et al.* 1999; Ralska-Jasiewiczowa *et al.* 2003; Makhnach *et al.* 2004; Kupryjanowicz 2007; Rutkowski *et al.* 2007; Zawisza & Szeroczynska 2007; Stančikaitė *et al.* 2008; Apolinarska & Hammarlund 2009).

In order to test the hypothesis of a particular eastern European pattern of early Holocene climatic amelioration, we present new high-resolution data from the sediment record of Lake Hańcza in northeastern Poland, the deepest lake in the Central-European Lowland. As part of the ESF project DecLakes (*Decadal Holocene and Lateglacial variability of the oxygen isotopic composition in precipitation over Europe reconstructed from deep-lake sediments*), this study combines microfacies analysis, µ-XRF geochemistry, pollen and stable isotope analyses to reconstruct the early to mid-Holocene climatic and environmental evolution in northeastern Poland. This is the first in a series of papers, focusing on climatic and environmental changes recorded in the Lake Hańcza sediments. Later contributions will address the vegetation development and ostracod assemblage changes in detail.

## 2.2 Study site

Lake Hańcza (54°16'N, 22°49'E, 229 m above sea level), is located about 20 km northwest of the town of Suwałki in the Suwałki-Augustów Lake District of northeastern Poland (Fig. 2.1A-C). The mesotrophic lake (maximum depth 108.5 m, surface area 3.1 km², volume 0.12 km³, catchment area 39.7 km²), which occupies a former subglacial channel incised into Saalian tills, is fed and drained by the Czarna Hańcza river. Catchment geology is dominated by Quaternary deposits of up to 280 m thickness, particularly glacial tills and glaciofluvial sands with intercalated interstadial/interglacial silts and clays (Ber 1974, 1987), that cover Cretaceous and Tertiary limestones and sandstones. Carbonate contents of 5–15% have been reported for various Pleistocene tills and glaciofluvial sands

in Poland (Bukowska-Jania & Pulina 1999). The Pomeranian Moraine, located about 7 km south of the lake (Ehlers & Gibbard 2004), is evidence for the last advance of the Scandinavian Ice Sheet at the end of the Weichselian glaciation. Age estimates for the moraine are highly variable, differing between ca. 18 500 cal. a BP (western Poland, derived from radiocarbon dating; Marks 2002 and references therein) and ca. 14 600 cal. a BP (northeastern Poland and Lithuania, derived from $^{10}$Be exposure dating; Rinterknecht *et al.* 2006).

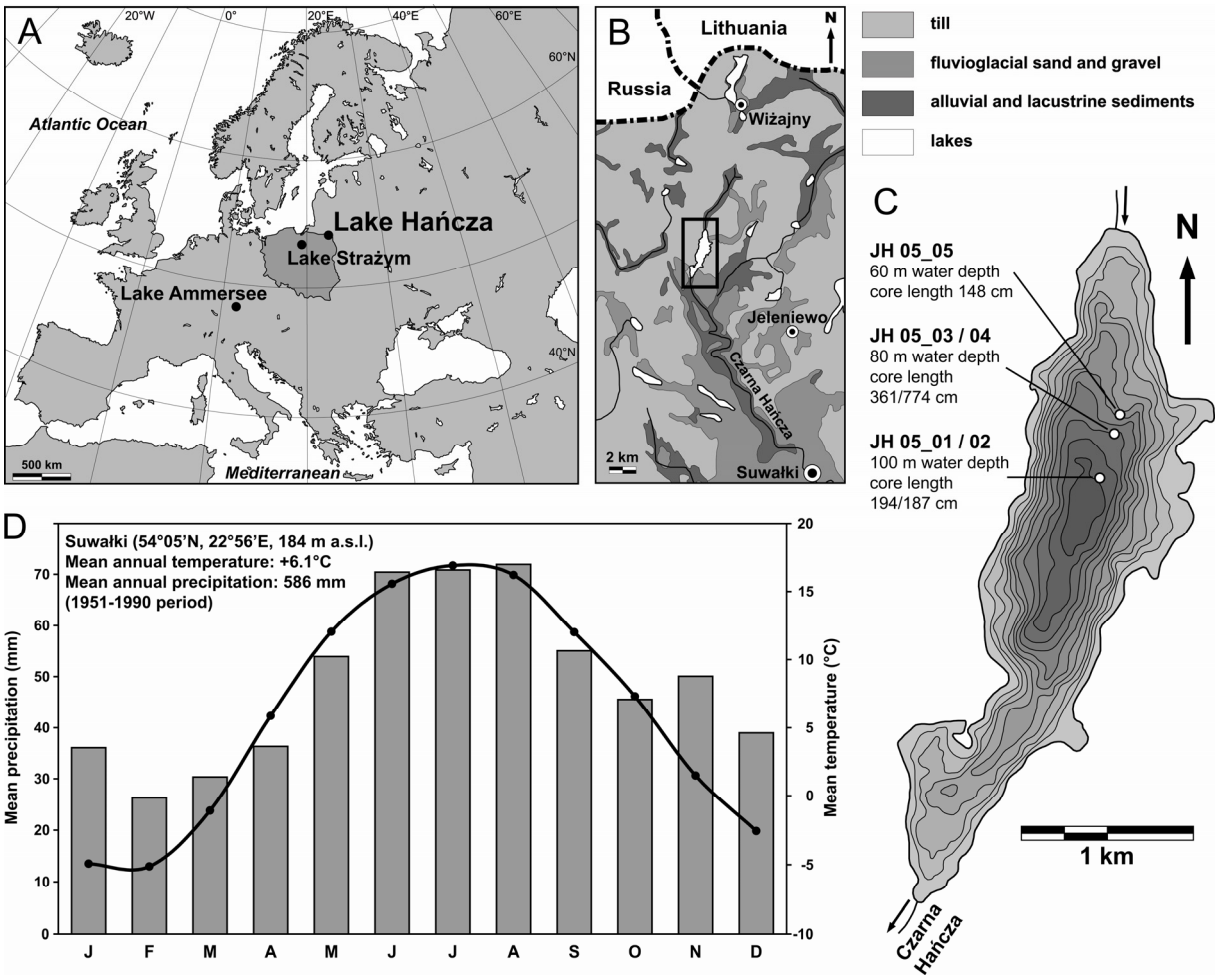


**Figure 2.1** (A) General geographic overview map with locations mentioned in the text. (B) Simplified geological map of the area surrounding Lake Hańcza (modified after Ber (1971)). (C) Bathymetric map of Lake Hańcza with coring locations. Isobaths are given at 10-m intervals. (D) Climate diagram for the weather station Suwałki (Vose *et al.* 1992).

Today, the study area is characterized by a humid continental climate with warm summers and cold winters. The mean annual air temperature is +6.1°C, with January and July means of -4.9°C and +16.9°C, respectively. Average annual precipitation in the region amounts to about 600 mm (Vose *et al.* 1992) (Fig. 2.1D), with highest rainfall during summer. Recent vegetation is dominated by nemoral forest communities with boreal influences. A significant proportion of *Picea abies* and the absence of *Fagus sylvatica* are characteristic differences from the western parts of Poland (Ralska-Jasiewiczowa & Latałowa 1996).

## 2.3 Methods

### *2.3.1 Fieldwork*

Five sediment cores, each consisting of 2-m-long segments, were recovered with a 90-mm-diameter UWITEC piston corer from the deep northern part of the lake (Fig. 2.1C). The two longest cores, from 80 m water depth (JH 05_03 and JH 05_04; Figs. 2.1C and 2.2A), comprise 361 and 774 cm of lake sediments and were selected as master cores.

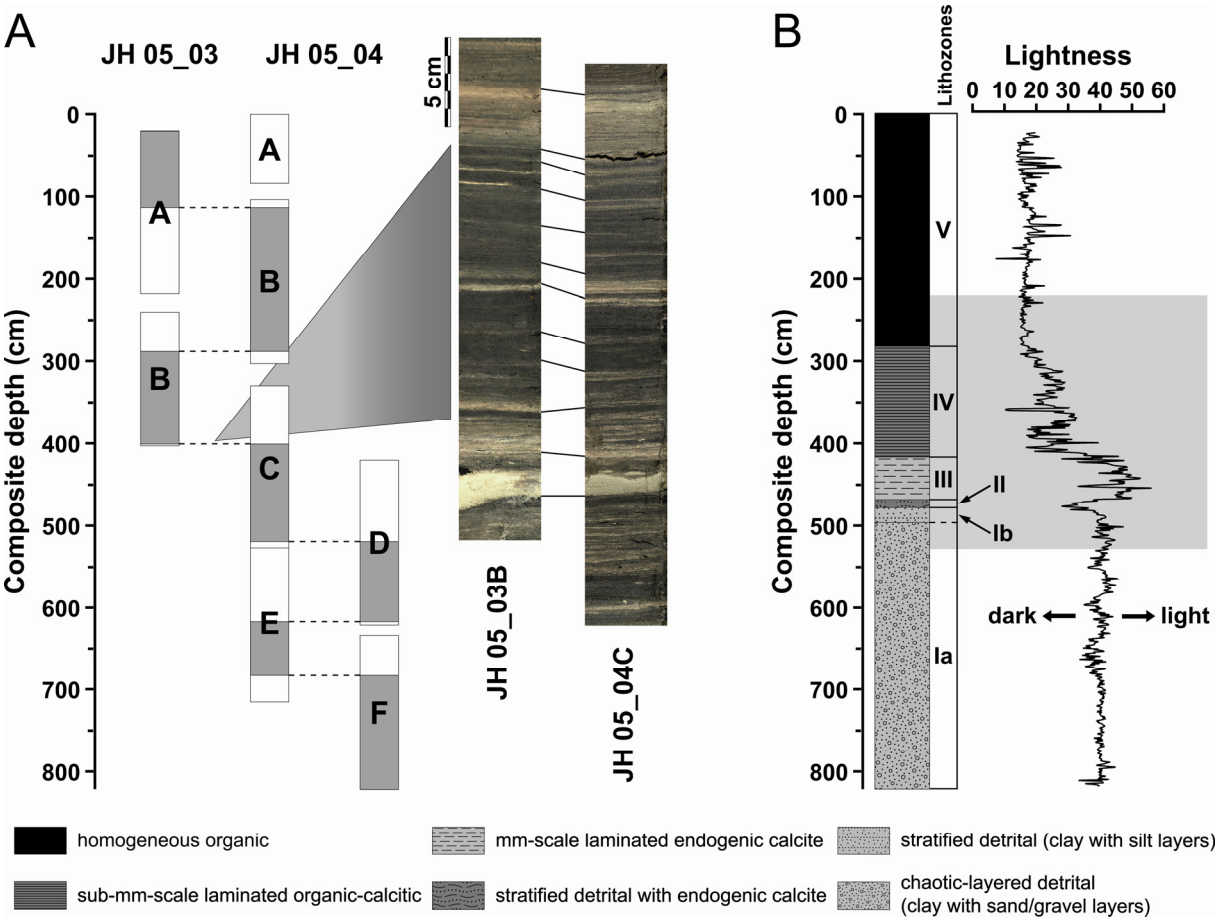


**Figure 2.2** (A) Correlation between the segments of cores JH 05_03 and JH 05_04. Grey shaded intervals indicate sections included in the composite profile. Detailed photographs of the core segments JH 05_03B and JH 05_04C illustrate the correlation through lithological marker layers. (B) Lithological composite profile of the complete Lake Hańcza sediment record. The grey shaded interval between 220 and 530 cm indicates the sequence investigated in this study. Sediment lightness L* was derived from spectrophotometry measurements (see text for details).

After photographing and lithostratigraphic description, the overlapping segments of the two cores were visually correlated by using distinct lithological marker layers, resulting in a continuous composite profile of about 820 cm length (Fig. 2.2). Continuous spectrophotometry measurements at 1-cm intervals were performed with a Minolta CM-2500d spectrophotometer on the fresh sediment

surface, covered with a thin transparent polyethylene film (Chapman & Shackleton 1998). The mean of reflectance, measured at 10-nm increments over the 400–700 nm wavelength range, results in the sediment lightness L* (Fig. 2.2B), given on a scale from 0 to 100 (black to white). Subsequently, the composite profile was sampled for all further analyses in the field lab to ensure precisely parallel samples for the multi-proxy approach. Detailed investigation focused on the core interval between 220 and 530 cm, which is characterized by major sedimentological changes.

### *2.3.2 Sedimentology and geochemistry*

Microfacies analysis and final core correlation were carried out under a ZEISS Axiophot polarization microscope at 25–400× magnification on a continuous series of large-scale petrographic thin sections, prepared from 10-cm-long overlapping sediment blocks according to the method described by Brauer *et al*. (1999b).

High-resolution micro X-ray fluorescence (µ-XRF) element scanning was carried out on a vacuum-operating EAGLE III XL µ-XRF spectrometer with a low-power Rh X-ray tube at 40 kV and 300 µA. Measurements were performed on a single scan line with 200 µm step width (250 µm spot size, 60 s counting time) on the impregnated sediment slabs from thin section preparation, allowing direct comparison of geochemical and microfacies data (Brauer *et al.* 2009). The fluorescent radiation emitted from the sample was recorded by an energy-dispersive Si (Li) detector and transformed into element information for each measuring point. Resulting element intensities for Al, Si, P, S and Ca are given semi-quantitatively as counts $s^{-1}$ (cps), reflecting relative changes in element composition.

Bulk sediment samples of 0.5 cm thickness for quantitative carbon geochemistry were taken almost continuously every 2 cm. Freeze-dried and homogenized samples (5–10 mg in Sn-capsules) were analyzed for total carbon (TC) using a EuroVector elemental analyzer EA 3000. Total organic carbon (TOC) was measured in a similar manner (3 mg in Ag-capsules) after pre-treatment with 20% HCl at 75°C. The analytical precision for all analyses is <0.3%. Total inorganic carbon (TIC) was estimated as the difference between TC and TOC. Calcite contents were calculated stoichiometrically from the TIC contents as thin section and X-ray diffractometry (XRD) analyses confirmed calcite as the dominant carbonate mineral. All results are expressed as per cent dry weight.

### *2.3.3 Stable isotopes*

For continuous $\delta^{18}O$ and $\delta^{13}C$ measurements on ostracods, 0.5-cm-thick sediment slices were disaggregated in 10% $H_2O_2$, wet-sieved (<125 µm) and rinsed in ethanol before drying. Juvenile *Candona neglecta* valves (mostly $5^{th}$–$8^{th}$ stage) were separated and mechanically cleaned. Subsets of up to 20 valves (5–80 µg) were analyzed for their stable isotope compositions at the Leibniz Laboratory in Kiel on a CARBO Kiel I/Finnigan MAT 251 $CO_2$ preparation and isotope ratio mass

spectrometer (IRMS) system. Results are given relative to the Vienna PeeDee Belemnite (VPDB) standard in the conventional δ-notation. The analytical precision is <0.04‰ for $\delta^{13}C$ and <0.07‰ for $\delta^{18}O$.

Bulk sediment samples (70–130 µg) containing more than 30% $CaCO_3$ were analyzed for the stable oxygen and carbon isotope compositions of endogenic calcite. Microfacies analysis revealed that contamination with detrital carbonates is negligible. Measurements were conducted at the GFZ Potsdam with a Finnigan MAT 253 IRMS connected to a Kiel IV carbonate device. Stable isotope ratios are expressed relative to the VPDB standard in the conventional δ-notation with an analytical precision of <0.04‰ and <0.06‰ for $\delta^{13}C$ and $\delta^{18}O$, respectively.

Water samples from Lake Hańcza and its inflow and outflow (Table 2.1) were analyzed for stable oxygen and hydrogen isotope compositions at the LSCE in Gif-sur-Yvette. A Finnigan MAT 252 IRMS coupled to a $CO_2$-equilibration line, and an automated inlet system connected to a specially designed mass spectrometer were used for $\delta^{18}O$ and $\delta^{2}H$ measurements, respectively (Vaughn *et al.* 1998). Results are given relative to the Vienna Standard Mean Ocean Water (VSMOW) standard in the conventional δ-notation with an analytical precision of <0.05‰ for $\delta^{18}O$ and <1‰ for $\delta^{2}H$.

**Table 2.1** Stable oxygen and hydrogen isotope composition of modern water samples from Lake Hańcza and regional precipitation.

| Source | $\delta^{18}O$ (‰ VSMOW) | $\delta^{2}H$ (‰ VSMOW) |
|---|---|---|
| Lake Hańcza inflow, 30.08.2005 | -9.20 | -67.02 |
| Lake Hańcza inflow, 19.04.2005 | -9.50 | -72.54 |
| Lake Hańcza outflow, 19.04.2005 | -7.05 | -58.13 |
| Lake Hańcza outflow, 31.08.2005 | -7.27 | -56.68 |
| Lake Hańcza surface water, 19.04.2005 | -7.23 | -58.47 |
| Lake Hańcza surface water, 03.09.2005 | -7.21 | -55.02 |
| Lake Hańcza 60 m water depth, 02.09.2005 | -7.51 | -58.15 |
| Lake Hańcza 80 m water depth, 02.09.2005 | -7.41 | -56.91 |
| downstream contributor Czarna Hańcza, 19.04.2005 | -10.11 | -72.54 |
| Cracow, precipitation[a] | -9.19 | -64.89 |
| Riga, precipitation[a] | -9.67 | -73.26 |
| Brest, precipitation[a] | -9.40 | -71.13 |

[a] Amount-weighted annual mean $\delta^{18}O$ and $\delta^{2}H$ of atmospheric precipitation according to the GNIP data base (IAEA/WMO 2006) for the stations Cracow (1975–2002), Riga (1981–1989) and Brest (1980–1983). Cracow, Riga and Brest are located ~500 km southwest, ~300 km northeast and ~250 km southeast of Lake Hańcza, respectively.

### *2.3.4 Pollen and ostracods*

Pollen analyses were carried out at the Adam Mickiewicz University in Poznań. Sediment samples of 1 $cm^3$ (1–3 cm sample increment) were prepared for microscope analysis following standard methods (Berglund & Ralska-Jasiewiczowa 1986), including treatment with cool HF and HCl and acetolysis for 3 min. Two *Lycopodium* tablets were added to each sample to calculate the pollen concentration (Stockmarr 1971). Samples were embedded in pure glycerine and stained with safranin. A minimum of 500 terrestrial pollen grains were analyzed, except for some Lateglacial samples with low pollen concentrations. Pollen percentages were calculated based on the sum of trees/shrubs (AP) and herbs (NAP, except aquatic and wetland plants). Pollen concentrations are given as pollen grains $cm^{-3}$ dry sediment. The pollen diagram was plotted using the TILIA/TILIA GRAPH software package (including zonation with CONISS; Grimm 1987, 1992).

Sediment slices of 0.5 cm thickness for ostracod analyses were taken at 5-cm intervals and prepared at the University of Gdańsk and the Institute for Limnology in Mondsee following standard techniques (Griffiths & Holmes 2000). After drying at 60°C for 24 h, samples were weighted, disaggregated in dilute $H_2O_2$, wet-sieved through a 125-µm mesh and rinsed in pure ethanol before drying. Separated ostracod valves were identified under a binocular microscope at 500× magnification using identification keys by Sywula (1974), Absolon (1978), Griffiths & Holmes (2000) and Meisch (2000), with taxonomy and nomenclature following the latter. Results are expressed as the total number of valves $g^{-1}$ dry sediment and as species/taxa relative abundances.

### *2.3.5 Radiocarbon dating*

Accelerator mass spectrometry (AMS) $^{14}C$ dating of 13 samples of terrestrial plant macrofossils, obtained from the studied core interval, was conducted at the Leibniz Laboratory in Kiel (Table 2.2). Conventional radiocarbon ages were calibrated using the OxCal 4.1 program (Ramsey 1995, 2001) with the IntCal04 calibration data set (Reimer *et al.* 2004).

## 2.4 Results

### *2.4.1 Sediment microfacies*

The Lake Hańcza sediment record can be subdivided into five main lithostratigraphical units (Fig. 2.2B). Lithozone I (821.5–477.5 cm) consists mainly of yellowish grey to brownish clay. While in the basal part (below 496.0 cm, Lithozone Ia) partly tilted sand and gravel layers are common, the upper part (496.0–477.5 cm, Lithozone Ib) contains only a few intercalated fine sand and silt layers.

X-ray diffractometry revealed quartz, feldspar and clay minerals as dominant, and dolomite, calcite and vivianite as minor sediment components. Sand and gravel layers contain mainly quartz but also a few detrital carbonates of up to 250 μm in diameter. Most grains are rounded, indicating glaciofluvial/fluvial transport processes. In the upper 5 cm of Lithozone Ib, several millimetre-thick black layers of finely dispersed microcrystalline pyrite (<5 μm) occur. Lithozone II (477.5–467.5 cm) represents a transitional zone with idiomorphic micritic calcite (<5 μm) abruptly appearing at its base. Subsequently, calcite contents gradually increase, coinciding with a decrease of siliciclastic components. The occurrence of pyrite layers in the lower half of Lithozone II causes a dark grey to blackish sediment colour. Lithozone III (467.5–417.0 cm) consists of faintly millimetre-scale-laminated, light grey lake marl, which contains abundant ostracod valves but only little amorphous organic matter and plant debris. Siliciclastics are also rare, except for one 1.2-cm-thick clay layer at ~463.0 cm and two millimetre-scale silt layers at ~443.0 cm. Above a 5-cm transition, representing the base of Lithozone IV (417.0–282.0 cm), organic matter contents significantly increase while calcite contents gradually decline. In some intervals distinct calcite varves of 0.25–0.5 mm thickness are preserved. These varves consist of a light layer of idiomorphic calcite and a brownish layer composed of organic debris and diatom frustules. Vivianite is enriched in the organic-rich laminae and appears abundantly up to ~380.0 cm. Within the brownish grey, organic-carbonatic sediments of Lithozone IV, one 1.3-cm-thick and one sub-millimetre-scale detrital siliciclastic silt layer are intercalated at about 400.0 cm. Lithozone V (above 282.0 cm) consists of an almost black, homogeneous diatom gyttja rich in plant remains and amorphous organic matter. Endogenic calcite is absent and minerogenic components are very rare.

### *2.4.2 Chronology*

Thirteen AMS $^{14}C$ dates on terrestrial plant macro remains (10 samples of leaf fragments, 3 samples of small pieces of wood) were obtained from the profile (Table 2.2). Calibrated ages of all samples are in stratigraphical order. Owing to its small size (~0.2 mg C), sample KIA34647 gave a large 2σ error range of ca. 700 years and is thus statistically indistinguishable from sample KIA34648, which was taken 1.5 cm above. Two dates were omitted from age modelling owing to probable reworking: (1) sample KIA34642 (351.5–352.0 cm), as it contains wood fragments and appears ca. 200 years too old compared to the neighbouring sample KIA34648 (360.0–360.5 cm); and (2) sample KIA33887 (516.0–517.5 cm), a wood fragment from the clastic high-energy deposits of Lithozone Ia that revealed a ca. 1000 year older age than sample KIA34650, which was obtained only 5 cm above. Consequently, the upper (younger) of these dates (KIA34650) was accepted, although we are aware that reworking cannot also be fully excluded for this wood sample. Therefore, the date must be considered as a maximum age.

**Table 2.2** AMS $^{14}$C dates obtained from terrestrial macrofossils from the Lake Hańcza sediment core. Italicised samples were not considered for the age-depth model (see explanations in the text). Conventional $^{14}$C ages were calibrated using OxCal 4.1 (Ramsey 1995, 2001) and the IntCal04 calibration dataset (Reimer *et al.* 2004).

| Sample / Lab. code | Composite depth (cm) | Dated material | Carbon content (mg) / $\delta^{13}$C (‰) | AMS $^{14}$C age ($^{14}$C a BP±1σ) | Calibrated age (cal. a BP, 2σ range) |
|---|---|---|---|---|---|
| KIA34649 | 239.5–240.0 | leaves[a] | 0.75 / -35.68±0.10 | 3794±44 | 3993–4403 |
| KIA34646 | 334.0–334.5 | leaves[a] | 1.73 / -28.80±0.09 | 4955±29 | 5608–5736 |
| *KIA34642* | *351.5–352.0* | *wood & leaf*[a] | *1.74 / -29.99±0.30* | *5873±36* | *6570–6787* |
| KIA34648 | 360.0–360.5 | leaves[a] | 1.11 / -30.41±0.06 | 6031±44 | 6750–6993 |
| KIA34647 | 361.5–362.0 | leaves[a] | 0.18 / -31.91±0.09 | 5828±149 | 6307–6989 |
| KIA34643 | 372.0–372.5 | leaves[a] | 1.06 / -30.23±0.10 | 6391±40 | 7262–7419 |
| KIA33884 | 378.5–379.0 | leaves[a] | 1.30 / -28.85±0.18 | 6531±35 | 7334–7556 |
| KIA34644 | 383.0–383.5 | leaves[a] | 0.60 / -30.88±0.17 | 6637±66 | 7428–7610 |
| KIA34645 | 386.5–387.0 | leaves[a] | 0.54 / -30.56±0.16 | 7070±68 | 7745–8012 |
| KIA33885 | 415.5–416.0 | leaves[a] | 1.13 / -24.63±0.35 | 8374±53 | 9264–9517 |
| KIA33886 | 434.5–435.0 | leaves[a] | 4.27 / -27.10±0.24 | 9016±35 | 10 162–10 241 |
| KIA34650 | 511.5–512.0 | wood | 4.60 / -25.03±0.13 | 10 922±46 | 12 832–12 937 |
| *KIA33887* | *516.0–517.5* | *wood* | *4.30 / -29.56±0.30* | *12 220±45* | *13 951–14 207* |

[a] undetermined terrestrial leaf fragments

The final core chronology is based on 11 calibrated ages (Table 2.2) and the biostratigraphically determined Younger Dryas-Holocene transition (477.5 cm) as an additional time marker. For the latter, an age of 11 590 varve (calendar) years BP was adopted from published varve chronologies (Brauer *et al.* 1999a). The age-depth model (Fig. 2.3) was developed using Bayesian sequence modelling (*P_Sequence* deposition model; *k*=1), implemented in the OxCal 4.1 program (Ramsey 2008). This approach allows consideration of sedimentological changes and subtraction of detrital layers in Lithozones III and IV, considered as sudden depositional events. The early to mid-Holocene chronology is considered robust, whereas the Lateglacial chronology remains uncertain, as it relies only on one dated wood sample.

As deduced from the age-depth model, the average sedimentation rate for Lithozones II to IV amounts to about 0.2–0.4 mm $a^{-1}$, in accordance with occasionally measured varve thickness. For the organic-rich sediments younger than ca. 4900 cal. a BP, the average sedimentation rate is about twice as high (~0.5–0.7 mm $a^{-1}$) as for the calcite-rich part, probably as a result of lower compaction. According to the age-depth model, major sedimentological changes occur at ca. 11 600 cal. a BP (top of Lithozone Ib, Lateglacial-Holocene transition, 477.5 cm,), ca. 11 250 cal. a BP (top of Lithozone II, 467.5 cm), ca. 9400 cal. a BP (top of Lithozone III, 417.0 cm) and ca. 4650 cal. a BP (top of Lithozone IV, 282.0 cm).

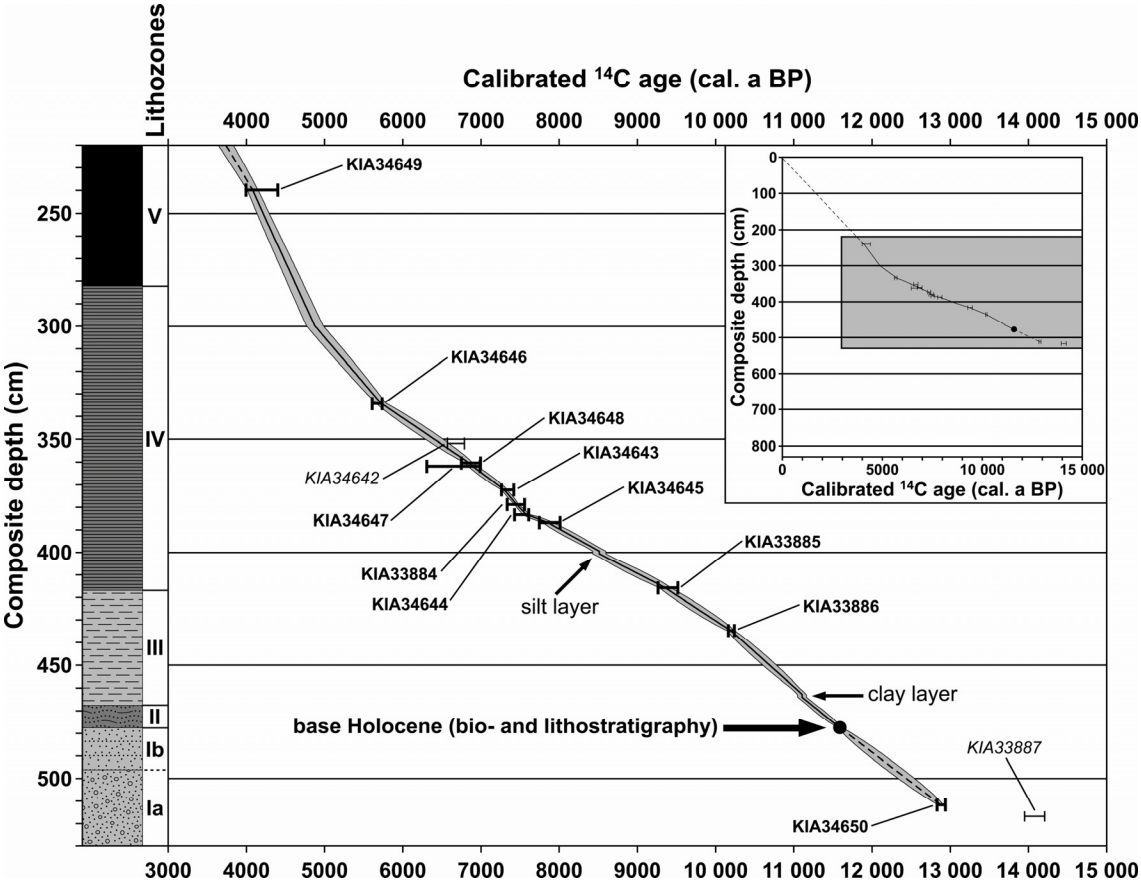


**Figure 2.3** Radiocarbon-derived age-depth model for the investigated sediment sequence from Lake Hańcza with the inset figure illustrating its position within the composite profile. Error bars for individual AMS $^{14}$C dates indicate calibrated 2σ ranges. Italicized samples were omitted from age-depth modelling. The line between individual radiocarbon dates and the Holocene base represents the age-depth model derived from the *P_Sequence* deposition model implemented in the OxCal 4.1 program (Ramsey 2008) with the grey shading representing its 1σ probability range. Dashed lines indicate sections where the chronology is uncertain as a result of probable reworking of the dated material and/or not confirmed by additional dates.

### *2.4.3 Geochemistry*

#### *µ-XRF element scanning*

The siliciclastic-dominated Lateglacial sediments (Lithozone I) exhibit elevated count rates of Si and Al (Fig. 2.4). Ca counts are low except for single spikes in several distinct sand layers, corresponding to the presence of detrital carbonates. The occurrence of pyrite-rich laminae is reflected by elevated S counts. The significant decrease of elements indicating siliciclastic input (Si, Al) at the onset of the Holocene (Lithozone II) is paralleled by a steep rise in Ca counts. Massive calcite precipitation in Lithozone III is reflected by maximum Ca count rates, whereas low counts for Si and Al prove very low allochthonous siliciclastic input. High P counts in Lithozone IV correspond to the abundant occurrence of vivianite. The cessation of calcite precipitation in Lithozone V is reflected by low Ca counts.

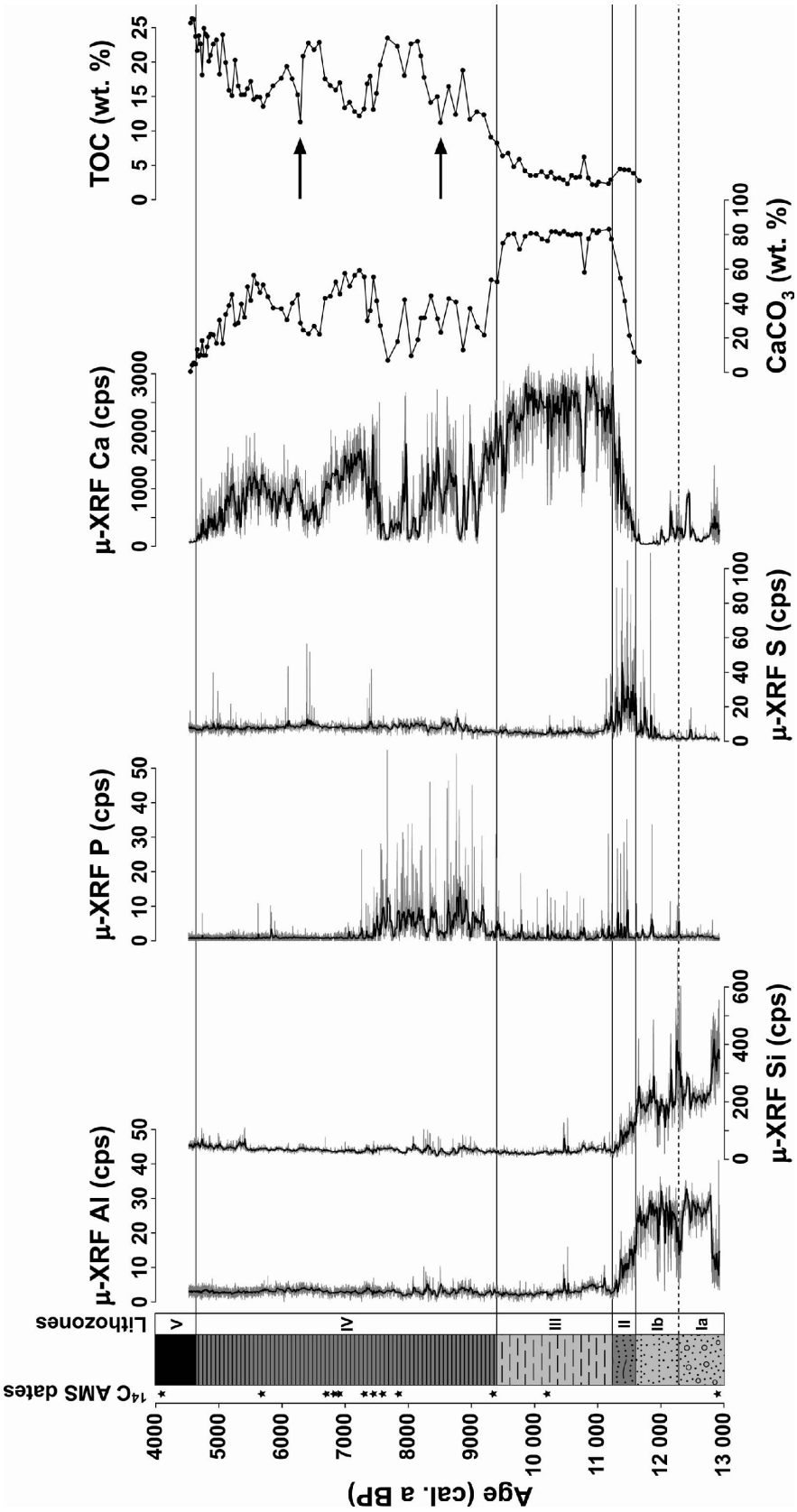


**Figure 2.4** Geochemistry of the Lake Hańcza sediment record as revealed by µ-XRF element scanning and quantitative carbon analyses. Thin grey lines in the µ-XRF data represent measurements with 200-µm resolution, while thick black lines indicate a 25-point running mean. Black arrows indicate the position of two detrital layers in Lithozone IV, affecting sample composition by minerogenic input and thus causing reduced TOC content.

*Carbon geochemistry*

Quantitative geochemical analyses (Fig. 2.4) support microfacies and µ-XRF data. Throughout the Lateglacial (Lithozone I), calcite contents remain below 6%, reflecting the sporadic occurrence of detrital carbonates. Calcite contents rapidly rise to more than 50% in Lithozone II, while TOC remains below 5%. The massive calcite precipitation in Lithozone III is reflected by $CaCO_3$ contents of ~80%. At the same time, TOC increases but still remains below 10%. Lithozone IV is characterized by an increase of TOC to about 15–20% and highly variable calcite contents. Microscopic evidence for high organic matter contents in Lithozone V is confirmed by a TOC rise to more than 25%, while $CaCO_3$ contents decrease to below 5%.

### *2.4.4 Stable isotope ratios*

*Ostracods*

High-resolution records of the stable oxygen ($\delta^{18}O_{ostracods}$) and carbon ($\delta^{13}C_{ostracods}$) isotope compositions of juvenile *Candona neglecta* valves were obtained for the interval from ca. 12 600 to 8200 cal. a BP (Fig. 2.5). Between ca. 12 600 and 10 000 cal. a BP, $\delta^{18}O_{ostracods}$ ranges between about -2.5 and -3.2‰, interrupted by a short negative excursion from ca. 11 400 to 11 200 cal. a BP, while $\delta^{13}C_{ostracods}$ values fluctuate between about -7.5 and -8.5‰. A shift to higher values occurs in both $\delta^{18}O_{ostracods}$ (from about -3.2 to -1.3‰) and $\delta^{13}C_{ostracods}$ (from about -8.3 to -6.7‰) between ca. 10 000 and 9000 cal. a BP. Beyond ca. 9000 cal. a BP, $\delta^{18}O_{ostracods}$ remains on an almost constant level while $\delta^{13}C_{ostracods}$ values vary between about -7.7‰ and -6.6‰.

*Bulk sediment samples*

Prior to 11 600 cal. a BP (Lithozone I), carbonates are predominantly detrital and thus do not reflect a climatic signal. Therefore, stable oxygen ($\delta^{18}O_{calcite}$) and carbon ($\delta^{13}C_{calcite}$) isotope ratios of bulk samples were measured only for the early to mid-Holocene time interval, exhibiting a pattern generally similar to the records obtained from ostracods (Fig. 2.5). From ca. 11 600 to 10 000 cal. a BP, $\delta^{18}O_{calcite}$ varies between about -8.7 and -8.1‰, while $\delta^{13}C_{calcite}$ values range between about -4.9 and -4.1‰. Between ca. 10 000 and 9000 cal. a BP, $\delta^{18}O_{calcite}$ values increase from about -8.7 to -7.0‰, while $\delta^{13}C_{calcite}$ rises from about -4.5 to -3.4‰. After reaching maximum values around 9000 cal. a BP, $\delta^{18}O_{calcite}$ decreases slightly by about 0.5‰, while $\delta^{13}C_{calcite}$ remains on an elevated level (around -3.5‰).

Calculation of calcification temperatures for endogenic calcite from the $\delta^{18}O_{ostracods}$ and $\delta^{18}O_{calcite}$ values using a temperature-dependent fractionation between water and calcite of -0.23‰ $°C^{-1}$ (Eicher

& Siegenthaler 1976), a vital offset of +2.2‰ for *Candona neglecta* (von Grafenstein *et al.* 1999b) and nearly constant calcification temperatures of ~4°C in the hypolimnion (von Grafenstein 2002) yields reasonable estimates (Fig. 2.5). The values vary between ~17 and 20°C during the early Holocene and apparently show a distinct short-term variability within the endogenic calcite-dominated Lithozone III but more stable values in Lithozone IV, which is characterized by lower calcite contents.

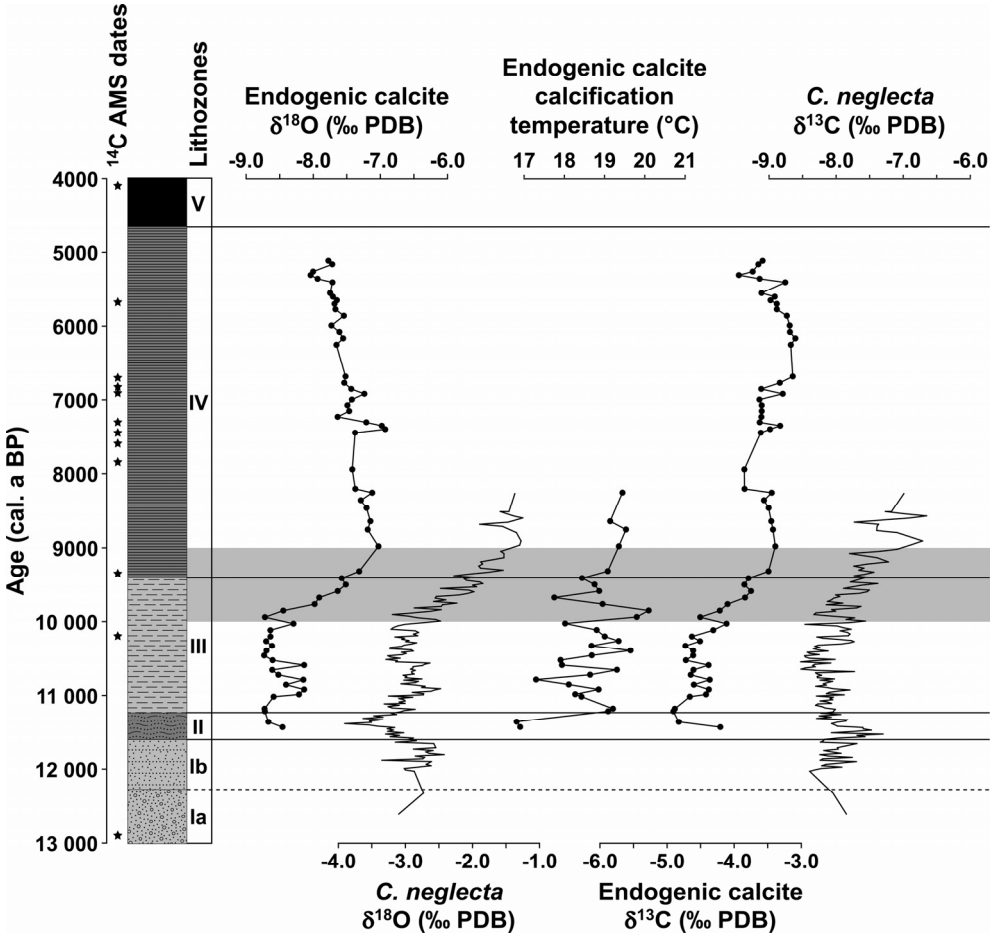


**Figure 2.5** Stable oxygen and carbon isotope ratios derived from juvenile *Candona neglecta* valves and bulk sediment endogenic calcite from Lake Hańcza. $\delta^{18}O$ values obtained from ostracods are not corrected for the species-specific vital offset. The grey shading indicates the period between 10 000 and 9000 cal. a BP, characterized by a prominent isotopic shift. The calcification temperature for endogenic calcite was calculated using the equation: $T_{calcite} = (\delta^{18}O_{ostracods}$ - vital offset - $\delta^{18}O_{calcite}) / (d\alpha/dT) + T_{hypo}$, with a vital offset of +2.2‰ for *C. neglecta* (von Grafenstein *et al.* 1999b), a temperature-dependent fractionation between water and calcite $d\alpha/dT$ of 0.23‰ $°C^{-1}$ (Eicher & Siegenthaler 1976) and a mean annual hypolimnetic water temperature $T_{hypo}$ of 4°C.

## *2.4.5 Pollen*

The pollen diagram reveals a succession of nine local pollen assemblage zones (LPAZ; Fig. 2.6), in accordance with the pattern of vegetation development for northeastern Poland (Ralska-Jasiewiczowa & Latałowa 1996; Ralska-Jasiewiczowa *et al.* 2004).

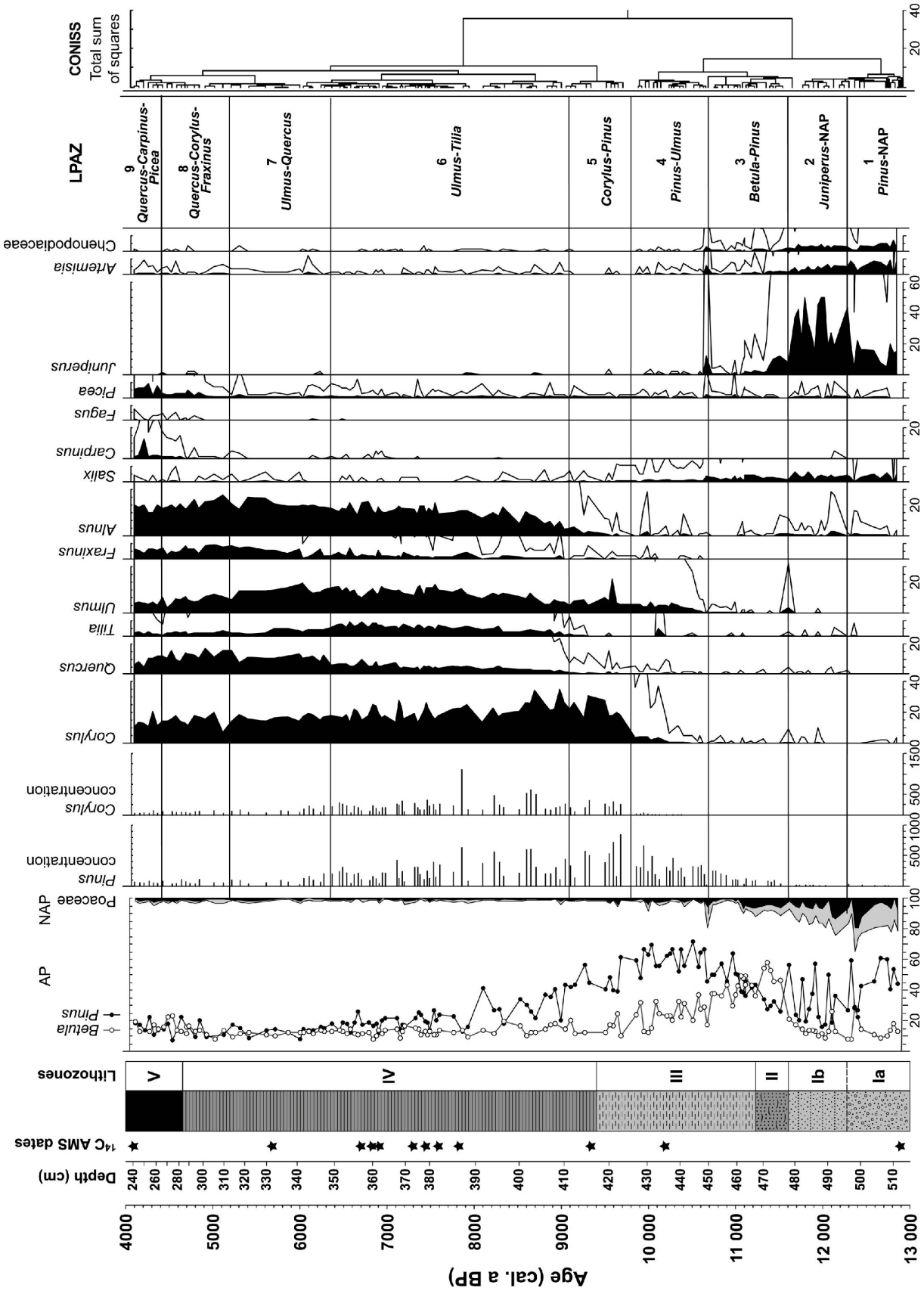


**Figure 2.6** Pollen percentage diagram for Lake Hańcza for the most important taxa discussed in the text. Pollen concentrations for *Pinus* and *Corylus* are given as pollen grains per cubic centimetre dry sediment. The outline curves represent a 10× exaggeration.

Despite the low pollen concentrations for LPAZ 1 and LPAZ 2, a shift in taxa with an increase of *Juniperus* (up to 50%) at the expense of *Pinus* and *Betula* occurs at the transition between theses zones. The upper limit of LPAZ 2, marked by the sharp decline of *Juniperus* and the simultaneous expansion of *Betula* (from <20% to >45%), defines the Lateglacial-Holocene transition. LPAZ 3 (ca. 11 600–10 700 cal. a BP) is characterized by the development of early Holocene pioneer *Betula-Pinus* forests (together up to 95%). At the same time, *Juniperus* almost disappears. The slow spread of deciduous trees starts in LPAZ 4 (ca. 10 700–9800 cal. a BP) with *Ulmus* and the subsequent establishment of *Corylus*. LPAZ 5 (ca. 9800–9100 cal. a BP) is characterized by the rapid spread of *Corylus* (up to 25–30%) as a first dominant mediocratic component and reflects the progressive afforestation at the Boreal-Atlantic transition. This coincides with a vegetation change in wet areas, where *Alnus* mainly replaces *Salix*. LPAZ 6 (ca. 9100–6350 cal. a BP) shows the further development of mixed deciduous forests with *Ulmus* (around 15%), *Quercus* (up to 5%), *Tilia* (5–10%), *Fraxinus* and *Corylus*. Deciduous trees dominate throughout LPAZ 7 (ca. 6350–5200 cal. a BP), whose upper boundary is defined by the *Ulmus* decline. LPAZ 8 (ca. 5200–4400 cal. a BP) is characterized by the decreasing abundance of *Ulmus* and *Tilia*, the spread of *Picea* and the first appearance of *Carpinus*. The main features of LPAZ 9 (younger than ca. 4400 cal. a BP) are, besides the still high abundance of *Quercus* and *Corylus*, increasing values for *Carpinus* and *Picea* (up to 5%) and the sporadic occurrence of *Fagus*, a species not present in recent forest communities in northeastern Poland (Ralska-Jasiewiczowa 1983).

### *2.4.6 Ostracods*

Sediments of the studied interval yielded valves of 17 ostracod species, of which six (Fig. 2.7) represent the autochthonous profundal fossil assemblage: *Candona candida*, *Candona neglecta*, *Fabaeformiscandona protzi*, *Cytherissa lacustris*, *Limnocytherina sanctipatricii* and *Leucocythere mirabilis* (the latter two considered as one taxon, Limnocytherinae). Valves of the other species were most probably subjected to post-mortem transport from shallow-water deposits and are thus discussed further as one group of littoral species. During the Lateglacial, ostracod abundance is relatively low. *C. candida*, *C. neglecta* and *C. lacustris* dominate the assemblage. The gradual disappearance of *C. lacustris* at the Lateglacial-Holocene transition marks a significant shift in the record. Parallel to the massive calcite precipitation in Lithozone III, total ostracod abundance increases to a maximum, with Candoninae and Limnocytherinae dominating the assemblage. Lower calcite contents in Lithozone IV are accompanied by decreasing preservation of ostracod valves, which are gradually replaced by diatom frustules subsequent to ca. 7700 cal. a BP. Within the low-calcite environment, *C. candida* and *C. neglecta* gradually disappear, while *F. protzi* and littoral species become more abundant. After about 4900 cal. a BP, no ostracods are preserved in the sediments.

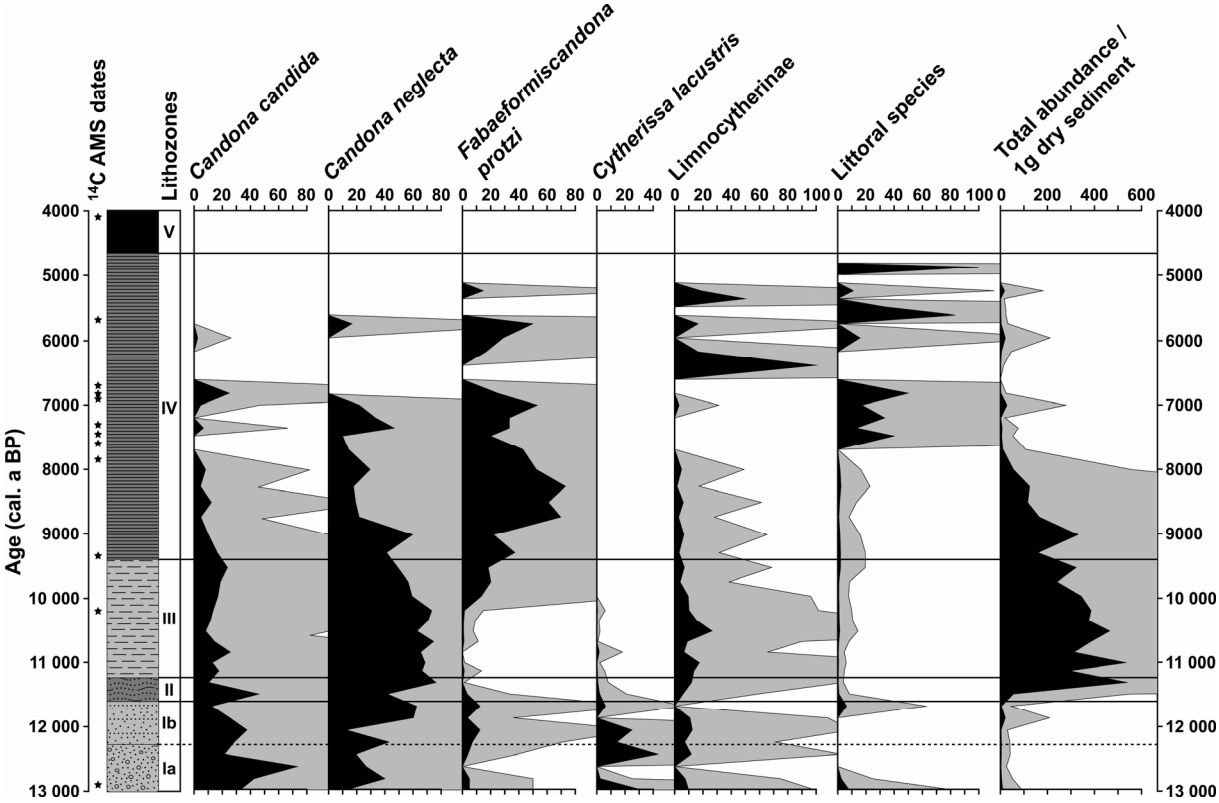


**Figure 2.7** Relative abundance of the most important ostracod species and total number of ostracod valves per gram dry sediment in the Lake Hańcza sediment record. Dark grey outline curves represent a 10× exaggeration. Beyond ca. 7700 cal. a BP and prior to ca. 11 600 cal. a BP, relative abundance changes might not be representative owing to the low number of ostracods.

## 2.5 Discussion

### *2.5.1 Lateglacial sedimentation*

The uncertain chronology and the depositional environment of the clastic-detrital basal sediments impede a climatic interpretation of the Lateglacial record. Sand- and gravel-dominated sediments that characterize the high-energy facies of Lithozone Ia suggest deposition by glaciofluvial processes during initial basin infill. These sediments were possibly deposited either subglacially in the channel or supraglacially with subsequent redeposition at the lake bottom after the melting of dead ice. The transition to a finer-grained, low-energy facies (Lithozone Ib) marks the onset of pelagic sedimentation, even if this was still detrital-dominated. The maximum age estimate of ca. 12 900 cal. a BP for this depositional shift suggests that dead ice probably remained in the Lake Hańcza basin until the Allerød, confirming results from the nearby Szeszupa depression (Ehlers *et al.* 1995) and other sites in northern Poland (Błaszkiewicz 2002).

Long preservation of stagnant ice was favoured by the great depth of the basin, persistent deep permafrost and a low terrestrial heat flow density of only ~40 mW $m^{-2}$ in the region (ca. 30–40% less than in other parts of northern Poland; Šafanda *et al.* 2004). A basal peat layer as an initial stage of organic sedimentation (Błaszkiewicz 2002) is not developed in Lake Hańcza.

### *2.5.2 Early Holocene environmental and climatic evolution*

Warming at the onset of the Holocene led to the initiation of biochemical calcite precipitation owing to increased lake productivity (Brauer & Casanova 2001). Rising temperatures further caused a stable water stratification, leading to anoxic conditions in the bottom waters as indicated by abundant iron sulphides (cf. Odegaard *et al.* 2003) and the small number of ostracod valves. In particular, the disappearance of *Cytherissa lacustris*, a poly-oxyphilic, inbenthic ostracod species that avoids sulphidic and organic sediments (Danielopol *et al.* 1990; Geiger 1993), corroborates this change in the deep-water habitat. The observed decline of shrub vegetation and the spread of *Betula* at the Lateglacial-Holocene boundary are in agreement with other pollen records from this region (Ralska-Jasiewiczowa *et al.* 2003; Kupryjanowicz 2007; Stančikaitė *et al.* 2008) and resulted in a gradual stabilization of catchment soils so that detrital sediment flux into the lake basin gradually decreased. The persistent occurrence of *Juniperus* and Chenopodiaceae indicates, however, that woodlands were still open during the early Holocene (Ralska-Jasiewiczowa *et al.* 2004), leading to this more gradual environmental response compared to sites more to the west/south in Germany and in central Poland (Brauer *et al.* 1999a; Merkt & Müller 1999; Ralska-Jasiewiczowa *et al.* 2003). A short-term drop of ~0.8‰ in the $\delta^{18}O_{ostracods}$ record between ca. 11 400 and 11 200 cal. a BP correlates with the lowest calculated calcification temperatures for endogenic calcite (Fig. 2.5) and probably reflects climatic deterioration during the Preboreal Oscillation (Björck *et al.* 1996; Björck *et al.* 1997; von Grafenstein *et al.* 1999a).

Predominant endogenic calcite formation between 11 250 and 9400 cal. a BP is a clear indication for high lake productivity in response to increased temperatures (Brunskill 1969; Kelts & Hsü 1978). During this period, detrital input almost ceased owing to the continuation of catchment stabilization by the spread of pioneer *Betula-Pinus* forests. However, three detrital layers indicate occasional extreme surface runoff events. In agreement with the migration pattern of vegetation reconstructed for Poland (Ralska-Jasiewiczowa *et al.* 2004), deciduous trees and particularly *Ulmus* and *Corylus* started to expand at ca. 10 600 and 10 200 cal. a BP, respectively. The establishment of *Corylus*, which is tolerant of seasonal drought, severe winters and relatively cool summers (Huntley 1993), prior to other deciduous trees, such as, for example, *Quercus*, suggests pronounced continental climatic conditions during this interval.

Between 10 000 and 9000 cal. a BP, a ~1.7‰ rise in both $\delta^{18}O_{calcite}$ and $\delta^{18}O_{ostracods}$ marks a further distinct step of climatic amelioration. A bias of the $\delta^{18}O_{calcite}$ record through isotopically enriched detrital carbonates from the catchment (Leng & Marshall 2004) is excluded, as microfacies analysis proved the endogenic origin of the measured calcite (cf. Mangili *et al.* 2010a). Furthermore, effects of the epilimnetic water temperature during calcite precipitation on the $\delta^{18}O_{calcite}$ record can be ruled out because of the parallel course of the $\delta^{18}O_{ostracods}$ record, which is independent of seasonal changes in surface water temperature (von Grafenstein 2002). Therefore, it is assumed that both $\delta^{18}O_{calcite}$ and $\delta^{18}O_{ostracods}$ reflect the average isotopic composition of the lake water, which in turn is controlled by the isotopic composition of precipitation ($\delta^{18}O_P$) and the lake water balance, i.e. the evaporation/inflow ratio (cf. von Grafenstein 2002). $\delta^{18}O_P$ is a function mainly of climatic factors, including air temperature (Dansgaard 1964; Siegenthaler & Eicher 1986; Różański *et al.* 1992), seasonality of precipitation (Drummond *et al.* 1995) and atmospheric circulation, causing moisture source changes (Yu *et al.* 1997; Hammarlund *et al.* 2002). In contrast, the lake water balance is only in part directly related to climate. Whereas evaporation is linked to summer temperatures, the amount of inflow is subject to complex catchment processes and is influenced by hydrological and vegetational changes (Seppä *et al.* 2005). In consequence, the observed $\delta^{18}O$ rise of about 1.7‰ between 10 000 and 9000 cal. a BP can be attributed to both climatic and environmental changes. On the one hand, a combination of rising temperatures, a shift in rainfall seasonality towards a dominance of isotopically heavier summer precipitation and a change in atmospheric circulation, leading to increased transport of Atlantic air masses, is assumed to have contributed to the observed shift in the Lake Hańcza $\delta^{18}O$ record. On the other hand, changes in the evaporation/inflow ratio probably also contributed to the isotopic enrichment of the lake water, as inferred from the present-day evaporation/inflow ratio of 0.14 (Bajkiewicz-Grabowska 2008). This is confirmed by a $\delta^{18}O$ enrichment of modern lake water of about 2.0–2.5‰ compared to the isotopic composition of the inflowing water and long-term precipitation (Table 2.1; Fig. 2.8), indicating the high sensitivity of the lake to evaporation and changes in catchment hydrology with respect to the oxygen isotope composition of the lake water (cf. von Grafenstein *et al.* 2000; von Grafenstein 2002). Between 10 000 and 9000 cal. a BP, the isotopic composition of the lake water was, in addition to evaporation from the lake surface, probably also influenced by changes in catchment hydrology owing to vegetation changes. The densification of vegetation cover should have resulted in higher evapotranspiration and thus in reduced discharge from the drainage basin into the lake (cf. Rosenmeier *et al.* 2002). An assumed 30% reduction of catchment runoff resulting from the establishment of dense deciduous forests would be sufficient to explain about half of the measured rise in $\delta^{18}O_{calcite}$ and $\delta^{18}O_{ostracods}$.

Because all the discussed effects would shift the oxygen isotope record in the same direction, namely towards more positive $\delta^{18}O$ values, it is difficult to quantitatively distinguish between them. However, it must be assumed that climatic factors and the vegetation development have both contributed to the observed rise in the $\delta^{18}O$ record of Lake Hańcza between 10 000 and 9000 cal. a BP.

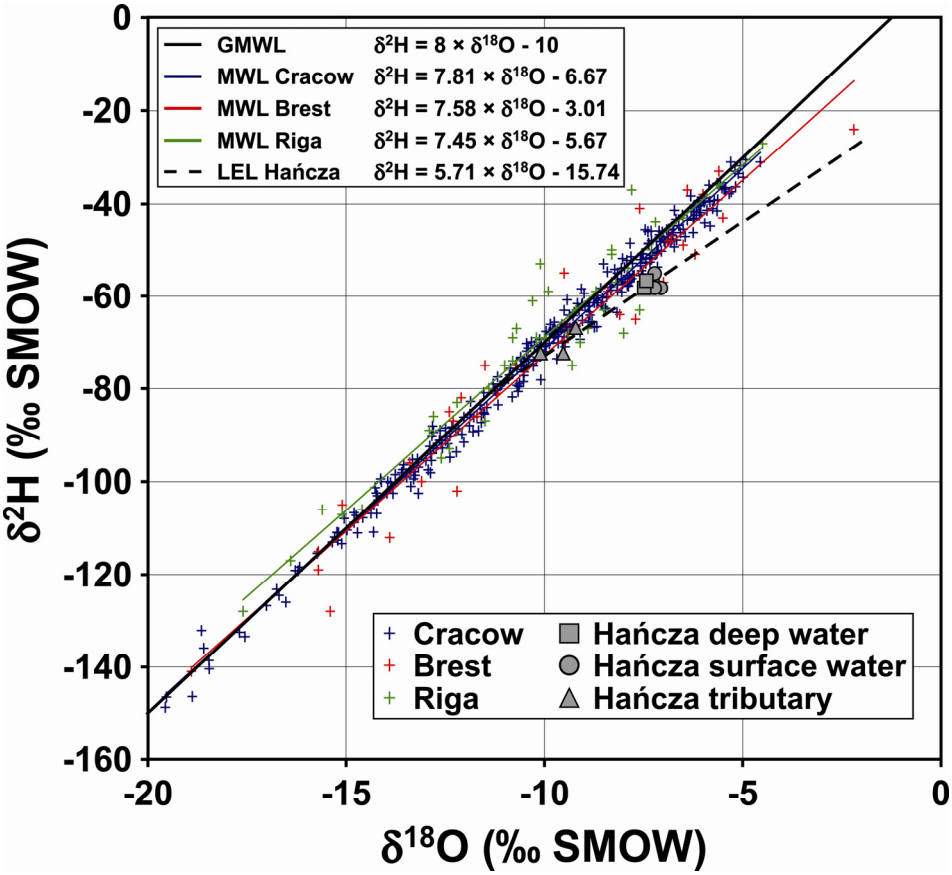


**Figure 2.8** Plot of $\delta^{18}O$ and $\delta^{2}H$ of long-term precipitation at the stations Cracow, Brest and Riga (IAEA/WMO 2006), the respective local meteoric water lines (MWL), and water samples from Lake Hańcza and its tributary (Table 1) with respect to the global meteoric water line (GMWL, Craig 1961). Water samples from Lake Hańcza plot on a local evaporation line (LEL), indicating evaporative enrichment of the lake water relative to regional long-term precipitation.

### *2.5.3 Palaeoclimatic implications*

So far, evidence for an early Holocene $\delta^{18}O$ rise in the southeastern Baltic region, as observed in the well-dated high-resolution record from Lake Hańcza, is scarce, as most of the published regional oxygen isotope records focus mainly on the Lateglacial (Goslar *et al.* 1993; Goslar *et al.* 1999; Hammarlund *et al.* 1999; Piotrowska *et al.* 2008; Apolinarska & Hammarlund 2009). However, a similar $\delta^{18}O$ increase has been observed in endogenic carbonates from Lake Strażym (Fig. 2.9) and Lake Mikołajki, about 100 and 250 km west of Lake Hańcza (Różański *et al.* 1988), and in southern Sweden (Hammarlund *et al.* 2003), pointing to the regional significance of this signal. Although vegetation evolution might also have influenced the $\delta^{18}O$ rise in the Lake Hańcza sediments, it is assumed that the record reflects the persistence of cool and more continental climate conditions in northeastern Poland prior to ca. 10 000 cal. a BP. The Lake Hańcza data therefore provide further evidence for earlier hypotheses of a special regional pattern of climatic evolution around the eastern Baltic, characterized by a delayed and attenuated warming during the first one and a half millennia of the Holocene (Subetto *et al.* 2002; Wohlfarth *et al.* 2002; Wohlfarth *et al.* 2007).

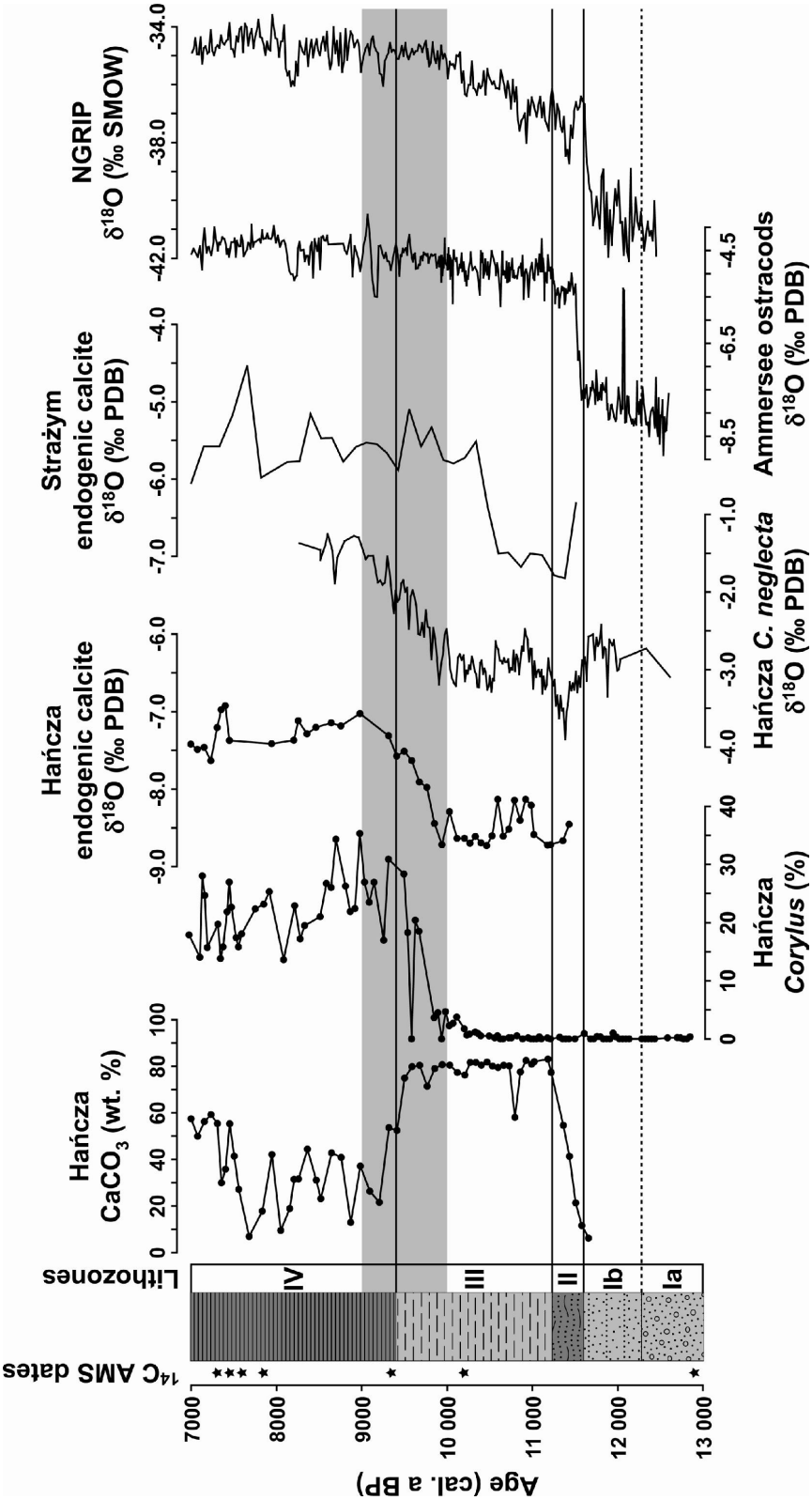


**Figure 2.9** Comparison of Lake Hańcza proxy data ($CaCO_3$ content, *Corylus* pollen, $\delta^{18}O$ of endogenic calcite and juvenile *Candona neglecta* valves) with oxygen isotope records from Lake Strażym (modified after Różański *et al.* (1988)), Lake Ammersee (von Grafenstein *et al.* 1999a) and the NGRIP ice core (GICC05 chronology, NGRIP Members 2004; Rasmussen *et al.* 2006; Vinther *et al.* 2006). All records are plotted on their individual time scales. The grey shading marks the period between 10 000 and 9000 cal. a BP, characterized by shifts in various proxies in the Lake Hańcza record, which probably reflect climatic amelioration.

This climatic scenario is attributed to the proximity of the remaining Scandinavian Ice Sheet, only ~600 km north of Lake Hańcza at the onset of the Holocene (Andersen *et al.* 1995; Mangerud 2004), which triggered a regional atmospheric circulation pattern in agreement with model runs (Kutzbach *et al.* 1993; Webb III *et al.* 1993). The persistence of a stable high-pressure cell above northern Europe, favoured by the ice sheet and probably amplified by the cold surface waters of the Baltic (Wohlfarth *et al.* 2007), resulted in an anticyclonic circulation (Yu & Harrison 1995; Harrison *et al.* 1996) with prevailing easterly winds (Fig. 2.10A). These probably transported $^{18}O$-depleted precipitation from the Barents Sea, which was ice-free since approximately 15 000 cal. a BP (Polyak *et al.* 1995), to the Lake Hańcza region and weakened the influence of Westerlies. Only after the final decay of the ice sheet between 10 000 and 9500 cal. a BP (Lundqvist & Mejdahl 1995), a more zonal circulation pattern was established in eastern Poland, associated with an increased influence of warm and moist air brought by the Westerlies from the Atlantic (Fig. 2.10B; Yu & Harrison 1995).

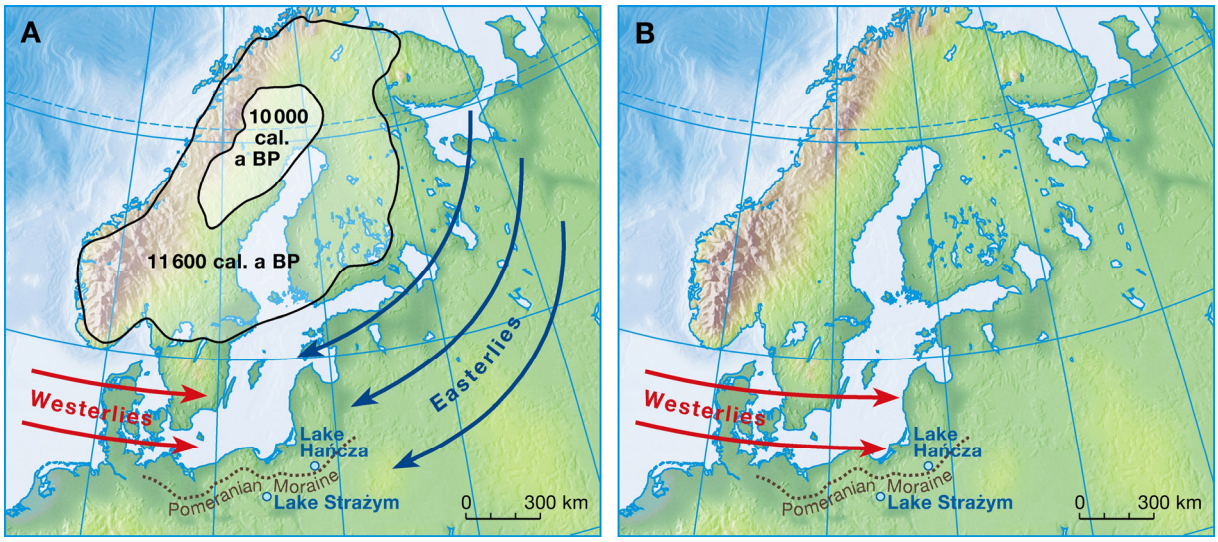


**Figure 2.10** Shifting early Holocene atmospheric circulation pattern in the southeastern Baltic inferred from Lake Hańcza proxy data. The Younger Dryas margin of the Scandinavian Ice Sheet is drawn according to Lundqvist & Wohlfarth (2001), Saarnisto & Saarinen (2001) and Mangerud (2004). The ice recession line for 10 000 cal. a BP corresponds to Lundqvist (1986). (A) Prior to ca. 10 000 cal. a BP, the easterly flow generated by the high-pressure cell above the remaining Scandinavian Ice Sheet brought cold and dry air from the northeast, thus preventing the advance of warm Westerlies into the Lake Hańcza region. (B) With the final decay of the Scandinavian Ice Sheet between 10 000 and 9500 cal. a BP (Lundqvist & Mejdahl 1995), the influence of easterly winds disappeared and warm and moist air brought by Westerlies reached the Lake Hańcza region.

A comparison of the Lake Hańcza data with the high-resolution oxygen isotope records from Lake Ammersee (southern Germany) and the Greenland ice cores (Fig. 2.9) underlines the particular regional pattern of climate evolution in the southeastern Baltic. While temperatures in southern Germany reached a plateau-like level immediately after the Preboreal Oscillation at about 11 200 cal. a BP (von Grafenstein *et al.* 1999a), Greenland temperatures gradually rose over ca. 2000 years until

they reached the early to mid-Holocene plateau (Rasmussen *et al.* 2006; Vinther *et al.* 2006). Although the end of the increasing temperature trend in Greenland coincides with the observed shift in Lake Hańcza, none of the mentioned records exhibits a comparable step-like $\delta^{18}O$ shift between 10 000 and 9000 cal. a BP. These differences in the early Holocene evolution of the records are thought to be related to the marked influence of the retreating Scandinavian Ice Sheet on atmospheric circulation in the Lake Hańcza region.

## 2.6 Conclusions

The well-dated sediment record of Lake Hańcza provides the first high-resolution early to mid-Holocene $\delta^{18}O$ and $\delta^{13}C$ records from endogenic calcite and ostracods for northeastern Poland, and, in combination with other proxy data, sheds light on the regional climatic and environmental evolution during the first half of the Holocene. The late Holocene and Lateglacial time intervals had to be excluded from detailed climatic interpretation because no suitable climate proxies could be derived from these sections of the sediment profile.

Endogenic calcite formation as an indication of a biologically productive lake started at the onset of the Holocene at about 11 600 cal. a BP. The lake-internal response to climatic amelioration was accompanied by the establishment of early boreal forests in the surroundings of the lake. The first ca. 350 years of the Holocene are characterized by gradually spreading woodlands and related soil stabilization, causing a decreasing trend in surface runoff and thus detrital matter flux. This interval of gradual environmental adjustment to improving climate conditions was interrupted by the Preboreal Oscillation, a ca. 200-year cool phase reflected by a 0.8 ‰ drop in $\delta^{18}O$.

A second major interval of climatic and environmental amelioration is observed between 10 000 and 9000 cal. a BP. This is reflected by a 1.7‰ rise in the $\delta^{18}O$ of ostracod valves and endogenic calcite, coincident with the spread of deciduous tree forests and likely reflecting rising temperatures and increased summer rainfall/moisture supply as a result of atmospheric circulation changes in the eastern Baltic. A comparable shift does not appear in high-resolution stable oxygen isotope records from southern Germany and Greenland and thus probably represents a regional delay in the response to early Holocene climatic improvement. This interpretation confirms earlier results from other lake records around the eastern Baltic.

## 2.7 Acknowledgements

This study has been funded by DFG (Germany, project no. BR2208/2-2, AN554/1-2), FWF (Austria, project no. I35-B06) and CNRS (France) under the European Science Foundation (ESF) EUROCORES Programme EuroCLIMATE (contract No. ERAS-CT-2003-980409 of the European Commission, DG Research, FP6, ESF project DecLakes no. 04-ECLIM-FP29). We thank Christopher

Bronk Ramsey (University of Oxford) for advice on using OxCal, Rudolf Naumann (GFZ Potsdam) for providing XRD measurements, Katarzyna Zamelczyk (University of Tromsø) for carbon geochemistry and bulk sediment stable isotope measurements, Andreas Hendrich (GFZ Potsdam) for drawing some figures, the coring/field lab crew and Lucyna Namiotko for help during the coring campaign, the laboratory staff at the contributing institutes for their assistance in the preparation of numerous samples, Anna and Tadeusz Słowikowscy (Błaskowizna at Lake Hańcza) for their exceptional hospitality and great help in organising the field lab, Teresa Świerubska (Suwałki Landscape Park) for her advice in the field, and Benjamin Gaede (University of Potsdam) for checking the language. We acknowledge the valuable comments of two anonymous reviewers and editorial remarks by Jan A. Piotrowski on an earlier version that helped us to improve this paper.

# 3 Environmental responses to Lateglacial climatic fluctuations recorded in the sediments of pre-Alpine Lake Mondsee (northeastern Alps)

Stefan Lauterbach[1], Achim Brauer[1], Nils Andersen[2], Dan L. Danielopol[3], Peter Dulski[1], Matthias Hüls[2], Krystyna Milecka[4], Tadeusz Namiotko[5], Milena Obremska[4], Ulrich von Grafenstein[6] and DecLakes participants[7]

[1] GFZ German Research Centre for Geosciences, Section 5.2 – Climate Dynamics and Landscape Evolution, D-14473 Potsdam, Germany

[2] Christian-Albrechts-University, Leibniz Laboratory for Radiometric Dating and Stable Isotope Research, D-24118 Kiel, Germany

[3] Austrian Academy of Sciences, Institute for Limnology, A-5310 Mondsee, Austria; present address: Austrian Academy of Sciences, Commission for the Stratigraphical & Palaeontological Research of Austria, c/o Institute of Earth Sciences, Geology and Palaeontology, University of Graz, A-8010 Graz, Austria

[4] Adam Mickiewicz University, Faculty of Geographical and Geological Science, Department of Biogeography and Palaeoecology, PL-61-680 Poznań, Poland

[5] University of Gdańsk, Department of Genetics, Laboratory of Limnozoology, PL-80-822 Gdańsk, Poland

[6] Laboratoire des Sciences du Climat et de l'Environnement, UMR CEA-CNRS, F-91191 Gif-sur-Yvette, France

[7] Soumaya Belmecheri (LSCE, Gif-sur-Yvette), Marc Desmet (ISTO, Tours), Helmut Erlenkeuser (Leibniz Laboratory, Kiel), Bernard Fanget (EDYTEM, Chambery), Jérôme Nomade (LGCA, Grenoble)

**published in *Journal of Quaternary Science* (in press, DOI: 10.1002/jqs.1448)**

***ABSTRACT*** *Investigation of the sedimentary record of pre-Alpine Lake Mondsee (Upper Austria) focused on the environmental reaction to rapid Lateglacial climatic changes. Results of this study reveal complex proxy responses that are variable in time and influenced by the long-term evolution of the lake and its catchment. A new field sampling approach facilitated continuous and precisely controlled parallel sampling at decadal to sub-annual resolution for µ-XRF element scanning, carbon geochemistry, stable isotope measurements on ostracods, pollen analyses and large-scale thin sections for microfacies analysis. The Holocene chronology is established through microscopic varve counting and supported by accelerator mass spectrometry (AMS) $^{14}C$ dating of terrestrial plant macrofossils, whereas the Lateglacial age model is based on $\delta^{18}O$ wiggle matching with the Greenland NGRIP record, using the GICC05 chronology. Microfacies analysis enables the detection of subtle sedimentological changes, proving that depositional processes even in rather large lake systems are highly sensitive to climate forcing. Comparing periods of major warming at the onset of the Lateglacial and Holocene and of major cooling at the onset of the Younger Dryas reveals differences in proxy responses, reflecting threshold effects and ecosystem inertia. Temperature increase, vegetation recovery, decrease of detrital flux and intensification of biochemical calcite precipitation at the onset of the Holocene took place with only decadal leads and lags over a ca. 100-year-period,*

*whereas the spread of woodlands and the reduction of detrital flux lagged the warming at the onset of the Lateglacial Interstadial by ca. 500–750 years. Cooling at the onset of the Younger Dryas is reflected by the simultaneous reaction of $\delta^{18}O$ and vegetation, but sedimentological changes (reduction of endogenic calcite content, increase in detrital flux) were delayed by about 150–300 years. Three short-term Lateglacial cold intervals, corresponding to Greenland isotope substages GI-1d, GI-1c2 and GI-1b, also show complex proxy responses that vary in time.*

## 3.1 Introduction

Rapid climatic changes across the Last Glacial-Holocene transition are documented in the Greenland ice cores (e.g. Johnsen *et al.* 1992; Rasmussen *et al.* 2006) and various lacustrine (e.g. von Grafenstein *et al.* 1999a; Birks & Ammann 2000; Brauer *et al.* 2000; Litt *et al.* 2001; Marshall *et al.* 2002; Magny *et al.* 2006; Yu 2007; Brauer *et al.* 2008) and marine (e.g. Haflidason *et al.* 1995; Hughen *et al.* 2000) palaeoclimate archives in the North Atlantic realm. Improved understanding of the regional environmental impact of these climatic changes is a prerequisite for assessing the effects of future climate variability on ecosystems and the dynamics of these processes. Within this context, continental archives are ideal to associate climatic changes directly with the environmental response in the human habitat. Previous studies on lacustrine records from the climate-sensitive region of the European Alps added a wealth of information on Lateglacial climate fluctuations (e.g. von Grafenstein *et al.* 1999a; Schwander *et al.* 2000) and their impact on terrestrial and aquatic ecosystems (e.g. Eicher & Siegenthaler 1976; Eicher *et al.* 1981; Ammann & Lotter 1989; Schmidt *et al.* 1998; Lotter 1999; Lotter *et al.* 2000; Heiri & Millet 2005; Finsinger *et al.* 2008) and depositional processes (e.g. Moscariello *et al.* 1998; Brauer & Casanova 2001). While high-resolution studies have shown that particularly small lake systems record even low-amplitude climatic changes and related environmental responses (e.g. Lotter *et al.* 1992; Litt & Stebich 1999; Ammann *et al.* 2000; Brauer *et al.* 2000), less is known about the climate sensitivity of lakes with a comparatively large catchment area. Hence, detailed investigation of the sedimentary record of pre-Alpine Lake Mondsee (Upper Austria) can aid our understanding of the impact of rapid Lateglacial climate fluctuations on the local ecosystem and the climate sensitivity of sedimentological processes in a rather large lake system. It furthermore provides new information on the regional climate development in the northeastern Alps and thus on the climatic differentiation in Europe during the Late- and Postglacial.

This study, associated with the European Science Foundation EuroCLIMATE project DecLakes (*Decadal Holocene and Lateglacial variability of the oxygen isotopic composition in precipitation over Europe reconstructed from deep-lake sediments*), presents detailed sediment microfacies data combined with high-resolution multi-proxy analyses obtained on a new Lateglacial to Holocene sediment core from Lake Mondsee, northeastern Alps, Austria.

Particular care was taken on the parallel sampling for all analyses, enabling direct comparison of various proxy data and detailed microscopic inspection of each individual sample interval. The main purpose of this paper is the detailed investigation of the variable proxy responses to rapid Lateglacial climatic fluctuations. Forthcoming publications will address in detail the ostracod assemblage succession and the interpretation of the stable isotope record in order to shed light on the complex relationships between air temperature, $\delta^{18}O$ in precipitation, $\delta^{18}O$ in lake water, water temperature and resulting $\delta^{18}O$ in ostracod valves.

## 3.2 Study site

Pre-Alpine Lake Mondsee is situated at the northern margin of the European Alps (47°49'N, 13°24'E, 481 m above sea level (a.s.l.)) in the Salzkammergut lake district of Upper Austria, about 40 km east of Salzburg (Fig. 3.1). The oligo-mesotrophic hardwater lake (maximum water depth ~68 m, surface area ~14.2 km², volume ~5.1 km³) can be subdivided into a shallow northern and a deeper southern basin (Jagsch & Megay 1982). Three major tributaries (Fuschler Ache, Zeller Ache and Wangauer Ache) and several minor streams discharge into the lake, which drains via the small river Seeache into Lake Attersee.

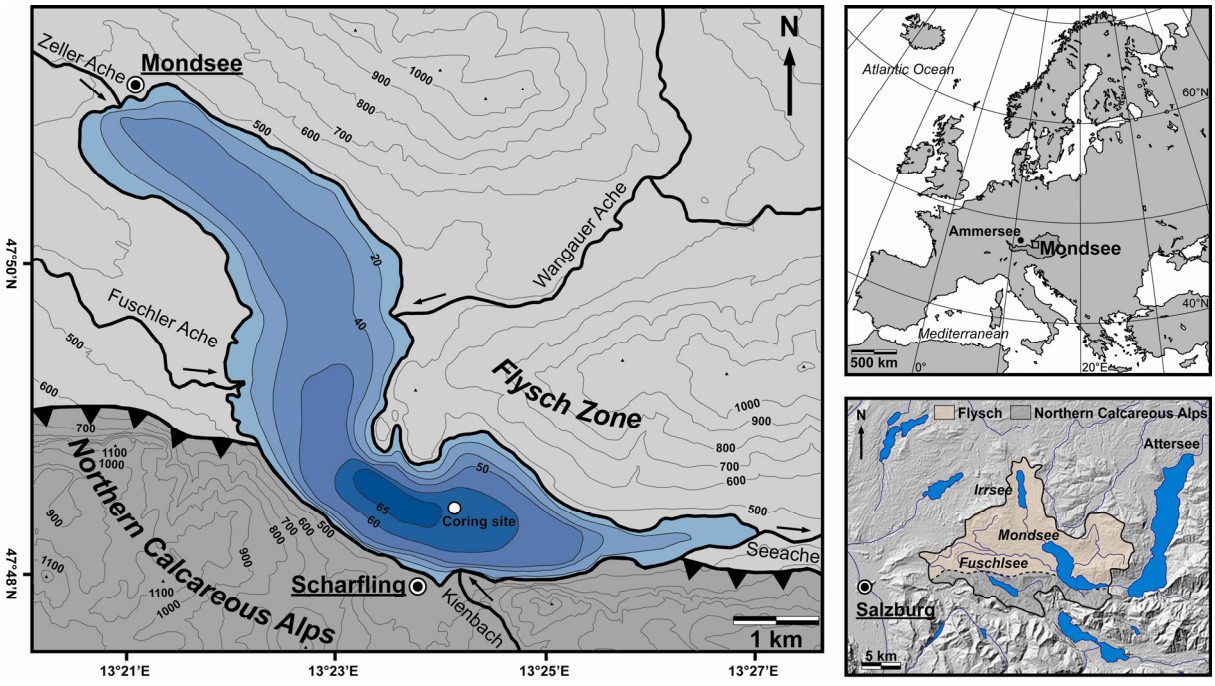


**Figure 3.1** Bathymetry of Lake Mondsee and simplified geological maps of the entire catchment and the surrounding area (modified after Nagl (1976) and van Husen (1989)). Isobaths are given with corresponding depths in metres below lake level. The small river Kienbach, which drains the Northern Calcareous Alps, is the main source of allochthonous detrital material to the coring site.

The catchment area of Lake Mondsee has a size of ~247 km², of which about 50% are covered by forests (Beiwl 2008). Two major geological units, separated by a thrust zone that follows the southern shoreline of Lake Mondsee, characterize the area (Fig. 3.1). The steep-sloped mountains of the Northern Calcareous Alps along the southern lakefront, which are composed of the Triassic Main Dolomite and Mesozoic limestones and reach elevations of up to 1782 m a.s.l., constitute about 25% of the catchment area. Cretaceous marls, shales and sandstones of the Rhenodanubic Flysch and local Quaternary deposits, which dominate the remaining ~75% of the catchment, characterize the gently sloped hills in the eastern, western and northern part of the catchment, generally not exceeding elevations of ~1000 m a.s.l. (van Husen 1989). During the Pleistocene, the lake basin, originally formed by tectonic processes, has been repeatedly overridden and substantially altered by glacier activity, finally by the Traun Glacier during the Würmian glaciation (van Husen 1979; Kohl 1998). Eemian palaeolake deposits on the northern shore, which are covered by Würmian tills (Klaus 1975; Drescher-Schneider & Papesch 1998), indicate the complex evolution and larger-than-present extent of the lake basin during earlier times. Direct glacier influence on the catchment rapidly ceased after the Last Glacial Maximum as indicated by kame deposits of the Ischler Stand (Bühl Stadial) about 15 km southeast of Lake Mondsee (van Husen 1977, 1997). The corresponding early phase of the Lateglacial ice decay (Reitner 2007) in the lower eastern Alpine valleys dates to ca. 18 000–19 000 cal. a BP (van Husen 1977; Schmidt *et al.* 1998; van Husen 2004; Klasen *et al.* 2007). After the ice retreat, the glacial basin was subsequently filled by meltwater, forming the present lake.

Today, the study area is characterized by an Alpine-influenced temperate climate with warm summers and frequent precipitation. The mean annual air temperature for the weather station Mondsee is +8.7°C with January and July means of -0.5°C and +17.8°C, respectively. The average annual precipitation amounts to about 1550 mm, with highest rainfall during summer (climate data for the period 1971–2000, Central Institute for Meteorology and Geodynamics (ZAMG), Vienna, Austria).

Past work on Lake Mondsee sediments mainly focused on recent and late Holocene limnological and sedimentological aspects (e.g. Löffler 1983; Behbehani *et al.* 1985; Danielopol *et al.* 1985; Irlweck & Danielopol 1985; Horsthemke 1986; Klee & Schmidt 1987; Herrmann 1990), but also included a low-resolution study on the Lateglacial to Holocene vegetation development (Schultze & Niederreiter 1990).

## 3.3 Fieldwork and methods

### *3.3.1 Fieldwork*

Two parallel sediment cores (1389 and 1172 cm long), each consisting of 2-m-long segments (Fig. 3.2), were recovered from the coring site (47°48’41”N, 13°24’09”E, 62 m water depth) in the southern lake basin (Fig. 3.1A) in June 2005 by using a 90-mm-diameter UWITEC piston corer.

Additionally, the undisturbed sediment-water interface was obtained in three short gravity cores recovered from the same site. A field lab was installed to facilitate on-site core opening, photographing and preliminary lithostratigraphical description. The overlapping segments of both cores were visually correlated by using more than 90 macroscopic lithological marker layers, resulting in a continuous composite profile of about 1500 cm length (Fig. 3.2). The subsequent continuous and precisely parallel sampling of the core segments for all proxy analyses was also carried out in the field lab.

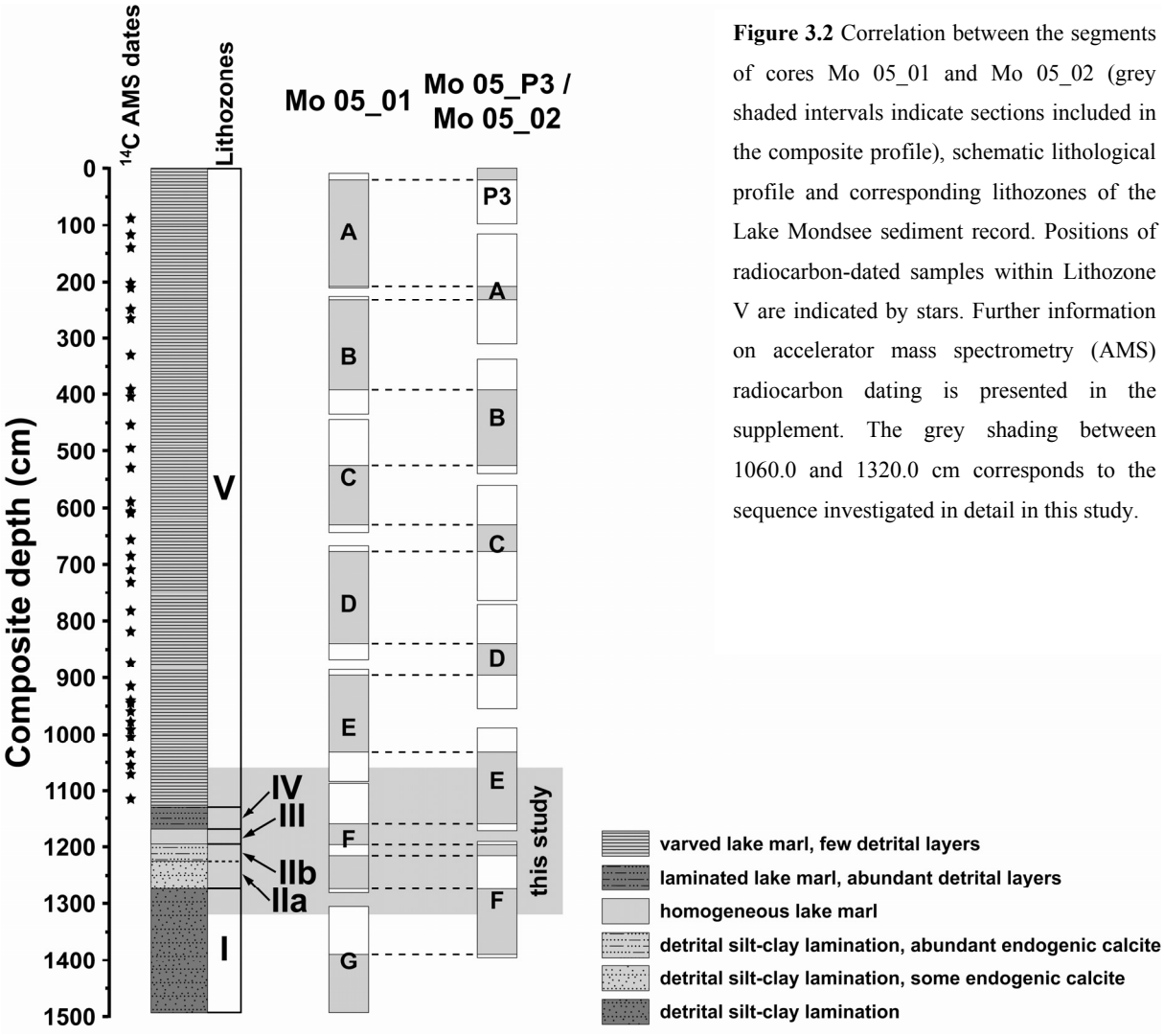


**Figure 3.2** Correlation between the segments of cores Mo 05_01 and Mo 05_02 (grey shaded intervals indicate sections included in the composite profile), schematic lithological profile and corresponding lithozones of the Lake Mondsee sediment record. Positions of radiocarbon-dated samples within Lithozone V are indicated by stars. Further information on accelerator mass spectrometry (AMS) radiocarbon dating is presented in the supplement. The grey shading between 1060.0 and 1320.0 cm corresponds to the sequence investigated in detail in this study.

### *3.3.2 Sediment microfacies analysis and varve counting*

Detailed sediment microfacies investigation, also confirming the preliminary macroscopic core correlation, was carried out on large-scale petrographic thin sections prepared from a continuous series of overlapping sediment blocks (100×20×10 mm) according to the method described by Brauer *et al*. (1999b). Thin sections were examined under a ZEISS Axiophot polarization microscope at 25–400× magnification.

Additionally, microscopic counting of biochemical calcite varves, including thickness measurements, was carried out within the uppermost 1129.0 cm of the profile. For a detailed account on the establishment of the varve chronology for the Holocene part of the profile and the supplementary accelerator mass spectrometry (AMS) radiocarbon dating of terrestrial plant macrofossils, the reader is referred to the supplement (Fig. 3.S1, Table 3.S1).

### *3.3.3 Geochemical analyses*

Bulk sediment samples for quantitative carbon geochemistry (0.5-cm-thick slices) from the interval 1112.0–1279.0 cm were analyzed continuously across climatic transitions, defined according to microfacies and stable isotope data, and with sample increments of 1–2 cm in the remaining sections. Total inorganic carbon (TIC) was measured coulometrically on freeze-dried and homogenized samples (~50 mg) by using a Ströhlein Coulomat 702 elemental analyzer. Total carbon (TC) was determined by combustion of sample material (100–200 mg) at 1350°C in a LECO CNS-2000 analyzer. Total organic carbon (TOC) was calculated as the difference between TC and TIC with an estimated analytical error of ~0.3%. All results are expressed as per cent dry weight.

Semi-quantitative major element scanning was carried out at 200 µm resolution on impregnated sediment slabs from thin section preparation between 1064.0 and 1302.0 cm, using a vacuum-operating EAGLE III XL micro X-ray fluorescence (µ-XRF) spectrometer with a low-power Rh X-ray tube at 40 kV and 300 µA (250 µm spot size, 60 s counting time, single scan line). The fluorescent radiation emitted from the sample was recorded by an energy-dispersive Si (Li) detector and transformed into element information for each measuring point. Element intensities for Mg, Al and Ca are expressed as counts $s^{-1}$ (cps), representing relative changes in element composition. Combined interpretation of high-resolution µ-XRF and microfacies data is enabled as the scanned sediment surfaces are identical to those prepared for thin sections (Brauer *et al.* 2009).

### *3.3.4 Stable isotopes*

For high-resolution stable isotope measurements on ostracods, 0.5-cm-thick sediment slices were taken continuously between 1060.0 and 1273.5 cm. Samples were disaggregated in 10% $H_2O_2$, wet sieved through a 125-µm mesh and rinsed in ethanol before drying. Subsequently, valves of juvenile ($5^{th}$–$8^{th}$ stage) *Candona neglecta* and *Fabaeformiscandona harmsworthi* (Namiotko *et al.* 2009) were separated and mechanically cleaned at the Institute for Limnology in Mondsee. Subsets of up to 20 valves (15–110 µg) of *Candona neglecta* (above 1212.0 cm) and *Fabaeformiscandona harmsworthi* (below 1212.0 cm) were analyzed for $\delta^{13}C$ and $\delta^{18}O$ at the Leibniz Laboratory in Kiel on a CARBO Kiel I / Finnigan MAT 251 $CO_2$ preparation and mass spectrometer system. Isotopic compositions are reported in the conventional δ-notation relative to the Vienna PeeDee Belemnite

(VPDB) standard. The analytical precision is <0.04‰ and <0.07‰ for $\delta^{13}C$ and $\delta^{18}O$, respectively. The change of the measured species at 1212.0 cm has no influence on the oxygen isotope record as $\delta^{18}O$ derived from different Candonidae is comparable because of the identical vital offset of about +2.2‰ compared to equilibrium calcite (von Grafenstein *et al.* 1999b).

### *3.3.5 Pollen*

For pollen analyses, carried out at the Adam Mickiewicz University in Poznań, 0.5-cm-thick sediment slices from the interval 1112.0–1279.0 cm were analyzed continuously across climatic transitions and with increments of up to 2.5 cm in the remaining sections. Two *Lycopodium* tablets were added to each sample for the calculation of pollen concentrations (Stockmarr 1971). Sample preparation followed the standard method described by Berglund and Ralska-Jasiewiczowa (1986), including treatment with cool HF and HCl, acetolysis, embedding in pure glycerine and staining with safranin. A minimum of 500 terrestrial pollen grains were counted and determined under a light microscope (400× magnification) for samples above 1200.0 cm, while less than 100 pollen grains per sample were counted below this depth due to the low pollen concentrations. The TILIA/TILIA GRAPH software package (including CONISS; Grimm 1987, 1992) was used for plotting and zonation of the pollen diagram. Pollen percentages were calculated upon the sum of terrestrial plants, including trees/shrubs (AP) and herbs/ferns (NAP) but excluding aquatic and wetland plants. Concentration values are expressed as pollen grains $cm^{-3}$ dry sediment.

## 3.4 Results

### *3.4.1 Sediment microfacies and geochemistry*

The Lake Mondsee sediment record is subdivided into five major lithostratigraphical units (Lithozones I to V), distinguished by (1) the amount of minerogenic detrital material, (2) the quantity of endogenic calcite and (3) the presence and structure of lamination (Figs. 3.2 and 3.3). Ca/Mg ratios (Fig. 3.4) allow the differentiation between intervals with predominantly detrital input (low ratios, high content of Mg-rich dolomitic material) and such with mainly autochthonous sedimentation (high ratios, dominant biochemical calcite precipitation). Polarization and scanning electron microscopy corroborate a close correspondence between high-Ca/Mg ratio intervals and the abundant occurrence of idiomorphic, biochemically precipitated calcite. We thus consider fluctuations in the broadly similar µ-XRF Ca and TIC records to mainly reflect changes in endogenic calcite contents. In contrast, the µ-XRF Mg record is regarded as a proxy for the input of detrital dolomite from the Northern Calcareous Alps. It largely coincides with the µ-XRF Al record, which is considered to reflect the second component of detrital input, the supply of siliciclastic detrital material from the Flysch Zone.

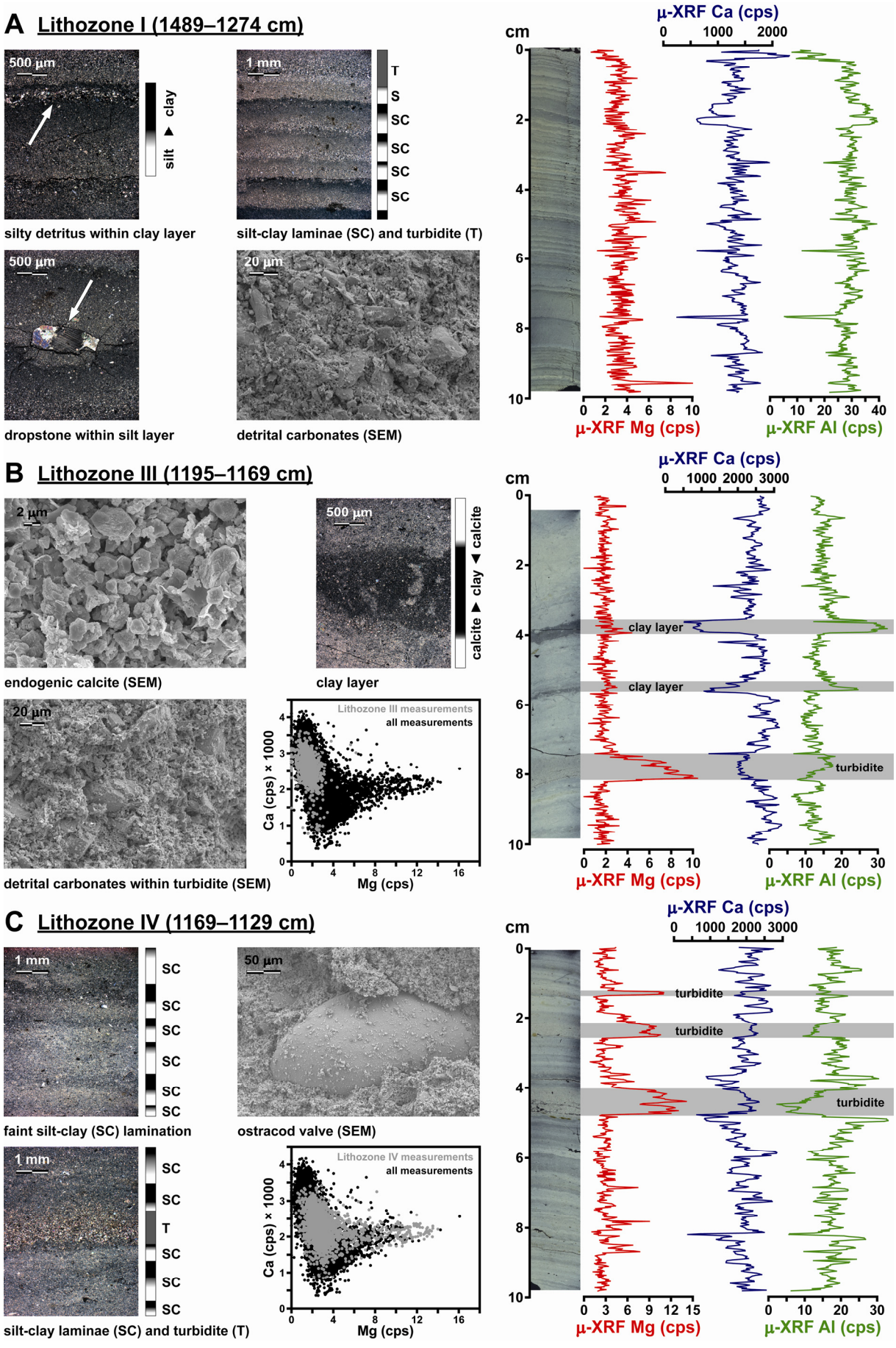
A Lithozone I (1489–1274 cm)
500 µm
silt ▲ clay
silty detritus within clay layer
1 mm
T
S
SC
SC
SC
SC
silt-clay laminae (SC) and turbidite (T)
500 µm
dropstone within silt layer
20 µm
detrital carbonates (SEM)
µ-XRF Ca (cps)
0 1000 2000
cm
µ-XRF Mg (cps)
µ-XRF Al (cps)
B Lithozone III (1195–1169 cm)
2 µm
endogenic calcite (SEM)
500 µm
calcite ▲ clay ▼ calcite
clay layer
20 µm
detrital carbonates within turbidite (SEM)
Lithozone III measurements
all measurements
Ca (cps) × 1000
Mg (cps)
clay layer
clay layer
turbidite
C Lithozone IV (1169–1129 cm)
1 mm
SC
SC
SC
SC
SC
SC
faint silt-clay (SC) lamination
50 µm
ostracod valve (SEM)
1 mm
SC
SC
T
SC
SC
SC
silt-clay laminae (SC) and turbidite (T)
Lithozone IV measurements
all measurements
turbidite
turbidite
turbidite

Lithozone I (1493.0–1274.0 cm) is composed of yellowish/brownish grey, distinctly laminated sediments. Regular light-dark couplets (average thickness ~1.0–1.5 mm; Fig. 3.3A) contain a darker (greyish) basal silt layer, which is composed of detrital carbonates and subordinated siliciclastics and reveals a sharp lower boundary. Towards the top, the silt layer grades into a lighter (yellowish) clay layer with decreasing carbonate content. The gradation of these silt-clay laminae reflects the temporally differentiated deposition of silt and clay by over- and interflows after spring meltwater discharge (Sturm & Matter 1978). Sporadic dropstones in the silt layer (Fig. 3.3A) indicate drift-ice transport and thus seasonal ice cover. About 160, silt- to fine sand-sized turbidites are intercalated within the regular silt-clay laminae. Although having an identical mineralogical composition, the distinctly graded turbidites are usually thicker (up to several centimetres) and frequently show erosional basal contacts (Fig. 3.3A), thus suggesting deposition by underflows (Sturm & Matter 1978). The predominantly dolomitic and siliciclastic composition of Lithozone I sediments is reflected by elevated Mg and Al counts, respectively (Fig. 3.4). As confirmed by microscopic analyses, the low Ca counts and TIC contents (<5.0%) exclusively reflect detrital carbonates.

The deposition of silt-clay laminae with intercalated turbidites continues throughout Lithozone II (1274.0–1195.0 cm). However, as observed in thin sections, the transitional boundary between Lithozones I and II can be defined by the first appearance of biochemically precipitated calcite and the decrease in average laminae thickness from ~1.0–1.5 mm to less than 1.0 mm. Sediment colour gradually changes from yellowish/brownish grey to light grey towards the top of Lithozone II. This is the result of the increasing amount of endogenic calcite, allowing the definition of two lithostratigraphical subzones.

---

**Figure 3.3** Typical sediment microfacies of different lithozones and results of µ-XRF element scanning of representative sediment slabs. Scanned thin sections (cross-polarized light) along the µ-XRF scans are displayed for comparison. Detail photographs were taken on thin sections under a ZEISS Axiophot polarization microscope at 25–50× magnification with cross-polarized light and on dried sediment samples under a scanning electron microscope (SEM). For further explanations on the figures see the text. (A) Laminated sediments of Lithozone I. Silt-clay laminae (SC) are composed of a basal silt layer of detrital carbonates and siliciclastics which grades into a clay layer. Frequently intercalated turbidites (T) represent deposition by underflows. Occasional silt-sized minerogenic detritus within the clayey sublayer reflects a secondary pulse of detrital flux. Dropstones within the silty sublayer originate from drift-ice transport. (B) Homogeneous lake marl of mainly microcrystalline endogenic calcite in Lithozone III. Two intercalated distinct clay layers (high Al and low Ca counts) and a turbidite composed of detrital carbonates (high Mg and intermediate Ca and Al counts) reflect occasional surface runoff events. The µ-XRF cross-plot reveals the high abundance of endogenic calcite (Ca counts) and low amounts of dolomitic detritus (Mg counts). (C) Faintly laminated sediment of Lithozone IV. Distinct turbidites intercalated within the silt-clay laminae are reflected by high Mg counts, whereas Ca and Al counts remain on a low/intermediate level. The µ-XRF cross-plot reflects the continuing presence of endogenic calcite (Ca counts) but also increased amounts of dolomitic detritus (Mg counts).

Microscopic inspection reveals that idiomorphic, microcrystalline calcite (<5 µm) is still rare below 1224.0 cm (Lithozone IIa), but becomes more abundant above (Lithozone IIb). This is reflected by a rise in Ca counts and TIC contents (from about 6.0 to 8.5%) throughout Lithozone IIb (Fig. 3.4) and most probably related to intensified biological productivity (Brauer & Casanova 2001). The parallel reduction of detrital flux, indicated by decreasing Al and Mg counts, results in a more faint lamination. A slight increase in TOC from about 0.3% to 0.5–0.8% around 1201.0 cm marks the onset of the gradual transition between Lithozones II and III.

Light grey, homogeneous lake marl, which predominantly consists of endogenic calcite, dominates throughout Lithozone III (1195.0–1169.0 cm). Only a few silt-sized detrital carbonates and siliciclastics are finely dispersed within the clay-sized matrix (Fig. 3.3B). The absence of a lamination is owed to the lack of episodic detrital input, which is indicated by low Al and Mg counts (Fig. 3.4). High amounts of endogenic calcite are reflected by maximum Ca counts and TIC contents of 8.5–10.0% (~70–80% $CaCO_3$), only interrupted by distinct reductions at 1195.5–1190.5 cm and 1181.0–1175.5 cm (Fig. 3.4). Within these two intervals, up to 4-mm-thick clay layers occur, corresponding to elevated Al counts (Figs. 3.3B and 3.4). The gradual transition towards Lithozone IV in the uppermost 5 cm of Lithozone III is characterized by the reappearance of regular episodic clay layers, resulting in a faint carbonate-clay lamination.

Lithozone IV (1169.0–1129.0 cm) is characterized by laminated light grey lake marl. Faint laminae couplets of about 1 mm thickness comprise, as observed in Lithozone II, a silty basal sublayer with detrital carbonates and an overlying clayey sublayer (Fig. 3.3C). Numerous yellowish-brownish, 0.3–8.0-mm-thick detrital layers with frequent erosional basal contacts are intercalated within the regular silt-clay laminae. These turbidites contain silt-sized detrital carbonates and siliciclastics and in most cases also fine-grained organic material. Higher detrital flux in Lithozone IV is reflected by an overall increase in Al and Mg counts, with distinct spikes in the Mg record reflecting the frequent occurrence of turbidites (Figs. 3.3C and 3.4). In contrast, endogenic calcite contents are reduced as indicated by decreasing Ca counts and TIC contents (Fig. 3.4), reaching lowest values between about 1168.0 and 1157.0 cm.

The sediments of Lithozone V (above 1129.0 cm) are composed of millimetre- to sub-millimetre-scale-laminated lake marl, that contains abundant ostracod valves and plant macro remains (leaves, needles, seeds and wood fragments). Sediment colour gradually changes from light to yellowish/brownish grey upcore, which is mainly related to the increasing abundance of organic matter.

---

**Figure 3.4** Results of µ-XRF element scanning (thin lines: measurements at 200 µm resolution, thick lines: 25-point running mean) and carbon geochemistry analyses obtained from the Lake Mondsee sediments across the Last Glacial-Holocene transition. µ-XRF Mg counts reflect input of detrital dolomite and Al counts those of detrital siliciclastics, whereas Ca counts and TIC contents reflect variations in the abundance of endogenic calcite.

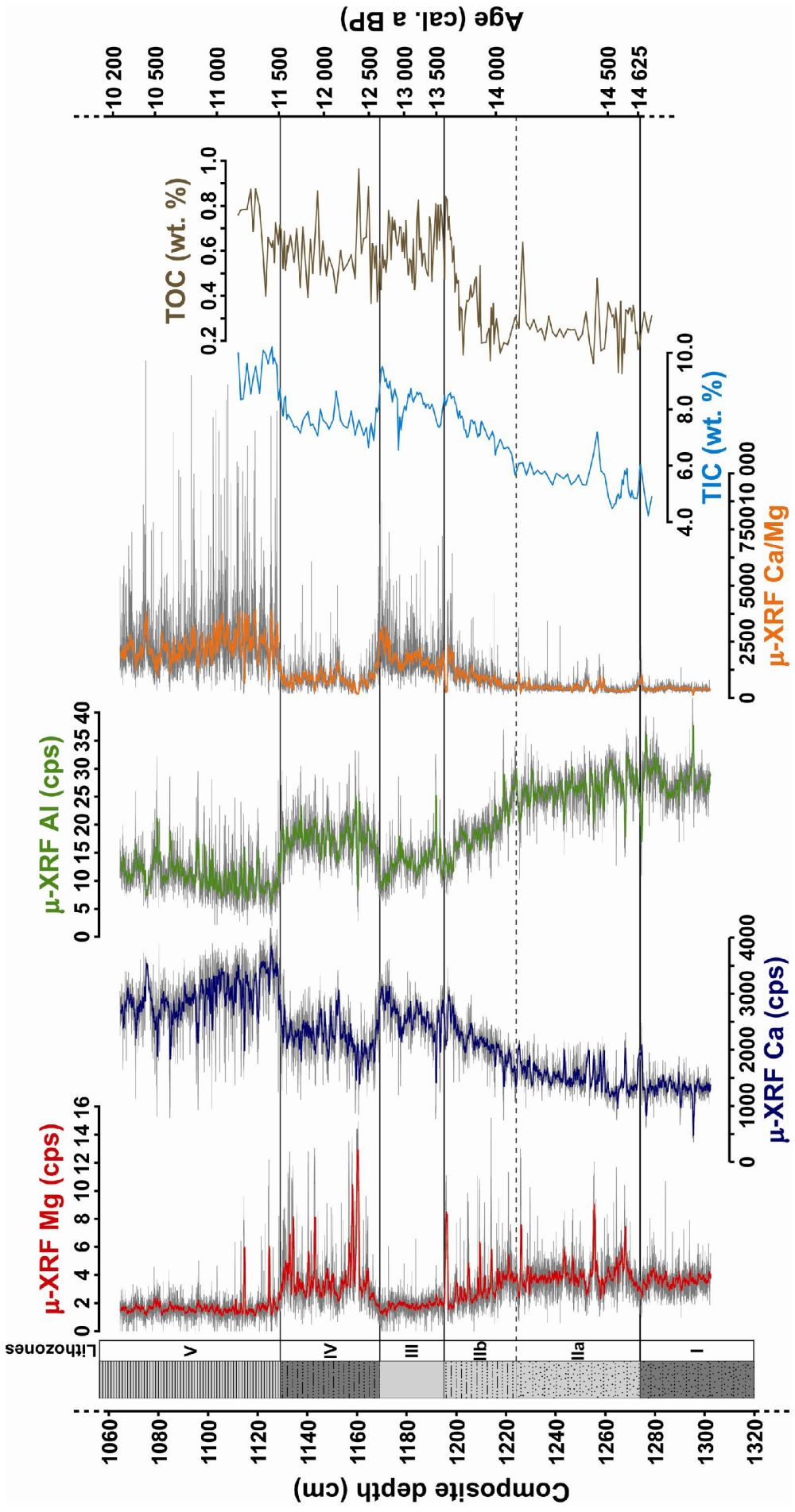
Age (cal. a BP)
10 200
10 500
11 000
11 500
12 000
12 500
13 000
13 500
14 000
14 500
14 625
TOC (wt. %)
0.2 0.4 0.6 0.8 1.0
TIC (wt. %)
4.0 6.0 8.0 10.0
µ-XRF Ca/Mg
0 2500 5000 7500 10 000
µ-XRF Al (cps)
0 5 10 15 20 25 30 35 40
µ-XRF Ca (cps)
0 1000 2000 3000 4000
µ-XRF Mg (cps)
0 2 4 6 8 10 12 14 16
Lithozones
V
IV
III
IIb
IIa
I
Composite depth (cm)
1060
1080
1100
1120
1140
1160
1180
1200
1220
1240
1260
1280
1300
1320

Intensified biochemical calcite precipitation is reflected by increased Ca counts and TIC contents of up to 10.0% (~70–85% $CaCO_3$) at the base of Lithozone V, whereas reduced Al and Mg counts prove the low minerogenic input (Fig. 3.4). Average varve thickness gradually increases from ~0.5 mm at the base of Lithozone V to ~2.0 mm in the uppermost 150 cm (Fig. 3.S1A), but shows only minor short-term fluctuations. Two types of detrital layers are intercalated within the regular varve succession: (1) macroscopic brownish detrital layers of up to several millimetres thickness, which are composed of detrital carbonates, subordinated siliciclastics and coarse organic debris and (2) microscopic detrital layers, which usually not exceed 100 µm in thickness and contain higher amounts of siliciclastics but only a few organic material (Swierczynski *et al.* 2009).

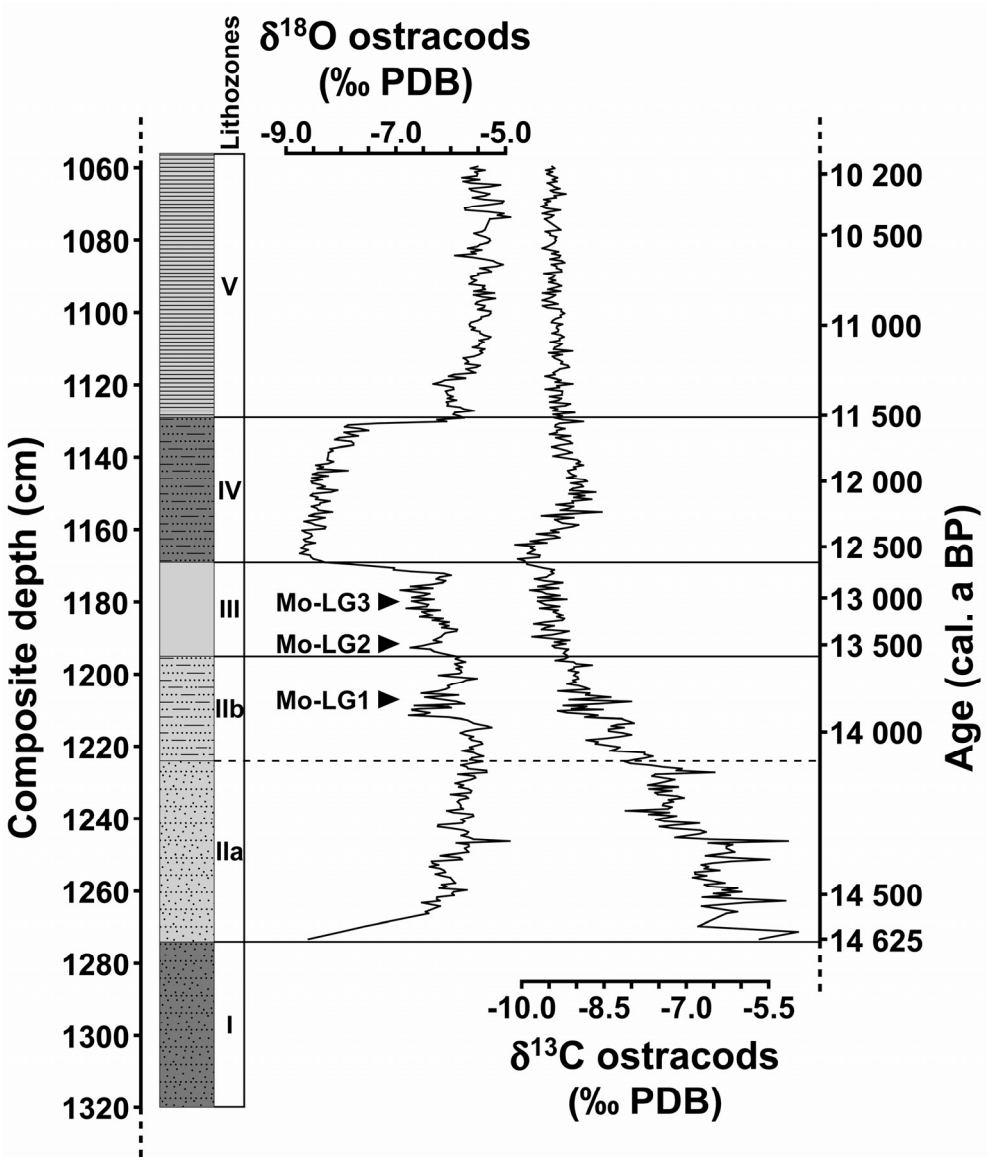


**Figure 3.5** Results of stable isotope measurements on juvenile ostracod (*Candona neglecta* and *Fabaeformiscandona harmsworthi*) valves obtained from the Lake Mondsee sediments across the Last Glacial-Holocene transition. $\delta^{18}O$ values, which are considered as a temperature proxy, are not corrected for the species-specific vital offset.

### *3.4.2 Stable isotope ratios*

The stable oxygen isotope record derived from the valves of juvenile Candonidae (Fig. 3.5) reveals the characteristic pattern of Lateglacial climatic changes, which is also seen in other Alpine oxygen isotope records (e.g. Eicher 1987; Lotter *et al.* 1992; von Grafenstein *et al.* 1999a; Schwalb 2003) and the Greenland ice cores (e.g. Johnsen *et al.* 1992; NGRIP Members 2004). The close correspondence to the $\delta^{18}O$ records from adjacent Lake Ammersee and Greenland (Fig. 3.7), which are mainly controlled by temperature variability (Johnsen *et al.* 1992; Stuiver *et al.* 1995; von Grafenstein *et al.* 1996; von Grafenstein *et al.* 1999a), but also the agreement with regional temperature reconstructions based on biotic proxy data (Heiri & Millet 2005), implies that the Lake Mondsee $\delta^{18}O$ record also reflects mainly a temperature signal. However, it might be additionally influenced by other factors, e.g. hydrological or atmospheric circulation changes.

Oxygen isotope ratios rapidly increase by ~2.0‰ at the base of Lithozone II (Pleniglacial-Lateglacial transition), while $\delta^{13}C$ values gradually decrease from about -5.5 to -9.0‰ in Lithozone II. Throughout Lithozones II and III, $\delta^{18}O$ ratios fluctuate around -6.0‰, superimposed by three minor negative excursions of about 0.8–1.5‰ at 1215.0–1201.5 cm, 1195.0–1191.5 cm and 1182.5–1175.0 cm, which are termed Mo-LG1, Mo-LG2 and Mo-LG3, respectively. $\delta^{13}C$ values decrease from about -9.0 to -10.0‰ within Lithozone III. Across the transition between Lithozone III and IV (1173.0–1168.0 cm), $\delta^{18}O$ decreases by about 2.5‰, reflecting the onset of the Younger Dryas. Throughout Lithozone IV, oxygen isotope ratios gradually rise by about 1.0‰, but remain below -7.5‰. Shortly before the base of Lithozone V at about 1131.5 cm, $\delta^{18}O$ ratios rapidly rise within 1.5 cm from about -8.0 to -6.0‰. $\delta^{13}C$ gradually increases from about -10.0 to -9.0‰ during the first half of Lithozone IV (1169.0–1159.0 cm) and then again decreases above ~1141.0 cm to about -9.5‰ in Lithozone V.

### *3.4.3 Pollen*

The pollen diagram exhibits a succession of seven local pollen assemblage zones (LPAZ; Fig. 3.6), in agreement with the regional Lateglacial vegetation development (Draxler 1977; Schmidt 1981; Draxler & van Husen 1987) and allowing the definition of biostratigraphic boundaries. Open plant communities (shrubs and herbs) dominate the interval below 1250.0 cm (Lithozone I and basal Lithozone II), but low pollen concentrations prevent detailed vegetation reconstruction. The lowermost pollen zone LPAZ 1 (1250.0–1216.0 cm) is characterized by dwarf shrub communities of *Juniperus*, *Salix* and *Betula nana* interspersed with herbs. LPAZ 2 (1216.0–1210.0 cm) reflects the rapid expansion of *Pinus* (up to 80%) and the decline of *Juniperus*. LPAZ 3 (1210.0–1201.0 cm) and LPAZ 4 (1201.0–1191.0 cm) reveal the further spread of *Pinus*, but heliophytic plants (Poaceae, Chenopodiaceae, *Artemisia*, *Juniperus*) still frequently occur.

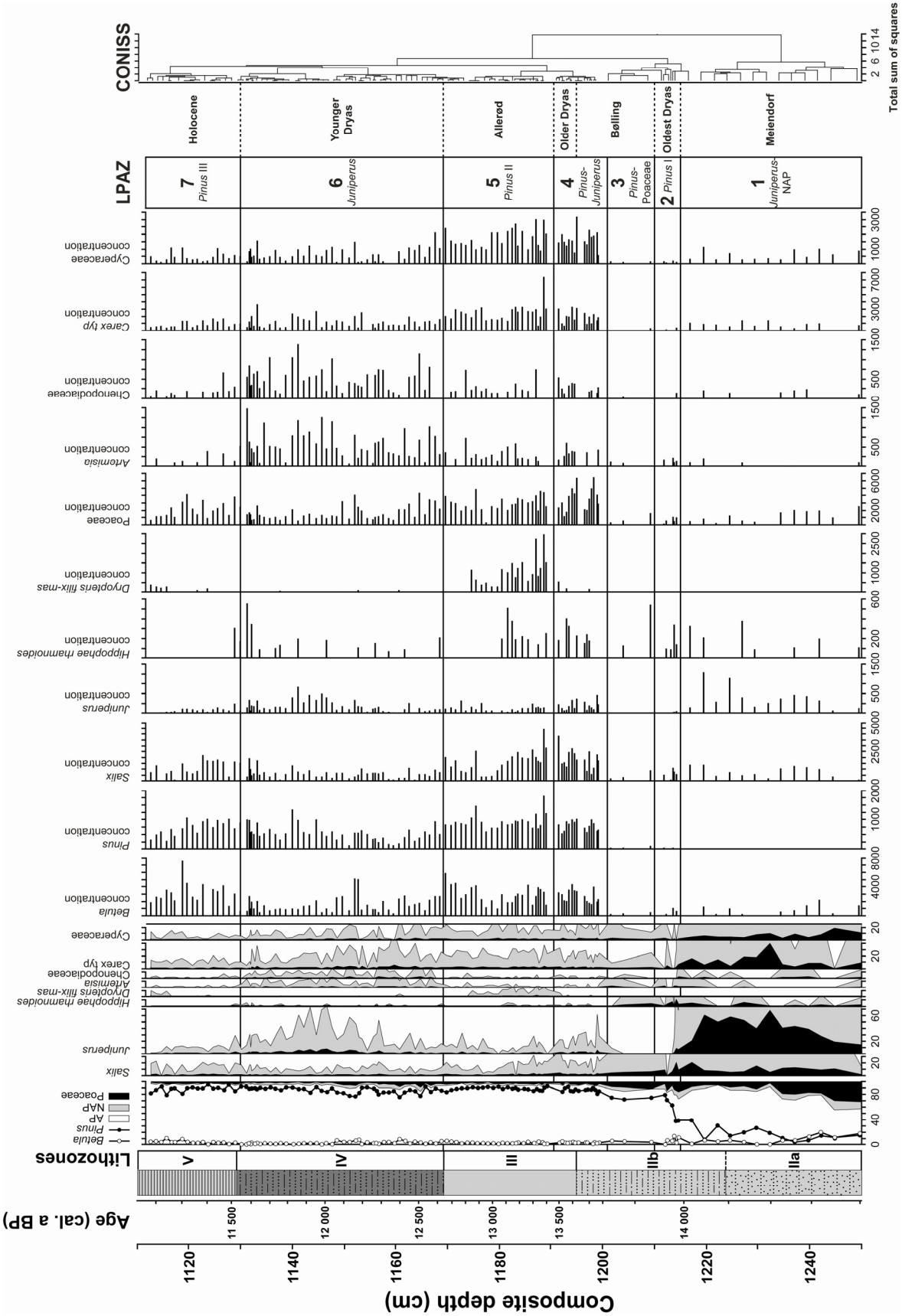


**Figure 3.6** Pollen percentage/concentration diagram for Lake Mondsee for selected taxa. Outline curves in the percentage diagrams represent a 10× exaggeration. Pollen concentrations are given as pollen grains $cm^{-3}$ dry sediment.

Declining values for *Juniperus* (below 2%) and NAP characterize LPAZ 5 (1191.0–1169.5 cm), which corresponds to the Allerød pollen zone. The presence of *Dryopteris filix-mas*, nowadays restricted to temperate climates (Zarzycki *et al.* 2002), indicates warmer climate conditions. The increase of *Artemisia* (up to 2%) and NAP (2–6%) marks the base of LPAZ 6 (1169.5–1130.0 cm), which corresponds to the Younger Dryas pollen zone and shows a clear bipartition with NAP prevailing in the lower part (below 1157.0 cm) and *Juniperus* dominating (up to 7%) above this depth. Opening of forest cover within this zone is indicated by fluctuations in the *Pinus* curve and decreased tree pollen concentrations. The onset of the Holocene at the base of LPAZ 7 (above 1130.0 cm) is reflected by the decline of Lateglacial shrubs and herbs.

### *3.4.4 Chronology*

The age-depth model for the Holocene part of the Lake Mondsee sediment record, which is largely equivalent to Lithozone V, was established through microscopic varve counting and is supported by AMS radiocarbon dating of terrestrial plant macrofossils. The base of Lithozone V at 1129.0 cm is dated to ca. 11 510 varve (calendar) years BP (for more details see the supplement).

*This part of the chapter is only published electronically as supporting online material and does not appear in the print version of the manuscript.*

### *Supplement – Establishment of the age-depth model for the Holocene part of the Lake Mondsee sediment record*

*Methods*

The age model for the Holocene part of the Lake Mondsee sediment record (Lithozone V) was established through microscopic varve counting on large-scale petrographic thin sections, carried out under a ZEISS Axiophot polarization microscope at 25–400× magnification. Continuous microscopic counting of biochemical calcite varves, including varve thickness measurements, was carried out in the distinctly annually laminated uppermost ~610 cm of the record. Between ~610 and 1129 cm, a varve-based sedimentation rate chronology was established because varve preservation was generally not sufficient for continuous counting. Here, counting and thickness measurements were performed only on the well-varved sections (~15%), which were used for calculating average sedimentation rates. In order to support the varve counting-based chronology for the Holocene part of the Lake Mondsee sediment record, accelerator mass spectrometry (AMS) $^{14}C$ dating of 35 samples of terrestrial plant macrofossils (leaf fragments, seeds, bark),

selected from the uppermost 1114.0 cm of the sediment profile (Table 3.S1), was performed at the Leibniz Laboratory in Kiel (Nadeau *et al.* 1997). Conventional radiocarbon ages were calibrated using the CALIB 5.0.1 program (Stuiver & Reimer 1993; Stuiver *et al.* 2005) with the IntCal04 calibration data set (Reimer *et al.* 2004).

For further confirmation of the dating of the uppermost part of the sediment record, comprising the deposits of the last ca. 50 years, $^{137}$Cs dating was carried out on oven-dried and homogenized bulk sediment samples from one surface gravity core in a low-background, well-type germanium detector at the Modane underground laboratory (Reyss *et al.* 1995). Sample specific activity for $^{137}$Cs is given in Becquerel per kilogram dry weight (Bq kg$^{-1}$).

**Table 3.S1** AMS $^{14}$C dates obtained from terrestrial macrofossils from the Holocene part of the Lake Mondsee record. Italicised samples substantially deviate from the varve-based age model (see explanations in the supplement). All conventional $^{14}$C ages were calibrated using the CALIB 5.0.1 program (Stuiver & Reimer 1993; Stuiver *et al.* 2005) with the IntCal04 calibration dataset (Reimer *et al.* 2004).

| Sample / Lab. code | Composite depth (cm) | Dated material | Carbon content (mg) / $\delta^{13}$C ± σ (‰) | AMS $^{14}$C age (a BP ± σ) | Calibrated age (cal. a BP, 2σ |
|---|---|---|---|---|---|
| KIA36603 | 87.50 | leaves[a] | 1.66 / -27.02±0.26 | 404±22 | 335–510 |
| KIA36604 | 117.00 | pine needle | 0.79 / -42.31±0.75 | 583±34 | 532–652 |
| *KIA32786* | *140.25* | *spruce needle* | *0.25 / -26.39±0.23* | *473±60* | *320–639* |
| *KIA29393* | *204.25* | *plant remains[b]* | *0.87 / -30.65±0.08* | *482±27* | *502–539* |
| KIA32787 | 212.25 | leaves[a] | 3.05 / -27.21±0.32 | 1265±24 | 1145–1280 |
| KIA36605 | 249.75 | leaves[a] | 0.72 / -28.99±0.30 | 1485±33 | 1303–1483 |
| KIA36606 | 265.75 | twig & leaves[a] | 1.02 / -26.90±0.29 | 1598±30 | 1410–1544 |
| KIA36607 | 327.75 | leaves[a] | 0.98 / -29.45±0.22 | 2130±27 | 2003–2297 |
| *KIA32789* | *393.00* | *bud scale* | *0.14 / -29.41±0.10* | *2091±132* | *1739–2349* |
| KIA32790 | 403.00 | plant remains[b] | 0.34 / -33.02±0.21 | 2373±56 | 2314–2702 |
| KIA32791 | 453.25 | willow leaf | 1.09 / -30.47±0.10 | 2801±29 | 2798–2974 |
| KIA36618 | 496.75 | leaves[a] | 3.10 / -29.36±0.16 | 3110±30 | 3256–3392 |
| KIA36608 | 529.50 | plant remains[b] | 1.65 / -25.09±0.20 | 3276±26 | 3445–3570 |
| KIA36609 | 530.50 | stem | 0.65 / -27.02±0.39 | 3369±40 | 3480–3697 |
| KIA36610 | 589.00 | plant remains[b] | 2.22 / -27.03±0.25 | 3618±33 | 3839–4070 |
| KIA36611 | 604.50 | plant remains[b] | 0.41 / -29.03±0.36 | 3697±56 | 3880–4228 |
| KIA29395 | 607.50 | plant remains[b] | 4.06 / -29.21±0.04 | 3848±26 | 4155–4407 |
| KIA39229 | 657.00 | leaves[a] | 1.61 / -28.99±0.09 | 4142±31 | 4570–4824 |
| KIA39230 | 685.00 | leaves[a] & needle | 2.28 / -28.77±0.12 | 4581±34 | 5058–5447 |

**Table 3.S1** continued

| Sample / Lab. code | Composite depth (cm) | Dated material | Carbon content (mg) / $\delta^{13}C \pm \sigma$ (‰) | AMS $^{14}C$ age (a BP ± σ) | Calibrated age (cal. a BP, 2σ |
|---|---|---|---|---|---|
| KIA32793 | 708.75 | twig & bark | 4.89 / -28.60±0.05 | 4668±28 | 5316–5566 |
| KIA36612 | 732.25 | wood & leaves | 0.97 / -27.69±0.13 | 4883±41 | 5488–5715 |
| KIA32794 | 782.25 | leaves[a] | 1.04 / -30.09±0.15 | 5462±36 | 6194–6310 |
| KIA36619 | 818.75 | plant remains[b] | 1.65 / -26.55±0.13 | 5809±36 | 6498–6717 |
| *KIA32795* | *873.00* | *plant remains[b]* | *0.28 / -32.70±0.23* | *6088±104* | *6727–7246* |
| KIA32796 | 916.50 | leaves[a] | 3.29 / -29.61±0.09 | 7129±36 | 7869–8014 |
| KIA39231 | 941.00 | twig | 0.95 / -29.41±0.12 | 7349±48 | 8026–8311 |
| *KIA32797* | *945.25* | *bark* | *5.11 / -27.57±0.07* | *7766±35* | *8449–8602* |
| KIA36616 | 958.75 | plant remains[b] | 0.69 / -25.24±0.42 | 7631±61 | 8344–8549 |
| KIA36615 | 977.00 | plant remains[b] | 2.88 / -30.85±0.19 | 8019±35 | 8767–9013 |
| KIA32798 | 993.00 | bud scale | 1.65 / -25.73±0.21 | 8192±41 | 9024–9273 |
| KIA36617 | 1005.50 | seed | 4.66 / -21.20±0.34 | 8300±32 | 9142–9432 |
| KIA29397 | 1034.75 | seed | 1.37 / -23.89±0.14 | 8638±48 | 9529–9700 |
| KIA34503 | 1056.25 | bud scale | 1.33 / -29.18±0.10 | 8874±57 | 9743–10 184 |
| *KIA32799* | *1071.00* | *leaves[a]* | *0.40 / -26.12±0.24* | *8586±101* | *9334–9903* |
| *KIA39232* | *1114.00* | *seed* | *0.29 / -23.17±0.58* | *8918±144* | *9551–10 368* |

[a] undetermined terrestrial leaf fragments

[b] various undetermined terrestrial plant remains (leaves, wood, seeds)

## *Results*

For the upper ~610 cm of the sediment record, representing the last ca. 4200 years, the chronology is based on continuous varve counting (Fig. 3.S1A), supported by $^{137}Cs$ dating in the uppermost part of the core (Fig. 3.S1B). Further confirmation of the varve chronology arises from microfacies evidence for independently dated events (Fig. 3.S1B): (1) a distinct, 4-mm-thick detrital layer related to a documented debris flow in July 1986 (Fig. 3.S1B, inset 1) (Swierczynski *et al.* 2009), that incorporates the $^{137}Cs$ fallout peak produced by the Chernobyl reactor accident in April 1986, (2) the massive spread of the diatom *Aulacoseira islandica* in 1982, indicating the onset of re-oligotrophication (Klee & Schmidt 1987; Schmidt 1991), (3) the onset of eutrophication in 1968 (Findenegg 1969) and (4) the input of clayey detrital material from dolomite washing during the construction of the nearby highway in 1961/62 (Einsele 1963). Results of repeated varve counts revealed a counting error of less than 3%.

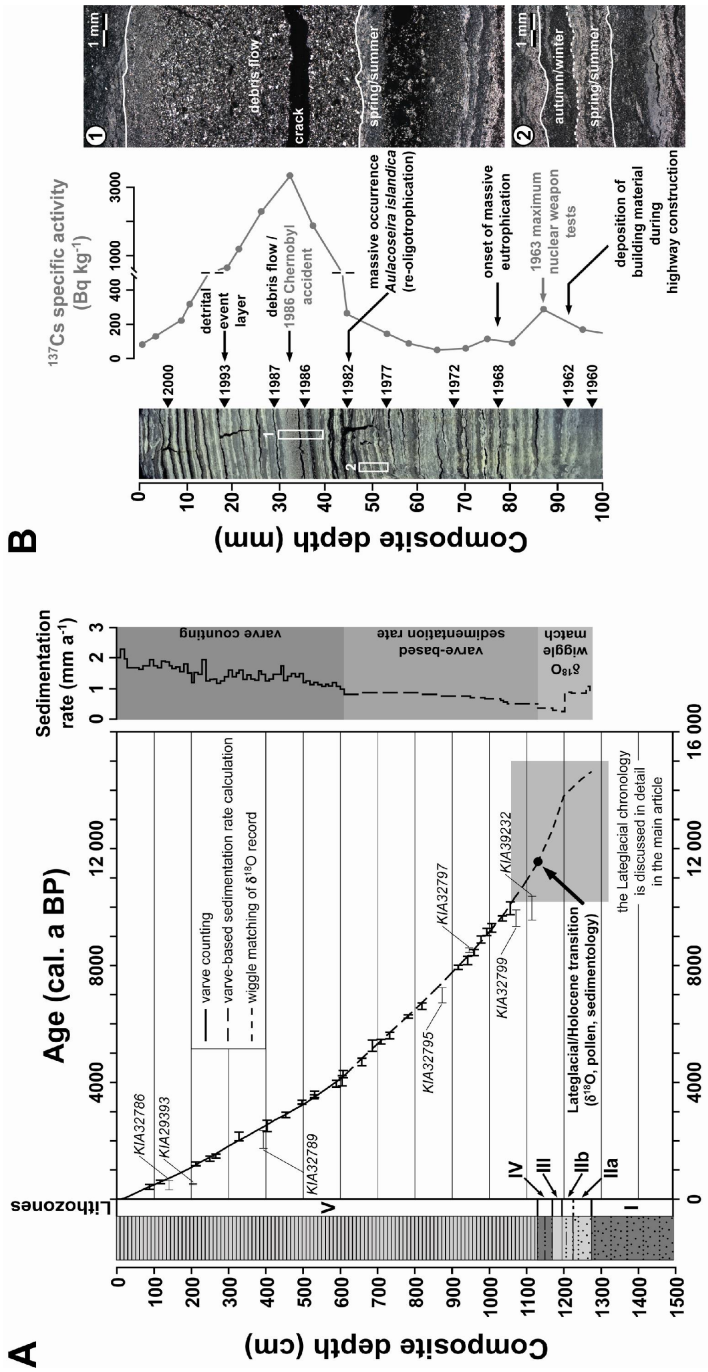


**Figure 3.S1** (A) Age-depth model of the Lake Mondsee sediment record based on microscopic varve counting, varve-based sedimentation rate calculation and $\delta^{18}O$ record wiggle matching (see text for details). Error bars for individual radiocarbon-dated samples indicate calibrated 2σ ranges. Named samples are probably erroneous (italicized in Table 3.S1). Average sedimentation rates are given in 10-cm intervals. (B) Results of $^{137}Cs$ dating of one gravity core. Calendar years next to the thin section scan (cross-polarized light) correspond to the adjacent light calcite summer layer or historical events (for details see the text). The high $^{137}Cs$ peak corresponding to the Chernobyl reactor accident is found within a debris flow layer deposited in summer 1986 (Swierczynski *et al.* 2009, inset 1). Recent biogenic calcite varves (inset 2) consist of (a) a light calcite layer that reveals a basal, coarse-grained sublayer (late spring) and an overlying fine-grained sublayer (summer) and (b) an overlying dark layer that contains amorphous organic material, clay minerals and diatom frustules (autumn to early spring).

Calibrated radiocarbon dates obtained from this interval agree well with the varve counting (Fig. 3.S1A), except three samples that yielded too young ages. For samples KIA32786 and KIA32789, this can be explained by the small sample sizes (0.25 and 0.14 mg C), favouring contamination with modern carbon (Wohlfarth *et al.* 1998), while for sample KIA29393 downcore displacement of the dated material during the coring is assumed. The varve-based sedimentation rate chronology established between ~610 and 1129 cm (Fig. 3.S1A) assigns an age of 11 507 varve (calendar) years BP to the base of Lithozone V (1129.0 cm) and is confirmed by 14 calibrated radiocarbon dates. Three small macrofossil samples (<0.4 mg C) from this interval (KIA32795, KIA32799 and KIA39232) also yielded too young calibrated $^{14}C$ ages, whereas sample KIA32797 appears to be ca. 100 years too old, probably due to redeposition of the dated material (bark).

For the Lateglacial interval, AMS $^{14}C$ dating and varve counting were not possible due to the lack of datable terrestrial macro remains and the failure to prove the annual origin of the fine lamination in Lithozones I, II and IV. Layer counting within the Lateglacial Interstadial interval (Lithozones II to IV) revealed a total of ~800 laminae couplets, which is significantly less than reported from proven annually laminated lake sediment records (e.g. Brauer *et al.* 1999b) and the Greenland ice cores (Rasmussen *et al.* 2006). However, a hiatus as a possible explanation for this difference is excluded because of the close agreement of the $\delta^{18}O$ record even for small-scale fluctuations with other Alpine isotope records (e.g. Eicher 1987; Lotter *et al.* 1992; von Grafenstein *et al.* 1999a). Therefore, the Lateglacial age model was compiled by wiggle matching the Lake Mondsee ostracod-derived $\delta^{18}O$ record to the NGRIP record from Greenland, using the recent GICC05 chronology (Rasmussen *et al.* 2006), which was corrected by an offset of -65 years (Muscheler *et al.* 2008) and transferred to the BP time scale. Six distinct isotopic marker points were identified in both the Lake Mondsee and the NGRIP $\delta^{18}O$ record (Fig. 3.7A) with the corresponding ages in the NGRIP record being used as tie points for the Lake Mondsee Lateglacial chronology (Table 3.1). Sample ages were linearly interpolated between the varve-dated base of Lithozone V and these tie points with thick turbidites being excluded as instantaneous (time-neutral) depositional events. Owing to the lack of isotopic markers in Lithozone I, no age model was established for the interval prior to 14 625 cal. a BP.

The Younger Dryas-Holocene boundary in the Lake Mondsee sediment record is defined by both biostratigraphy, namely the top of LPAZ 6 at 1130.0 cm, and the pronounced $\delta^{18}O$ rise between 1131.5 and 1130.0 cm. The assigned age of 11 580–11 540 cal. a BP is similar to the Lake Meerfelder Maar varve chronology (11 590 varve (calendar) years BP; Brauer *et al.* 1999a), the German pine chronology (11 570 cal. a BP; Friedrich *et al.* 1999) and the corrected NGRIP GICC05 chronology (11 605-11 545 cal. a BP; Rasmussen *et al.* 2006; Muscheler *et al.* 2008).

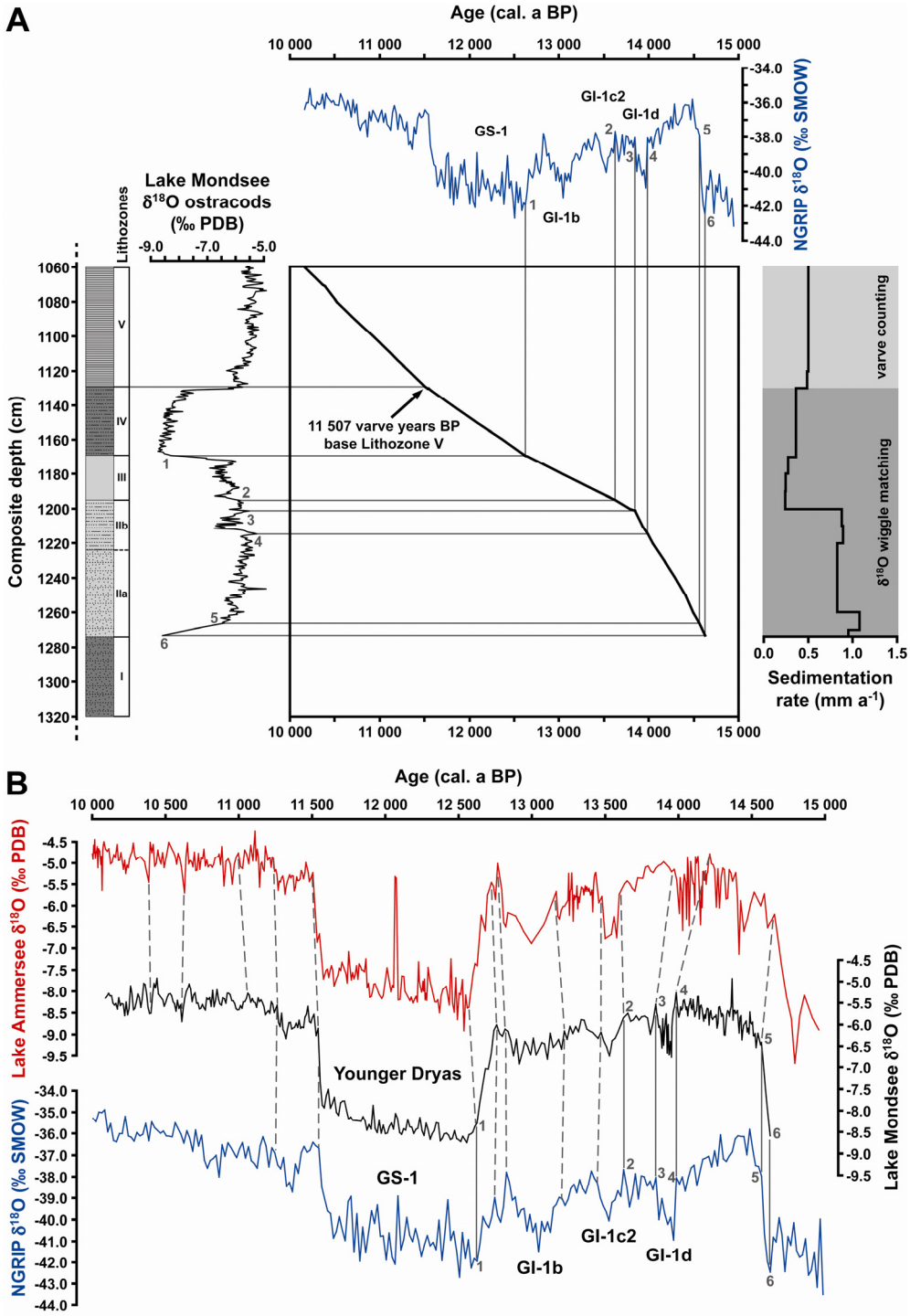


**Figure 3.7** (A) Age-depth model of the Lateglacial part of the Lake Mondsee sediment record based on wiggle matching between the $\delta^{18}O$ records from Lake Mondsee and NGRIP, the latter plotted according to the GICC05 chronology (Rasmussen *et al.* 2006), corrected by an offset of -65 years (Muscheler *et al.* 2008). For further information on the chronological tie points please see the text and Table 3.1. (B) Comparison of the NGRIP, Lake Mondsee and Lake Ammersee (von Grafenstein *et al.* 1999a) $\delta^{18}O$ records. Solid lines and Arabic numerals in both figures indicate the six tie points used for the construction of the Lateglacial age model (Table 3.1). The varve counting-based age of 11 507 varve (calendar) years BP for the base of Lithozone V at 1129.0 cm in the Lake Mondsee record is used as an additional tie point for the Lateglacial age model. Additional dashed lines reveal the close agreement between the records. Slight differences between the Lake Mondsee and Lake Ammersee $\delta^{18}O$ records prior to ca. 13 500 cal. a BP might be an artefact of the different approaches used for establishing the chronologies.

Temporal resolution for pollen, stable isotope and carbon geochemistry data is in the order of ca. 5–60 years throughout the investigated interval with highest resolutions across climatic transitions. µ-XRF measurements are continuously sub-annually resolved.

**Table 3.1** Chronological tie points used for the establishment of the Lateglacial age-depth model of the Lake Mondsee sediment record. Isotopic marker points in the Lake Mondsee $\delta^{18}O$ record are given with their depth in the composite profile and corresponding ages in the NGRIP record (Rasmussen *et al.* 2006). Sample ages between these tie points were interpolated linearly.

| Marker point | Marker point description | Age (cal. a BP) | Lake Mondsee composite depth (cm) |
|---|---|---|---|
| | base of Lithozone V in Lake Mondsee, age determined by varve chronology | 11 507 | 1129.00 |
| 1 | end of GI-1/GS-1 transition in Greenland | 12 625[a] | 1169.25 |
| 2 | onset of Greenland isotope substage GI-1c2 | 13 625 [a] | 1195.25 |
| 3 | end of Greenland isotope substage GI-1d | 13 845 [a] | 1201.25 |
| 4 | onset of Greenland isotope substage GI-1d | 13 985 [a] | 1214.75 |
| 5 | end of Pleniglacial-Lateglacial $\delta^{18}O$ rise in Greenland | 14 565 [a] | 1266.25 |
| 6 | onset of Pleniglacial-Lateglacial $\delta^{18}O$ rise in Greenland | 14 625 [a] | 1273.25 |

[a] the Greenland GICC05 chronology (Rasmussen *et al.* 2006) was transferred from years b2k (before AD 2000) into cal. a BP (before present/AD 1950) and shifted by -65 years (Muscheler *et al.* 2008)

## 3.5 Discussion

### *3.5.1 Proxy response to warming at the onset of the Lateglacial and Holocene*

The Pleniglacial period was characterized by predominantly clastic-detrital sedimentation, which reflects extensive catchment erosion favoured by the sparse, shrub- and herb-dominated vegetation. Subsequent rapid warming at the onset of the Lateglacial Interstadial is clearly reflected by the marked $\delta^{18}O$ rise at the base of Lithozone IIa (Figs. 3.5 and 3.8), which according to the correlation with the NGRIP chronology occurred between 14 625 and 14 565 cal. a BP.

Detrital input slightly decreased but prevailed for another ca. 500 years until 14 100 cal. a BP (base of Lithozone IIb), indicating a rather slow initial catchment stabilization. During the following

ca. 250 years (14 100–13 850 cal. a BP), the decrease of allochthonous matter flux accelerated (Fig. 3.4), likely as a result of the establishment of dense *Pinus* forests and related catchment stabilization. Gradual soil development during the first ca. 750 years of the Lateglacial is also indicated by decreasing $\delta^{13}C$ values, reflecting the increased supply of $^{13}C$-depleted $CO_2$ from soil respiration (Hammarlund *et al.* 1997). The timing of the *Pinus* expansion in the Lake Mondsee record around 14 000 cal. a BP is consistent with results from other Alpine sites (Draxler 1977; Ammann & Lotter 1989; Lotter 1999; Schmidt *et al.* 2002). As temperatures at the northern Alpine margin were sufficient for forest establishment already several hundred years earlier (Ammann 1989), which is also indicated by the Lake Mondsee $\delta^{18}O$ record, the delay in the spread of *Pinus* forests rather reflects not a climatic signal but migrational lags (Gaillard 1985; Ammann *et al.* 1994) and slow soil development. Delayed forest establishment might have been amplified by discontinuous permafrost (Hoek 2001), which was preserved in the catchment area during the early Lateglacial Interstadial (van Husen 1997). Permafrost persistence could also explain the high detrital matter flux until ca. 14 100 cal. a BP, as reduced seepage would have caused enhanced surface runoff and erosion (Stebich *et al.* 2009). Although microscopic evidence for the first occurrence of endogenic calcite at the base of Lithozone IIa clearly indicates a synchronous productivity increase in response to the warming at about 14 600 cal. a BP, the major rise in Ca counts and TIC contents occurred only after 14 100 cal. a BP. This might be related to dilution effects through the dominant detrital matter flux (Loizeau *et al.* 2001) during the first ca. 500 years of the Lateglacial Interstadial.

In contrast to the gradual environmental changes at the onset of the Lateglacial Interstadial, environmental response to the Holocene warming was more rapid and reveals less pronounced leads and lags between proxy data (Fig. 3.9). Both the reduction of surface runoff and the increase in calcite precipitation started synchronously with the rapid 2‰ $\delta^{18}O$ rise, but continued for further ca. 60 years after $\delta^{18}O$ had already reached Holocene levels. Also the decline of shrub vegetation and the recovery of *Pinus* forests occurred parallel to the pronounced $\delta^{18}O$ rise between ca. 11 580 and 11 540 cal. a BP. In particular, the biostratigraphically defined end of the Younger Dryas (LPAZ 6) coincides with the end of the $\delta^{18}O$ rise. Immediate forest recovery in response to the temperature rise was possible because *Pinus* forests had survived locally during the Younger Dryas, proving the importance of ecological preconditions for the reflection of climatic changes in the pollen record (cf. Jones *et al.* 2002).

---

**Figure 3.8** Detailed comparison of selected proxy data from the Lake Mondsee sediment record during the Lateglacial Interstadial. Grey shaded areas indicate periods of major proxy changes given with their approximate duration in years. Oxygen isotope ratios obtained from juvenile ostracod valves (not corrected for the species-specific vital offset) are considered as a temperature proxy. Thin lines in the results of µ-XRF element scanning represent measurements at 200 µm resolution. Thick lines indicate a 25-point running mean. Small-scale cold events seen in the oxygen isotope record (Mo-LG2 and Mo-LG3; for further explanations see the text) are reflected by reductions in TIC and Ca counts, both considered as a proxy for biochemically precipitated calcite. Al counts reflect the corresponding increase of siliciclastic detrital input and particularly the occurrence of clay layers during cooling events Mo-LG2 and Mo-LG3. The *Pinus* pollen record reveals that small-scale coolings had no/only minor influence on local forest vegetation.

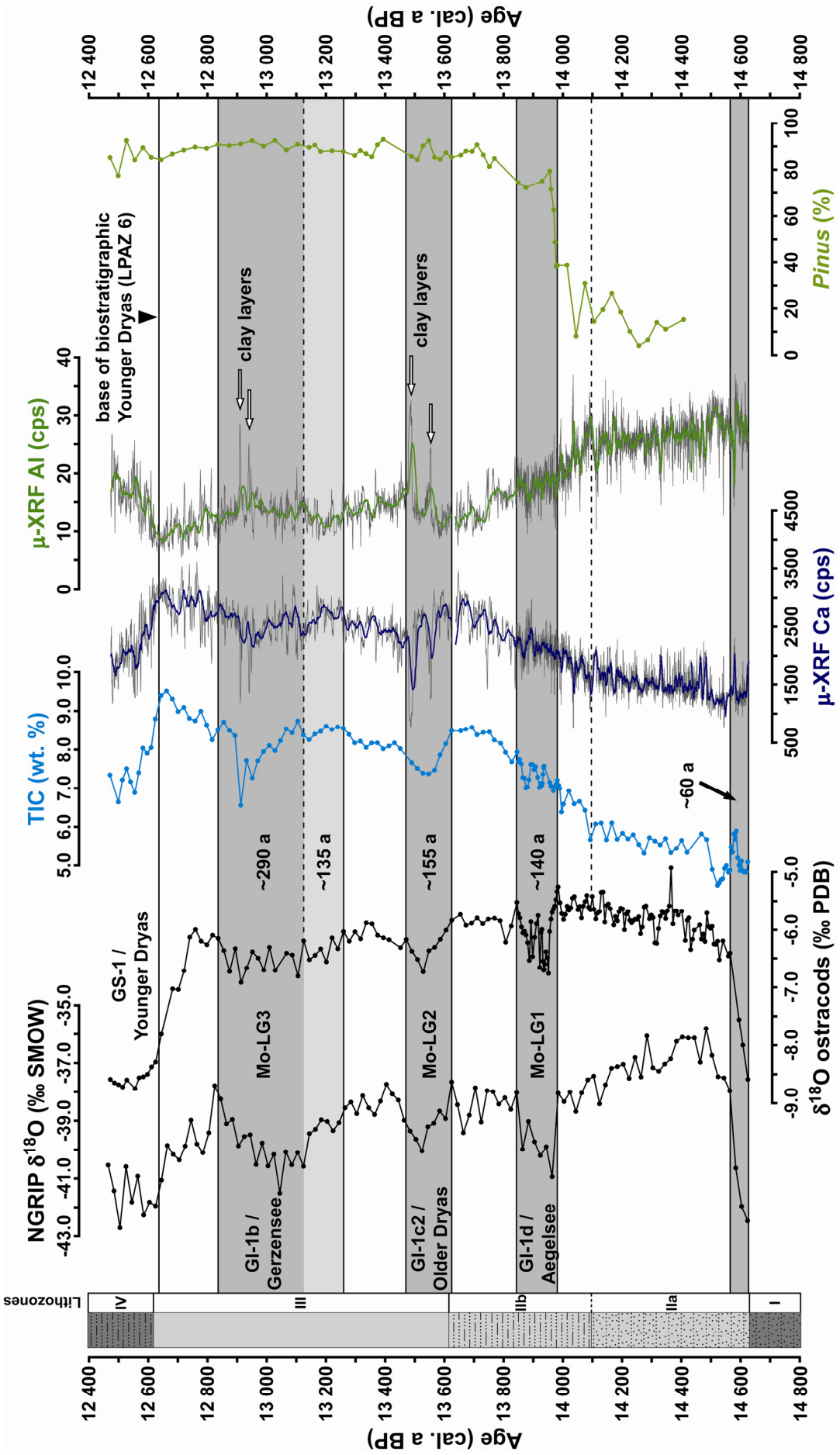
Age (cal. a BP)
12 400
12 600
12 800
13 000
13 200
13 400
13 600
13 800
14 000
14 200
14 400
14 600
14 800
Lithozones
IV
III
IIb
IIa
I
NGRIP δ18O (‰ SMOW)
-43.0 -41.0 -39.0 -37.0 -35.0
GS-1 / Younger Dryas
Gi-1b / Gerzensee
Mo-LG3
Gi-1c2 / Older Dryas
Mo-LG2
Gi-1d / Aegelsee
Mo-LG1
~290 a
~135 a
~155 a
~140 a
~60 a
TIC (wt. %)
5.0 6.0 7.0 8.0 9.0 10.0
μ-XRF Al (cps)
0 10 20 30 40
μ-XRF Ca (cps)
500 1500 2500 3500 4500
δ18O ostracods (‰ PDB)
-9.0 -8.0 -7.0 -6.0 -5.0
Pinus (%)
0 20 40 60 80 100
base of biostratigraphic Younger Dryas (LPAZ 6)
clay layers
clay layers

### *3.5.2 Proxy response to cooling at the onset of the Younger Dryas*

Climatic deterioration at the beginning of the Younger Dryas is well reflected by a 2.5‰ drop in $\delta^{18}O$ between ca. 12 760 and 12 590 cal. a BP. The slight *Pinus* decrease, which started already parallel to the $\delta^{18}O$ drop, was followed by the increase of NAP (used for the biostratigraphic definition of the Younger Dryas onset at the base of LPAZ 6) within the second half of the oxygen isotope decrease at about 12 640 cal. a BP. This indicates a short response time of local vegetation to climatic forcing. Simultaneous changes in vegetation and oxygen isotopes at the onset of Younger Dryas have also been described from Switzerland (Ammann *et al.* 2000) and Poland (Goslar *et al.* 1993). In the Lake Mondsee record, the expansion of shrub, grassland and herb communities at the base of LPAZ 6 was accompanied by a reduction in tree pollen concentrations, indicating opening of forest cover and reduced flowering in response to cooler climate conditions (Rundgren & Ingólfsson 1999). However, vegetation feedback was not as pronounced as at sites closer to ecotone boundaries, i.e. at higher altitudes (Ammann *et al.* 1993; Birks & Ammann 2000; Wick 2000) or closer to the remaining Scandinavian Ice Sheet (Goslar *et al.* 1993; Litt & Stebich 1999; Merkt & Müller 1999).

In contrast to the vegetation response, changes in the sedimentation regime around the onset of the Younger Dryas were rather complex. Microfacies analysis reveals a first minor increase in detrital matter flux (reappearance of faint silt-clay laminae) parallel to the onset of the $\delta^{18}O$ decrease. This indicates that, similar to the end of the Younger Dryas, a subtle sedimentological change occurred synchronously with the climatic shift. However, more pronounced changes in the sedimentation regime as the reduction of calcite precipitation and the increase of allochthonous flux only occurred at the end of the temperature decrease around 12 620 cal. a BP and continued for ca. 60 years after $\delta^{18}O$ had already reached the low Younger Dryas level (Fig. 3.9). The delay in the reduction of calcite precipitation is difficult to explain because the presence of endogenic calcite in the sediments is influenced by a variety of factors, e.g. temperature, lake productivity or water chemistry. For example, a gradual increase in aridity or the establishment of permafrost might have reduced the availability of carbonate ions through groundwater flux and thus caused a delayed reduction in calcite precipitation. It could also reflect temperature threshold effects as endogenic calcite formation can persist even under low temperatures (Ohlendorf & Sturm 2001).

---

**Figure 3.9** Detailed comparison of selected proxy data from the Lake Mondsee sediment record across the Allerød-Younger Dryas and Younger Dryas-Holocene transitions. Grey shaded areas indicate periods of major proxy changes with their approximate duration given in years. Oxygen isotope ratios obtained from juvenile ostracod valves are not corrected for the species-specific vital offset. Thin grey lines in the results of µ-XRF element scanning represent measurements at 200 µm resolution. Thick coloured lines indicate a 25-point running mean. µ-XRF Ca counts are considered as a proxy for biochemically precipitated calcite, whereas Mg counts reflect detrital input (dolomite). Pollen records of NAP and *Juniperus* are plotted as representatives for shrub/herb vegetation.

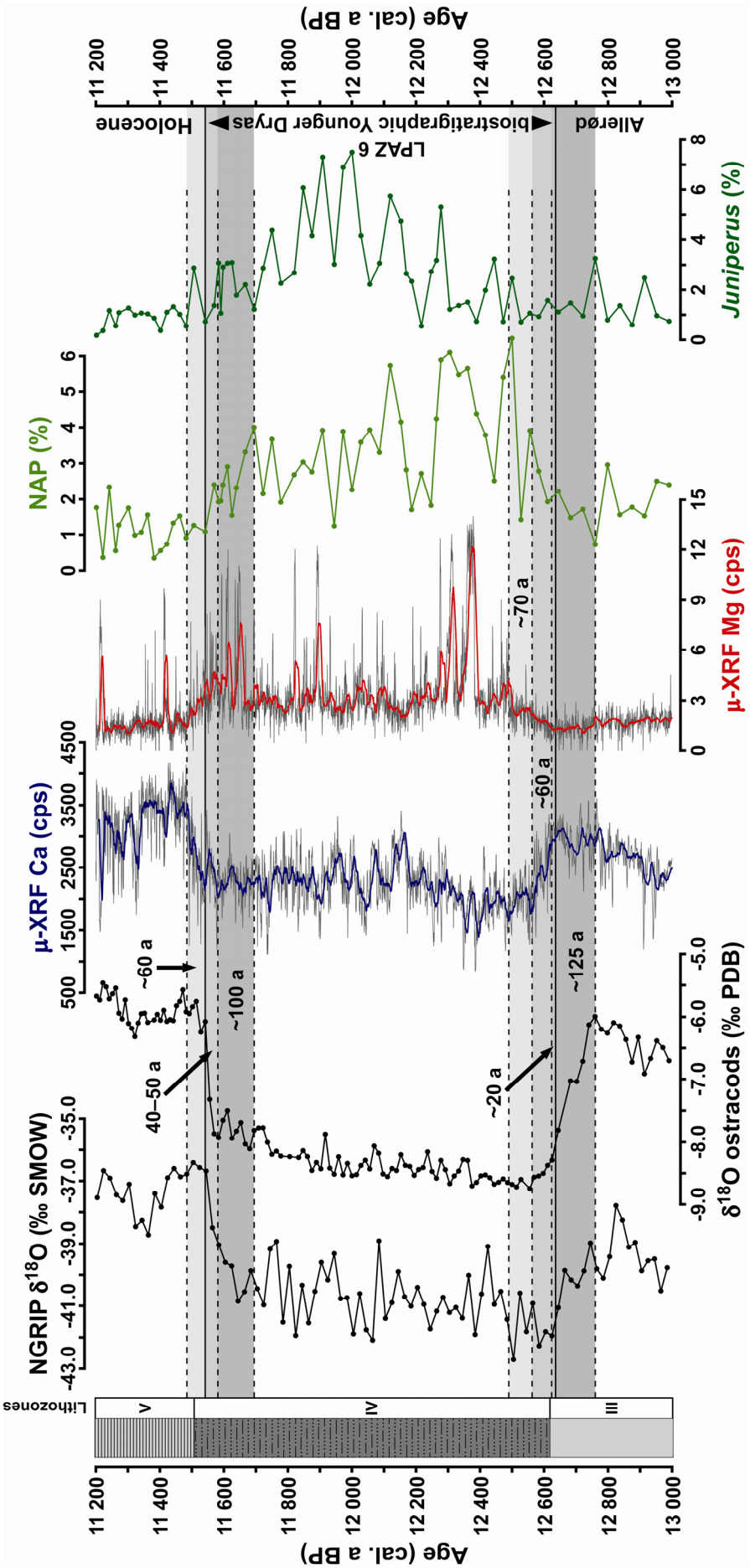
Age (cal. a BP)
11 200
11 400
11 600
11 800
12 000
12 200
12 400
12 600
12 800
13 000
Holocene
Younger Dryas
Allerød
biostratigraphic
LPAZ 6
Juniperus (%)
0
2
4
6
8
NAP (%)
0
1
2
3
4
5
6
μ-XRF Mg (cps)
0
3
6
9
12
15
μ-XRF Ca (cps)
500
1500
2500
3500
4500
δ18O ostracods (‰ PDB)
-5.0
-6.0
-7.0
-8.0
-9.0
NGRIP δ18O (‰ SMOW)
-35.0
-37.0
-39.0
-41.0
-43.0
~60 a
~100 a
40–50 a
~70 a
~60 a
~20 a
~125 a
Lithozones
V
IV
III

Moreover, also seasonality might have played a role as endogenic calcite formation is a proxy for spring/summer conditions and there is evidence from model studies (Isarin *et al.* 1998) and proxy data (Lücke & Brauer 2004) that Younger Dryas winter cooling was more severe than the drop in summer temperatures. The delay in the first occurrence of distinct turbidites, which were deposited only ca. 130 years after the general increase of detrital flux, could be related to the gradual build-up of discontinuous permafrost in the catchment (cf. Stebich *et al.* 2009), but might also reflect the persistence of perennial snow fields or the build-up of small local glaciers in the Northern Calcareous Alps.

### *3.5.3 Proxy response to short-term Lateglacial coolings*

The relatively warm conditions during the Lateglacial Interstadial are punctuated by three short negative $\delta^{18}O$ excursions of 0.8–1.5‰, labelled as Mo-LG1, Mo-LG2 and Mo-LG3, which are interpreted as cold intervals (Fig. 3.8).

Mo-LG1 is characterized by a ~1.5‰ drop in $\delta^{18}O$, which lasted about 140 years (ca. 13 985–13 845 cal. a BP) and corresponds to Greenland isotope substage GI-1d (Björck *et al.* 1998), the Aegelsee oscillation in Switzerland (Lotter *et al.* 1992) and a period of higher detrital flux (MK-4) in Lake Meerfelder Maar (Brauer *et al.* 2000). Rapid fluctuations superimposed on the general decrease in $\delta^{18}O$ may result from the high temporal resolution (ca. 4 years per sample) during this interval as a consequence of the high sedimentation rate in Lithozone IIb. As Mo-LG1 occurred still within the 750-year period of elevated detrital matter flux during the early Lateglacial Interstadial, the $\delta^{18}O$ decrease is not clearly reflected by sedimentological changes (Fig. 3.8). Also vegetation development reveals an ambiguous response to the Mo-LG1 cooling as the replacement of *Juniperus* by *Pinus* forests rather indicates successive forest stabilization than climatic deterioration. Thus, climatic and vegetational development during this period appear to be decoupled, most probably owing to the superimposed migration processes (Ammann *et al.* 1994).

Cold interval Mo-LG2, which is characterized by a ~1.0‰ drop in $\delta^{18}O$, lasted ca. 155 years (ca. 13 625–13 470 cal. a BP). It correlates to a short period of lower $\delta^{18}O$ values in the Lake Ammersee record (von Grafenstein *et al.* 1999a), to the ca. 180-year-long isotope substage GI-1c2 in the Greenland ice core records (Björck *et al.* 1998; Rasmussen *et al.* 2006) and probably to the Older Dryas pollen zone in the Eifel Maar lakes (Brauer *et al.* 2000). In contrast to Mo-LG1, the $\delta^{18}O$ decrease coincides with a marked negative oscillation in Ca counts and TIC contents, reflecting the response of calcite precipitation to decreasing temperatures (Brunskill 1969; Kelts & Hsü 1978). Two distinct negative spikes in the Ca record and corresponding positive Al peaks are due to the presence of discrete clay layers (Figs. 3.3 and 3.8), reflecting siliciclastic detrital matter deposition by extreme surface runoff events. The direct coupling between climate change and sedimentological response during cold interval Mo-LG2 provides evidence that under certain conditions even sedimentation in a

large lake system is sensitive to minor climate changes. In contrast to the clear sedimentological shift, the pollen record reveals only a subdued response during Mo-LG2, suggesting that local forest cover at this time was sufficiently stable to compensate for the low-amplitude cooling. Although subtle changes in different *Pinus* species (Schmidt *et al.* 2002) cannot be excluded, the temperature decrease was, even if higher herb pollen and lower *Pinus* and *Betula* concentrations indicate a slight reduction in forest cover, not sufficient to exceed a critical threshold necessary for a major shift in forest composition. This probably reflects a certain insensitivity of vegetation at sites far from ecotone boundaries to small-scale climatic changes (Wohlfarth *et al.* 1994; Walker 1995).

The ~0.8‰ decrease in $\delta^{18}O$ during Mo-LG3 lasted for ca. 290 years (ca. 13 125–12 835 cal. a BP) and corresponds to Greenland isotope substage GI-1b (Björck *et al.* 1998) and the Gerzensee oscillation in Switzerland (Eicher & Siegenthaler 1976; Lotter *et al.* 1992). The peak amplitude of the gradual $\delta^{18}O$ decrease appears to be smaller than for the preceding two cold intervals, which is different than in Lake Ammersee (von Grafenstein *et al.* 1999a) and the Greenland ice cores (Rasmussen *et al.* 2006) and might be related to variations in local hydrology. The temperature decrease during Mo-LG3 was directly paralleled by a reduction in calcite precipitation after about 13 125 cal. a BP, reflected by drops in TIC contents and Ca counts, (Fig. 3.8). Moreover, rising temperatures at the end of Mo-LG3 (ca. 12 910–12 835 cal. a BP) were paralleled by immediately increasing endogenic calcite contents. It is also striking that even the gradual $\delta^{18}O$ decrease by about 0.5‰ during the ca. 135 years prior to Mo-LG3 is reflected by fluctuations in endogenic calcite contents. Although two discrete clay layers, reflected by discrete Al peaks, indicate sporadic surface runoff events, the interval between ca. 13 615 and 12 620 cal. a BP is characterized by rather low detrital contents and thus low erosion rates. This might be related to (1) increased aridity and thus decreased snow meltwater discharge/surface runoff, (2) increased infiltration of precipitation due to the disappearance of permafrost or (3) further soil stabilization through the spread of dense and stable late Allerød forest communities dominated by *Pinus*. Their ability to compensate low-amplitude cooling (Lotter *et al.* 1992; Wick 2000) would explain the lack of a clear vegetational response to the Mo-LG3 cooling. The subdued reaction is restricted to slight reductions in the concentrations of tree pollen and *Dryopteris filix-mas* spores, indicating reduced flowering due to climatic cooling during this interval.

## 3.6 Conclusions

The combination of continuous microfacies data and sub-decadally to sub-annually resolved multi-proxy analyses provides new information on the environmental response of a rather large pre-Alpine lake system to rapid Lateglacial climatic fluctuations.

Major warmings at the onset of the Lateglacial and Holocene reveal differential environmental responses, largely controlled by the ecological and climatic preconditions. While lake productivity

responded immediately to the warming at 14 600 cal. a BP, the spread of woodlands in the surroundings and the decrease of detrital flux lagged the temperature increase by 500–750 years. Causes for the delay were persistent permafrost, plant-specific migrational lags and slow catchment stabilization. In contrast, immediate ecosystem recovery within ca. 100 years in response to the Holocene temperature rise was favoured by already established forest cover and stable soils. Shifts in local vegetation and temperature at the onset of the Younger Dryas occurred broadly synchronously. Although subtle sedimentological changes occurred at about the same time, the pronounced reduction of calcite precipitation, the general increase of detrital flux and the deposition of distinct detrital layers lagged the onset of the cooling by 150–300 years. This complex sedimentological response reflects the inertia of a large lake system, but probably also seasonal effects.

Sedimentological responses to short-term Lateglacial coolings are complex and largely determined by the environmental preconditions. As sedimentological changes during cold intervals are commonly characterized by variations in detrital flux, they are better recognizable during intervals of mainly autochthonous sedimentation (Mo-LG2, Mo-LG3), but hardly detectable for intervals with predominantly detrital sedimentation (Mo-LG1). The absence of a clear vegetational response to the low-amplitude Lateglacial coolings indicates a low climate sensitivity of local *Pinus* woodlands once a stable forest cover was established.

## 3.7 Acknowledgements

This study, carried out within the frame of the European Science Foundation EUROCORES Programme EuroCLIMATE (contract No. ERAS-CT-2003-980409 of the European Commission, DG Research, FP6, ESF project DecLakes no. 04-ECLIM-FP29), has been made possible thanks to the support and funding from the national agencies FWF (Austria, project no. I35-B06), DFG (Germany, project no. BR2208/2-2, AN554/1-2) and CNRS (France). We thank Jean-Louis Reyss (LSCE, Gif-sur-Yvette) for $^{137}$Cs dating, Rudolf Naumann (GFZ, Potsdam) for providing XRD measurements, Juliane Herwig (GFZ, Potsdam) for assistance with the scanning electron microscope, Manuela Dziggel (GFZ, Potsdam) for help with some figures, Georg Schettler (GFZ, Potsdam) for help with carbon geochemistry analyses, Gertraud Roidmayr (Institute for Limnology, Mondsee) for picking ostracods and Richard Niederreiter (UWITEC, Mondsee) and Johann Knoll (Institute for Limnology, Mondsee) for assistance during the coring campaign. The laboratory staff at the contributing institutes are acknowledged for preparing numerous samples and running measurements smoothly. Furthermore, we are indebted to the Institute for Water Ecology, Fisheries and Lake Research in Scharfling, particularly Albert Jagsch, for providing logistical support in organising the field lab. We acknowledge the valuable comments of Roland Schmidt (Institute for Limnology, Mondsee), Michel Magny (Université Franche-Comté, Besançon) and an anonymous reviewer on an earlier version of the manuscript.

# 4 Were there overshooting warm temperatures in Central Europe after the abrupt 8.2 ka and 9.1 ka cold events?

Nils Andersen[1], Stefan Lauterbach[2], Dan L. Danielopol[3], Tadeusz Namiotko[3,4], Matthias Hüls[1], Helmut Erlenkeuser[1], Achim Brauer[2], Ulrich von Grafenstein[5] and DecLakes participants[6]

[1] Christian-Albrechts-University, Leibniz Laboratory for Radiometric Dating and Stable Isotope Research, D-24118 Kiel, Germany

[2] GFZ German Research Centre for Geosciences, Section 5.2 – Climate Dynamics and Landscape Evolution, D-14473 Potsdam, Germany

[3] Austrian Academy of Sciences, Institute for Limnology, A-5310 Mondsee, Austria; present address: Austrian Academy of Sciences, Commission for the Stratigraphical & Palaeontological Research of Austria, c/o Institute of Earth Sciences, Geology and Palaeontology, University of Graz, A-8010 Graz, Austria

[4] University of Gdańsk, Department of Genetics, Laboratory of Limnozoology, PL-80-822 Gdańsk, Poland

[5] Laboratoire des Sciences du Climat et de l'Environnement, UMR CEA-CNRS, F-91191 Gif-sur-Yvette, France

[6] Ángel Baltanás (UAM, Madrid), Soumaya Belmecheri (LSCE, Gif-sur-Yvette), Marc Desmet (ISTO, Tours), Bernard Fanget (EDYTEM, Chambery), Jérôme Nomade (LGCA, Grenoble)

***ABSTRACT*** *A new varve-dated high-resolution oxygen isotope record of deep-living ostracods from Lake Mondsee (Austria) indicates the occurrence of pronounced cold spells around 8200 and 9100 cal. a BP in Central Europe. The total duration (ca. 150 years) and the absolute dating of the so-called 8.2 ka event are in perfect agreement with results from other palaeoclimate archives. Interestingly, our data also indicate overshooting air temperatures of about +0.7°C directly after the 8.2 ka cold phase. This ca. 100-year-long temperature overshooting in Central Europe is consistent with results from coupled climate models and occurred synchronous to overshooting temperatures in Greenland, thus probably reflecting a temperature increase on a hemispheric scale, driven by enhanced Atlantic meridional overturning circulation (MOC). This strengthening of the MOC most likely also caused synchronous migrations of the Arctic Front and the Intertropical Convergence Zone (ITCZ), reflected in proxy records from the North Atlantic and the Cariaco Basin, respectively. In contrast to the 8.2 ka cold phase, no overshooting warm temperatures are recognized directly after the 9.1 ka cold phase in the Lake Mondsee oxygen isotope record, most likely due to the relative weakness and short duration (ca. 70 years) of this cold phase and the only subdued subsequent MOC resumption. In addition, a prominent warm period in Central Europe around 8800 cal. a BP that apparently corresponds to a wet period in the Cariaco Basin, was probably also driven by strong MOC. These results indicate the complex behaviour of the global climate system and should be considered when modelling the MOC resumption after abrupt cooling events.*

## 4.1 Introduction

Although the Holocene is generally considered as a period of relatively stable climate conditions, numerous studies have shown that it was interrupted by several short low-amplitude cold periods (cf. Mayewski *et al.* 2004; Wanner *et al.* 2008). Among these, the so-called 8.2 ka event, which has been detected in various palaeoclimate archives worldwide (cf. Rohling & Pälike 2005), represents the most significant Holocene climate anomaly. Although initially presented as an example for the sensitivity of the North Atlantic oceanic circulation to weak freshwater forcing (Alley *et al.* 1997), it was most likely triggered by the catastrophic drainage of the ice-dammed lakes Agassiz and Ojibway (von Grafenstein *et al.* 1998; Barber *et al.* 1999; Wiersma & Renssen 2006; Renssen *et al.* 2007), causing a shutdown of the meridional overturning circulation (MOC) in the North Atlantic (Ellison *et al.* 2006; LeGrande *et al.* 2006; Kleiven *et al.* 2008) and subsequent cooling in the surrounding areas. However, very little is known about climate recovery after the 8.2 ka cold phase, although a "climate overshoot" around 7900 cal. a BP has been described by Ellison *et al*. (2006) and model results also indicate a significant overshooting of the MOC by more than 30% (e.g. Stouffer *et al.* 2006; Renold *et al.* 2010). Moreover, the synchrony of the response to freshwater discharges in different areas (e.g. Daley *et al.* 2009) and the internal structure of the 8.2 ka cold phase are also still matter of debate. For example, in some records the 8.2 ka cold period is separated into two cooling events (Ellison *et al.* 2006), eventually forced by two distinct freshwater outbursts (Teller *et al.* 2002) and/or the retarded melting of drifting icebergs from the collapse of the Hudson Bay ice dome (Wiersma & Jongma 2010), but not all high-resolution studies show this bipartition of the 8.2 ka cold phase (e.g. Boch *et al.* 2009). Global impact of MOC variability during the 8.2 ka cold period has been postulated on the basis of precisely dated stalagmite oxygen isotope records (Cheng *et al.* 2009), revealing an antiphase relationship between weak Asian summer monsoon and strong South American summer monsoon. This was probably related to shifts in the latitudinal position of the Intertropical Convergence Zone (ITCZ), driven by MOC variability. Another prominent Holocene cold phase occurred prior to 9000 cal. a BP. Although either termed 9.1 ka (e.g. Boch *et al.* 2009), 9.2 ka (e.g. Fleitmann *et al.* 2008) or 9.3 ka event (e.g. von Grafenstein *et al.* 1999a; Rasmussen *et al.* 2007) in different records, all these climate perturbations most likely refer to the same cold phase (see below). A rapid freshwater discharge event, although of uncertain origin and probably much smaller magnitude than those triggering the 8.2 ka event, has also been proposed to trigger this cold period (Fleitmann *et al.* 2008; Yu *et al.* 2010).

This study presents a new sub-decadally resolved $\delta^{18}O$ record obtained from the valves of deep-living ostracods found in the sediments of Lake Mondsee (Austria). By discussing the reflection of the cold periods around 8200 and 9100 cal. a BP as well as the possible occurrence of subsequent temperature overshoots in the Lake Mondsee record and putting the results in a large-scale context, we provide new information that improves the understanding of rapid climate fluctuations during the Holocene.

## 4.2 Material and methods

Two parallel sediment cores were recovered with a 90-mm-diameter UWITEC piston corer from the deep southern basin (62 m water depth) of Lake Mondsee (Fig. 4.1; 47°48'N, 13°24'E, 481 m above sea level, surface area ~14.2 km², catchment area ~247 km²), an oligo-mesotrophic hardwater lake located in Upper Austria, about 40 km east of Salzburg. The overlapping segments of the two sediment cores were correlated, resulting in a continuous ca. 15-m-long composite profile. The age model of the Holocene sediment record was established by counting of biochemical calcite varves on large-scale petrographic thin sections and is confirmed by accelerator mass spectrometry (AMS) $^{14}C$ dating of terrestrial plant macrofossils collected from the sediment cores (Fig. 4.S1 and Table 4.S1; for further details on the sediment core and the age model see Lauterbach *et al.* (in press)). The sediments of the composite profile were sampled at consecutive 0.5-cm-intervals (equivalent to a temporal resolution of ca. 7–8 years). The oxygen isotope composition ($\delta^{18}O$) of juvenile specimens of the ostracod *Candona neglecta*, prepared from the sediment samples (for details see the supplement), was analyzed with a MAT 251 mass spectrometer combined with a Kiel 1 (prototype) device.


**Figure 4.1** Overview map with the location of Lake Mondsee and other proxy records mentioned in the text and the average positions of the Intertropical Convergence Zone (ITCZ) in January and July and the Arctic Front.

*This part of the chapter will be only published electronically as supporting online material and does not appear in the print version of the manuscript.*

## *Supplement – Chronology of the Lake Mondsee $\delta^{18}O$ record across the 8.2 ka event*

The primary chronology of the Lake Mondsee sediment core and thus also that of the $\delta^{18}O$ record is based on counting of biochemical calcite varves (for details see Lauterbach *et al.* (i*n press*)). Two independent varve counts by different examiners yielded a maximum difference of about 50 years during the last ca. 2000 years, equal to a counting error of less than 3%. For the varve chronology of the interval around the 8.2 ka cold event we thus consider a similar uncertainty of ±50 years as a reasonable estimate. This error range is indicated in Figure 4.S1 by dashed lines.

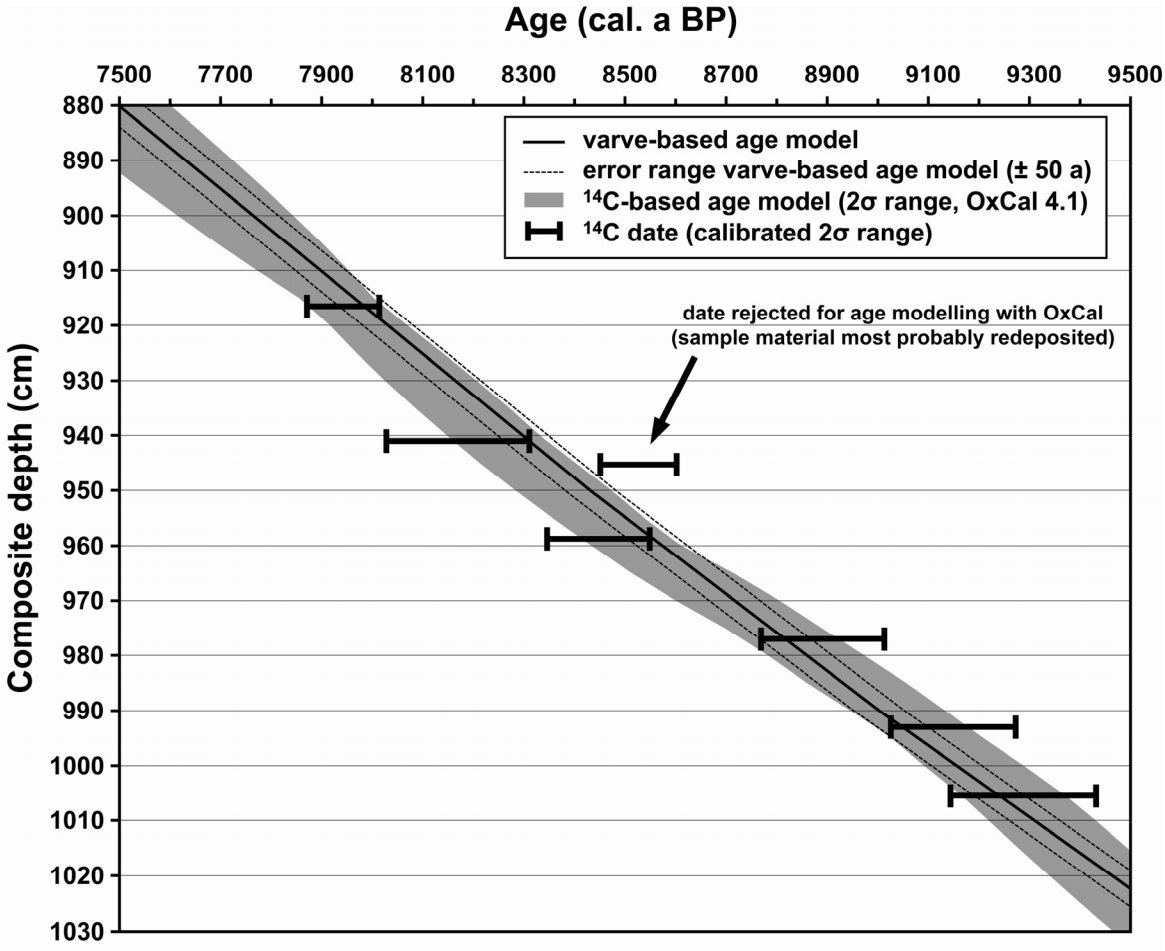


**Figure 4.S1** Comparison of the primary varve-based age model (given with a counting uncertainty of ±50 years as dashed lines) of the Lake Mondsee record and the secondary radiocarbon-based age model (shown as the 2σ probability range in grey), which has been established using OxCal (Ramsey 1995, 2001, 2008) to evaluate the reliability of the varve chronology. Individual AMS $^{14}C$ dates on terrestrial plant macrofossils are given with their 2σ probability ranges.

In order to further evaluate the reliability of the varve-based age model, we calculated a secondary age model based on AMS $^{14}$C dates from terrestrial plant macrofossils, which were dated at the Leibniz Laboratory for Radiometric Dating and Stable Isotope Research in Kiel, Germany (Lauterbach *et al.* in press). Twelve conventional radiocarbon dates (Table 4.S1) were calibrated using the OxCal 4.1 program (Ramsey 1995, 2001) with the IntCal09 calibration data set (Reimer *et al.* 2009). Two of these dates were omitted from subsequent $^{14}$C age modelling as they are inconsistent with the primary varve chronology, probably due to the very small sample size (KIA32795) and reworking of the dated material (KIA32797). The other ten calibrated ages were used as input parameters for the radiocarbon-based age-depth model (Fig. 4.S1), which was developed using the Bayesian-based *P_Sequence* deposition model (the model parameter *k* was set to 1) implemented in the OxCal 4.1 program (Ramsey 2008). In order to avoid model inconsistencies (e.g. large error ranges) at the upper and lower boundaries of the interval under investigation (7500–9500 cal. a BP), which usually occur when there is no dated sample, we chose a much larger interval for establishing the $^{14}$C-based model (ca. 6200–10 000 cal. a BP).

**Table 4.S1** Selected AMS $^{14}$C dates of terrestrial macrofossils from the Lake Mondsee sediment core. All conventional $^{14}$C ages were calibrated using the OxCal 4.1 program (Ramsey 1995, 2001) with the IntCal09 calibration data set (Reimer *et al.* 2009). Italicized samples were rejected from age modelling with OxCal (for further explanations see the text). For a full account on radiocarbon dates from the Lake Mondsee sediment record and the primary varve-based age model see Lauterbach *et al.* (in press).

| Sample / Lab. code | Composite depth (cm) | Dated material | Carbon content (mg) / $\delta^{13}$C ± σ (‰) | AMS $^{14}$C age (a BP ± σ) | Calibrated age (cal. a BP, 2σ |
|---|---|---|---|---|---|
| KIA32794 | 782.25 | leaves[a] | 1.04 / -30.09±0.15 | 5462±36 | 6194–6310 |
| KIA36619 | 818.75 | plant remains[b] | 1.65 / -26.55±0.13 | 5809±36 | 6498–6717 |
| *KIA32795* | *873.00* | *plant remains[b]* | *0.28 / -32.70±0.23* | *6088±104* | *6727–7246* |
| KIA32796 | 916.50 | leaves[a] | 3.29 / -29.61±0.09 | 7129±36 | 7869–8014 |
| KIA39231 | 941.00 | twig | 0.95 / -29.41±0.12 | 7349±48 | 8026–8311 |
| *KIA32797* | *945.25* | *bark* | *5.11 / -27.57±0.07* | *7766±35* | *8449–8602* |
| KIA36616 | 958.75 | plant remains[b] | 0.69 / -25.24±0.42 | 7631±61 | 8344–8549 |
| KIA36615 | 977.00 | plant remains[b] | 2.88 / -30.85±0.19 | 8019±35 | 8767–9013 |
| KIA32798 | 993.00 | bud scale | 1.65 / -25.73±0.21 | 8192±41 | 9024–9273 |
| KIA36617 | 1005.50 | seed | 4.66 / -21.20±0.34 | 8300±32 | 9142–9432 |
| KIA29397 | 1034.75 | seed | 1.37 / -23.89±0.14 | 8638±48 | 9529–9700 |
| KIA34503 | 1056.25 | bud scale | 1.33 / -29.18±0.10 | 8874±57 | 9743–10 184 |

[a] undetermined terrestrial leaf fragments

[b] various undetermined terrestrial plant remains (leaves, wood, seeds)

The final $^{14}C$-based age model yielded an agreement index $A_{model}$ of 70.2%, which is fairly above the critical threshold of 60% and thus proves the robustness of the model (Ramsey 1995, 2008). Comparison of the varve- and radiocarbon-based age models reveals a very close overall agreement with both models being statistically indistinguishable within their uncertainty ranges in the interval under investigation (7500–9500 cal. a BP) and thus supports the reliability of the primary varve-based age model.

***Supplement – Stable isotope measurements***

For oxygen isotope analyses, 0.5-cm-thick slices of bulk sediment were disaggregated in a 10% $H_2O_2$ solution. Ostracods were concentrated by wet sieving (>125µm) and afterwards rinsed in ethanol to avoid contamination with dissolved carbonate in tab water (von Grafenstein *et al.* 1998). From each sediment slice, juvenile specimens of the ostracod *Candona neglecta* (instars 5–8) were selected. The oxygen isotope composition ($\delta^{18}O$) of subsets of 14–15 ostracod valves (30–90 µg) was analyzed with a MAT 251 mass spectrometer combined with a preparative Kiel 1 (prototype) device. For evolving carbon dioxide, carbonates were reacted with 100% phosphoric acid ($H_3PO_4$) under vacuum at 75°C. The oxygen isotope composition of the ostracod valves is given relative to the Vienna PeeDee Belemnite (VPDB) standard in the conventional δ-notation with an analytical uncertainty of <0.07‰.

## 4.3 Results

In the Lake Mondsee $\delta^{18}O$ record (Figs. 4.2E, 4.3B and 4.S2C), the climate anomaly commonly referred to as the 8.2 ka event is preceded by a minor cooling around 8300 cal. a BP with a drop in $\delta^{18}O$ by about 0.4‰. The subsequent main cold phase around 8200 cal. a BP is characterized by a decrease in $\delta^{18}O$ by about 1.0‰. At the end of this cold phase, $\delta^{18}O$ values slowly increased by 1.3‰, reaching $\delta^{18}O$ values 0.4‰ above the 8.3 ka-reference level between ca. 8100 and 8000 cal. a BP. The duration of the minor cold phase was about 60 years, while the major cold phase, i.e. the 8.2 ka event *sensu stricto*, lasted from ca. 8225 to 8075 cal. a BP and reveals a clear asymmetry with a more rapid cooling (ca. 55 years) and a slow subsequent warming (ca. 95 years). The timing of the 8.2 ka event in the Lake Mondsee record as well as its duration of about 150 years (with a central cooling period of about 70 years) perfectly fit the results from the Greenland ice cores (Kobashi *et al.* 2007; Thomas *et al.* 2007) and other varved lake sediment records (e.g. Prasad *et al.* 2009; Zillén & Snowball 2009).

The total amplitude of the 8.2 ka event, compared to the long-term mean $\delta^{18}O$, is almost similar for different oxygen isotope records from Europe: ~1.2‰ in Lake Mondsee (Figs. 4.2E and 4.3B), ~1.2‰ in Lake Hawes Water in NW England (Fig. 4.3A; Marshall *et al.* 2007), ~1.1 ‰ in stalagmites

from Katerloch Cave in Austria (Fig. 4.3D and 4.3E; Boch *et al.* 2009) and ~1.0 ‰ in Lake Ammersee in Germany (Fig. 4.3C; von Grafenstein *et al.* 1998). Considering a temperature gradient of about 0.6‰/°C (von Grafenstein *et al.* 1998; Boch *et al.* 2009), these maximum amplitudes are equal to a cooling by about 2°C in the lake records, while Boch *et al*. (2009) estimated a slightly stronger cooling by about 3°C from analysis of the Katerloch Cave stalagmites, considering in addition the equilibrium oxygen isotopic fractionation factor between drip water and calcite.

The major climate perturbation around 9100 cal. a BP is characterized by a drop in $\delta^{18}O$ by about 0.8‰, lasting for about 70 years (Fig. 4.2E), which again reveals a close agreement with results from other studies (e.g. von Grafenstein *et al.* 1999a; Rasmussen *et al.* 2007). However, the absolute dating of this event in different archives varies between 9100 and 9300 cal. a BP (von Grafenstein *et al.* 1999a; Rasmussen *et al.* 2007; Fleitmann *et al.* 2008; Boch *et al.* 2009), which is most probably owed to chronological uncertainties. In consequence, climate events discussed in this study and particularly the interval referred here to as the 9.1 ka cold period, which we interpret as synchronous, do not necessarily show a strictly synchronous timing in the figures. Nevertheless, by using a mechanistic approach for coupling terrestrial, marine and ice core records and by considering model results, we are confident that the pronounced climate shifts in the different records occurred indeed synchronously.

Owing to its large catchment/surface area ratio and the high average annual precipitation (~1500 mm $a^{-1}$) in the region, modern lake water of Lake Mondsee is only very slightly enriched in $\delta^{18}O$ and $\delta^{2}H$ (-10.2‰ and -72.1‰, respectively) compared to the long-term isotopic composition of local precipitation (-10.5‰ and -75.5‰). The past oxygen isotope composition of the lake water ($\delta^{18}O_L$), calculated from deep-lake ostracod $\delta^{18}O$, should therefore provide a robust quantitative record of the oxygen isotope composition of past precipitation ($\delta^{18}O_P$). Hence, as $\delta^{18}O_P$ in Central Europe is mainly controlled by air temperature (Różański *et al.* 1992; Baldini *et al.* 2008), the oxygen isotope record from Lake Mondsee is supposed to mainly reflect air temperature variability.

## 4.4 Discussion

### *4.4.1 Evidence for overshooting warm temperatures and atmosphere/ocean circulation changes after the 8.2 ka event*

Distinct freshwater pulses from proglacial lakes Agassiz and Ojibway (Teller *et al.* 2002) caused two abrupt reductions of surface water temperatures in the North Atlantic around 8500 and 8300 cal. a BP (Ellison *et al.* 2006) as indicated by elevated percentages of the planktonic foraminifer *Neogloboquadrina pachyderma* sinistral (blue bars in Fig. 4.2D). Subsequent to the lowering of surface water temperatures, the strength of deep-water currents and thus MOC intensity significantly decreased during the 8.2 ka cold period (Fig. 4.2C) as reflected by a decrease in the mean grain size of sortable silt (SS) in the North Atlantic (Ellison *et al.* 2006).

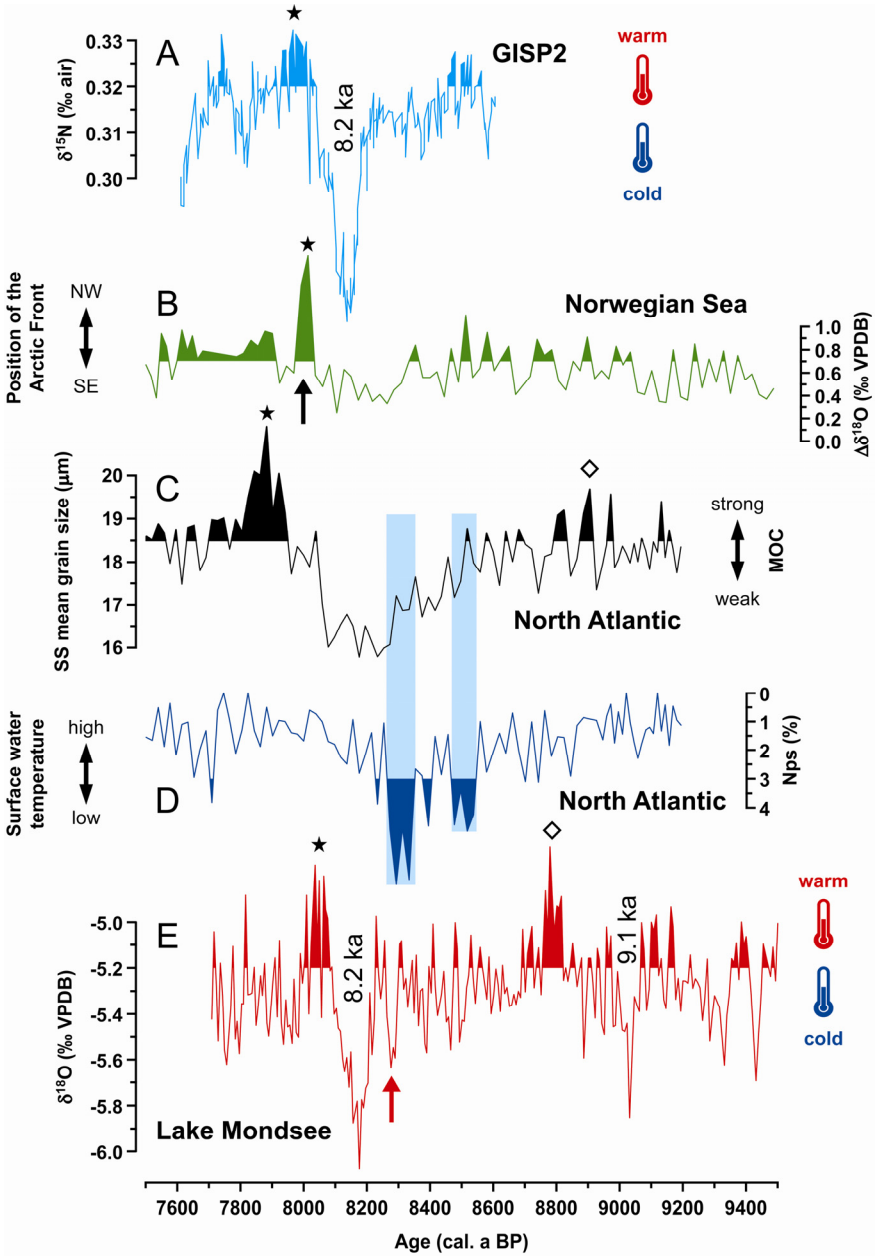


**Figure 4.2** Comparison of different palaeoclimate records for the interval 7500–9500 cal. a BP, indicating changes in the intensity of the Atlantic meridional overturning circulation (MOC) and associated shifts in air temperature in the North Atlantic realm. A: Nitrogen isotopes from the GISP2 ice core as a proxy for Greenland air temperature (Kobashi *et al.* 2007). B: Difference between $\delta^{18}O$ of *Neogloboquadrina pachyderma* sinistral (Nps) and *Neogloboquadrina pachyderma* dextral (Npd) from MD95-2011 (Norwegian Sea) as a proxy for the migration of the Arctic Front (Risebrobakken *et al.* 2003). Migration of the Arctic Front towards the northwest is indicated by a large contrast in $\delta^{18}O$ of both species (black arrow). C: Mean grain size of sortable silt (SS) from MD99-2251 (North Atlantic) as a proxy for MOC intensity (Ellison *et al.* 2006). D: Percentages of *Neogloboquadrina pachyderma* sinistral (Nps) from MD99-2251 (North Atlantic) as proxy for surface water temperature. Cold phases are indicated by high percentages of Nps (Ellison *et al.* 2006). Blue bars highlight two major reductions of surface water temperature in the North Atlantic prior to the decrease in MOC intensity during the 8.2 ka cold period, which have most probably been triggered by freshwater discharge from proglacial lakes Agassiz and Ojibway. E: Oxygen isotope composition of juvenile *Candona neglecta* valves from Lake Mondsee. The red arrow indicates the first minor cooling event at ca. 8300 cal. a BP. Solid asterisks and open diamonds mark climate overshoots, regarded to be synchronous in the different records.

Directly after the 8.2 ka cold period, enhanced MOC activity was observed (asterisk in Fig. 4.2C; Ellison *et al.* 2006), causing increased heat transport to the northern hemisphere and consequently higher temperatures there (Stouffer *et al.* 2006). This interpretation is in agreement with overshooting warm temperatures in Greenland directly after the 8.2 ka cold period. The increase in Greenland air temperature is most clearly reflected in the nitrogen isotope record from the GISP2 ice core (asterisk in Fig. 4.2A; Kobashi *et al.* 2007), being considered as a much better proxy for changes in Greenland air temperature than the oxygen isotope data (Fig. 4.S2B; Thomas *et al.* 2007), which are supposed to be biased by temporal shifts in the oxygen isotope-temperature relationship (Kobashi *et al.* 2007).

The occurrence of overshooting warm air temperatures in the North Atlantic realm subsequent to the 8.2 ka cold period is confirmed by our results from the Lake Mondsee record, where $\delta^{18}O$ values after the 8.2 ka cold period are about 0.4‰ higher than those before the cooling (asterisks in Figs. 4.2E, 4.3B and 4.S2C). Also the short duration of this temperature overshoot in Lake Mondsee (only ca. 100 years) is similar to other proxy records in the North Atlantic realm (Figs. 4.2 and 4.3). For example, an increase in $\delta^{18}O$ by about 0.4‰ above the pre-8.2 ka cold period level is also observed in the record from Lake Hawes Water (Fig. 4.3A; Marshall *et al.* 2007), which is regarded to mainly reflect the $\delta^{18}O$ composition of past precipitation and thus temperature variability. In agreement with a strengthening of the MOC, increases in $\delta^{18}O$ in both records could be explained by a temperature overshoot of about +0.7°C in Central Europe and NW England. This closely agrees with results from coupled ocean-atmosphere climate models, indicating overshooting annual mean surface temperatures of +0.5°C subsequent to Holocene cooling events (Renssen *et al.* 2007) and particularly a positive temperature anomaly of about 0.2–0.3°C after the 8.2 ka cold period (Wiersma & Renssen 2006). As a likely cause for this temperature overshoot, various models indicate an enhanced resumption of the MOC with a 30% increase above the pre-8.2 ka cold period level (e.g. Stouffer *et al.* 2006; Renold *et al.* 2010). A slightly subdued $\delta^{18}O$ overshoot after the 8.2 ka cold period is also observed in the stalagmite records from Katerloch Cave (Figs. 4.3D and 4.3E; Boch *et al.* 2009), but there is no clear evidence for overshooting warm temperatures in the oxygen isotope record from Lake Ammersee (Fig. 4.3C; von Grafenstein *et al.* 1999a). However, this might be explained by the lower temporal resolution of this data set, the smaller sample size and the lower hydrological sensitivity of the lake (2.7 years water renewal time compared to 1.7 years in Lake Mondsee).

In addition to causing temperature variations, changing MOC intensities would also drive the migration of oceanic (e.g. the Arctic Front) and atmospheric front systems (e.g. the ITCZ) (Stouffer *et al.* 2006; Cheng *et al.* 2009) by influencing the meridional thermal gradients. Reduced MOC during the 8.2 ka cold period would force the ITCZ and the associated rain belts to move southwards (Stouffer et al., 2006; Renssen et al., 2006), while the enhanced MOC during the climate overshoot would force the ITCZ to migrate northwards (Renold *et al.* 2010). Similar displacements can be assumed for the Arctic Front. Displacement of the ITCZ is documented in the Cariaco Basin grey scale record (Fig. 4.3F; Hughen *et al.* 2000).

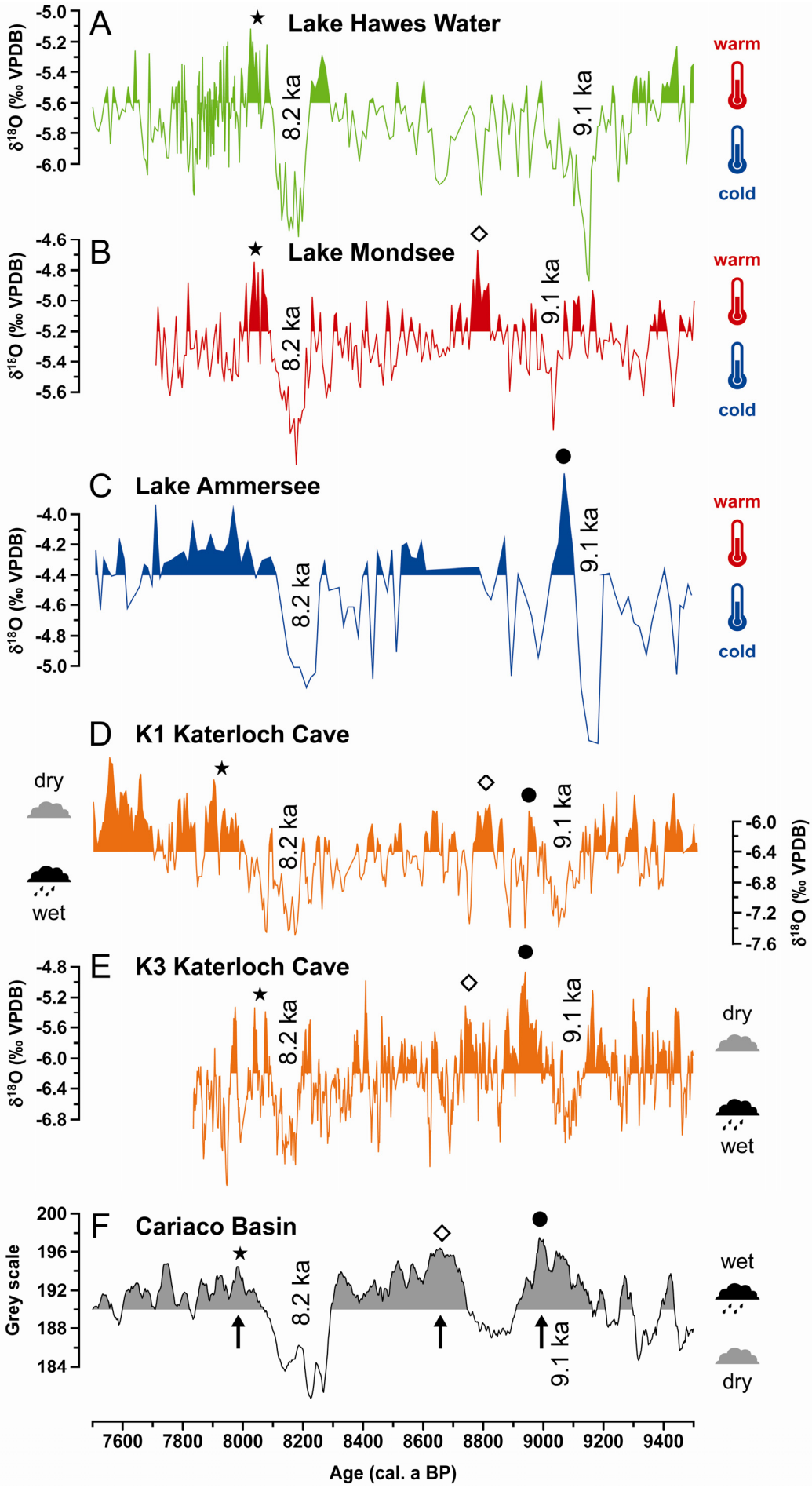
A
Lake Hawes Water
δ18O (‰ VPDB)
-5.0
-5.2
-5.4
-5.6
-5.8
-6.0
8.2 ka
9.1 ka
warm
cold
B
Lake Mondsee
-4.6
-4.8
-5.0
-5.2
-5.4
-5.6
C
Lake Ammersee
-4.0
-4.2
-4.4
-4.6
-4.8
-5.0
D
K1 Katerloch Cave
dry
wet
-6.0
-6.4
-6.8
-7.2
-7.6
E
K3 Katerloch Cave
-4.8
-5.2
-5.6
-6.0
-6.4
-6.8
F
Cariaco Basin
Grey scale
200
196
192
188
184
7600
7800
8000
8200
8400
8600
8800
9000
9200
9400
Age (cal. a BP)

As a consequence of a weak MOC during the 8.2 ka cold period, the ITCZ was shifted southwards, causing dry conditions in the southern Caribbean, which is reflected by light sediment colours in the Cariaco Basin grey scale record (Fig. 4.3F). In contrast, overshooting of the MOC after the 8.2 ka cold period initiated a synchronous northward shift of the ITCZ, causing wet climate conditions in the Cariaco Basin as reflected by dark sediment colours in the grey scale record. The migration of the Arctic Front has been tracked by investigating the offset between the oxygen isotope compositions of the left (Nps) and right coiling (Npd) forms of the planktonic foraminifer *Neogloboquadrina pachyderma* in the Norwegian Sea (Fig. 4.2B; Risebrobakken *et al.* 2003). While there is no difference between the $\delta^{18}O$ of both forms in areas north of the Arctic Front, there is a significant offset between the $\delta^{18}O$ of Nps and Npd in areas south of the Arctic Front. By using this relationship, a short-term northwestward shift of the Arctic Front can be identified directly after the 8.2 ka cold period (asterisk in Fig. 4.2B), which most likely occurred synchronous to the temperature overshoot in the Lake Mondsee record.

### *4.4.2 Were there overshooting warm temperatures after the 9.1 ka event?*

Overshooting oxygen isotope values directly after the 9.1 ka cold period are observed in the stalagmite records from Katerloch Cave (Fig. 4.3D and 4.3E; Boch *et al.* 2009) and also in the Lake Ammersee record (Fig. 4.3C; von Grafenstein *et al.* 1999a), but no such overshooting is visible in the records from Lake Hawes Water (Fig. 4.3A; Marshall *et al.* 2007) and Lake Mondsee (Fig. 4.3B). The differences between the adjacent oxygen isotope records from Lake Mondsee, Lake Ammersee and Katerloch Cave (the latter two are located only ~170 km west and ~175 km southeast of Lake Mondsee, respectively) for the interval bracketing the 9.1 ka cold period might be explained by differences in the temperature sensitivity of the individual records and, in the case of Lake Ammersee, by the less-constrained chronology and the lower sampling resolution (the overshoot after the 9.1 ka cold phase is only a one-point-phenomenon here). It could also be a consequence of threshold effects, i.e. the cooling during the 9.1 ka cold period was probably too short (~70 years in Lake Mondsee) and not strong enough to provoke a substantial shutdown of the MOC and in consequence a subsequent pronounced recovery. This interpretation is confirmed by the proxy records from the North Atlantic (Fig. 4.2), indicating only a weak shutdown and following recovery of the MOC around 9000 cal. a BP.

---

**Figure 4.3** High-resolution oxygen isotope records from European lakes and stalagmites in comparison to the Cariaco Basin grey scale record. A: $\delta^{18}O$ of authigenic calcite from Lake Hawes Water in NW England (Marshall *et al.* 2007). The original time scale was shifted by 200 years towards younger ages to improve the assumed fit with the other records during the 8.2 ka and 9.1 ka cold periods. B: $\delta^{18}O$ of juvenile *Candona neglecta* valves from Lake Mondsee. C and D: $\delta^{18}O$ of stalagmites K1 and K3 from Katerloch Cave in Austria (Boch *et al.* 2009). Due to the much larger fluctuations, the oxygen isotope scale was reduced by a factor of 2. E: Grey scale record of marine sediments from the Cariaco Basin (Hughen *et al.* 2000). Solid asterisks, open diamonds and solid circles mark climate events, regarded to be synchronous in the different records. Black arrows mark northward shifts of the ITCZ.

*This figure will be only published electronically as supporting online material and does not appear in the print version of the manuscript.*

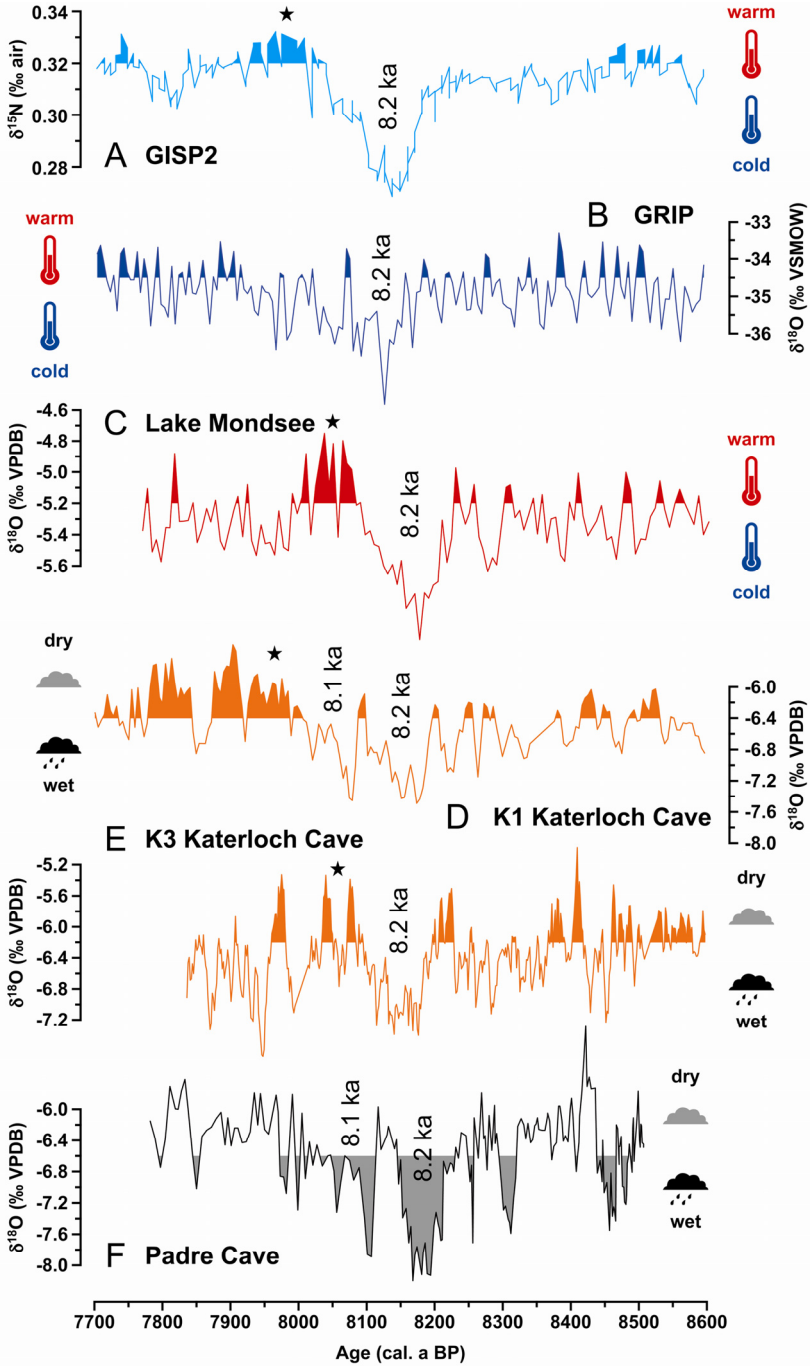


**Figure 4.S2** Detailed comparison of high-resolution climate proxy records across the 8.2 ka cold phase. A: Nitrogen isotopes from the GISP2 ice core as a proxy for Greenland air temperature (Kobashi *et al.* 2007). B: Oxygen isotopes from the GRIP ice core (Thomas *et al.* 2007). C: Oxygen isotopes of juvenile *Candona neglecta* valves from Lake Mondsee. D and E: Oxygen isotopes from stalagmites K1 and K3 from Katerloch Cave in Austria (Boch *et al.* 2009). F: Oxygen isotopes from stalagmite PAD07 from Padre Cave in Brazil, reflecting the intensity of the South American summer monsoon (Cheng *et al.* 2009). Solid asterisks mark the temperature overshoot interpreted as synchronous in the different records.

A comparatively short climate overshoot would also be more difficult to distinguish from the regular centennial-scale variations in the European oxygen isotope records. Furthermore, for Katerloch Cave, the partly significant differences between the two stalagmites also indicate that these records do not reflect air temperature alone. As stated by Boch *et al*. (2009), probably other factors such as changing atmospheric circulation patterns or precipitation intensities also played a role. This interpretation is confirmed by 1) the amplitudes of $\delta^{18}O$ variability for the stalagmite records, which is about twice as high as for the lake records (note the different scaling for stalagmites and lake records in Figs. 4.3D, 4.3E, 4.S2D and 4.S2E) and 2) the close similarity with the monsoon record from Padre Cave in Brazil (Fig. 4.S2F; Cheng *et al.* 2009), which is primarily driven by precipitation intensity and not temperature. Such an interpretation is also in agreement with the more complex structure of the 8.2 ka cold period in the Katerloch Cave records, a pattern also seen in the oxygen isotope records from the GRIP ice core (Fig. 4.S2B; Thomas *et al.* 2007) and Padre Cave (Fig. 4.S2F). In particular, for the period between ca. 8500 and 8100 cal. a BP, the Katerloch K3 $\delta^{18}O$ record shows a close similarity with the Padre Cave $\delta^{18}O$ record, while for the period between ca. 8300 and 7800 cal.a BP there is a close similarity between the Katerloch K1 $\delta^{18}O$ record and the Padre Cave and GRIP $\delta^{18}O$ records.

The role of the Alps as an effective barrier for meridional moisture transport (Sodemann & Zubler 2010) could also be a possible explanation for the observed differences between the oxygen isotope records from Lake Mondsee and Katerloch Cave during the interval directly after the 9.1 ka cold period. While Lake Mondsee is situated at the northern flank of the Alps and therefore under direct influence of Atlantic air masses coming from the NW, the Katerloch Cave is located at the southeastern rim of the Alps. Here the influence of Atlantic air masses is partly blocked by the Alps and the contribution of moisture coming from the Mediterranean is higher. According to model results, the modern mean annual moisture contribution from the Mediterranean in the Southern Alps (33.2%) is nearly twice as high as in the Northern Alps (17.3%) (Sodemann & Zubler 2010). Moreover, the mean annual moisture contribution from the North Atlantic in the Northern and Southern Alps is 43.8% and 33.3%, respectively. As a consequence, the observed differences between the two records might also be caused by the different contributions of North Atlantic and Mediterranean air masses and the isotopic contrast between these moisture source areas. Differences in the response to Holocene cooling events north and south of the Alps have also been highlighted by previous studies. For instance, Magny *et al*. (2003) postulated wetter condition in response to Holocene cooling phases for the European mid-latitudes (~43–50°N), contrasting drier conditions around the Mediterranean. Such climate conditions could explain the interruption of sapropel S1 formation in the Mediterranean (Magny *et al.* 2003) and a maximum in fire intensity in southern Europe (Davis & Stevenson 2007), which occurred synchronously to the 8.2 ka cold period.

Interestingly, a prominent period of higher oxygen isotope values is found in the Lake Mondsee record about 300 years after the 9.1 ka cold period (open diamonds in Fig. 4.3B). This warm period around 8800 cal. a BP is also reflected by slightly elevated oxygen isotope values in the records from

Katerloch Cave (Figs. 4.3D and 4.3E; Boch *et al.* 2009) and the Greenland ice cores (Rasmussen *et al.* 2007). A supposed drying during the 9.1 ka cold period is hardly visible in the Cariaco Basin grey scale record (Fig. 4.3F), which is in agreement with an only insignificant decrease in MOC intensity during this cooling (Fig. 4.2C), However, a subsequent prominent wet period in the low latitudes, starting around 8800 cal. a BP, is reflected in the Cariaco Basin grey scale record (Fig. 4.3F). This wet period was probably driven by a northward shift of the ITCZ, caused by a slight increase in MOC intensity (Fig. 4.2C) analogue to the response after the 8.2 ka.

Because of the lacking evidence for a $\delta^{18}O$ rise in the records of Lake Mondsee and Lake Hawes Water immediately after the 9.1 ka cold period, we conclude that, in contrast to the 8.2 ka cold period, there was probably no significant temperature increase directly after this cooling. Considering the discussed influence of moisture source changes on the $\delta^{18}O$ records, elevated oxygen isotope values recognized in the Katerloch Cave stalagmites directly after the 9.1 ka cold period are probably mainly caused by changes in precipitation intensity, indicating relatively dry conditions in the Southern Alps at this time. These occurred synchronously to a northward shift of the ITCZ, visible as a wet period in the Cariaco Basin grey scale record.

## 4.5 Conclusions

Overshooting warm temperatures of about +0.7°C directly after the 8.2 ka cold period, caused by a pronounced recovery of the MOC, are documented for Central Europe. A short dry period in Central Europe directly after the 9.1 ka cold phase, occurring synchronously to a wet period in the Cariaco Basin, might be driven by a northward shift of the ITCZ, thus indicating an interval of stronger MOC also at this time. However, the lacking evidence for overshooting warm temperatures in Central Europe directly after the 9.1 ka cold period indicates that the recovery of the MOC might have been less pronounced than after the 8.2 ka cold period and not sufficient to provoke a substantial warming in Central Europe. In addition, a short warm period in Central Europe around 8800 cal. a BP, which is most likely not directly related to the 9.1 ka cold phase, occurred apparently synchronous to another northward shift of the ITCZ. This indicates that intensification of the MOC and significant migrations of the ITCZ during the Holocene also occurred independently from freshwater discharge events. These findings have to be considered when modelling the MOC resumption after abrupt freshwater discharges adequately and could be used for model validation.

## 4.6 Acknowledgements

This study was carried out within the framework of the European Science Foundation (ESF) EUROCORES Programme EuroCLIMATE (ESF project DecLakes no. 04-ECLIM-FP29). We thank the ESF for coordination and the national agencies FWF (Austria, project no. I35-B06),

DFG (Germany, project no. AN554/1-2 and BR2208/2-2) and CNRS (France) for support and funding. We thank Gertraud Roidmayr and Maria Pichler (Institute for Limnology, Mondsee) for picking ostracods, Dieter Berger, Gabriele Arnold and Michael Köhler (GFZ, Potsdam) for preparing high-quality sediment thin sections, Richard Niederreiter (UWITEC, Mondsee) and Johann Knoll (Institute for Limnology, Mondsee) for assistance during the coring campaign and Albert Jagsch for providing access to the facilities of the Institute for Water Ecology, Fisheries and Lake Research in Scharfling.

# 5 A sedimentary record of Holocene surface runoff events and earthquake activity from Lake Iseo (Southern Alps, Italy)

Stefan Lauterbach[1], Emmanuel Chapron[2], Achim Brauer[1], Matthias Hüls[3], Adrian Gilli[4], Fabien Arnaud[5], Andrea Piccin[6], Jérôme Nomade[7], Marc Desmet[8], Ulrich von Grafenstein[9] and DecLakes participants[10]

[1] GFZ German Research Centre for Geosciences, Section 5.2 – Climate Dynamics and Landscape Evolution, D-14473 Potsdam, Germany

[2] Université d'Orléans, Institut des Sciences de la Terre d'Orléans, Observatoire des Sciences de l'Univers en région Centre, UMR 6113 CNRS/INSU, F-45071 Orléans, France

[3] Christian-Albrechts-University, Leibniz Laboratory for Radiometric Dating and Stable Isotope Research, D-24118 Kiel, Germany

[4] Swiss Federal Institute of Technology (ETH) Zurich, Geological Institute, CH-8092 Zurich, Switzerland

[5] Université de Savoie, Centre Interdisciplinaire Scientifique de la Montagne, Laboratoire EDYTEM, UMR 5204 CNRS, F-73376 Le Bourget-du-Lac, France

[6] Regione Lombardia, Direzione Generale Territorio e Urbanistica, Struttura Sistema Informativo Territoriale, I-20124 Milan, Italy

[7] Université Joseph Fourier, Observatoire des Sciences de l'Univers de Grenoble, Laboratoire de Géodynamique des Chaînes Alpines, F-38041 Grenoble, France

[8] Université François Rabelais de Tours, Institut des Sciences de la Terre d'Orléans – Equipe de Tours, UMR 6113 CNRS/INSU, F-37200 Tours, France

[9] Laboratoire des Sciences du Climat et de l'Environnement, UMR CEA-CNRS, F-91191 Gif-sur-Yvette, France

[10] Soumaya Belmecheri (LSCE, Gif-sur-Yvette), Helmut Erlenkeuser (Leibniz Laboratory, Kiel), Ángel Baltanás, (Universidad Autónoma, Madrid), Dan L. Danielopol (Institute for Limnology, Mondsee), Georg Hoffmann (LSCE, Gif-sur-Yvette), Christian Wolff (GFZ, Potsdam)

**accepted for publication in *The Holocene* (pending minor revisions)**

***ABSTRACT*** *This study presents a record of Holocene surface runoff events and earthquakes, preserved in the sediments of pre-Alpine Lake Iseo, northern Italy. A combined approach of high-resolution seismic surveying, detailed sediment microfacies analysis, non-destructive core-scanning techniques and accelerator mass spectrometry (AMS) $^{14}C$ dating of terrestrial macrofossils is used to detect and date these events in order to shed light on past regional seismic activity and the influence of climate variability and human impact on allochthonous detrital matter flux into the lake. The 19-m-long investigated sediment sequence of faintly layered lake marl contains frequent centimetre- to decimetre-scale sandy-silty detrital layers. During the early to mid-Holocene, these small-scale detrital layers, reflecting sediment supply by extreme surface runoff events, reveal a distinct centennial-scale recurrence pattern, which is in accordance with regional lake-level highstands and minima in solar activity and thus apparently mainly climate-controlled. After ca. 4200 cal. a BP,*

*intervals of high detrital flux occasionally also correlate with periods of enhanced human settlement activity, reflecting the complex influence of climate variability and anthropogenic impact on catchment erosion processes. Furthermore, five up to 2.40-m-thick large-scale event layers, composed of basal mass-wasting deposits overlain by large-scale turbidites, were identified, which are supposed to be triggered by strong earthquakes. The uppermost large-scale event layer can be correlated to a documented $M_w$=6.0 earthquake in AD 1222 in Brescia. The four other large-scale event layers are supposed to correspond to previously undocumented regional earthquakes around 350 BC, 570 BC, 2540 BC and 6210 BC, which most probably also reached magnitudes in the order of $M_w$=5.0–6.5.*

## 5.1 Introduction

Damaging earthquakes as well as large floods, debris flows and surface runoff events constitute serious natural hazards to modern societies. The assessment of these hazards mainly relies on a thorough understanding of the particular recurrence patterns and underlying trigger mechanisms. As such studies require long continuous event records but historical data are mostly limited to only short periods (i.e. the past ca. 500–1000 years), lake sediments have been successfully used to establish long records of palaeoseismicity (e.g. Chapron *et al.* 1999; Schnellmann *et al.* 2002; Migowski *et al.* 2004; Monecke *et al.* 2004; Nomade *et al.* 2005; Strasser *et al.* 2006), river flooding (Arnaud *et al.* 2005; Chapron *et al.* 2005; Bøe *et al.* 2006; Moreno *et al.* 2008; Debret *et al.* 2010), debris flow activity (Dapples *et al.* 2002; Irmler *et al.* 2006) and extreme surface runoff events (Mangili *et al.* 2005). Owing to its high population density and importance for national economy, north-central Italy is particularly vulnerable to the effects of natural hazards. However, until now, regional lake sediment records have only rarely been utilized to reconstruct past earthquake activity (e.g. Fanetti *et al.* 2008). Furthermore, while several studies in the northwestern Alps addressed hydrological changes during the Holocene (e.g. Magny 1993a,b; Magny 2004; Magny *et al.* 2010), regional data on palaeohydrological changes for northern and central Italy are still sparse (Magny *et al.* 2007; Magny *et al.* 2009a). This is of particular interest as changes in the hydrological cycle might have influenced the recurrence of floods, landslides and surface runoff events in the region and in addition also affected prehistoric societies (Magny 2004; Arbogast *et al.* 2006). Within this context, also the influence of anthropogenic settlement activity on precipitation-triggered catchment erosion is still matter of debate (Dapples *et al.* 2002; Irmler *et al.* 2006; Schneider *et al.* 2010).

As part of the European Science Foundation project DecLakes (*Decadal Holocene and Lateglacial variability of the oxygen isotopic composition in precipitation over Europe reconstructed from deep-lake sediments*), this study introduces the sedimentary record of pre-Alpine Lake Iseo, northern Italy. A combined seismic and sedimentological approach is used to identify exceptional depositional events, namely large- and small-scale turbidites and mass-wasting deposits, in a sediment core from the Sale Marasino Basin, a subbasin of Lake Iseo. Based on a core chronology established

through accelerator mass spectrometry (AMS) $^{14}C$ dating of terrestrial macrofossils, this allows the reconstruction of (1) local surface runoff activity, reflecting both climate variability and human impact in the surrounding area, and (2) major regional earthquakes throughout the Holocene.

## 5.2 Study site and tectonic setting

Lake Iseo (Latin name Sebino), the fourth largest lake in northern Italy (surface area ~60.9 km²), is located in the foothill zone of the Lombardian Southern Alps at 185 m a.s.l., about 20 km northwest of Brescia (Fig. 5.1A and 5.1B). According to Bini *et al.* (1978), the present lake basin, which in the northern and central part is surrounded by more than 1200-m-high mountain ranges, is the result of Pleistocene glacier activity, reshaping a pre-existent Late Miocene erosional canyon. The Oglio River is, besides some minor streams and the Borlezza River in the northwest, the main inflow and only outflow of Lake Iseo (Garibaldi *et al.* 1999). Monte Isola Island in the central part of the lake is one of the largest lake islands in Europe (surface area ~4 km², peak elevation ~420 m above lake level).

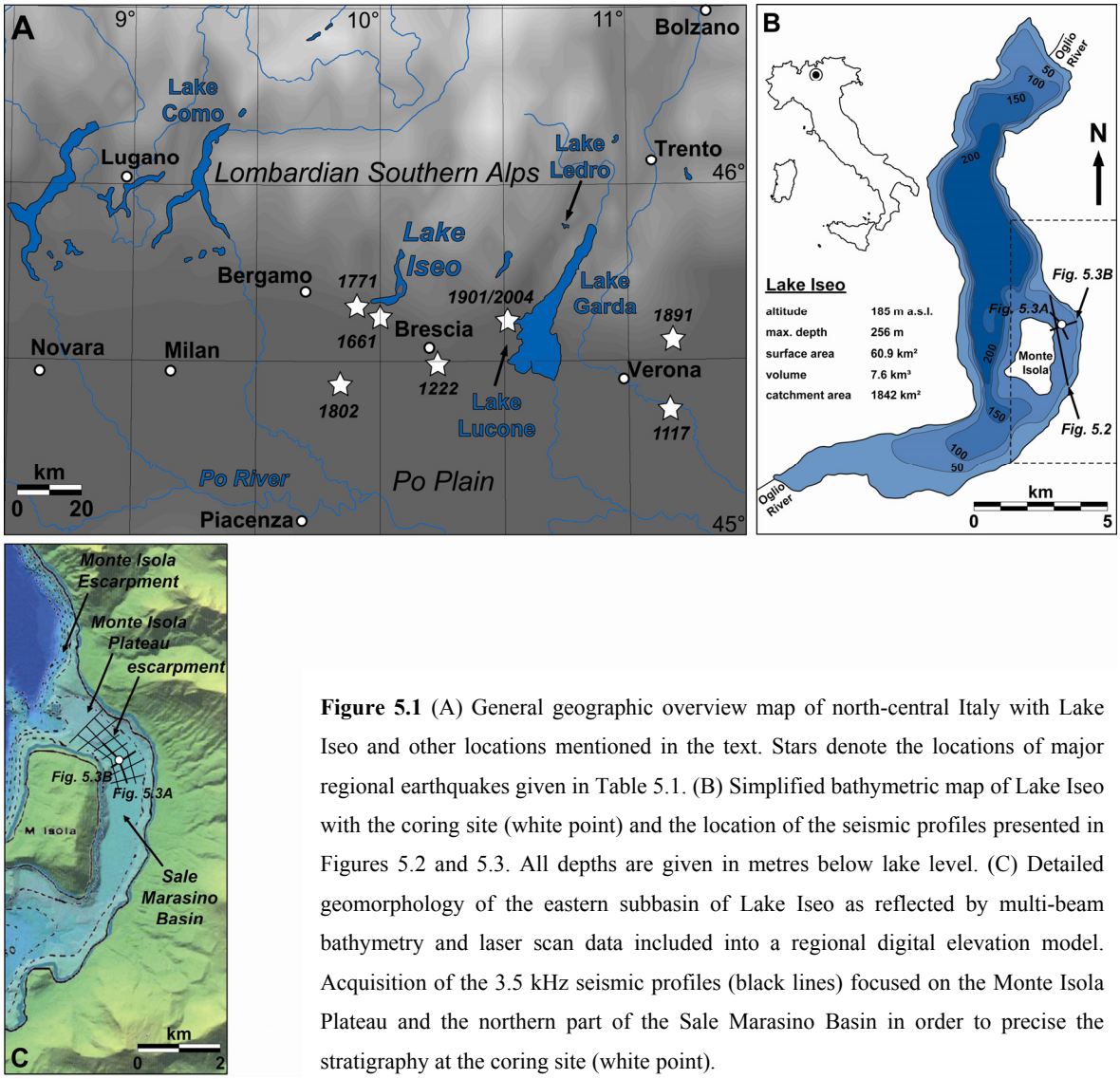


**Figure 5.1** (A) General geographic overview map of north-central Italy with Lake Iseo and other locations mentioned in the text. Stars denote the locations of major regional earthquakes given in Table 5.1. (B) Simplified bathymetric map of Lake Iseo with the coring site (white point) and the location of the seismic profiles presented in Figures 5.2 and 5.3. All depths are given in metres below lake level. (C) Detailed geomorphology of the eastern subbasin of Lake Iseo as reflected by multi-beam bathymetry and laser scan data included into a regional digital elevation model. Acquisition of the 3.5 kHz seismic profiles (black lines) focused on the Monte Isola Plateau and the northern part of the Sale Marasino Basin in order to precise the stratigraphy at the coring site (white point).

The combination of multi-beam bathymetry (EM3000) and laser scan survey (LIDAR) data from a previous study on the geomorphology of the Lake Iseo basin (Bini *et al.* 2007) with a digital elevation model (Fig. 5.1C) allows to illustrate the main morphological features of the area surrounding the eastern subbasin of Lake Iseo between Monte Isola Island and the eastern lake shore. This subbasin, which is at its northern margin separated from the deep central basin (maximum water depth ~256 m) by the submerged Monte Isola Escarpment (Bini *et al.* 2007), can be divided into a shallower northern (Monte Isola Plateau (MIP), water depth ~79 m) and a deeper southern part (Sale Marasino Basin (SMB), water depth ~100 m), where the coring site is located. They are separated by a small, NE–SW trending escarpment of about 20 m height. While the western margin of the SMB is characterized by the steep slopes of Monte Isola Island, the eastern flank reveals numerous gullies and canyons as well as subaquatic detrital fans (Bini *et al.* 2007). Triassic to Jurassic dolomites and limestones together with Plio-Pleistocene fluvial and glacial deposits represent the main geological units exposed along the shorelines in the vicinity of the coring site (Bini *et al.* 2007; Cassinis *et al.* 2009).

The regional tectonic setting, particularly the formation of a fold-and-thrust belt since the Late Oligocene, is the result of the post-collisional phase of the Alpine orogeny (e.g. Dal Piaz *et al.* 2003 and references therein). Although crustal shortening in the Lombardian Southern Alps has previously been assumed to slow or even cease during the Late Miocene (Fantoni *et al.* 2004; Castellarin *et al.* 2006), recent geomorphological studies revealed that the complete thrust front was tectonically active throughout the Plio-Pleistocene (Burrato *et al.* 2003; Chunga *et al.* 2007; Sileo *et al.* 2007; Livio *et al.* 2009). The crustal shortening, which still proceeds with rates of ~1.1 mm $a^{-1}$ in the Lake Iseo area (Serpelloni *et al.* 2005), is mainly accommodated by blind thrusts and fault-propagation folding of Pleistocene strata (Sileo et al., 2007; Livio et al., 2009), reflected by a few regional historical earthquakes with moment magnitudes of $M_w \geq 5.0$ and epicentral intensities of $I_0 \geq$ VII (Boschi *et al.* 2000; CPTI Working Group 2004; Guidoboni *et al.* 2007) (Table 5.1).

**Table 5.1** Major earthquakes during the past ca. 900 years in the vicinity of Lake Iseo. All data are given according to Italian earthquake catalogues (CPTI Working Group, 2004; Guidoboni *et al.*, 2007).

| Year | Location | Distance from Lake Iseo | Moment magnitude $M_w$ | Epicentral intensity $I_0$ |
|---|---|---|---|---|
| AD 2004[a] | Salò | ~35 km southeast | 5.0 | VII-VIII |
| AD 1901[a] | Salò | ~35 km southeast | 5.7 | VIII |
| AD 1891 | Valle d'Illasi | ~90 km southeast | 5.7 | VIII-IX |
| AD 1802 | Soncino | ~40 km southwest | 5.7 | VIII |
| AD 1771 | Sarnico | southern lake shore | 4.8 | VI |
| AD 1661 | Montecchio | southern lake shore | 5.2 | VII |
| AD 1222 | Brescia | ~25 km southeast | 6.0 | VIII-IX |
| AD 1117 | Verona | ~75 km southeast | 6.5 | IX-X |

[a] instrumentally recorded

In general, seismic activity in the Lake Iseo area is mainly confined to an arcuate zone extending about 30–40 km to the south and southeast of the lake (CPTI Working Group 2004; Guidoboni *et al.* 2007). This zone comprises the WSW–ENE trending Val Trompia fold-and-thrust belt and its continuation in the Lake Garda region, the SSW–NNE trending Giudicarie Fault System (Castellarin & Cantelli 2000; Fantoni *et al.* 2004; Livio *et al.* 2009).

## 5.3 Fieldwork and methods

### *5.3.1 Seismic reflection surveys*

During the first seismic reflection survey on Lake Iseo in 2002, which was carried out with a broad-band (300–2400 kHz) single-channel boomer device (Bini *et al.* 2007), only one axial profile was acquired across the eastern subbasin (Fig. 5.2). This profile was used to select the coring site (45°43'11"N, 10°06'20"E), which is located at about 100 m water depth, close to the deepest part of the SMB (Figs. 5.1B and 5.1C), within an area of relatively well-stratified sediments.

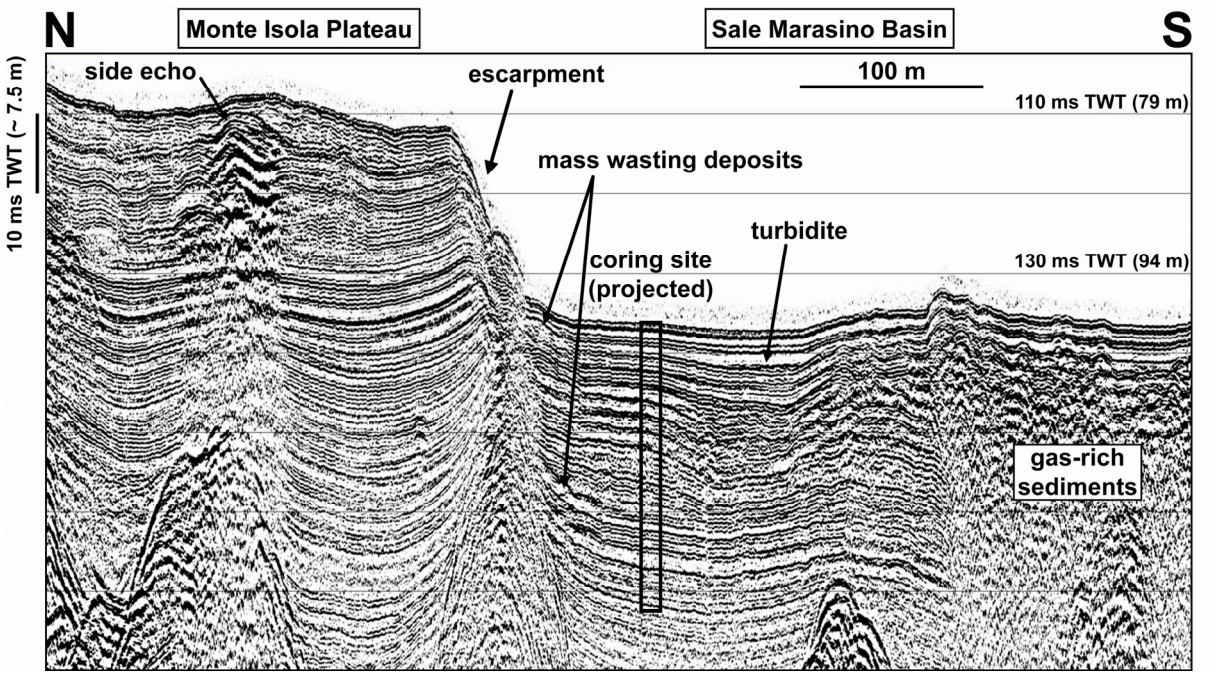


**Figure 5.2** High-resolution seismic profile (boomer) across the eastern subbasin of Lake Iseo, illustrating the main sedimentary environments that characterize this part of the lake and have previously been documented by Bini *et al.* (2007). This seismic profile, which is localized in Figure 5.1, was used to select the coring site. The frequent occurrence of mass-wasting deposits and the identification of a large-scale turbidite deposit in the Sale Marasino Basin suggest that subaquatic landslides essentially originate from the escarpment that separates the basin from the Monte Isola Plateau.

In 2007, a new high-resolution seismic reflection survey was performed across the MIP and the SMB by using the 3.5 kHz pinger device and Octopus acquisition system of the ETH Zurich, mounted on an inflatable boat. A dense grid of seismic profiles was acquired, precisely imaging the stratigraphy of the sedimentary basin infill at the coring site (Figs. 5.3A and 5.3B). Seismic data processing (band-pass filtering) and interpretation were performed at the University of Orléans by using the programs SeiSee and KINGDOM Suite, respectively.

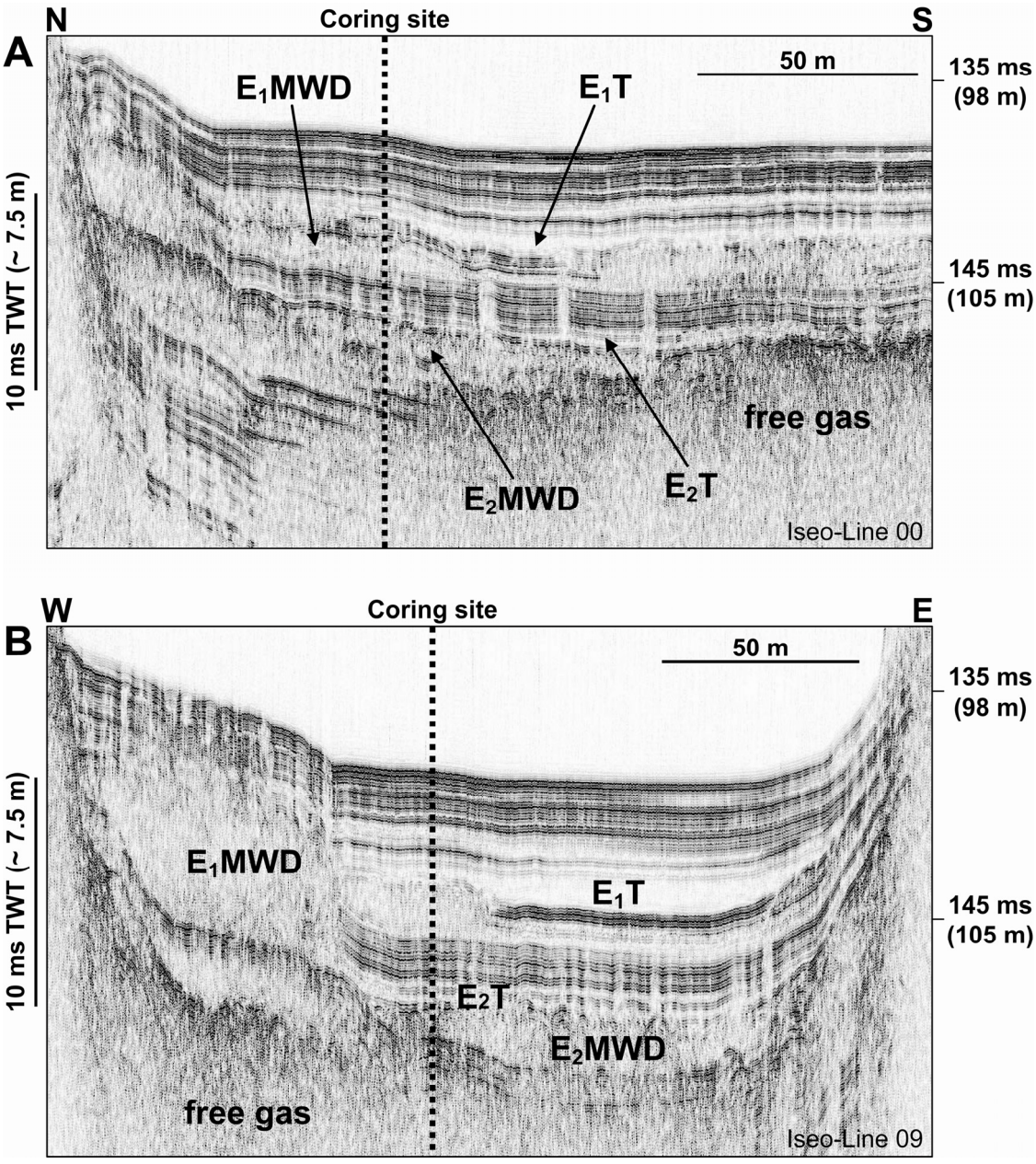


**Figure 5.3** Two high-resolution seismic profiles (3.5 kHz), acquired in N-S (A) and E-W (B) direction and intersecting close to the coring location, illustrate the basin infill geometry of the northern Sale Marasino Basin at the coring site. The occurrence of free gas in the sediments at about 7 m below the lake floor, which limits acoustic imaging below this depth, is indicated together with the large-scale mass-wasting ($E_1$MWD and $E_2$MWD) and turbidite deposits ($E_1$T and $E_2$T) discussed in the text.

### *5.3.2 Coring*

Three parallel sediment cores (SEB 05_02, SEB 06_03 and SEB 06_04), each consisting of 2-m-long segments, were recovered from the coring site during the field campaigns in 2005 and 2006 by using a 90-mm-diameter UWITEC piston corer. Additionally, three short gravity cores (SEB 05_02P1, SEB 06_03P1 and SEB 06_03P2) were retrieved in order to obtain the undisturbed sediment-water interface. All core segments were already split into halves, lithostratigraphically described, photographed and subsampled on-site in a field lab. The segments of the three long sediment cores and gravity core SEB 06_03P2 were visually correlated by using more than 80 macroscopically visible lithological marker layers, resulting in an about 19-m-long continuous composite profile (Fig. 5.4A). Due to core loss and the lack of overlapping segments in the parallel cores, the two lowermost segments of core SEB 06_03 could not be linked to the continuous composite profile and thus remain floating with their position given according to the intended depth in the coring protocol.

### *5.3.3 Sediment properties and dating*

Continuous measurements of diffuse spectral reflectance (1-cm intervals) of all core segments were carried out prior to subsampling in the field lab with a Minolta CM-2500d spectrophotometer (0.8 mm spot size) on the fresh sediment surface, covered with a thin transparent polyethylene film (Chapman & Shackleton 1998). The mean reflectance intensity, measured at 10-nm increments over the 400–700 nm wavelength range, results in the sediment lightness L*, given on a scale from 0 (black) to 100 (white).

For detailed sediment microfacies analysis, which was carried out at the GFZ in Potsdam, a set of large-scale petrographic thin sections was prepared from overlapping sediment blocks (100×20×10 mm), taken continuously from all cores of the composite profile, according to the method described by Brauer *et al*. (1999b) and Brauer and Casanova (2001). Thin sections were examined under a ZEISS Axiophot polarization microscope at 25–400× magnification.

Magnetic susceptibility measurements were conducted on split cores at 0.5-cm steps with a Bartington MS2E point sensor mounted on a GEOTEK multi-sensor core logger at the University of Franche-Comté in Besançon. Results are expressed as SI units.

Twenty-nine samples of terrestrial plant macrofossils (wood, small twigs, seeds, leaf fragments) were selected from the cores of the composite profile (Table 5.2) and AMS $^{14}$C-dated at the Leibniz Laboratory in Kiel. Conventional radiocarbon ages were calibrated using the OxCal 4.1 program (Ramsey 1995, 2001) with the IntCal09 calibration data set (Reimer *et al.* 2009). All calibrated ages are reported as 2σ ranges.

**Table 5.2** AMS $^{14}C$ dates obtained from terrestrial macrofossils from Lake Iseo. All conventional radiocarbon dates were calibrated using OxCal 4.1 (Ramsey, 1995, 2001) with the IntCal09 calibration dataset (Reimer *et al.*, 2009). Italicised samples were not considered for the age-depth model (for explanations see the results chapter).

| Sample / Lab. code | Composite depth (cm) | Dated material | Carbon content (mg) / $\delta^{13}C \pm \sigma$ (‰) | AMS $^{14}C$ age (a BP ± σ) | Calibrated age (cal. a BP, 2σ range) |
|---|---|---|---|---|---|
| KIA39233 | 59.50 | twig | 1.34 / -26.94 ± 0.49 | 134 ± 25 | 9–275[a] |
| KIA39234 | 101.00 | twig | 5.85 / -27.79 ± 0.27 | 209 ± 27 | -4–303[a] |
| KIA39235 | 159.50 | wood & leaf fragments[b] | 1.56 / -23.80 ± 0.13 | 677 ± 29 | 561–679 |
| KIA39236 | 190.00 | twigs | 2.38 / -26.24 ± 0.34 | 672 ± 26 | 561–675 |
| *KIA33098* | *354.00* | *wood* | *4.27 / -25.79 ± 0.11* | *1370 ± 22* | *1269–1316* |
| *KIA29385* | *412.00* | *olive seed* | *4.60 / -28.04 ± 0.08* | *1225 ± 24* | *1068–1257* |
| *KIA29388* | *414.00* | *plant remains[b]* | *4.57 / -25.30 ± 0.11* | *1256 ± 25* | *1091–1277* |
| KIA33099 | 457.00 | wood & twig | 5.33 / -26.53 ± 0.10 | 1296 ± 24 | 1178–1287 |
| KIA36621 | 606.00 | plant remains[b] | 5.40 / -27.29 ± 0.50 | 2201 ± 32 | 2135–2327 |
| KIA33100 | 614.25 | wood | 4.38 / -26.34 ± 0.09 | 2232 ± 24 | 2155–2335 |
| KIA36622 | 822.00 | plant remains[b] | 2.30 / -27.40 ± 0.38 | 2434 ± 27 | 2354–2699 |
| KIA29390 | 1127.00 | plant remains[a] | 1.87 / -27.62 ± 0.20 | 3016 ± 27 | 3081–3335 |
| KIA29386 | 1128.25 | wood | 3.92 / -28.40 ± 0.57 | 3018 ± 25 | 3082–3335 |
| KIA33109 | 1276.00 | beech nut | 4.28 / -27.62 ± 0.11 | 3319 ± 29 | 3473–3631 |
| KIA33101 | 1372.75 | wood | 2.48 / -25.87 ± 0.09 | 3728 ± 26 | 3985–4151 |
| KIA33102 | 1383.50 | twig | 4.62 / -29.81 ± 0.16 | 3803 ± 25 | 4090–4286 |
| KIA33103 | 1423.00 | shell of beech nut | 4.67 / -27.59 ± 0.36 | 3854 ± 33 | 4155–4411 |
| KIA29387 | 1503.25 | wood | 2.98 / -27.47 ± 0.15 | 4206 ± 29 | 4628–4846 |
| KIA33110 | 1503.75 | twigs & wood | 1.91 / -28.68 ± 0.16 | 4240 ± 28 | 4655–4859 |
| KIA29392 | 1626.00 | plant remains[b] | 1.84 / -28.11 ± 0.12 | 5484 ± 36 | 6207–6394 |
| KIA33104 | 1762.00 | wood | 4.82 / -28.90 ± 0.19 | 7124 ± 36 | 7866–8014 |
| KIA33112 | 1851.50 | wood & leaf | 3.53 / -24.95 ± 0.08 | 8382 ± 35 | 9302–9484 |
| KIA33105 | 1852.50 | wood | 0.92 / -29.50 ± 0.11 | 8296 ± 52 | 9129–9444 |
| KIA33106 | 1857.50 | wood & plant remains[b] | 3.01 / -29.37 ± 0.14 | 8369 ± 37 | 9297–9476 |
| *KIA33107* | *2088.00* | *twig* | *3.34 / -25.31 ± 0.09* | *11 931 ± 47* | *13 636–13 940* |
| *KIA33108* | *2134.00* | *wood & leaves* | *3.97 / -26.13 ± 0.13* | *12 470 ± 49* | *14 175–15 024* |
| *KIA39237* | *2376.00* | *wood & bark* | *4.84 / -27.91 ± 0.40* | *13 225 ± 54* | *15 475–16 680* |
| *KIA39238* | *2386.00* | *twig* | *5.20 / -25.45 ± 0.34* | *13 232 ± 65* | *15 463–16 700* |
| *KIA30286* | *2449.00* | *plant remains[b]* | *0.73 / -28.87 ± 0.22* | *14 950 ± 126* | *17 859–18 567* |

[a] This sample falls within a $^{14}C$ plateau caused by an increase in solar activity (Maunder minimum) and fossil fuel burning (Suess effect). It is thus only possible to determine a comparatively large calibration range.

[b] various undetermined terrestrial plant remains (leaves, wood, seeds)

## 5.4 Results

### *5.4.1 Seismic stratigraphy*

On the boomer profile, the northern part of the SMB is characterized by a well-stratified acoustic facies, reaching more than 40 ms two-way-travel time (TWT) in thickness (Fig. 5.2). In contrast, the very limited acoustic penetration of only 5 ms TWT in the southern SMB suggests the local occurrence of free gas in the basin infill. South of the coring site, a large turbidite deposit, characterized by a transparent acoustic facies and laterally developing onlaps, is identified at 140 ms TWT. At the edge of the escarpment that separates the SMB and the MIP, several lense-shaped bodies with a transparent to chaotic acoustic facies indicate local mass-wasting deposits that may have reworked sediments at the coring site. On the MIP, acoustic penetration locally reaches about 70 ms TWT. Several small-scale lense-shaped bodies with a chaotic acoustic facies, which are found within the upper 20 ms TWT, indicate recurrent but spatially limited subaquatic mass-wasting events.

Acoustic penetration of the pinger profiles in the SMB is limited to 10–15 ms TWT below the lake floor, suggesting free gas in the deeper sediments (Figs. 5.3A and 5.3B). Within the upper acoustic level, which reveals well-stratified and parallel continuous reflections, several intercalated large-scale mass-wasting deposits can be clearly identified. The uppermost transparent layer, which is interpreted as a large-scale turbidite and termed $E_1T$, is characterized by a high-amplitude basal reflection and develops lateral onlaps along the eastern, western and northern edges of the basin. This layer caps a lense-shaped mass-wasting deposit with a chaotic to transparent acoustic facies and irregular basal and upper boundaries, which is termed $E_1MWD$ and reaches its maximum thickness near the base of the escarpment and thins towards the southeast. A second transparent layer, which is considered as a large-scale turbidite and termed $E_2T$, reaches its maximum thickness in the deepest part of the basin and also develops onlaps at the basin edges. It locally drapes a lense-shaped mass-wasting deposit, termed $E_2MWD$, which is characterized by a chaotic to transparent acoustic facies and an irregular upper boundary, but also several chaotic internal high-amplitude reflections that locally absorb the acoustic signal. This mass-wasting deposit seems to be thicker at the foot of the escarpment and extends over the complete width of the SMB.

### *5.4.2 Sediment microfacies and proxy data*

*Regular pelagic sedimentation and small-scale detrital layers*

The sediment record of Lake Iseo can be subdivided into three major lithostratigraphical units. The uppermost 21.0 cm of the sediment profile consist of a black organic gyttja and are characterized by a

sediment lightness L* smaller than ~20. This unit is supposed to represent deposition during the recent phase of eutrophication, i.e. approximately the past five to six decades.

The second unit, comprising the largest part of the sediment record (21.0–2078.0 cm), is composed of light to brownish grey, partly blackish, silt- to clay-sized lake marl that displays a faint centimetre-scale layering. Major constituents are microcrystalline endogenic calcite, clay minerals, finely dispersed detrital carbonates and siliciclastics (up to 100 µm in diameter), amorphous organic matter, diatom frustules and ostracod valves. Locally, a faint millimetre-scale lamination of light, carbonate-rich layers and dark layers, containing clay minerals, amorphous organic matter and diatom frustules, is observed. However, the macroscopic layering is mainly owed to the lithological contrast between the autochthonous lake marl and frequently intercalated, brownish grey sand/silt layers. These small-scale detrital layers are mainly composed of angular allochthonous carbonates and siliciclastics (feldspar, quartz and mica) between 50 and 500 µm in diameter, but often also contain terrestrial plant material (e.g. wood, leaves, seeds, fruits), charcoal particles and fragments of gastropods and bivalves. Two types of small-scale detrital layers can be distinguished. Distinct layers (0.5–18.5 cm thick) reveal a clear upward gradation from sand/silt to clay (Fig. 5.4B, picture e) and sharp, occasionally erosional, basal contacts. Matrix-supported detrital layers are thinner than graded layers (<0.5 cm) and show no gradation. As the coarse-grained minerogenic detritus is finely dispersed in the lake marl, only indistinct boundaries are observed. Small-scale detrital layers are reflected by distinct fluctuations in sediment lightness towards lighter (L*>40, high content of detrital carbonates) or darker (L*<35, abundant organic material) colour and by peaks in magnetic susceptibility (Fig. 5.4A and 5.4B, picture d), which is attributed to the concentration of allochthonous magnetic minerals (Thompson *et al.* 1975) and larger grain sizes (Bradshaw & Thompson 1985).

Sediments of the third lithostratigraphical unit occur only in the two lowermost floating core segments below 2078.0 cm composite depth. These deposits reveal a distinct centimetre-scale lamination of light grey silt layers and frequently intercalated brownish to reddish clay and sand layers.

---

**Figure 5.4** (A) Results of diffuse spectral reflectance (sediment lightness L*) and magnetic susceptibility measurements on the Lake Iseo composite profile and the two lowermost floating core segments. Stars indicate radiocarbon dates (black – included in the age-depth model, white – excluded). Grey horizontal bars indicate the position of earthquake-induced large-scale event layers $E_1$ to $E_5$. Arrows indicate the position of sediment microfacies structures presented in Figure 5.4B. (B) Sediment microfacies of large-scale mass-wasting deposits, regular pelagic sediments and small-scale detrital layers as revealed from large-scale petrographic thin sections (pictures a–e) and core photographs (picture d). Large-scale mass-wasting deposits are characterized by destroyed layering and liquefaction structures (pictures a and c) and chaotic sediment sequences with randomly dispersed up to gravel-sized intraclasts (picture b). The regular pelagic lake marl is intercalated by frequent small-scale turbidites and matrix-supported detrital layers (pictures d and e), which are well reflected by peaks in magnetic susceptibility (picture d).

*Large-scale event layers*

Within the sediments of the second lithostratigraphical unit, five large-scale event layers occur, which exhibit a characteristic sedimentological bipartition. The uppermost event layer $E_1$ (216.0–452.0 cm) reveals a 128.3-cm-thick basal sequence of similar composition as the regular pelagic lake marl. However, the macroscopic sediment appearance is wet and unconsolidated and microfacies analysis reveals a largely destroyed and indistinct layering, extensive sediment homogenization and occasional liquefaction structures (Fig. 5.4B, picture a). This sequence can be correlated to the large-scale mass-wasting deposit $E_1$MWD in the seismic stratigraphy. It is overlain by a 107.7-cm-thick graded layer with a distinct, about 10-cm-thick sandy base with abundant organic macro remains, rapidly fining upwards into silt and clay. This layer is interpreted as a large-scale turbidite, corresponding to event layer $E_1$T in the seismic stratigraphy. While the signature of the basal mass-wasting deposit in the core-scanning data is ambiguous owing to the partly preserved primary sediment structure, the overlying, rather homogeneous turbidite is clearly visible through almost constant sediment lightness (Fig. 5.4A).

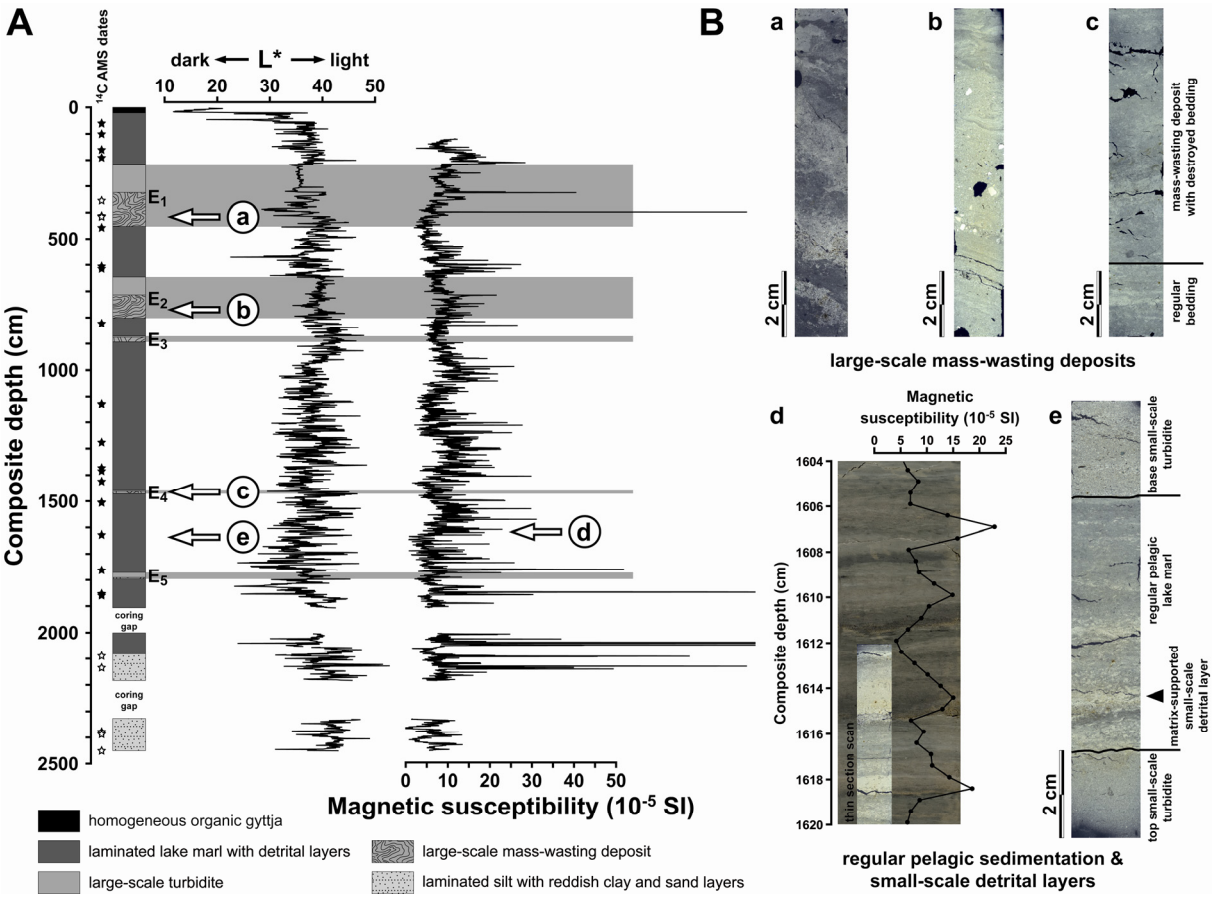

Event layer $E_2$ (646.1–802.0 cm) contains a 89.0-cm-thick basal part, which is characterized by a chaotic sequence of (1) autochthonous lake marl with destroyed and tilted layering, (2) small-scale graded sand/silt layers and lenses (up to 8.5 cm thick) and (3) homogenized, clay-sized autochthonous sediment with randomly dispersed gravel-sized dolomitic and siliciclastic intraclasts and lumps of finely-laminated lake marl (Fig. 5.4B, picture b). This sequence, which can be correlated to the large-scale mass-wasting deposit $E_2$MWD in the seismic stratigraphy, is overlain by a 66.9-cm-thick graded layer that exhibits a distinct upward fining from coarse sand to clay. This corresponds to the large-scale turbidite $E_2$T in the seismic stratigraphy. Relatively constant sediment lightness clearly reflects extensive sediment homogenization throughout the entire event layer $E_2$ (Fig. 5.4A). Strong fluctuations and high peaks (up to $20 \times 10^{-5}$ SI units) in magnetic susceptibility within the basal mass-wasting deposit reflect finely the dispersed sand- and gravel-sized carbonate detritus, while rather constant values within the overlying turbidite mirror extensive sediment homogenization and upward-fining.

Besides the two exceptionally thick events $E_1$ and $E_2$, three other large-scale event layers are found in the lower part of the profile. However, owing to their limited thickness and to the occurrence of free gas in the deeper sediments, these layers are not seen in the seismic sections. Event layer $E_3$ (871.1–893.5 cm) contains a 17.8-cm-thick basal mass-wasting deposit of macroscopically wet and homogeneous appearance, which is characterized by destroyed and folded layering and overlain by a 4.6-cm-thick turbidite. The 7.9-cm-thick basal mass-wasting deposit of event layer $E_4$ (1458.7–1470.5 cm) also exhibits destroyed layering (Fig. 5.4B, picture c) and is capped by a 3.9-cm-thick turbidite. Event layer $E_5$ (1771.0–1796.0 cm) contains a 5.5-cm-thick basal mass-wasting deposit with destroyed and folded layering, which is overlain by a 19.5-cm-thick sequence of three separate turbidites.

### *5.4.3 Chronology*

All 29 terrestrial macrofossil samples obtained for AMS radiocarbon dating (24 samples from the upper ~19 m of the profile and 5 other samples from the two floating core segments) were derived from detrital layers and thus might tend to give too old calibrated ages because of sample reworking. However, several cross-datings on wood, which is prone to reworking, and other, presumably less affected, terrestrial macro remains (leaf fragments, seeds, etc.) obtained from the same or adjacent event layers (KIA33112/KIA33105/KIA33106, KIA29387/KIA33110, KIA29390/KIA29386, KIA36621/KIA33100, KIA29385/KIA29388) reveal consistent calibrated ages with overlapping 2σ ranges. It is thus inferred that reworking of wood samples in most cases should be negligible.

The Bayesian-based *P_Sequence* deposition model with the parameter $k$=0.5 (depositional events per unit length), implemented in the OxCal 4.1 program (Ramsey 2008), was used for generating an age-depth model for the continuous upper ~19 m of the sediment record (Fig. 5.5).

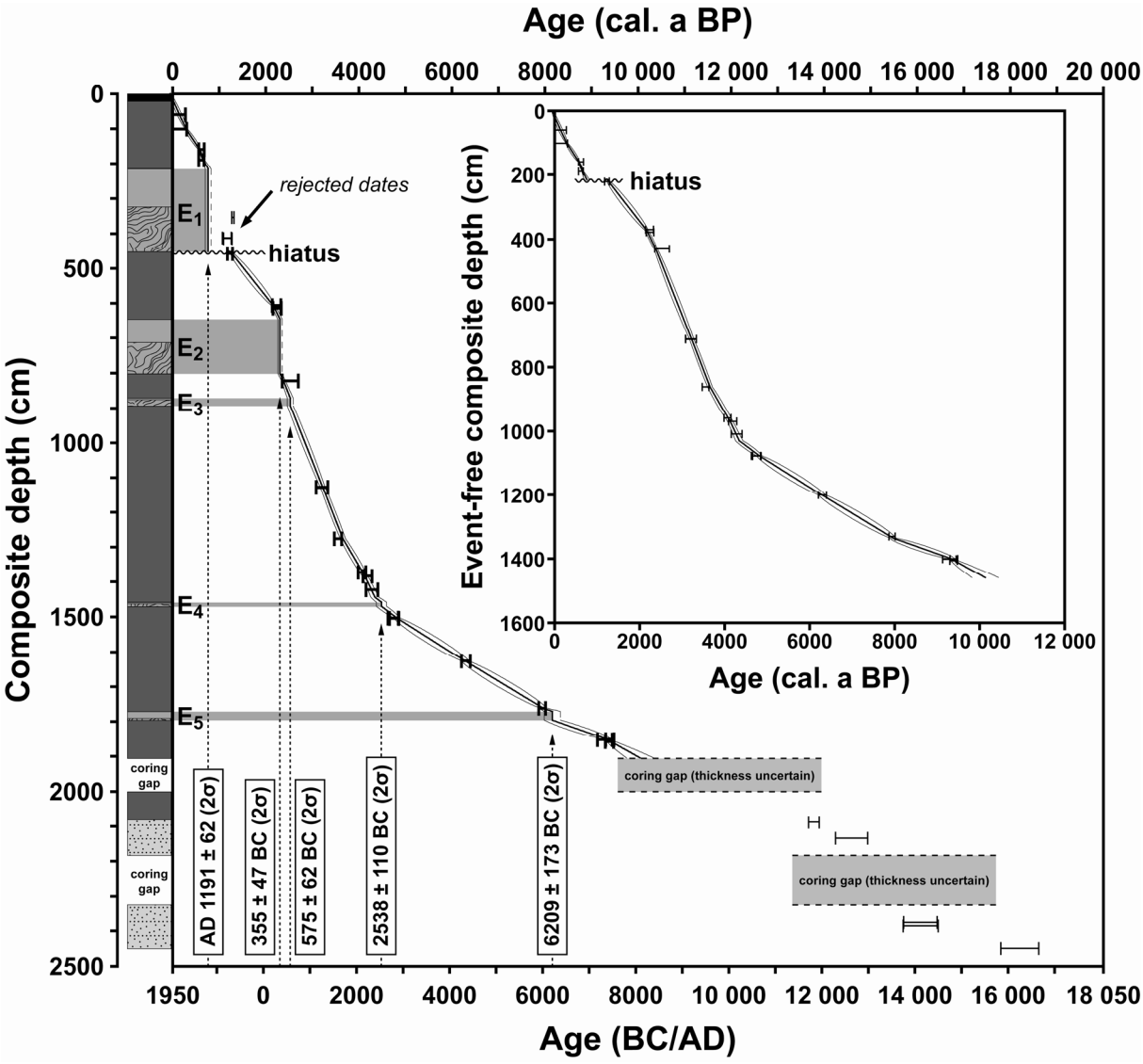


**Figure 5.5** Age-depth model for the Lake Iseo sediment record derived from AMS $^{14}C$ dating of terrestrial macrofossils (Table 5.2). Error bars for individual radiocarbon dates indicate calibrated 2σ ranges (bold – included in the age-depth model, thin – excluded). The bold line between individual radiocarbon dates represents the age-depth model derived from the *P_Sequence* deposition model (*k*=0.5) implemented in the OxCal 4.1 program (Ramsey 2008). Adjacent dashed lines represent the 2σ probability range of the age-depth model. The inset figure illustrates the age-depth model corrected for large-scale event layers. Grey horizontal bars indicate the position of earthquake-induced large-scale event layers $E_1$ to $E_5$, given with the corresponding ages in years BC/AD.

Out of the 24 dated samples from this interval, three samples (KIA33098, KIA29385 and KIA29388) were rejected as they were obtained from large-scale event layer $E_1$ and thus do not belong to an *in-situ* sediment sequence. The remaining 21 calibrated ages and an age of -56 cal. a BP for the sediment-water interface (coring campaign in spring 2006) were used as input parameters for age-depth modelling. As large-scale event layers correspond to instantaneous ("time-neutral") depositional events, the final age-depth model was calculated based on a corrected composite depth with the thickness of these event layers being subtracted (Fig. 5.5).

The final age-depth model yielded a model agreement index $A_{model}$ of 72.5%, which is fairly above the threshold of 60% (Ramsey 1995, 2008). Although also small-scale graded and matrix-supported detrital layers represent instantaneous depositional events, these were not removed from the final age-depth model, because their reflection in the magnetic susceptibility record enables the investigation of their recurrence pattern. An alternative age-depth model, where all small-scale graded detrital layers thicker than 1.5 cm were removed, reveals, however, only negligible deviations from the original age-depth model, in general not exceeding the 2σ confidence interval (i.e. 100–200 years) between individual radiocarbon dated samples.

The continuous upper ~19 m of the Lake Iseo sediment record cover approximately the past 10 000 years (Fig. 5.5). As revealed from the modelled age of 759±62 cal. a BP for the top of large-scale event layer $E_1$ and a radiocarbon date of 1233±54 cal. a BP obtained from a sample (KIA33099) 5 cm below this event, we suggest an erosional hiatus of ca. 500 years (equivalent to about 1 m of sediment) below event layer $E_1$. Due to their floating stratigraphical position, no age model was constructed for the two lowermost core segments of the profile. However, radiocarbon dates of 15 463–16 700 and 17 859–18 567 cal. a BP (KIA39238 and KIA30286, Table 5.2) from the top and the base of the lowermost core segment, respectively, indicate that postglacial lacustrine sediments in the SMB have an age of at least ca. 18 000 cal. a BP (the base of the lacustrine deposits was not recovered). Presuming that the dated material is not reworked, this in turn yields an older minimum age for the retreat of the Last Glacial Maximum glacier from the lake basin than the previous estimate of >16 000 cal. a BP (Bini *et al.* 2007).

Sedimentation rates for both the original and the alternative age-depth model are lowest (~0.5–1.0 mm $a^{-1}$) between ca. 10 000 and 4300 cal. a BP, then increase to ~2.5–3.5 mm $a^{-1}$ from ca. 4300 to 2200 cal. a BP and slightly decrease to ~1.5–2.5 mm $a^{-1}$ during the last ca. 2200 years (all values excluding the large-scale event layers and the ca. 500-year-long hiatus). Modelled ages for the two large event layers $E_1$ and $E_2$ are AD 1191±62 (759±62 cal. a BP) and 355±47 BC (2305±47 cal. a BP), respectively, while the three smaller event layers $E_3$, $E_4$ and $E_5$ date to 575±62 BC (2525±62 cal. a BP), 2538±110 BC (4488±110 cal. a BP) and 6209±173 BC (8159±173 cal. a BP), respectively (Fig. 5.5).

## 5.5 Discussion

### *5.5.1 Holocene runoff events and their relation to climate variability and human impact*

Frequent small-scale detrital layers in the Lake Iseo sediment record, containing abundant allochthonous minerogenic components and terrestrial plant macrofossils, reflect episodical detrital flux from the catchment. Owing to the clear upward-fining and the occasionally observed erosional basal contacts, the graded detrital layers are interpreted as lacustrine turbidites, deposited by high-

density currents acting as underflows (hyperpycnal flows; Sturm & Matter 1978; Mulder & Chapron 2010). In contrast, non-graded matrix-supported detrital layers might reflect either successive settling of detrital material from low-density currents acting as inter- or overflows (Sturm & Matter 1978; Chapron *et al.* 2002) or represent the distal depositional facies of underflows, entering the lake basin at larger distance from the coring site (Mangili *et al.* 2005). In any case, the most probable processes for the transport of allochthonous material from the catchment into the lake are either extreme surface runoff events, channelized through subaerial gullies and subaquatic canyons, or propagating terrestrial debris flows and landslides (Hsü & Kelts 1985; Sletten *et al.* 2003; Mangili *et al.* 2005; Irmler *et al.* 2006) from the hills along the shorelines of the lake, which are all expected to be triggered by exceptionally high precipitation or snowmelt discharge events. The frequent occurrence of mass movements on the SMB slopes throughout the Holocene has also been proven by the seismic survey of Bini et al. (2007), revealing several detrital fans, interpreted as landslide accumulations, along the eastern shoreline. In contrast, river flooding (Lambert *et al.* 1976; Sturm & Matter 1978; Bøe *et al.* 2006) or subaquatic mass flows after the gravitational collapse of slope or delta deposits (Girardclos *et al.* 2007) are unlikely to cause small-scale detrital layers as (1) there is no major tributary close to the coring site and flood-induced turbidity currents originating from the Oglio River are unlikely to cross the Monte Isola Escarpment (Fig. 5.1) and (2) the frequent occurrence of small-scale detrital layers indicates the absence of long-term sediment storage and thus loading effects on the slopes.

Based on sediment microfacies and magnetic susceptibility data, 12 intervals with increased abundance of small-scale detrital layers and generally increased background flux of detrital matter were identified within the Lake Iseo sediment sequence during the Holocene (Fig. 5.6), revealing a distinct centennial-scale recurrence pattern. These intervals of increased detrital flux occur at ca. 9800, 9400–8700, 8000–7900, 7600–6900, 6700, 6300–5900, 5700–4900, 4750, 4200–3300, 2950–2700, 2400–1700 and 750–500 cal. a BP. Although no magnetic susceptibility data are available for the past ca. 500 years, sediment microfacies inspection revealed two further intervals with several small-scale turbidites clustering at ca. 300–200 and 150 cal. a BP. During the early to mid-Holocene, i.e. prior to ca. 4200 cal. a BP, periods of increased detrital flux reveal a correspondence with maxima in atmospheric residual $\Delta^{14}C$ (Stuiver *et al.* 1998), which are considered to represent periods of low solar activity (Beer 2000; Muscheler *et al.* 2000) and in turn are commonly associated with wet/cold climate conditions (van Geel *et al.* 1998; Mauquoy *et al.* 2008). These are thought to favour increased catchment erosion through extreme surface runoff events. Hence, intervals of abundant increased detrital matter flux in Lake Iseo during the early Holocene also reveal a good overall agreement with periods of high lake-levels in the northwestern Alps and central Italy (Magny 2004; Magny *et al.* 2007) as well as flooding activity in the northwestern Alps (Debret *et al.* 2010), which are in general also dependent on wet climate conditions. This close agreement between the different proxy records supports the previously supposed significance of Holocene wet-dry cycles over a wide regional scale in the Alpine region (Magny *et al.* 2007).

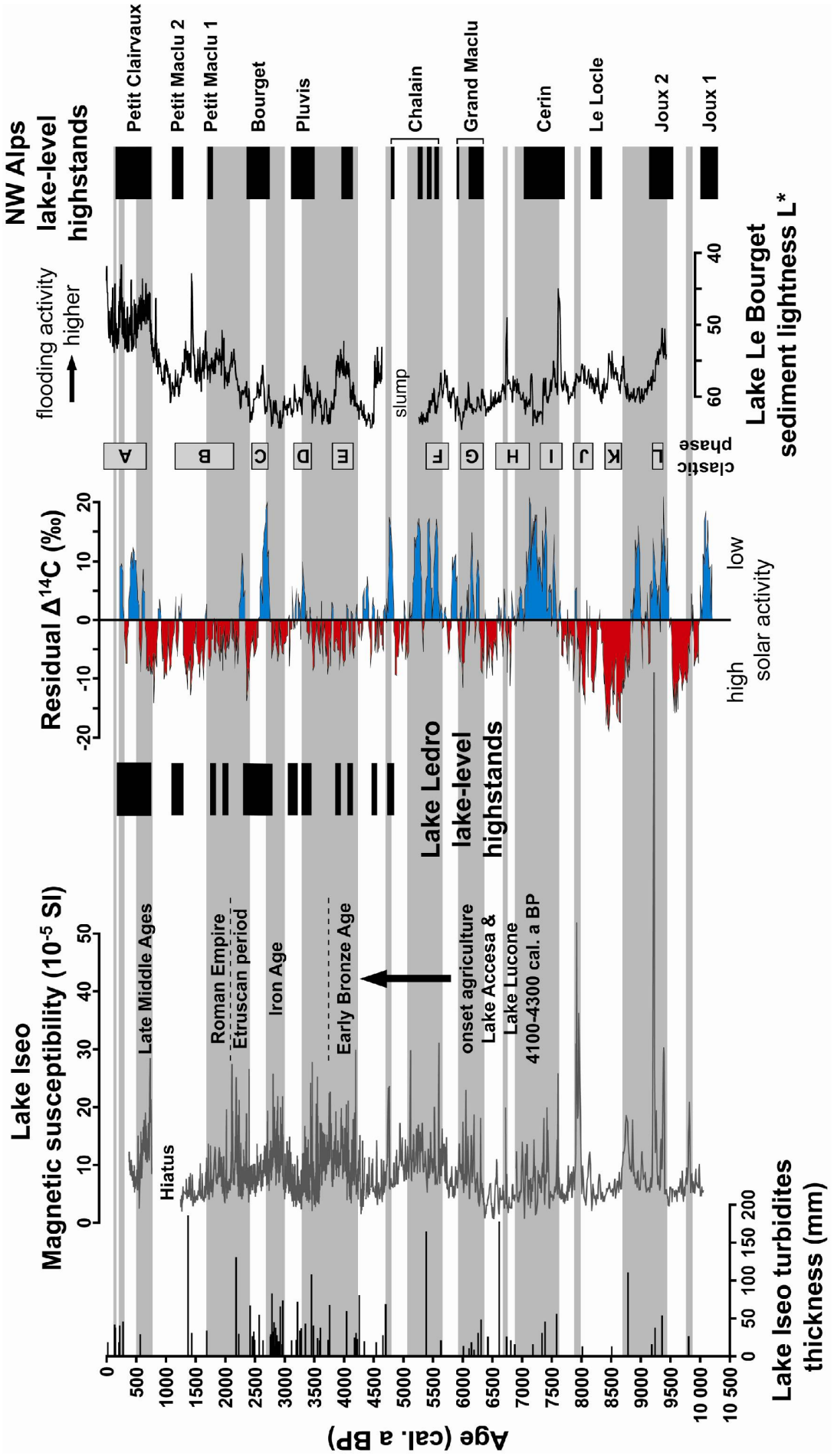
NW Alps
lake-level
highstands
Petit Clairvaux
Petit Maclu 2
Petit Maclu 1
Bourget
Pluvis
Chalain
Grand Maclu
Cerin
Le Locle
Joux 2
Joux 1
flooding activity
higher
slump
Lake Le Bourget
sediment lightness L*
clastic
phase
A
B
C
D
E
F
G
H
I
J
K
L
Residual Δ14C (‰)
high
solar activity
low
Lake Ledro
lake-level
highstands
Lake Iseo
Magnetic susceptibility (10-5 SI)
Late Middle Ages
Roman Empire
Etruscan period
Iron Age
Early Bronze Age
onset agriculture
Lake Accesa &
Lake Lucone
4100-4300 cal. a BP
Hiatus
Lake Iseo turbidites
thickness (mm)
Age (cal. a BP)

After about 4200 cal. a BP, intervals of increased detrital flux in the Lake Iseo record appear to be partly decoupled from periods of low solar activity (Fig. 5.6) and regional lake-level highstands (Magny 2004; Magny *et al.* 2009a), indicating that catchment erosion during the late Holocene might be also controlled by factors other than climate. It has previously been shown that minima in the residual $\Delta^{14}C$ record, reflecting periods of high solar activity and thus dry/warm climate conditions and low lake-levels, were paralleled by increased human impact, e.g. agricultural activity and the construction of lake-dwellings (Tinner *et al.* 2003; Magny 2004). In consequence, the apparent occasional correlation between intervals of high solar activity and enhanced detrital matter flux in Lake Iseo during the late Holocene could be related to increased human impact, particularly during climatically favourable dry/warm periods, in the vicinity of the lake since the Late Neolithic to Early Bronze Age. Although the Lake Iseo area was already settled prior to ca. 5000 cal. a BP as revealed from rock art in the Camonica Valley (de Saulieu 2007), the hypothesis of an onset of significant human influence on detrital flux in Lake Iseo around 4300–4200 cal. a BP is supported by contemporaneous significant increases in pollen indicators for agricultural activity in other records along the southern margin of the Alps (Pini 2002; Tinner *et al.* 2003; Valsecchi *et al.* 2006) and in north-central Italy (Drescher-Schneider *et al.* 2007). It has previously been shown that human activity (in particular agriculture and forest clearance) strongly affects catchment erosion and thus supply of allochthonous material to a lake (Dapples *et al.* 2002). Furthermore, the absence of an increase in net detrital layer thickness after ca. 4200 cal. a BP indicates that the general late Holocene sedimentation rate increase is mainly a reflection of higher background detrital flux, which in turn might be related to the onset of continuous human impact at this time.

The first period of presumably mainly human-controlled detrital matter flux lasted until ca. 3300 cal. a BP, contemporaneous with the Late Bronze Age reduction of indicators for agricultural activity in the nearby Lake Lucone pollen record (Valsecchi *et al.* 2006) and at other locations in the Southern Alps (Finsinger & Tinner 2006).

---

**Figure 5.6** Comparison of Lake Iseo proxy records for detrital matter flux (small-scale turbidites, magnetic susceptibility) with cultural stages in north-central Italy and the first significant increase of taxa indicating agricultural activity in the Lake Accesa (Drescher-Schneider *et al.* 2007) and Lake Lucone (Valsecchi *et al.* 2006) pollen records, lake-level highstands in Lake Ledro (Magny *et al.* 2009a), the record of atmospheric residual $\Delta^{14}C$ as a proxy for solar activity (Stuiver *et al.* 1998), the Lake Le Bourget flooding record (Debret *et al.* 2010) and lake-level highstands in the northwestern Alps (Magny 2004). Grey horizontal bars indicate periods of increased supply of detrital matter in the Lake Iseo sediment record, characterized by abundant turbidites and high magnetic susceptibility. Prior to ca. 4200 cal. a BP, these periods reveal a close correspondence with intervals of high lake-levels in north-central Italy and the northwestern Alps, increased detrital flux through flooding in Lake Le Bourget and low solar activity, indicating wet/cold climate conditions. This indicates a predominant influence of climate variability on detrital matter flux to Lake Iseo. After ca. 4200 cal. a BP, detrital input into the lake appears to be controlled by a complex interplay between climatic factors (wet/cold conditions) and anthropogenic impact. This is indicated by intervals of high detrital flux occurring during periods of dry/warm climate conditions (high solar activity), which overlap with prominent settlement phases.

This furthermore coincides with the widespread abandonment of lake-dwellings in the Alps around the Middle-Late Bronze Age transition (Magny 1993c; Tinner *et al.* 2003; Magny *et al.* 2009b), attributed to a shift towards unfavourable wet/cold climate conditions (Magny 2004). The next interval of high detrital matter flux in the Lake Iseo record at ca. 2950–2700 cal. a BP broadly corresponds to the Iron Age settlement phase, but also incorporates the prominent period of low solar activity and thus wet climate conditions around 2800 cal. a BP (van Geel *et al.* 1996), which also favoured enhanced flooding and glacier activity in the Alps (Guyard *et al.* 2007a; Debret *et al.* 2010). This indicates a complex interplay between the influences of climate and human impact on erosion processes during the late Holocene, apparently also valid for the subsequent intervals of increased catchment erosion at 2400–1700 and 750–500 cal. a BP, which broadly correspond to the Etruscan/Roman Empire period and the Late Middle Ages, respectively. Although there is indication for contemporaneous increases of human impact in the area from the adjacent Lake Lucone pollen record (Valsecchi *et al.* 2006), these intervals partly also incorporate periods of wet/cold climate conditions, e.g. around 1800–1700 and 750–650 cal. a BP, as revealed from lake-level records (Magny 2004). The latest periods of increased detrital flux mainly cluster around the Maunder and Dalton solar minima of the Little Ice Age and therefore could reflect wet/cold climate conditions (cf. Chapron *et al.* 2002; Arnaud *et al.* 2005; Chapron *et al.* 2005) but also increased human impact, in particular deforestation for firewood production.

### *5.5.2 Prehistoric earthquake activity in the vicinity of Lake Iseo*

The five large-scale event layers within the Lake Iseo sediment record reveal a characteristic bipartite structure with basal mass-wasting deposits (slump deposits according to Mulder and Cochonat (1996) and Guyard *et al.* (2007b)) and overlying large-scale turbidites (Fig. 5.4). Similar deposits have previously been identified in numerous lakes and attributed to past earthquake activity (Siegenthaler *et al.* 1987; Chapron *et al.* 1999; Schnellmann *et al.* 2002; Monecke *et al.* 2004; Blass *et al.* 2005; Moernaut *et al.* 2007; Bertrand *et al.* 2008; Fanetti *et al.* 2008). Although large-scale turbidites could also have been generated by gravitationally induced subaquatic mass flows (Hsü & Kelts 1985; Girardclos *et al.* 2007) or extreme surface runoff/flood events (e.g. Lambert *et al.* 1976; Sturm & Matter 1978; Sletten *et al.* 2003; Mangili *et al.* 2005; Bøe *et al.* 2006), a triggering by large earthquakes is more likely than the former mechanisms because (1) frequent small-scale detrital layers throughout the sediment profile prove the continuous supply of allochthonous material and thus the absence of long-term sediment loading on the slopes and (2) there is no tributary discharging to the SMB and channelized surface flow from extreme rainfall runoff is unlikely to generate hyperpycnal flows of the dimension necessary for the deposition of the two large-scale turbidites within event layers $E_1$ and $E_2$ (Mulder & Chapron 2010).

The hypothesis of a seismic triggering of the large-scale event layers is further supported by comparison with historical earthquake records in the region. Particularly the earthquakes of AD 1117 in Verona and AD 1222 in Brescia with inferred epicentral intensities / magnitudes of $I_0$=IX–X / $M_w$=6.5 and $I_0$=VIII–IX / $M_w$=6.0, respectively, which are considered as the two most destructive historical seismic events in north-central Italy (Boschi *et al.* 2000; CPTI Working Group 2004; Guidoboni *et al.* 2007) and have been intensively studied by evaluation of historical sources, archaeoseismology and geomorphological evidence (Guidoboni 1986; Galadini & Galli 2001; Galadini *et al.* 2001; Guidoboni *et al.* 2005; Livio *et al.* 2009), might have affected the study site. Macroseismic intensities of these events in the Lake Iseo area were still in the order of VII to VIII (Guidoboni *et al.* 2007), although the documentation of local effects attributed to the AD 1117 event is rather ambiguous (Guidoboni *et al.* 2005; Stucchi *et al.* 2008). Recent studies have shown that earthquakes exceeding intensities of even VI to VII at the respective site are sufficient to cause liquefaction features within lake sediments (Obermeier 1996; Monecke *et al.* 2004), but also landslides, slope failures and seiches (Siegenthaler *et al.* 1987; Serva 1994; Chapron *et al.* 1999) and in consequence large-scale subaquatic mass movements (i.e. slides or slumps), evolving into mass flows and turbidites (Inouchi *et al.* 1996). The modelled age of AD 1191±62 for large-scale event layer E1 impedes the unequivocal assignment to either the AD 1117 or the AD 1222 earthquake. However, based on the relationship between earthquake strength, epicentral distance and the generation of large-scale turbidites (Inouchi *et al.* 1996), we consider large-scale event layer $E_1$ to be more likely triggered by the adjacent AD 1222 Brescia earthquake (epicentral distance ~25 km) rather than by the more distant AD 1117 Verona earthquake (epicentral distance ~75 km). The second major event layer $E_2$ is supposed to represent a previously undocumented earthquake around 350 BC. With respect to the spatial pattern and maximum magnitudes/intensities of the historically documented earthquakes in the region (CPTI Working Group 2004; Guidoboni *et al.* 2007), the triggering earthquake most probably occurred within a radius of about 30–40 km and reached a magnitude and intensity of $M_w$=5.0–6.5 and $I_0$=VII–IX, respectively. An explanation for the different sediment facies of the basal mass-wasting deposits of both large-scale event layers could be a different distance of the initial slope failure, resulting in a proximal-distal pattern as observed for turbidites, debris flows and slump-generated deposits in Lake Zurich (Hsü & Kelts 1985).

Although the three lower large-scale event layers $E_3$, $E_4$ and $E_5$, dating to 575±62 BC, 2538±110 BC and 6209±173 BC, respectively (Fig. 5.5), are relatively thin compared to event layers $E_1$ and $E_2$, they are also supposed to reflect previously undocumented prehistoric earthquakes with magnitudes of at least $M_W$=5.0. The reduced thickness of these event layers indicates, however, not necessarily that the triggering earthquakes were significantly smaller than those causing event layers $E_1$ and $E_2$. Possible explanations could be either more distal initial slope failures for the event layers $E_3$, $E_4$ and $E_5$ than for the two larger event layers or the generally lower background supply of detrital material during the early Holocene.

Enhanced detrital matter flux due to the increased human activity in the catchment since the Bronze Age might have increased the amount of sediment available for mobilization through slope failures induced by the earthquakes of AD 1222 and 350 BC.

## 5.6 Conclusions

Prior to ca. 4200 cal. a BP, the occurrence of small-scale turbidites and intervals of generally increased detrital matter flux in the Lake Iseo sediment record reveals a correspondence with periods of low solar activity, increased flooding in large Alpine rivers and regional lake-level highstands, reflecting wet and cold climate conditions. This indicates that catchment erosion during the early to mid-Holocene was mainly driven by natural climate variability. With the increase of human impact in the vicinity of the lake after ca. 4200 cal. a BP, intervals of increased occurrence of small-scale turbidites and detrital matter flux and thus enhanced catchment erosion appear to be partly decoupled from climatic fluctuations (wet and cold climate conditions) but rather influenced by anthropogenic land use activity.

Five large-scale event layers composed of basal mass-wasting deposits and overlying turbidites were identified within the profile, which are attributed to major regional earthquakes. Radiocarbon dating provides evidence for a correlation of the uppermost event layer with a documented $M_w$=6.0 earthquake in AD 1222 in Brescia. The four older large-scale event layers are supposed to be related to previously undocumented earthquakes, which occurred prior to the period covered by regional earthquake catalogues around 350 BC, 570 BC, 2540 BC and 6210 BC and most probably also exceeded $M_w$=5.0.

## 5.7 Acknowledgements

This study is part of the DecLakes project within the frame of the European Science Foundation EUROCORES Programme EuroCLIMATE (contract No. ERAS-CT-2003-980409 of the European Commission, DG Research, FP6, ESF project DecLakes no. 04-ECLIM-FP29) and has been funded by the national agencies DFG (Germany, project no. BR2208/2-2, AN554/1-2), CNRS (France) and MEC (Spain, project no. CGL2005-23766-E/CLI). We are indebt to the owners of the Riva di San Pietro camping site for facilitating the field lab. Gabriele Arnold, Dieter Berger and Michael Köhler (GFZ Potsdam) are acknowledged for preparing high-quality thin sections. Maxime Debret (Université de Rouen) kindly provided the Lake Le Bourget data.

# 6 Summary

## 6.1 Main results and conclusions

Although each of the previous chapters of my thesis is an independent work, focusing on a certain region of Europe, covering a specific time interval, utilizing different methodological approaches and addressing a slightly different aspect of past climate variability, all these manuscripts deal with one common topic, the reconstruction of climatic and environmental changes in Europe during the Lateglacial and Holocene. Considering one of my main objectives and also the major aim of the DecLakes project, the identification of regional peculiarities of Lateglacial and Holocene climate variability in Europe during the past 15 000 years and their relation to climatic changes on a larger, extraregional to hemispheric, scale, the investigation of the sediment records of Lake Hańcza (northeastern Poland), Lake Mondsee (Upper Austria) and Lake Iseo (northern Italy) yielded a number of important results for the understanding of past climate dynamics. Moreover the records also provided important insights into the responses of different sedimentary regimes and ecosystems to climatic changes. In the following, I will first present the most important results of the individual studies concerning regional climatic and environmental evolution since the Lateglacial and finally draw some more general conclusions concerning the utilization of sedimentological proxy data in palaeoclimate studies.

The focus of my work on the sediment record of Lake Hańcza was to reconstruct the Lateglacial to early Holocene climate development in eastern Central Europe and to identify possible differences to palaeoclimate records located further to the west. By combining my results of detailed sediment microfacies analysis on large-scale petrographic thin sections and µ-XRF element scanning with pollen analyses and stable isotope measurements on ostracods and bulk endogenic calcite, I was able to identify an interval of environmental and climatic improvement during the early Holocene that clearly post-dates the initial climatic amelioration at the Younger Dryas-Holocene transition. This interval between ca. 10 000 and 9000 cal. a BP was characterized by a pronounced 1.7‰ rise in the oxygen isotope composition of ostracod valves and endogenic calcite and the parallel spread of deciduous forests, likely reflecting rising temperatures and increased humidity. These climatic changes are attributed to a major reorganization of atmospheric circulation in the eastern Baltic in response to the final disappearance of the Scandinavian Ice Sheet. Apparently, relatively cold and dry climate conditions persisted in the eastern Baltic during the first ca. 1500 years of the Holocene, likely as a result of the persistence of the Scandinavian Ice Sheet and an associated specific regional atmospheric circulation pattern during this interval. As a result of a stable high-pressure cell above the ice sheet, persistent anticyclonic circulation (Yu & Harrison 1995; Harrison *et al.* 1996) likely blocked the influence of warm and moist air coming from the Atlantic and thus attenuated the early Holocene climatic amelioration in the eastern Baltic region.

This circulation pattern only disappeared with the final decay of the Scandinavian Ice Sheet around 9500 cal. a BP (Lundqvist & Mejdahl 1995), allowing for further climatic improvement. The observed attenuated early Holocene climatic amelioration in northeastern Poland differs from the climate evolution seen in high-resolution palaeoclimate records from Central Europe (von Grafenstein *et al.* 1999a) and Greenland (Rasmussen *et al.* 2006; Vinther *et al.* 2006) and thus probably represents a particular regional pattern of early Holocene climate development. My results confirm previous studies from other lake sediment records in northwestern Russia (Subetto *et al.* 2002; Wohlfarth *et al.* 2002; Wohlfarth *et al.* 2007) and in consequence indicate that large areas southeast of the retreating Scandinavian Ice Sheet have undergone an early Holocene climate development that clearly differs from that in Greenland and Central and Western Europe.

Work on the sediment record of pre-Alpine Lake Mondsee so far concentrated on two of the time intervals that were focus of the DecLakes project. Within the first study, I applied a multi-proxy approach to the Lateglacial part of this sediment sequence to investigate the response of depositional processes and different environmental parameters to rapid climate fluctuations in a comparatively large lake system. In general, the depositional regime, reflected by allochthonous detrital matter supply and biochemical calcite precipitation, revealed an unexpectedly high sensitivity and pronounced response to climate forcing. Interestingly, even small-scale Lateglacial climate fluctuations such as the Gerzensee and Aegelsee cold oscillations (Eicher & Siegenthaler 1976; Lotter *et al.* 1992) can be tracked in the Lake Mondsee sediments by using high-resolution sedimentological and geochemical analyses. However, while it could be shown that changes in local vegetation occurred broadly synchronously with Lateglacial temperature changes, the response of the sedimentary regime to climate variability is characterized by temporally complex relationships between different proxy parameters. For instance, the decrease of detrital matter flux and the intensification of biochemical calcite precipitation at the onset of the Holocene took place quasi-synchronously with the marked temperature rise, while the reduction of detrital flux lagged the initial Lateglacial warming around 14 600 cal. a BP by ca. 500–750 years. This different behaviour of the sedimentary system during periods of major warming is mainly attributed to the different environmental preconditions. In particular, the delayed reduction of detrital flux at the onset of the Lateglacial Interstadial can be mainly attributed to the persistence of permafrost and relatively slow catchment stabilization, owed to the only gradual establishment of forests in the vicinity of the lake. In contrast the rapid response of the depositional system at the onset of the Holocene was most likely favoured by already established forest cover and stable soils. A complex reaction of the sedimentary regime to climate forcing can also be observed at the onset of the Younger Dryas cooling. Here, the reduction of biochemical calcite precipitation and the increase of detrital flux show a delay of 150–300 years compared to the onset of the cooling, which is supposed to reflect the inertia of a large lake system, but probably also seasonal effects. In summary, major climate shifts during the Lateglacial are characterized by complex and temporally variable proxy responses to climatic forcing, which are controlled by ecosystem inertia and

the long-term evolution of the lake and its catchment. In consequence, only the sound knowledge of the individual boundary conditions at a given site enables the reliable assessment of the impact of future climate change on the local ecosystem and thus the human habitat.

The second study on the Lake Mondsee sediment record utilized the main proxy obtained within the DecLakes project, the oxygen isotope composition of ostracod valves, to study two prominent climate deteriorations during the Holocene, the so-called 8.2 ka and 9.1 ka cold events. These abrupt coolings, which have been identified in numerous palaeoclimate records in the circum-North Atlantic region (e.g. von Grafenstein *et al.* 1999a; Kobashi *et al.* 2007; Rasmussen *et al.* 2007; Seppä *et al.* 2007; Boch *et al.* 2009), are supposed to have been triggered by shutdowns of the Atlantic meridional overturning circulation (MOC) (Ellison *et al.* 2006; LeGrande *et al.* 2006; Kleiven *et al.* 2008) after catastrophic freshwater discharges to the North Atlantic (von Grafenstein *et al.* 1998; Barber *et al.* 1999; Teller *et al.* 2002; Wiersma & Renssen 2006; Renssen *et al.* 2007; Yu *et al.* 2010). A sound understanding of the spatial extent and internal structure of these two cold events in Central Europe as well as the underlying trigger mechanisms and a possible subsequent climate recovery could aid a better understanding of global-scale climate dynamics, which is important for the reliable assessment of future climate change. By combining microscopic varve counting and AMS $^{14}C$ dating of terrestrial plant macrofossils, I was able to establish a robust chronological framework for the oxygen isotope record. As one outcome of this work, the duration (ca. 150 years) as well as the absolute dating (8225–8075 cal. a BP) of the 2°C-cooling during the 8.2 ka cold event reveal a good agreement with results from the Greenland ice cores (Kobashi *et al.* 2007; Thomas *et al.* 2007) and other varved lake sediment records in Europe (e.g. Prasad *et al.* 2009; Zillén & Snowball 2009). Interestingly, a sudden ca. 100-year-long temperature overshoot of ~0.7°C directly after the 8.2 ka cold period could be identified, which is also seen in other proxy records around the North Atlantic (Kobashi *et al.* 2007; Marshall *et al.* 2007), thus most probably representing a hemispheric-scale climate signal. This abrupt warming was most likely triggered by an enhanced resumption of the MOC after the 8.2 ka cold event, also initiating substantial shifts of oceanic and atmospheric front systems (i.e. the Arctic Front and the Intertropical Convergence Zone) in the North Atlantic realm (Stouffer *et al.* 2006; Cheng *et al.* 2009). Although there is also evidence from the North Atlantic for an overshoot in MOC intensity after the 9.1 ka cold period (Ellison *et al.* 2006), there is no indication for overshooting warm temperatures in the Lake Mondsee record during this interval. A possible explanation could be the rather low amplitude and the shorter duration of the 9.1 ka cold event, resulting in a less pronounced subsequent recovery of the MOC (Ellison *et al.* 2006). This overshoot in MOC intensity was most likely not strong enough to trigger a substantial rise in air temperatures in Central Europe. Furthermore, a short warm period around 8800 cal. a BP could be identified in the Lake Mondsee record, apparently occurring synchronous to a shift in atmospheric circulation over the North Atlantic (Cheng *et al.* 2009) but not directly related to changes in MOC intensity. These findings indicate the complex behaviour of the global climate system and should be considered when modelling future abrupt climate events.

Arising from the already macroscopically visible frequent occurrence of coarse-grained clastic-detrital material within the sediment record of Lake Iseo, I decided to focus my work on this sediment sequence on investigating the recurrence pattern of allochthonous detrital flux in order to contribute to a better understanding of the influences of climate variability and anthropogenic impact on catchment erosion processes. By applying a multi-proxy approach of non-destructive core scanning techniques and detailed sediment microfacies analysis on a continuous set of more than 300 large-scale petrographic thin sections, I was able to identify several intervals with increased contents of sand- to silt-sized allochthonous material, occurring either as distinct small-scale graded layers or finely dispersed within the regular clayey-silty pelagic sediments. The coarse-grained material is thought to have been transported from the catchment into the lake by surface runoff after strong precipitation events. In consequence, the derived data set represent the first record of extreme surface runoff events for northern Italy that covers almost the entire Holocene. Based on a comparison with Alpine lake-level (Magny 2004) and flood records (Debret *et al.* 2010) as well as with the record of atmospheric residual $\Delta^{14}C$ as a proxy for solar activity (Stuiver *et al.* 1998; Beer 2000; Muscheler *et al.* 2000), I was able to show that the recurrence of increased detrital flux in Lake Iseo during the early to mid-Holocene reveals a close correspondence with regional lake-level highstands and flooding periods as well as with periods of low solar activity, indicating relatively wet and cold climate conditions (van Geel *et al.* 1998; Mauquoy *et al.* 2008). Hence, detrital flux into the lake during this interval was apparently mainly controlled by natural climate variability. In contrast, during the late Holocene, i.e. after ca. 4200 cal. a BP, increased detrital flux into the basin and thus enhanced catchment erosion through extreme surface runoff not always coincides with periods of wet and cold climate conditions and thus appears to be partly decoupled from climate variability. Although the detrital flux was most probably still triggered by extreme surface runoff after heavy precipitation or strong snow melt, its occasional correlation with periods of increased anthropogenic land use activity in northern Italy (Valsecchi *et al.* 2006; Drescher-Schneider *et al.* 2007) indicates the complex interplay between natural climate variability and human impact on catchment erosion processes, a fact that should be considered when interpreting lake sediment records of periodical detrital matter supply in terms of climate variability.

My work on the Holocene sediment record of Lake Iseo also yielded results, which do not have a direct relation to climate variability, but nevertheless are important for the understanding of the depositional system and the regional geological setting. During the detailed microfacies investigation of the sediments, five large-scale detrital event layers were identified that revealed a completely different internal structure than the normal graded surface runoff event layers, thus being supposed to have different origin. Moreover, their distribution within the lake basin could partly be tracked by high-resolution seismic surveying, indicating a large spatial extent. These event layers are composed of basal mass-wasting deposits, showing large-scale slumping, liquefaction structures and sediment homogenization, and overlying large-scale turbidites. Owing to this characteristic sediment

microfacies (cf. Siegenthaler *et al.* 1987; Chapron *et al.* 1999; Schnellmann *et al.* 2002; Monecke *et al.* 2004; Blass *et al.* 2005; Moernaut *et al.* 2007; Bertrand *et al.* 2008; Fanetti *et al.* 2008), these large-scale event layers are supposed to have been triggered by major regional earthquakes. This interpretation is endorsed by the correlation of the uppermost radiocarbon-dated event layer with a documented and intensively studied $M_w$=6.0 earthquake in AD 1222 near Brescia, about 25 km southeast of Lake Iseo (Guidoboni 1986; Boschi *et al.* 2000; CPTI Working Group 2004; Guidoboni *et al.* 2007; Livio *et al.* 2009). In consequence, the four older large-scale event layers are supposed to be related to previously undocumented major earthquakes in the vicinity of Lake Iseo, reaching magnitudes most probably larger than $M_w$=5.0. As these earthquakes occurred around 350 BC, 570 BC, 2540 BC and 6210 BC, i.e. prior to the period covered by regional earthquake catalogues (Boschi *et al.* 2000; CPTI Working Group 2004; Guidoboni *et al.* 2007), the results from the Lake Iseo sediment record contribute to a better understanding of regional historical seismic activity and could improve the assessment of the seismic hazard in the region.

Besides these very site-specific and climate-related outcomes of my work on the three lake sediment sequences, some more general conclusions considering the value of sedimentological and geochemical proxy data for palaeoclimate studies and the climate sensitivity of large lake systems can be drawn. All studies reveal an unexpectedly high sensitivity of the sedimentary regimes and ecosystems of comparatively large lake systems to past climatic and environmental changes. Besides the imprint of large-scale climate dynamics, also small-scale and more regional climate fluctuations can be detected. However, as the sedimentological response of large lake systems to such small-scale climatic changes is often rather subtle, it is mandatory to apply high-resolution analytical methods to detect these changes in the sediments. Moreover, as single proxy records provide only a limited view on past climatic and environmental changes and thus might lead to erroneous conclusions, only the combination of a variety of different proxies obtained from one sediment record allows for the reliable reconstruction of the environmental development in response to climatic changes and human impact at a given site. It is also important to mention that the response of depositional processes and local environment to climatic changes is largely determined by the local climatic boundary conditions, the individual characteristics of the lake and its surrounding and the environmental preconditions, e.g. glaciation history of the catchment area, local topography, bedrock properties, catchment and basin morphology and size, vegetation history and soil development. Only the sound knowledge of these individual characteristics allows the reliable interpretation of the proxy data derived from a particular lake sediment record in terms of past environmental and climatic changes. As an example, a palaeoenvironmental reconstruction for the Lake Hańcza area without the knowledge of the vegetational development would have been biased with respect to the apparent influence of the vegetation change between 10 000 and 9000 cal. a BP on the $\delta^{18}O$ record. In addition, an interpretation of the $\delta^{18}O$ record in terms of climatic changes without a profound knowledge of the sedimentary record would have possibly also yielded erroneous conclusions. Only the detailed inspection of the

Lateglacial sediments, which were subject to extensive redeposition, indicates that the lacking reflection of a rise in $\delta^{18}O$ at the Younger Dryas-Holocene transition must be related to the Lateglacial depositional environment, which not allows an interpretation of the $\delta^{18}O$ record in terms of climate evolution during this interval. It should be also kept in mind when interpreting lake sediment records in terms of climate variability that anthropogenic impact in the catchment area might influence proxy responses and that natural climate variability and human interferences are not always easily discernable and probably often superimposed. For example, catchment geology and morphology might be of less importance for the location of the coring site in lakes with small topographic contrasts in the surrounding area such as Lake Hańcza. However, this becomes more important in lakes with a more complex catchment morphology. This is partly observed in the Lake Mondsee sediment record, where small scale detrital layers frequently occur but are, however, well confined and clearly discernable from the regular pelagic sediments. Nevertheless, this arises to a major problem in Lake Iseo, where the allochthonous detrital material from surface runoff and also earthquake events is partly hardly discernible from the pelagic sediments. A more careful selection of the coring site with respect to basin and catchment morphology and also a detailed seismic survey prior to the coring campaign could have helped in this particular case to achieve a sediment record more appropriate for high-resolution oxygen isotope studies.

## 6.2 Further perspectives

As each of the studies within this thesis focuses on a rather specific topic and also covers only a relatively narrow time interval, particularly the long sediment sequences of Lake Mondsee and Lake Iseo hold a high potential to yield further interesting results concerning different aspects of past climatic and environmental changes in the Alpine region. One topic to be addressed is the ongoing discussion about the relation between global warming and the recurrence of extreme precipitation events and floods (e.g. Frei *et al.* 1998; Mudelsee *et al.* 2003), posing a serious hazard to modern societies. For Lake Mondsee, a very recent study, that covered the sedimentation history of the last ca. 100 years and where I was involved as a co-author (Fig. 6.1; Swierczynski *et al.* 2009), proved the potential of this lake sediment record as an archive of Holocene flood and debris flow events. By extending the time interval covered by instrumental records and historical sources, such a long flood record could contribute significantly to the understanding of flood recurrence and the underlying trigger mechanisms in the past and thus could yield important information for future flood hazard assessment.

At present, this work continues within the frame of the PhD thesis of Tina Swierczynski, aiming at reconstructing flood and debris flow recurrence for the entire Holocene. However, first preliminary results of my work already indicate interesting relationships between increased flood and debris flow activity and periods of climatic cooling (e.g. during the coldest period of the Little Ice Age) or

increased human impact (e.g. during the past ca. 200 years) (Fig. 6.2). Within this context, it is necessary to mention a very recent work on the sediments of Lake Ammersee, also located at the northern margin of the Alps, which addressed the relation between flood occurrence and large-scale atmospheric circulation processes (Czymzik *et al.* 2010). By showing that the occurrence of detrital input through floods in Lake Ammersee is coupled to certain weather regimes and that flood occurrence during the past ca. 450 years reveals a close correspondence to minima in solar activity as reflected in the record of atmospheric residual $\Delta^{14}C$ (Stuiver *et al.* 1998; Beer 2000; Muscheler *et al.* 2000), Czymczik *et al*. (2010) concluded that low solar activity favours certain flood-prone weather regimes and thus has an influence on large-scale atmospheric circulation processes and flood recurrence. A comparison of the Lake Ammersee flood record with a preliminary 1000-year-long record of detrital event layers (floods and debris flows) from Lake Mondsee, both reflecting sediment supply after extreme precipitation events (Fig. 6.2), reveals very close similarities between the two lake records during the last ca. 450 years.

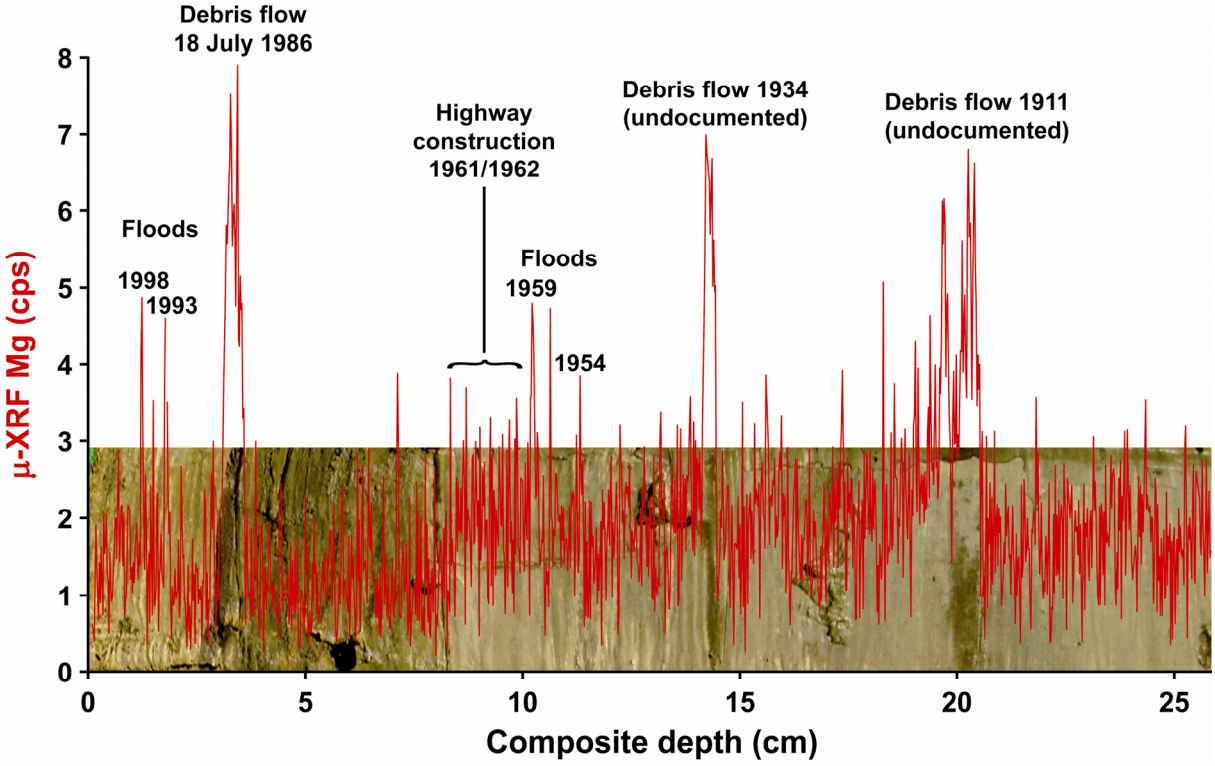


**Figure 6.1** High-resolution μ-XRF element scan across the uppermost 26 cm of the Lake Mondsee sediment core. Peaks in Mg clearly correspond to brownish macroscopic debris flow layers but also to microscopic flood layers, both containing dolomitic minerogenic detritus originating from the Northern Calcareous Alps (for further explanations see Chapter 3). As also the diffuse detrital input during the highway construction in the early 1960s (Einsele 1963) is reflected, continuous μ-XRF scanning along the entire sediment record could be used for the identification of intervals with higher amounts of clastic-detrital input. The dark sediment colour between ca. 4 and 8 cm does not reflect detrital input but the phase of eutrophication between ca. 1968 and 1982 (Findenegg 1969; Klee & Schmidt 1987; Schmidt 1991). This figure was modified from (Swierczynski *et al.* 2009) by using new own results.

Besides the increased occurrence of detrital layers in both records since about AD 1800, which probably reflects increased human impact in the respective catchment areas, there is also a close agreement for the interval AD 1550 to AD 1800, where enhanced flood/debris flow occurrence in both records is mainly coupled to phases of low solar activity (i.e. the coldest phases of the Little Ice Age) (Stuiver *et al.* 1998; Beer 2000; Muscheler *et al.* 2000), which is generally considered to reflect cold and wet climate conditions (van Geel *et al.* 1998; Mauquoy *et al.* 2008). However, prior to about AD 1550, hydrologically triggered depositional events (floods and debris flows) in Lake Mondsee are not only restricted to periods of low solar activity but instead reveal a more complex recurrence pattern. In agreement with my results from Lake Iseo, this might indicate that, although precipitation was still the trigger for the deposition of these event layers, also anthropogenic land use has a significant influence on erosion processes and thus the supply of detrital material to the lake.

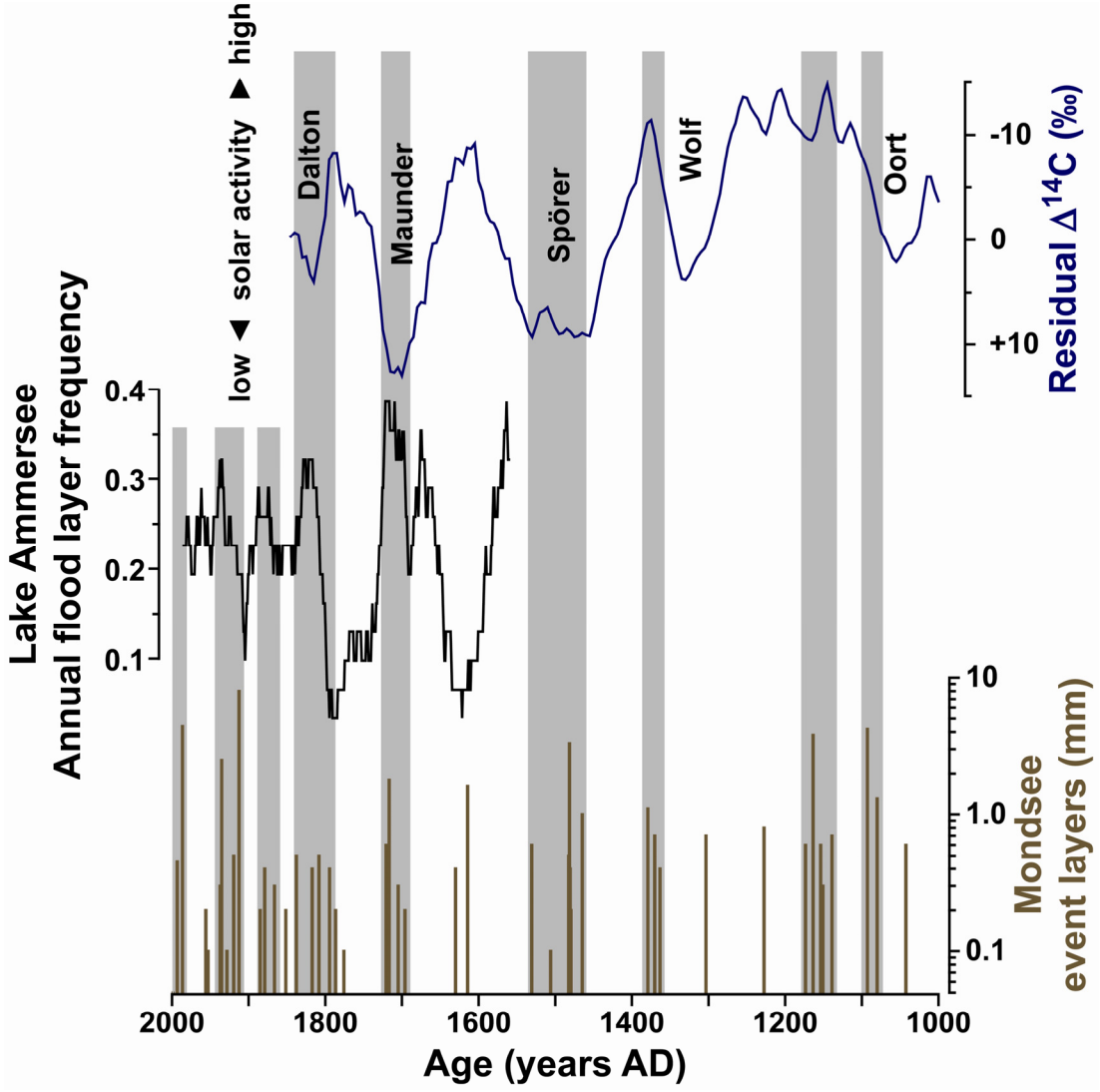


**Figure 6.2** Comparison of a preliminary record of detrital layer recurrence (thickness measurements were carried out on large-scale petrographic thin sections) in Lake Mondsee with the Lake Ammersee flood record (Czymzik *et al.* 2010) and the record of atmospheric residual $\Delta^{14}C$ (Stuiver *et al.* 1998) as a proxy for solar activity during the last 1000 years.

Hence, although the understanding of the trigger mechanisms and the temporal distribution of extreme surface runoff or flood events and their reflection in lake sediment records clearly demands further investigations, it is possible that the relationship between solar activity, atmospheric circulation and extreme precipitation events inferred from the Lake Ammersee flood record (Czymzik *et al.* 2010) might be partly a result of the short duration of this record and probably is not valid on longer time scales.

Interestingly, a close relationship between anthropogenic impact and the occurrence of catchment erosion processes, reflected by the occurrence of debris flow layers in the Lake Mondsee sediments, appears to have existed already during prehistorical times. Although studies that aim at tracking episodes of agricultural activity would either need high-resolution pollen analyses or even more sophisticated approaches such as molecular biomarker techniques (e.g. Jacob *et al.* 2009), a first estimate of the human impact on the Lake Mondsee environment can already be made by the sedimentological investigations that were part of my studies. The local establishment of lake-dwellings along the shores of Lake Mondsee is dated to the late Neolithic, i.e. to ca. 4500–5900 cal. a BP (Table 6.1; Felber 1970; Felber & Pak 1973; Felber 1974, 1975; Felber 1985), generally considered to coincide with the first pronounced phase of agricultural activity in the Alpine region (Behre 2007).

**Table 6.1** Radiocarbon dates obtained from remnants of Neolithic lake-dwellings in Lake Mondsee. Conventional $^{14}C$ ages (Felber 1970; Felber & Pak 1973; Felber 1974, 1975, 1985) were calibrated using OxCal 4.1 (Ramsey 1995, 2001) with the IntCal09 calibration dataset (Reimer *et al.*, 2009).

| Sample | Location | Dated material | Conventional $^{14}C$ age ($^{14}C$ a BP ± σ) | Calibrated age (cal. a BP, 2σ range) |
|---|---|---|---|---|
| VRI-250 | Mooswinkl | pile from lake-dwelling (probably *Populus*) | 4560±100 | 4883–5576 |
| VRI-331 | Mooswinkl | pile from lake-dwelling (*Picea abies*) | 4350±90 | 4657–5294 |
| VRI-332 | Mooswinkl | pile from lake-dwelling (*Picea abies*) | 4260±90 | 4525–5213 |
| VRI-333 | Mooswinkl | pile from lake-dwelling (*Picea abies*) | 4430±110 | 4826–5445 |
| VRI-311 | Scharfling | pile from lake-dwelling (*Picea abies*) | 4940±120 | 5331–5931 |
| VRI-312 | Scharfling | pile from lake-dwelling (*Acer pseudoplatanus*) | 4870±100 | 5326–5891 |
| VRI-313 | Scharfling | pile from lake-dwelling (*Fagus sylvatica*) | 4660±90 | 5054–5590 |
| VRI-314 | Scharfling | pile from lake-dwelling (*Picea abies*) | 4780±90 | 5312–5707 |
| VRI-823 | See | pile from lake-dwelling (undetermined) | 4660±80 | 5062–5589 |
| VRI-37 | See | pile from lake-dwelling (undetermined) | 4910±130 | 5325–5920 |
| VRI-68 | See | pile from lake-dwelling (undetermined) | 4750±90 | 5306–5653 |
| VRI-119 | See | pile from lake-dwelling (undetermined) | 4800±90 | 5319–5714 |

Interestingly, a pronounced increase in the occurrence of detrital event layers, mainly macroscopically visible turbidites related to debris flow events, can be found in the sediments between ca. 4500–5000 varve (calendar) years BP (Fig. 6.3). Also prior to this interval, debris flow occurrence appears to be slightly increased compared to the long-term average. Moreover, the decrease in the frequency of detrital layers in the sediment record around 4500 cal. a BP exactly coincides with the disappearance of lake-dwellings at Lake Mondsee, which occurred synchronously to other records around the Alps and has been related to a combination of climate change and cultural factors (cf. Magny 2004). Hence, a detailed study on the recurrence of detrital event layers in combination with pollen or biomarker analyses could yield new information on the human occupation and land use activity in the region as well as on its impact on erosion processes.

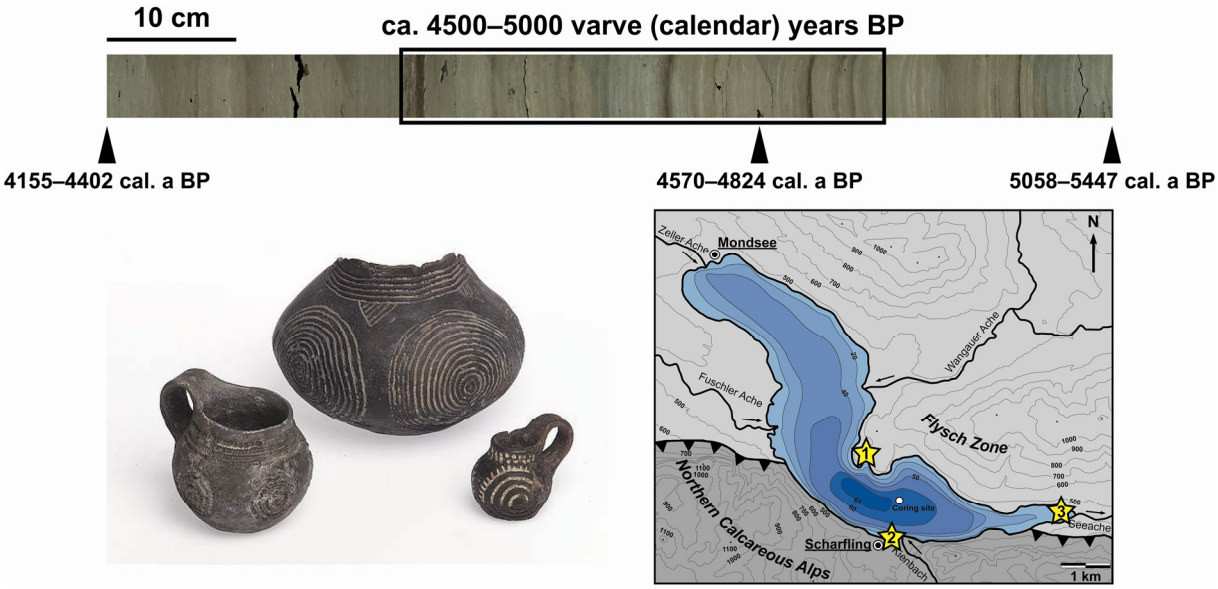


**Figure 6.3** Core photograph of Lake the Mondsee sediments deposited between ca. 4200 and 5150 varve (calendar) years BP. Calibrated AMS radiocarbon dates (2σ) obtained from terrestrial plant macrofossils from the sediment core are given for comparison. The most striking feature of this interval is the increased abundance of brownish detrital layers between ca. 4500 and 5000 cal. a BP. This interval partly coincides with the phase of late Neolithic lake-dwellings, whose remnants were found at three locations (indicated by stars): Mooswinkl Bay (1), Scharfling (2) and See (3). Besides wooden piles of lake-dwellings, also numerous artefacts were found, as for example typical pottery of the late Neolithic Mondsee group/culture (picture by courtesy of the copyright owner Oberösterreichische Landesmuseen, Abteilung Ur- und Frühgeschichte; picture by E. Grilnberger).

A further perspective of the Lake Mondsee sediment record, where work is already in progress and which is of particular interest for the understanding of the relationships between extreme hydrological events and global climate change, is the completion of the Lake Mondsee oxygen isotope record for the entire Holocene and its interpretation in terms of temperature variability. As the results in chapters 3 and 4 of my thesis have shown, this record bears the potential to provide a high-resolution quantitative record of past temperature variability in Central Europe of even better quality as the Lake

Ammersee $\delta^{18}O$ record (von Grafenstein *et al.* 1999a), particularly because of the better age control and the higher hydrological sensitivity of Lake Mondssee.

Further work on Lake Iseo is already planned and a first important step has been made with a successful field campaign in September 2010. New sediment cores were recovered from a site where, according to the seismic studies, sedimentation might be less affected by the supply of detrital matter from the catchment and the shallow-water zone. Preliminary oxygen isotope data obtained from the old sediment record that I have studied, revealed large fluctuations of 2–4‰ throughout the Holocene, which certainly do no reflect a climatic signal. The microscopic inspection of samples with $\delta^{18}O$ values strongly deviating from the average Holocene level showed that such outliers are directly related to detrital layers from surface runoff events. These are supposed to transport also shallow-water ostracods, which calcify at higher temperatures than ostracods from the profundal, to the deep lake basin and thus are responsible for the observed bias of the oxygen isotope record. Although conspicuous samples from distinct detrital layers can be identified by microfacies analysis and removed from the data set, the frequent input of allochthonous material throughout the record implies that also oxygen isotope samples that are inconspicuous at first sight may contain littoral ostracods. Hence, an oxygen isotope record derived from the old sediment core is hardly interpretable in terms of climate variability, but new cores from a more appropriate coring site might yield a continuous undisturbed sediment profile and thus provide the material for the establishment of the first high-resolution oxygen isotope record from the Southern Alps that covers the Holocene and Lateglacial. In addition, this new sediment core might provide the possibility for tephrochronological studies, particularly the detection of microtephras (e.g. Turney 1998), which has been impeded in the old core because of the continuously high input of coarse-grained allochthonous material. This would on the one hand allow a refinement of the radiocarbon-based chronology by correlation with the well-dated tephrochronological reference site Lake Monticchio in southern Italy (Wulf *et al.* 2004). On the other hand, it would also enable the correlation with other palaeoclimate records from the Mediterranean (e.g. Calanchi *et al.* 1998; Magny *et al.* 2007), in order to achieve a more regional picture of climate development since the Last Glacial Maximum and to aid the understanding of the prevalent influences on oxygen isotope records south of the Alps. Furthermore, as the Laacher See Tephra, one of the best-dated Lateglacial chronological markers (Brauer *et al.* 1999b), has recently been identified in another lake sediment record south of the Alps (Finsinger *et al.* 2008), tephrochronological studies on a new sediment core from Lake Iseo could also provide the possibility to correlate this record with other stable oxygen isotope records from north of the Alps and to draw implications on palaeoclimatic teleconnections on a European scale.

# 7 References

Absolon, A. 1978: Die Gattung *Candona* (Ostracoda) im Quartär von Europa. *Rozpravy Československé Akademie Věd 88*, 1–75.

Alley, R. B., Mayewski, P. A., Sowers, T., Stuiver, M., Taylor, K. C. & Clark, P. U. 1997: Holocene climatic instability: A prominent, widespread event 8200 yr ago. *Geology 25*, 483–486.

Ammann, B. 1989: Periods of rapid environmental change around 12500 and 10000 years B.P., as recorded in Swiss lake deposits. *Journal of Paleolimnology 1*, 269–277.

Ammann, B., Birks, H. J. B., Brooks, S. J., Eicher, U., von Grafenstein, U., Hofmann, W., Lemdahl, G., Schwander, J., Tobolski, K. & Wick, L. 2000: Quantification of biotic responses to rapid climatic changes around the Younger Dryas – a synthesis. *Palaeogeography, Palaeoclimatology, Palaeoecology 159*, 313–347.

Ammann, B., Birks, H. J. B., Drescher-Schneider, R., Juggins, S., Lang, G. & Lotter, A. F. 1993: Patterns of variation in late-glacial pollen stratigraphy along a northwest-southeast transect through Switzerland – A numerical analysis. *Quaternary Science Reviews 12*, 277–286.

Ammann, B. & Lotter, A. F. 1989: Late-Glacial radiocarbon- and palynostratigraphy on the Swiss Plateau. *Boreas 18*, 109–126.

Ammann, B., Lotter, A. F., Eicher, U., Gaillard, M.-J., Wohlfarth, B., Haeberli, W., Lister, G., Maisch, M., Niessen, F. & Schlüchter, C. 1994: The Würmian Late-glacial in lowland Switzerland. *Journal of Quaternary Science 9*, 119–125.

Andersen, B. G., Lundqvist, J. & Saarnisto, M. 1995: The Younger Dryas margin of the Scandinavian Ice Sheet – An introduction. *Quaternary International 28*, 145–146.

Andersen, K. K., Svensson, A., Johnsen, S. J., Rasmussen, S. O., Bigler, M., Röthlisberger, R., Ruth, U., Siggaard-Andersen, M.-L., Peder Steffensen, J., Dahl-Jensen, D., Vinther, B. M. & Clausen, H. B. 2006: The Greenland Ice Core Chronology 2005, 15–42ka. Part 1: constructing the time scale. *Quaternary Science Reviews 25*, 3246–3257.

Apolinarska, K. & Hammarlund, D. 2009: Multi-component stable isotope records from Late Weichselian and early Holocene lake sediments at Imiołki, Poland: palaeoclimatic and methodological implications. *Journal of Quaternary Science 24*, 948–959.

Arbogast, R.-M., Jacomet, S., Magny, M. & Schibler, J. 2006: The significance of climate fluctuations for lake level changes and shifts in subsistence economy during the late Neolithic (4300–2400 B.C.) in central Europe. *Vegetation History and Archaeobotany 15*, 403–418.

Arnaud, F., Revel, M., Chapron, E., Desmet, M. & Tribovillard, N. 2005: 7200 years of Rhone river flooding activity in Lake Le Bourget, France: a high-resolution sediment record of NW Alps hydrology. *The Holocene 15*, 420–428.

Bajkiewicz-Grabowska, E. 2008: Bilans wodny jeziora Hańcza. *In* Kozłowski, J., Poczyczyński, P. & Zdanowski, B. (eds.): *Środowisko i ichtiofauna jeziora Hańcza*, 25–36. Wydawnictwo IRS, Olsztyn.

Baldini, L. M., McDermott, F., Foley, A. M. & Baldini, J. U. L. 2008: Spatial variability in the European winter precipitation $\delta^{18}$O-NAO relationship: Implications for reconstructing NAO-mode climate variability in the Holocene. *Geophysical Research Letters 35*, L04709.

Barber, D. C., Dyke, A., Hillaire-Marcel, C., Jennings, A. E., Andrews, J. T., Kerwin, M. W., Bilodeau, G., McNeely, R., Southon, J., Morehead, M. D. & Gagnon, J. M. 1999: Forcing of the cold event of 8,200 years ago by catastrophic drainage of Laurentide lakes. *Nature 400*, 344–348.

Baroni, C., Zanchetta, G., Fallick, A. E. & Longinelli, A. 2006: Mollusca stable isotope record of a core from Lake Frassino, northern Italy; hydrological and climatic changes during the last 14 ka. *The Holocene 16*, 827–837.

Beer, J. 2000: Long-term indirect indices of solar variability. *Space Science Reviews 94*, 53–66.

Behbehani, A. R., Handl, M., Horsthemke, E., Schmidt, R. & Schneider, J. 1985: Possible lake level fluctuations within the Mondsee and Attersee. *In* Danielopol, D. L., Schmidt, R. & Schultze, E. (eds.): *Contributions to the paleolimnology of the Trumer Lakes (Salzburg) and the lakes Mondsee, Attersee and Traunsee (Upper Austria)*, 136–148. Limnologisches Institut der Österreichischen Akademie der Wissenschaften, Mondsee.

Behre, K.-E. 2007: Evidence for Mesolithic agriculture in and around central Europe? *Vegetation History and Archaeobotany 16*, 203–219.

Beiwl, C. 2008: *Atlas der natürlichen Seen Österreichs mit einer Fläche ≥ 50 ha. Morphometrie – Typisierung - Trophie.* 147 pp. Bundesamt für Wasserwirtschaft, Vienna.

Ber, A. 1971: *Arkusz Suwałki. Mapa Geologiczna Polski 1:200 000.* Państwowy Instytut Geologiczny, Warszawa.

Ber, A. 1974: Czwartorzęd Pojezierza Suwalskiego – The Quaternary of the Suwałki Lake District (in Polish with English summary). *Instytut Geologiczny Biuletyn 269*, 23–105.

Ber, A. 1987: Glaciotectonic deformation of glacial landforms and deposits in the Suwałki Lakeland (NE Poland). *In* van der Meer, J. J. M. (ed.): *Tills and Glaciotectonics*, 135–143. A. A. Balkema, Rotterdam.

Berglund, B. E. & Ralska-Jasiewiczowa, M. 1986: Pollen analysis. *In* Berglund, B. E. (ed.): *Handbook of Holocene Palaeoecology and Palaeohydrology*, 455–484. John Wiley & Sons, Chichester.

Bertrand, S., Charlet, F., Chapron, E., Fagel, N. & De Batist, M. 2008: Reconstruction of the Holocene seismotectonic activity of the Southern Andes from seismites recorded in Lago Icalma, Chile, 39°S. *Palaeogeography Palaeoclimatology Palaeoecology 259*, 301–322.

Bini, A., Cita, M. B. & Gaetani, M. 1978: Southern Alpine lakes: hypothesis of an erosional origin related to the Messinian entrenchment. *Marine Geology 27*, 271–288.

Bini, A., Cobari, D., Falletti, P., Fassina, M., Perotti, C. R. & Piccin, A. 2007: Morphology and geological setting of Iseo Lake (Lombardy) through multibeam bathymetry and high-resolution seismic profiles. *Eclogae Geologicae Helvetiae 100*, 23–40.

Birks, H. H. & Ammann, B. 2000: Two terrestrial records of rapid climatic change during the glacial-Holocene transition (14,000–9,000 calendar years B.P.) from Europe. *Proceedings of the National Academy of Sciences of the United States of America 97*, 1390–1394.

Björck, S., Kromer, B., Johnsen, S., Bennike, O., Hammarlund, D., Lemdahl, G., Possnert, G., Rasmussen, T. L., Wohlfarth, B., Hammer, C. U. & Spurk, M. 1996: Synchronized terrestrial-atmospheric deglacial records around the North Atlantic. *Science 274*, 1155–1160.

Björck, S., Rundgren, M., Ingolfsson, O. & Funder, S. 1997: The Preboreal oscillation around the Nordic seas: terrestrial and lacustrine responses. *Journal of Quaternary Science 12*, 455–465.

Björck, S., Walker, M. J. C., Cwynar, L. C., Johnsen, J., Knudsen, K.-L., Lowe, J. J., Wohlfarth, B. & INTIMATE Members 1998: An event stratigraphy for the Last Termination in the North Atlantic region based on the Greenland ice-core record: a proposal by the INTIMATE group. *Journal of Quaternary Science 13*, 283–292.

Blass, A., Anselmetti, F. S., Grosjean, M. & Sturm, M. 2005: The last 1300 years of environmental history recorded in the sediments of Lake Sils (Engadine, Switzerland). *Eclogae Geologicae Helvetiae 98*, 319–332.

Błaszkiewicz, M. 2002: Spätglaziale und frühholozäne Seebeckenentwicklung im östlichen Teil von Pommern (Polen). *Greifswalder Geographische Arbeiten 26*, 11–14.

Boch, R., Spötl, C. & Kramers, J. 2009: High-resolution isotope records of early Holocene rapid climate change from two coeval stalagmites of Katerloch Cave, Austria. *Quaternary Science Reviews 28*, 2527–2538.

Bøe, A.-G., Dahl, S. O., Lie, Ø. & Nesje, A. 2006: Holocene river floods in the upper Glomma catchment, southern Norway: a high-resolution multiproxy record from lacustrine sediments. *The Holocene 16*, 445–455.

Boschi, E., Guidoboni, E., Ferrari, G., Mariotti, D., Valensise, G. & Gasperini, P. 2000: Catalogue of strong Italian earthquakes from 461 B.C. to 1997. *Annali di Geofisica 43*, 609–868.

Bradshaw, R. & Thompson, R. 1985: The use of magnetic measurements to investigate the mineralogy of Icelandic lake sediments and to study catchment processes. *Boreas 14*, 203–215.

Brauer, A. & Casanova, J. 2001: Chronology and depositional processes of the laminated sediment record from Lac d'Annecy, French Alps. *Journal of Paleolimnology 25*, 163–177.

Brauer, A., Dulski, P., Mangili, C., Mingram, J. & Liu, J. 2009: The potential of varves in high-resolution paleolimnological studies. *PAGES News 17*, 96–98.

Brauer, A., Endres, C., Günter, C., Litt, T., Stebich, M. & Negendank, J. F. W. 1999a: High resolution sediment and vegetation responses to Younger Dryas climate change in varved lake sediments from Meerfelder Maar, Germany. *Quaternary Science Reviews 18*, 321–329.

Brauer, A., Endres, C. & Negendank, J. F. W. 1999b: Lateglacial calendar year chronology based on annually laminated sediments from Lake Meerfelder Maar, Germany. *Quaternary International 61*, 17–25.

Brauer, A., Günter, C., Johnsen, S. J. & Negendank, J. F. W. 2000: Land-ice teleconnections of cold climate periods during the last Glacial/Interglacial transition. *Climate Dynamics 16*, 229–239.

Brauer, A., Haug, G. H., Dulski, P., Sigman, D. M. & Negendank, J. F. W. 2008: An abrupt wind shift in western Europe at the onset of the Younger Dryas cold period. *Nature Geoscience 1*, 520–523.

Brunskill, G. J. 1969: Fayetteville Green Lake, New York. II. Precipitation and sedimentation of calcite in a meromictic lake with laminated sediments. *Limnology and Oceanography 14*, 830–847.

Bukowska-Jania, E. & Pulina, M. 1999: Calcium carbonate in deposits of the last Scandinavian glaciation and contemporary chemical denudation in western Pomerania, NW Poland, in the light of modern processes in Spitsbergen. *Zeitschrift für Geomorphologie - Supplement 119*, 27–41.

Burrato, P., Ciucci, F. & Valensise, G. 2003: An inventory of river anomalies in the Po Plain, Northern Italy: evidence for active blind thrust faulting. *Annals of Geophysics 46*, 865–882.

Calanchi, N., Cattaneo, A., Dinelli, E., Gasparotto, G. & Lucchini, F. 1998: Tephra layers in late Quaternary sediments of the central Adriatic Sea. *Marine Geology 149*, 191–209.

Cassinis, G., Corbari, D., Falletti, P. & Perotti, C. R. 2009: *Note illustrative della carta geologica d'Italia alla scala 1: 50.000. Foglio 99 Iseo.* 263 pp. APAT, Servizio Geologico d'Italia, Roma.

Castellarin, A. & Cantelli, L. 2000: Neo-Alpine evolution of the southern Eastern Alps. *Journal of Geodynamics 30*, 251–274.

Castellarin, A., Vai, G. B. & Cantelli, L. 2006: The Alpine evolution of the Southern Alps around the Giudicarie faults: A Late Cretaceous to Early Eocene transfer zone. *Tectonophysics 414*, 203–223.

Chapman, M. R. & Shackleton, N. J. 1998: What level of resolution is attainable in a deep-sea core? Results of a spectrophotometer study. *Paleoceanography 13*, 311–315.

Chapron, E., Arnaud, F., Noël, H., Revel, M., Desmet, M. & Perdereau, L. 2005: Rhone River flood deposits in Lake Le Bourget: a proxy for Holocene environmental changes in the NW Alps, France. *Boreas 34*, 404–416.

Chapron, E., Beck, C., Pourchet, M. & Deconinck, J. F. 1999: 1822 earthquake-triggered homogenite in Lake Le Bourget (NW Alps). *Terra Nova 11*, 86–92.

Chapron, E., Desmet, M., de Putter, T., Loutre, M. F., Beck, C. & Deconinck, J. F. 2002: Climatic variability in the northwestern Alps, France, as evidenced by 600 years of terrigenous sedimentation in Lake Le Bourget. *The Holocene 12*, 177–185.

Cheng, H., Fleitmann, D., Edwards, R. L., Wang, X., Cruz, F. W., Auler, A. S., Mangini, A., Wang, Y., Kong, X., Burns, S. J. & Matter, A. 2009: Timing and structure of the 8.2 kyr B.P. event inferred from $\delta^{18}O$ records of stalagmites from China, Oman, and Brazil. *Geology 37*, 1007–1010.

Chunga, K., Livio, F., Michetti, A. M. & Serva, L. 2007: Synsedimentary deformation of Pleistocene glaciolacustrine deposits in the Albese con Cassano Area (Southern Alps, Northern Italy), and possible implications for paleoseismicity. *Sedimentary Geology 196*, 59–80.

CPTI Working Group 2004: *Catalogo Parametrico dei Terremoti Italiani 2004 (CPTI04)*. INGV, Bologna (http://emidius.mi.ingv.it/CPTI/).

Craig, H. 1961: Isotopic Variations in Meteoric Waters. *Science 133*, 1702–1703.

Crowley, T. J. 2000: Causes of Climate Change Over the Past 1000 Years. *Science 289*, 270–277.

Czymzik, M., Dulski, P., Plessen, B., von Grafenstein, U., Naumann, R. & Brauer, A. 2010: A 450 year record of spring-summer flood layers in annually laminated sediments from Lake Ammersee (southern Germany). *Water Resources Research 46*, W11528.

Dal Piaz, G. V., Bistacchi, A. & Massironi, M. 2003: Geological outline of the Alps. *Episodes 26*, 175–180.

Daley, T. J., Street-Perrott, F. A., Loader, N. J., Barber, K. E., Hughes, P. D. M., Fisher, E. H. & Marshall, J. D. 2009: Terrestrial climate signal of the "8200 yr B.P. cold event" in the Labrador Sea region. *Geology 37*, 831–834.

Danielopol, D. L., Carbonel, P. & Colin, J.-P. (eds.) 1990: *Cytherissa* (Ostracoda) – the *Drosophila* of paleolimnology. *Bulletin de l'Institut de Geologie du Bassin d'Aquitaine 47–48,* 310 pp.

Danielopol, D. L., Geiger, W., Tölderer-Farmer, M., Orellana, C. P. & Terrat, M. N. 1985: The ostracoda of Mondsee: spatial and temporal changes during the last fifty years. *In* Danielopol, D. L., Schmidt, R. & Schultze, E. (eds.): *Contributions to the paleolimnology of the Trumer Lakes (Salzburg) and the lakes Mondsee, Attersee and Traunsee (Upper Austria)*, 99–119. Limnologisches Institut der Österreichischen Akademie der Wissenschaften, Mondsee.

Dansgaard, W. 1964: Stable isotopes in precipitation. *Tellus 16*, 436–468.

Dapples, F., Lotter, A. F., van Leeuwen, J. F. N., van der Knaap, W. O., Dimitriadis, S. & Oswald, D. 2002: Paleolimnological evidence for increased landslide activity due to forest clearing and land-use since 3600 cal BP in the western Swiss Alps. *Journal of Paleolimnology 27*, 239–248.

Davis, B. A. S. & Stevenson, A. C. 2007: The 8.2 ka event and early-mid holocene forests, fires and flooding in the central Ebro desert, NE Spain. *Quaternary Science Reviews 26*, 1695–1712.

de Saulieu, G. 2007: Gravures rupestres et statues-menhirs alpines du Chalcolithique à l'Âge du Bronze moyen : reflets de processus sociaux. *In* Hervé, R., Magny, M. & Mordant, C. (eds.): *Environnements et cultures à l'Âge du Bronze en Europe occidentale*, 357–374. Éditions du CTHS, Paris.

Debret, M., Chapron, E., Desmet, M., Rolland-Revel, M., Magand, O., Trentesaux, A., Bout-Roumazeille, V., Nomade, J. & Arnaud, F. 2010: North western Alps Holocene paleohydrology recorded by flooding activity in Lake Le Bourget, France. *Quaternary Science Reviews 29*, 2185–2200.

Draxler, I. 1977: Pollenanalytische Untersuchungen von Mooren zur spät- und postglazialen Vegetationsgeschichte im Einzugsgebiet der Traun. *Jahrbuch der Geologischen Bundesanstalt Wien 120*, 131–163.

Draxler, I. & van Husen, D. 1987: Zur Vegetationsgeschichte und Stratigraphie des Würmspätglazials des Traungletschergebietes. *Mitteilungen der Kommission für Quartärforschung der Österreichischen Akademie der Wissenschaften 7*, 37–49.

Drescher-Schneider, R., de Beaulieu, J.-L., Magny, M., Walter-Simonnet, A.-V., Bossuet, G., Millet, L., Brugiapaglia, E. & Drescher, A. 2007: Vegetation history, climate and human impact over the last 15,000 years at Lago dell'Accesa (Tuscany, Central Italy). *Vegetation History and Archaeobotany 16*, 279–299.

Drescher-Schneider, R. & Papesch, W. 1998: A contribution towards the reconstruction of Eemian vegetation and climate in central Europe: first results of pollen and oxygen-isotope investigations from Mondsee, Austria. *Vegetation History and Archaeobotany 7*, 235–240.

Drummond, C. N., Patterson, W. P. & Walker, J. C. G. 1995: Climatic forcing of carbon-oxygen isotopic covariance in temperate-region marl lakes. *Geology 23*, 1031–1034.

Ebbesen, H. & Hald, M. 2004: Unstable Younger Dryas climate in the northeast North Atlantic. *Geology 32*, 673–676.

Ehlers, J., Āboltiņš, O., Ber, A., Dobracka, E., Dobracki, R., Donner, J., Dreimanis, A., Florek, W., Gaigalas, A., Hang, T., Heinsalu, A., Jurgaitis, A., Karukäpp, R., Koivisto, M., Krzywicki, T., Lisicki, S., Makowska, A., Markots, A., Melešytė, M., Miidel, A., Mojski, J. E., Morawski, W., Nitz, B., Raukas, A., Saarse, L., Satkšnas, J., Siiräinen, A., Strautnieks, I., Subotowicz, W., Tavast, E., Tomczak, A., Zelčs, V. & Zilans, A. 1995: Baltic Traverse. *In* Schirmer, W. (ed.): *Quaternary field trips in Central Europe, Vol. 1*, 119–188. Verlag Dr. Friedrich Pfeil, München.

Ehlers, J. & Gibbard, P. L. (eds.) 2004: Quaternary glaciations: extent and chronology, Part 1: Europe. *Developments in Quaternary Science 2,* 488 pp. Elsevier, Amsterdam.

Eicher, U. 1987: Die spätglazialen sowie die frühpostglazialen Klimaverhältnisse im Bereiche der Alpen: Sauerstoffisotopenkurven kalkhaltiger Sedimente. *Geographica Helvetica 1987/2*, 99–104.

Eicher, U. & Siegenthaler, U. 1976: Palynological and oxygen isotope investigations on Late-Glacial sediment cores from Swiss lakes. *Boreas 5*, 109–117.

Eicher, U., Siegenthaler, U. & Wegmüller, S. 1981: Pollen and oxygen isotope analyses on late- and post-glacial sediments of the Tourbière de Chirens (Dauphiné, France). *Quaternary Research 15*, 160–170.

Einsele, E. 1963: Schwere Schädigungen der Fischerei und der biologischen Verhältnisse im Mondsee durch Einbringung von lehmig-tonigem Berg-Abraum. Der spezielle Fall und seine allgemeinen Lehren. *Österreichs Fischerei 16*, 1–9.

Ellison, C. R. W., Chapman, M. R. & Hall, I. R. 2006: Surface and deep ocean interactions during the cold climate event 8200 years ago. *Science 312*, 1929–1932.

Fanetti, D., Anselmetti, F. S., Chapron, E., Sturm, M. & Vezzoli, L. 2008: Megaturbidite deposits in the Holocene basin fill of Lake Como (southern Alps, Italy). *Palaeogeography, Palaeoclimatology, Palaeoecology 259*, 323–340.

Fantoni, R., Bersezio, R. & Forcella, F. 2004: Alpine structure and deformation chronology at the southern Alps-Po Plain border in Lombardy. *Bollettino della Società Geologica Italiana 123*, 463–476.

Felber, H. 1970: Vienna Radium Institute radiocarbon dates I. *Radiocarbon 12*, 298–318.

Felber, H. 1974: Vienna Radium Institute radiocarbon dates V. *Radiocarbon 16*, 277–283.

Felber, H. 1975: Vienna Radium Institute radiocarbon dates VI. *Radiocarbon 17*, 247–254.

Felber, H. 1985: Vienna Radium Institute radiocarbon dates XV. *Radiocarbon 27*, 616–622.

Felber, H. & Pak, E. 1973: Vienna Radium Institute radiocarbon dates IV. *Radiocarbon 15*, 425–434.

Findenegg, I. 1969: Die Eutrophierung des Mondsees im Salzkammergut. *Wasser- und Abwasser-Forschung 4*, 139–144.

Finsinger, W., Belis, C., Blockley, S. P. E., Eicher, U., Leuenberger, M., Lotter, A. F. & Ammann, B. 2008: Temporal patterns in lacustrine stable isotopes as evidence for climate change during the late glacial in the Southern European Alps. *Journal of Paleolimnology 40*, 885–895.

Finsinger, W. & Tinner, W. 2006: Holocene vegetation and land-use changes in response to climatic changes in the forelands of the southwestern Alps, Italy. *Journal of Quaternary Science 21*, 243–258.

Fleitmann, D., Mudelsee, M., Burns, S. J., Bradley, R. S., Kramers, J. & Matter, A. 2008: Evidence for a widespread climatic anomaly at around 9.2 ka before present. *Paleoceanography 23*, PA1102.

Frei, C., Schär, C., Lüthi, D. & Davies, H. C. 1998: Heavy precipitation processes in a warmer climate. *Geophysical Research Letters 25*, 1431–1434.

Friedrich, M., Kromer, B., Spurk, M., Hofmann, J. & Kaiser, K. F. 1999: Paleo-environment and radiocarbon calibration as derived from Lateglacial/Early Holocene tree-ring chronologies. *Quaternary International 61*, 27–39.

Gaillard, M.-J. 1985: Late-glacial and Holocene environments of some ancient lakes in the western Swiss Plateau. *Dissertationes Botanicae 87*, 273–336.

Galadini, F. & Galli, P. 2001: Archaeoseismology in Italy: Case studies and implications on long-term seismicity. *Journal of Earthquake Engineering 5*, 35–68.

Galadini, F., Galli, P., Molin, D. & Ciurletti, G. 2001: Searching for the source of the 1117 earthquake in Northern Italy: a multidisciplinary approach. *In* Glade, T., Albini, P. & Francés, F. (eds.): *The Use of Historical Data in Natural Hazard Assessments*, 3–27. Kluwer Academic Publishers, Dordrecht, Netherlands.

Garibaldi, L., Mezzanotte, V., Brizzio, M. C., Rogora, M. & Mosello, R. 1999: The trophic evolution of Lake Iseo as related to its holomixis. *Journal of Limnology 58*, 10–19.

Geiger, W. 1993: *Cytherissa lacustris* (Ostracoda, Crustacea): Its use in detecting and reconstructing environmental changes at the sediment-water interface. *Verhandlungen der Internationalen Vereinigung für theoretische und angewandte Limnologie 25*, 1102–1107.

Girardclos, S., Schmidt, O. T., Sturm, M., Ariztegui, D., Pugin, A. & Anselmetti, F. S. 2007: The 1996 AD delta collapse and large turbidite in Lake Brienz. *Marine Geology 241*, 137–154.

Goslar, T., Bałaga, K., Arnold, M., Tisnerat, N., Starnawska, E., Kuźniarski, M., Chróst, L., Walanus, A. & Więckowski, K. 1999: Climate-related variations in the composition of the Lateglacial and Early Holocene sediments of Lake Perespilno (eastern Poland). *Quaternary Science Reviews 18*, 899–911.

Goslar, T., Kuc, T., Ralska-Jasiewiczowa, M., Różański, K., Arnold, M., Bard, E., van Geel, B., Pazdur, M. F., Szeroczyńska, K., Wicik, B., Więckowski, K. & Walanus, A. 1993: High-resolution lacustrine record of the Late Glacial/Holocene transition in Central Europe. *Quaternary Science Reviews 12*, 287–294.

Griffiths, H. I. & Holmes, J. A. 2000: *Non-marine Ostracods and Quaternary Palaeoenvironments.* 188 pp. Quaternary Research Association Technical Guide 8, Quaternary Research Association, London.

Grimm, E. C. 1987: CONISS: a FORTRAN 77 program for stratigraphically constrained cluster analysis by the method of incremental sum of squares. *Computers & Geosciences 13*, 13–35.

Grimm, E. C. 1992: TILIA and TILIA GRAPH: Pollen spreadsheet and graphics programs. *8th International Palynological Congress*, Aix-en-Provence, Program and Abstracts, p. 56, September 6–12. 1992.

Grootes, P., Stuiver, M., White, J. W. C., Johnsen, S. J. & Jouzel, J. 1993: Comparison of oxygen isotope records from the GISP2 and GRIP Greenland ice cores. *Nature 366*, 552–554.

Grootes, P. M. & Stuiver, M. 1997: Oxygen 18/16 variability in Greenland snow and ice with $10^{-3}$- to $10^{-5}$-year time resolution. *Journal of Geophysical Research 102*, 26455–26470.

Guidoboni, E. 1986: The earthquake of December 25, 1222: analysis of a myth. *Geologia Applicata e Idrogeologia 21*, 413–424.

Guidoboni, E., Comastri, A. & Boschi, E. 2005: The "exceptional" earthquake of 3 January 1117 in the Verona area (northern Italy): A critical time review and detection of two lost earthquakes (lower Germany and Tuscany). *Journal of Geophysical Research 110*, B12309.

Guidoboni, E., Ferrari, G., Mariotti, D., Comastri, A., Tarabusi, G. & Valensise, G. 2007: CFTI4Med – Catalogue of strong earthquakes in Italy (461 B.C.–1997) and Mediterranean area (760 B.C.–1500).

Gulliksen, S., Birks, H. H., Possnert, G. & Mangerud, J. 1998: A calendar age estimate of the Younger Dryas-Holocene boundary at Kråkenes, western Norway. *The Holocene 8*, 249–259.

Guyard, H., Chapron, E., St-Onge, G., Anselmetti, F. S., Arnaud, F., Magand, O., Francus, P. & Mélières, M.-A. 2007a: High-altitude varve records of abrupt environmental changes and mining activity over the last 4000 years in the Western French Alps (Lake Bramant, Grandes Rousses Massif). *Quaternary Science Reviews 26*, 2644–2660.

Guyard, H., St-Onge, G., Chapron, E., Anselmetti, F. S. & Francus, P. 2007b: The AD 1881 earthquake-triggered slump and late Holocene flood-induced turbidites from proglacial Lake Bramant, western French Alps. *In* Lykousis, V., Sakellariou, D. & Locat, J. (eds.): *Submarine Mass Movements and Their Consequences*. Advances in Natural and Technological Hazards Research 27, 279–286.

Haflidason, H., Sejrup, H. P., Kristensen, D. K. & Johnsen, S. J. 1995: Coupled response of the late glacial climatic shifts of northwest Europe reflected in Greenland ice cores: Evidence from the northern North Sea. *Geology 23*, 1059–1062.

Hammarlund, D., Aravena, R., Barnekow, L., Buchardt, B. & Possnert, G. 1997: Multi-component carbon isotope evidence of early Holocene environmental change and carbon-flow pathways from a hard-water lake in northern Sweden. *Journal of Paleolimnology 18*, 219–233.

Hammarlund, D., Barnekow, L., Birks, H. J. B., Buchardt, B. & Edwards, T. W. D. 2002: Holocene changes in atmospheric circulation recorded in the oxygen-isotope stratigraphy of lacustrine carbonates from northern Sweden. *The Holocene 12*, 339–351.

Hammarlund, D., Björck, S., Buchardt, B., Israelson, C. & Thomsen, C. T. 2003: Rapid hydrological changes during the Holocene revealed by stable isotope records of lacustrine carbonates from Lake Igelsjön, southern Sweden. *Quaternary Science Reviews 22*, 353–370.

Hammarlund, D., Björck, S., Buchardt, B. & Thomsen, C. T. 2005: Limnic responses to increased effective humidity during the 8200 cal. yr BP cooling event in southern Sweden. *Journal of Paleolimnology 34*, 471–480.

Hammarlund, D., Edwards, T. W. D., Björck, S., Buchardt, B. & Wohlfarth, B. 1999: Climate and environment during the Younger Dryas (GS-1) as reflected by composite stable isotope records of lacustrine carbonates at Torreberga, southern Sweden. *Journal of Quaternary Science 14*, 17–28.

Harrison, S. P., Yu, G. & Tarasov, P. E. 1996: Late Quaternary lake-level record from northern Eurasia. *Quaternary Research 45*, 138–159.

Heiri, O. & Millet, L. 2005: Reconstruction of Late Glacial summer temperatures from chironomid assemblages in Lac Lautrey (Jura, France). *Journal of Quaternary Science 20*, 33–44.

Herrmann, M. 1990: *Oberflächenkartierung der Mooswinklbucht/Mondsee und Untersuchungen zur Tiefenstruktur.* Thesis, Georg-August-Universität, Göttingen, Germany.

Hoek, W. Z. 2001: Vegetation response to the ~14.7 and ~11.5 ka cal. BP climate transitions: is vegetation lagging climate? *Global and Planetary Change 30*, 103–115.

Horsthemke, E. 1986: *Sedimentgeologische Untersuchungen zum Problem von Seespiegel-schwankungen im Bereich der neolithischen Siedlung der Station See im Mondsee (Salzkammergut, Österreich).* Thesis, Georg-August-Universität Göttingen, Germany.

Hsü, K. J. & Kelts, K. 1985: Swiss lakes as a geological laboratory. Part I: Turbidity currents. *Naturwissenschaften 72*, 315–321.

Hughen, K. A., Southon, J. R., Lehman, S. J. & Overpeck, J. T. 2000: Synchronous radiocarbon and climate shifts during the last deglaciation. *Science 290*, 1951–1954.

Huntley, B. 1993: Rapid early-Holocene migration and high abundance of hazel (*Corylus avellana* L.): alternative hypotheses. *In* Chambers, F. M. (ed.): *Climate Change and Human Impact on the Landscape*, 205–215. Chapman & Hall, London.

IAEA/WMO 2006: Global Network of Isotopes in Precipitation. The GNIP Database. (http://isohis.iaea.org).

Inouchi, Y., Kinugasa, Y., Kumon, F., Nakano, S., Yasumatsu, S. & Shiki, T. 1996: Turbidites as records of intense palaeoearthquakes in Lake Biwa, Japan. *Sedimentary Geology 104*, 117–125.

Irlweck, K. & Danielopol, D. L. 1985: Caesium-137 and lead-210 dating of recent sediments from Mondsee (Austria). *Hydrobiologia 128*, 175–185.

Irmler, R., Daut, G. & Mäusbacher, R. 2006: A debris flow calendar derived from sediments of lake Lago di Braies (N. Italy). *Geomorphology 77*, 69–78.

Isarin, R. F. B., Renssen, H. & Vandenberghe, J. 1998: The impact of the North Atlantic Ocean on the Younger Dryas climate in northwestern and Central Europe. *Journal of Quaternary Science 13*, 447–453.

Jacob, J., Disnar, J.-R., Arnaud, F., Gauthier, E., Billaud, Y., Chapron, E. & Bardoux, G. 2009: Impacts of new agricultural practices on soil erosion during the Bronze Age in the French Prealps. *The Holocene 19*, 241–249.

Jagsch, A. & Megay, K. 1982: Mondsee. *In* Wurzer, E. (ed.): *Seenreinhaltung in Österreich*, 155–163. Bundesministerium für Land- und Forstwirtschaft, Wien.

Johnsen, S. J., Clausen, H. B., Dansgaard, W., Fuhrer, K., Gundestrup, N., Hammer, C. U., Iversen, P., Jouzel, J., Stauffer, B. & Steffensen, J. P. 1992: Irregular glacial interstadials recorded in a new Greenland ice core. *Nature 359*, 311–313.

Jones, R. T., Marshall, J. D., Crowley, S. F., Bedford, A., Richardson, N., Bloemendal, J. & Oldfield, F. 2002: A high resolution, multiproxy Late-glacial record of climate change and intrasystem responses in Northwest England. *Journal of Quaternary Science 17*, 329–340.

Kelts, K. & Hsü, K. J. 1978: Freshwater carbonate sedimentation. *In* Lerman, A. (ed.): *Lakes: Chemistry, Geology, Physics*, 295–324. Springer, New York.

Klasen, N., Fiebig, M., Preusser, F., Reitner, J. M. & Radtke, U. 2007: Luminescence dating of proglacial sediments from the Eastern Alps. *Quaternary International 164–65*, 21–32.

Klaus, W. 1975: Das Mondsee-lnterglazial, ein neuer Florenfundpunkt der Ostalpen. *Jahrbuch des oberösterreichischen Musealvereines 120a*, 315–344.

Klee, R. & Schmidt, R. 1987: Eutrophication of Mondsee (Upper Austria) as indicated by the diatom stratigraphy of a sediment core. *Diatom Research 2*, 55–76.

Kleiven, H. F., Kissel, C., Laj, C., Ninnemann, U. S., Richter, T. O. & Cortijo, E. 2008: Reduced North Atlantic Deep Water Coeval with the Glacial Lake Agassiz Freshwater Outburst. *Science 319*, 60–64.

Kobashi, T., Severinghaus, J. P., Brook, E. J., Barnola, J. M. & Grachev, A. M. 2007: Precise timing and characterization of abrupt climate change 8200 years ago from air trapped in polar ice. *Quaternary Science Reviews 26*, 1212–1222.

Koç Karpuz, N. & Jansen, E. 1992: A high-resolution diatom record of the last deglaciation from the SE Norwegian Sea: documentation of rapid climatic changes. *Paleoceanography 7*, 499–520.

Kohl, H. 1998: Das Eiszeitalter in Oberösterreich Teil II: Die eiszeitliche Vergletscherung in Oberösterreich. *Jahrbuch des oberösterreichischen Musealvereines 143a*, 175–390.

Krivova, N. A. & Solanki, S. K. 2004: Solar variability and global warming: a statistical comparison since 1850. *Advances in Space Research 34*, 361–364.

Kupryjanowicz, M. 2007: Postglacial development of vegetation in the vicinity of the Wigry Lake. *Geochronometria 27*, 53–66.

Kutzbach, J. E., Guetter, P. J., Behling, P. J. & Selin, R. 1993: Simulated climatic changes: results of the COHMAP climate-model experiments. *In* Wright, H. E., Kutzbach, J. E., Webb III, T., Ruddiman, W. F., Street-Perrott, F. A. & Bartlein, P. J. (eds.): *Global Climates since the Last Glacial Maximum*, 24–93. University of Minnesota Press, Minneapolis.

Lambert, A. M., Kelts, K. & Marshall, N. F. 1976: Measurements of density underflows from Walensee, Switzerland. *Sedimentology 23*, 87–105.

Lauterbach, S., Brauer, A., Andersen, N., Danielopol, D. L., Dulski, P., Hüls, M., Milecka, K., Namiotko, T., Obremska, M., von Grafenstein, U. & DecLakes participants Environmental responses to Lateglacial climatic fluctuations recorded in the sediments of pre-Alpine Lake Mondsee (northeastern Alps). *Journal of Quaternary Science* (in press), DOI: 10.1002/jqs.1448.

LeGrande, A. N., Schmidt, G. A., Shindell, D. T., Field, C. V., Miller, R. L., Koch, D. M., Faluvegi, G. & Hoffmann, G. 2006: Consistent simulations of multiple proxy responses to an abrupt climate change event. *Proceedings of the National Academy of Sciences of the United States of America 103*, 837–842.

Leng, M. J. & Marshall, J. D. 2004: Palaeoclimate interpretation of stable isotope data from lake sediment archives. *Quaternary Science Reviews 23*, 811–831.

Litt, T., Brauer, A., Goslar, T., Merkt, J., Bałaga, K., Müller, H., Ralska-Jasiewiczowa, M., Stebich, M. & Negendank, J. F. W. 2001: Correlation and synchronisation of Lateglacial continental sequences in northern central Europe based on annually laminated lacustrine sediments. *Quaternary Science Reviews 20*, 1233–1249.

Litt, T. & Stebich, M. 1999: Bio- and chronostratigraphy of the lateglacial in the Eifel region, Germany. *Quaternary International 61*, 5–16.

Livio, F. A., Berlusconi, A., Michetti, A. M., Sileo, G., Zerboni, A., Trombino, L., Cremaschi, M., Mueller, K., Vittori, E., Carcano, C. & Rogledi, S. 2009: Active fault-related folding in the epicentral area of the December 25, 1222 ($I_0$ = IX MCS) Brescia earthquake (Northern Italy): Seismotectonic implications. *Tectonophysics 476*, 320–335.

Löffler, H. 1983: Aspects of the history and evolution of Alpine lakes in Austria. *Hydrobiologia 100*, 143–152.

Loizeau, J.-L., Span, D., Coppee, V. & Dominik, J. 2001: Evolution of the trophic state of Lake Annecy (eastern France) since the last glaciation as indicated by iron, manganese and phosphorus speciation. *Journal of Paleolimnology 25*, 205–214.

Lotter, A. F. 1999: Late-glacial and Holocene vegetation history and dynamics as shown by pollen and plant macrofossil analyses in annually laminated sediments from Soppensee, central Switzerland. *Vegetation History and Archaeobotany 8*, 165–184.

Lotter, A. F., Birks, H. J. B., Eicher, U., Hofmann, W., Schwander, J. & Wick, L. 2000: Younger Dryas and Allerød summer temperatures at Gerzensee (Switzerland) inferred from fossil pollen and cladoceran assemblages. *Palaeogeography, Palaeoclimatology, Palaeoecology 159*, 349–361.

Lotter, A. F., Eicher, U., Siegenthaler, U. & Birks, H. J. B. 1992: Late-glacial climatic oscillations as recorded in Swiss lake sediments. *Journal of Quaternary Science 7*, 187–204.

Lowe, J. J. & Hoek, W. Z. 2001: Inter-regional correlation of palaeoclimatic records for the last glacial-interglacial transition; a protocol for improved precision recommended by the INTIMATE project group. *Quaternary Science Reviews 20*, 1175–1187.

Lücke, A. & Brauer, A. 2004: Biogeochemical and micro-facial fingerprints of ecosystem response to rapid Late Glacial climatic changes in varved sediments of Meerfelder Maar (Germany). *Palaeogeography, Palaeoclimatology, Palaeoecology 211*, 139–155.

Lundqvist, J. 1986: Late Weichselian glaciation and deglaciation in Scandinavia. *Quaternary Science Reviews 5*, 269–292.

Lundqvist, J. & Mejdahl, V. 1995: Luminescence dating of the deglaciation in northern Sweden. *Quaternary International 28*, 193–197.

Lundqvist, J. & Wohlfarth, B. 2001: Timing and east-west correlation of south Swedish ice marginal lines during the Late Weichselian. *Quaternary Science Reviews 20*, 1127–1148.

Magny, M. 1993a: Holocene fluctuations of lake levels in the French Jura and sub-Alpine ranges, and their implications for past general circulation patterns. *The Holocene 3*, 306–313.

Magny, M. 1993b: Solar influences on Holocene climatic changes illustrated by correlations between past lake-level fluctuations and the atmospheric $^{14}C$ record. *Quaternary Research 40*, 1–9.

Magny, M. 1993c: Un cadre climatique pour les habitats lacustres préhistoriques? *Comptes Rendus de l'Academie des Sciences 316*, 1619–1625.

Magny, M. 2004: Holocene climate variability as reflected by mid-European lake-level fluctuations and its probable impact on prehistoric human settlements. *Quaternary International 113*, 65–79.

Magny, M., Aalbersberg, G., Bégeot, C., Benoit-Ruffaldi, P., Bossuet, G., Disnar, J.-R., Heiri, O., Laggoun-Defarge, F., Mazier, F., Millet, L., Peyron, O., Vannière, B. & Walter-Simonnet, A.-V. 2006: Environmental and climatic changes in the Jura mountains (eastern France) during the Lateglacial-Holocene transition: a multi-proxy record from Lake Lautrey. *Quaternary Science Reviews 25*, 414–445.

Magny, M., Arnaud, F., Holzhauser, H., Chapron, E., Debret, M., Desmet, M., Leroux, A., Millet, L., Revel, M. & Vannière, B. 2010: Solar and proxy-sensitivity imprints on paleohydrological records for the last millennium in west-central Europe. *Quaternary Research 73*, 173–179.

Magny, M., Bégeot, C., Guiot, J. & Peyron, O. 2003: Contrasting patterns of hydrological changes in Europe in response to Holocene climate cooling phases. *Quaternary Science Reviews 22*, 1589–1596.

Magny, M., de Beaulieu, J. L., Drescher-Schneider, R., Vanniere, B., Walter-Simonnet, A. V., Miras, Y., Milleta, L., Bossueta, G., Peyron, O., Bruglapaglia, E. & Leroux, A. 2007: Holocene climate changes in the central Mediterranean as recorded by lake-level fluctuations at Lake Accesa (Tuscany, Italy). *Quaternary Science Reviews 26*, 1736–1758.

Magny, M., Galop, D., Bellintani, P., Desmet, M., Didier, J., Haas, J. N., Martinelli, N., Pedrotti, A., Scandolari, R., Stock, A. & Vanniere, B. 2009a: Late-Holocene climatic variability south of the Alps as recorded by lake-level fluctuations at Lake Ledro, Trentino, Italy. *The Holocene 19*, 575–589.

Magny, M., Peyron, O., Gauthier, E., Rouèche, Y., Bordon, A., Billaud, Y., Chapron, E., Marguet, A., Pétrequin, P. & Vannière, B. 2009b: Quantitative reconstruction of climatic variations during the Bronze and early Iron ages based on pollen and lake-level data in the NW Alps, France. *Quaternary International 200*, 102–110.

Makhnach, N., Zernitskaja, V., Kolosov, I. & Simakova, G. 2004: Stable oxygen and carbon isotopes in Late Glacial-Holocene freshwater carbonates from Belarus and their palaeoclimatic implications. *Palaeogeography Palaeoclimatology Palaeoecology 209*, 73–101.

Mangerud, J. 2004: Ice sheet limits in Norway and on the Norwegian continental shelf. *In* Ehlers, J. & Gibbard, P. L. (eds.): *Quaternary glaciations: extent and chronology, Part 1: Europe*, 271–294. Elsevier, Amsterdam.

Mangili, C., Brauer, A., Moscariello, A. & Naumann, R. 2005: Microfacies of detrital event layers deposited in Quaternary varved lake sediments of the Piànico-Sèllere Basin (northern Italy). *Sedimentology 52*, 927–943.

Mangili, C., Brauer, A., Plessen, B., Dulski, P., Moscariello, A. & Naumann, R. 2010a: Effects of detrital carbonate on stable oxygen and carbon isotope data from varved sediments of the interglacial Piànico palaeolake (Southern Alps, Italy). *Journal of Quaternary Science 25*, 135–145.

Mangili, C., Plessen, B., Wolff, C. & Brauer, A. 2010b: Climatic implications of annual to decadal resolution stable isotope data from calcite varves of the Piànico interglacial lake record, Southern Alps. *Global and Planetary Change 71*, 168–174.

Mann, M. E., Bradley, R. S. & Hughes, M. K. 1998: Global-scale temperature patterns and climate forcing over the past six centuries. *Nature 392*, 779–787.

Marks, L. 2002: Last glacial maximum in Poland. *Quaternary Science Reviews 21*, 103–110.

Marshall, J. D., Jones, R. T., Crowley, S. F., Oldfield, F., Nash, S. & Bedford, A. 2002: A high resolution Late-Glacial isotopic record from Hawes Water, Northwest England. Climatic oscillations: calibration and comparison of palaeotemperature proxies. *Palaeogeography, Palaeoclimatology, Palaeoecology 185*, 25–40.

Marshall, J. D., Lang, B., Crowley, S. F., Weedon, G. P., van Calsteren, P., Fisher, E. H., Holme, R., Holmes, J. A., Jones, R. T., Bedford, A., Brooks, S. J., Bloemendal, J., Kiriakoulakis, K. & Ball, J. D. 2007: Terrestrial impact of abrupt changes in the North Atlantic thermohaline circulation: Early Holocene, UK. *Geology 35*, 639–642.

Mauquoy, D., Yeloff, D., Van Geel, B., Charman, D. J. & Blundell, A. 2008: Two decadally resolved records from north-west European peat bogs show rapid climate changes associated with solar variability during the mid-late Holocene. *Journal of Quaternary Science 23*, 745–763.

Mayewski, P. A., Rohling, E. E., Stager, C. J., Karlen, W., Maasch, K. A., Meeker, L. D., Meyerson, E. A., Gasse, F., van Kreveld, S., Holmgren, K., Lee-Thorp, J., Rosqvist, G., Rack, F., Staubwasser, M., Schneider, R. R. & Steig, E. J. 2004: Holocene climate variability. *Quaternary Research 62*, 243–255.

McKenzie, J. A. 1985: Carbon isotopes and productivity in the lacustrine and marine environment. *In* Stumm, W. (ed.): *Chemical processes in lakes*, 99–118. John Wiley & Sons, New York.

McManus, J. F., Oppo, D. W. & Cullen, J. L. 1999: A 0.5-million-year record of millennial-scale climate variability in the North Atlantic. *Science 283*, 971–975.

Meisch, C. 2000: Freshwater Ostracoda of western and central Europe. *In* Schwoerbel, J. & Zwick, P. (eds.): *Süßwasserfauna von Mitteleuropa. Band 8/3*. 522 pp. Spektrum Akademischer Verlag, Heidelberg.

Merkt, J. & Müller, H. 1999: Varve chronology and palynology of the Lateglacial in Northwest Germany from lacustrine sediments of Hämelsee in Lower Saxony. *Quaternary International 61*, 41–59.

Migowski, C., Agnon, A., Bookman, R., Negendank, J. F. W. & Stein, M. 2004: Recurrence pattern of Holocene earthquakes along the Dead Sea transform revealed by varve-counting and radiocarbon dating of lacustrine sediments. *Earth and Planetary Science Letters 222*, 301–314.

Moernaut, J., De Batist, M., Charlet, F., Heirman, K., Chapron, E., Pino, M., Brümmer, R. & Urrutia, R. 2007: Giant earthquakes in South-Central Chile revealed by Holocene mass-wasting events in Lake Puyehue. *Sedimentary Geology 195*, 239–256.

Monecke, K., Anselmetti, F. S., Becker, A., Sturm, M. & Giardini, D. 2004: The record of historic earthquakes in lake sediments of central Switzerland. *Tectonophysics 394*, 21–40.

Moreno, A., Valero-Garcés, B., González-Sampériz, P. & Rico, M. 2008: Flood response to rainfall variability during the last 2000 years inferred from the Taravilla Lake record (Central Iberian Range, Spain). *Journal of Paleolimnology 40*, 943–961.

Moscariello, A., Schneider, A. M. & Filippi, M. L. 1998: Late glacial and early Holocene palaeoenvironmental changes in Geneva Bay (Lake Geneva, Switzerland). *Palaeogeography, Palaeoclimatology, Palaeoecology 140*, 51–73.

Mudelsee, M., Börngen, M., Tetzlaff, G. & Grunewald, U. 2003: No upward trends in the occurrence of extreme floods in central Europe. *Nature 425*, 166–169.

Mulder, T. & Chapron, E. 2010: Flood deposits in continental and marine environments: Character and significance. *In* Slatt, R. M. & Zavala, C. (eds.): *Sediment transfer from shelf to deep water - Revisiting the delivery system*. AAPG Studies in Geology 61, 1–30.

Mulder, T. & Cochonat, P. 1996: Classification of offshore mass movements. *Journal of Sedimentary Research 66*, 43–57.

Muscheler, R., Beer, J., Wagner, G. & Finkel, R. C. 2000: Changes in deep-water formation during the Younger Dryas event inferred from $^{10}$Be and $^{14}$C records. *Nature 408*, 567–570.

Muscheler, R., Kromer, B., Björck, S., Svensson, A., Friedrich, M., Kaiser, K. F. & Southon, J. 2008: Tree rings and ice cores reveal $^{14}$C calibration uncertainties during the Younger Dryas. *Nature Geoscience 1*, 263–267.

Nadeau, M. J., Schleicher, M., Grootes, P. M., Erlenkeuser, H., Gottdang, A., Mous, D. J. W., Sarnthein, J. M. & Willkomm, H. 1997: The Leibniz-Labor AMS facility at the Christian-Albrechts University, Kiel, Germany. *Nuclear Instruments and Methods in Physics Research Section B: Beam Interactions with Materials and Atoms 123*, 22–30.

Nagl, H. 1976: Geographische Untersuchungen. *Attersee. Vorläufige Ergebnisse des OECD–Seeneutrophierungs- und des MaB–Programms*, 8–28. Gmunden.

Namiotko, T., Danielopol, D. L., Pichler, M. & von Grafenstein, U. 2009: Occurrence of an Arctic ostracod species, *Fabaeformiscandona harmsworthi* (Scott, 1899) (Ostracoda, Candonidae) in late glacial sediments of Lake Mondsee (Austria). *Crustaceana 82*, 1209–1212.

NGRIP Members 2004: High-resolution record of Northern Hemisphere climate extending into the last interglacial period. *Nature 431*, 147–151.

Nomade, J. 2005: *Chronologie et sédimentologie du remplissage du Lac d'Annecy depuis le Tardiglaciaire: Implications paléoclimatologiques et paléohydrologiques*. PhD Thesis, Université Joseph Fourier, Grenoble, France.

Nomade, J., Chapron, E., Desmet, M., Reyss, J.-L., Arnaud, F. & Lignier, V. 2005: Reconstructing historical seismicity from lake sediments (Lake Laffrey, Western Alps, France). *Terra Nova 17*, 350–357.

Obermeier, S. F. 1996: Use of liquefaction-induced features for paleoseismic analysis - An overview of how seismic liquefaction features can be distinguished from other features and how their regional distribution and properties of source sediment can be used to infer the location and strength of Holocene paleo-earthquakes. *Engineering Geology 44*, 1–76.

Odegaard, C., Rea, D. K. & Moore, T. C. 2003: Stratigraphy of the mid-Holocene black bands in Lakes Michigan and Huron: Evidence for possible basin-wide anoxia. *Journal of Paleolimnology 29*, 221–234.

Ohlendorf, C. & Sturm, M. 2001: Precipitation and dissolution of calcite in a Swiss high alpine lake. *Arctic, Antarctic, and Alpine Research 33*, 410–417.

Pini, R. 2002: A high-resolution Late-Glacial – Holocene pollen diagram from Pian di Gembro (Central Alps, Northern Italy). *Vegetation History and Archaeobotany 11*, 251–262.

Piotrowska, N., Pazdur, A., Hałas, S. & Rutkowski, J. 2008: Carbon and oxygen isotope record in carbonate sediments of Lake Wigry (NE Poland). *Geophysical Research Abstracts 10*, EGU2008-A-00608. *EGU General Assembly*, Vienna, 13–18 April 2008.

Polyak, L., Lehman, S. J., Gataullin, V. & Jull, A. J. T. 1995: Two-step deglaciation of the southeastern Barents Sea. *Geology 23*, 567–571.

Prasad, S., Witt, A., Kienel, U., Dulski, P., Bauer, E. & Yancheva, G. 2009: The 8.2 ka event: Evidence for seasonal differences and the rate of climate change in western Europe. *Global and Planetary Change 67*, 218–226.

Ralska-Jasiewiczowa, M. 1983: Isopollen maps for Poland: 0–11000 years B.P. *New Phytologist 94*, 133–175.

Ralska-Jasiewiczowa, M., Goslar, T., Madeyska, T. & Starkel, L. 1998: *Lake Gościąż, Central Poland – A monographic study Part 1*. 340 pp. W. Szafer Institute of Botany, Polish Academy of Sciences, Cracow.

Ralska-Jasiewiczowa, M., Goslar, T., Różański, K., Wacnik, A., Czernik, J. & Chróst, L. 2003: Very fast environmental changes at the Pleistocene/Holocene boundary, recorded in laminated sediments of Lake Gościąż, Poland. *Palaeogeography Palaeoclimatology Palaeoecology 193*, 225–247.

Ralska-Jasiewiczowa, M. & Latałowa, M. 1996: Poland. *In* Berglund, B. E., Birks, H. J. B., Ralska-Jasiewiczowa, M. & Wright, H. E. (eds.): *Palaeoecological events during the last 15000 years*, 403–472. John Wiley & Sons, Chichester.

Ralska-Jasiewiczowa, M., Latałowa, M., Wasylikowa, K., Tobolski, K., Madeyska, E., Wright Jr., H. E. & Turner, C. 2004: *Late Glacial and Holocene history of vegetation in Poland based on isopollen maps.* 444 pp. W. Szafer Institute of Botany, Polish Academy of Sciences, Cracow.

Ramsey, C. B. 1995: Radiocarbon calibration and analysis of stratigraphy: the OxCal program. *Radiocarbon 37*, 425–430.

Ramsey, C. B. 2001: Development of the radiocarbon calibration program. *Radiocarbon 43*, 355–363.

Ramsey, C. B. 2008: Deposition models for chronological records. *Quaternary Science Reviews 27*, 42–60.

Rasmussen, S. O., Andersen, K. K., Svensson, A. M., Steffensen, J. P., Vinther, B. M., Clausen, H. B., Siggaard-Andersen, M.-L., Johnsen, S. J., Larsen, L. B., Dahl-Jensen, D., Bigler, M., Röthlisberger, R., Fischer, H., Goto-Azuma, K., Hansson, M. E. & Ruth, U. 2006: A new Greenland ice core chronology for the last glacial termination. *Journal of Geophysical Research 111*, D06102.

Rasmussen, S. O., Vinther, B. M., Clausen, H. B. & Andersen, K. K. 2007: Early Holocene climate oscillations recorded in three Greenland ice cores. *Quaternary Science Reviews 26*, 1907–1914.

Reimer, P. J., Baillie, M. G. L., Bard, E., Bayliss, A., Beck, J. W., Bertrand, C. J. H., Blackwell, P. G., Buck, C. E., Burr, G. S., Cutler, K. B., Damon, P. E., Edwards, R. L., Fairbanks, R. G., Friedrich, M., Guilderson, T. P., Hogg, A. G., Hughen, K. A., Kromer, B., McCormac, G., Manning, S., Ramsey, C. B., Reimer, R. W., Remmele, S., Southon, J. R., Stuiver, M., Talamo, S., Taylor, F. W., van der Plicht, J. & Weyhenmeyer, C. E. 2004: IntCal04 terrestrial radiocarbon age calibration, 0-26 cal kyr BP. *Radiocarbon 46*, 1029–1058.

Reimer, P. J., Baillie, M. G. L., Bard, E., Bayliss, A., Beck, J. W., Blackwell, P. G., Ramsey, C. B., Buck, C. E., Burr, G. S., Edwards, R. L., Friedrich, M., Grootes, P. M., Guilderson, T. P., Hajdas, I., Heaton, T. J., Hogg, A. G., Hughen, K. A., Kaiser, K. F., Kromer, B., McCormac, F. G., Manning, S. W., Reimer, R. W., Richards, D. A., Southon, J. R., Talamo, S., Turney, C. S. M., van der Plicht, J. & Weyhenmeye, C. E. 2009: IntCal09 and Marine09 radiocarbon age calibration curves, 0-50,000 years cal BP. *Radiocarbon 51*, 1111–1150.

Reitner, J. M. 2007: Glacial dynamics at the beginning of Termination I in the Eastern Alps and their stratigraphic implications. *Quaternary International 164–65*, 64–84.

Renold, M., Raible, C. C., Yoshimori, M. & Stocker, T. F. 2010: Simulated resumption of the North Atlantic meridional overturning circulation - Slow basin-wide advection and abrupt local convection. *Quaternary Science Reviews 29*, 101–112.

Renssen, H., Goosse, H. & Fichefet, T. 2007: Simulation of Holocene cooling events in a coupled climate model. *Quaternary Science Reviews 26*, 2019–2029.

Reyss, J. L., Schmidt, S., Legeleux, F. & Bonte, P. 1995: Large, low background well-type detectors for measurements of environmental radioactivity. *Nuclear Instruments & Methods in Physics Research - Section A: Accelerators, Spectrometers, Detectors and Associated Equipment 357*, 391–397.

Rinterknecht, V. R., Clark, P. U., Raisbeck, G. M., Yiou, F., Bitinas, A., Brook, E. J., Marks, L., Zelcs, V., Lunkka, J. P., Pavlovskaya, I. E., Piotrowski, J. A. & Raukas, A. 2006: The last deglaciation of the southeastern sector of the Scandinavian Ice Sheet. *Science 311*, 1449–1452.

Risebrobakken, B., Jansen, E., Andersson, C., Mjelde, E. & Hevrøy, K. 2003: A high-resolution study of Holocene paleoclimatic and paleoceanographic changes in the Nordic Seas. *Paleoceanography 18*, 1017.

Rohling, E. J. & Pälike, H. 2005: Centennial-scale climate cooling with a sudden cold event around 8,200 years ago. *Nature 434*, 975–979.

Rosenmeier, M. F., Hodell, D. A., Brenner, M., Curtis, J. H., Martin, J. B., Anselmetti, F. S., Ariztegui, D. & Guilderson, T. P. 2002: Influence of vegetation change on watershed hydrology: implications for paleoclimatic interpretation of lacustrine $\delta^{18}O$ records. *Journal of Paleolimnology 27*, 117–131.

Różański, K., Araguas-Araguas, L. & Gonfiantini, R. 1992: Relation-between long-term trends of oxygen-18 isotope composition of precipitation and climate. *Science 258*, 981–985.

Różański, K., Harmata, K., Noryśkiewicz, B., Ralska-Jasiewiczowa, M. & Wcisło, D. 1988: Palynological and isotope studies on carbonate sediments from some Polish lakes - Preliminary results. *In* Lang, G. & Schlüchter, C. (eds.): *Lake, mire and river environments during the last 15000 years*, 41–49. A. A. Balkema, Rotterdam.

Ruddiman, W. F. 2003: The Anthropogenic greenhouse era began thousands of years ago. *Climatic Change 61*, 261–293.

Rundgren, M. & Ingólfsson, Ó. 1999: Plant survival in Iceland during periods of glaciation? *Journal of Biogeography 26*, 387–396.

Rutkowski, J., Krol, K. & Szczepanska, J. 2007: Lithology of the profundal sediments in Slupianska Bay (Wigry Lake, NE Poland) - Introduction to interdisciplinary study. *Geochronometria 27*, 47–52.

Saarnisto, M. & Saarinen, T. 2001: Deglaciation chronology of the Scandinavian Ice Sheet from the Lake Onega Basin to the Salpausselkä End Moraines. *Global and Planetary Change 31*, 387–405.

Šafanda, J., Szewczyk, J. & Majorowicz, J. 2004: Geothermal evidence of very long glacial temperatures on a rim of the Fennoscandian ice sheet. *Geophysical Research Letters 31*, L07211.

Schmidt, R. 1981: Grundzüge der spät- und postglazialen Vegetations- und Klimageschichte des Salzkammergutes (Österreich) aufgrund palynologischer Untersuchungen von See- und Moorprofilen. *Mitteilungen der Kommission für Quartärforschung der Österreichischen Akademie der Wissenschaften 3*, 1–96.

Schmidt, R. 1991: Recent re-oligotrophication in Mondsee (Austria) as indicated by sediment diatom and chemical stratigraphy. *Verhandlungen der Internationalen Vereinigung für theoretische und angewandte Limnologie 24*, 963–967.

Schmidt, R., van den Bogaard, C., Merkt, J. & Müller, J. 2002: A new Lateglacial chronostratigraphic tephra marker for the south-eastern Alps: The Neapolitan Yellow Tuff (NYT) in Längsee (Austria) in the context of a regional biostratigraphy and palaeoclimate. *Quaternary International 88*, 45–56.

Schmidt, R., Wunsam, S., Brosch, U., Fott, J., Lami, A., Marchetto, A., Löffler, H., Müller, H. W., Pražáková, M. & Schwaighofer, B. 1998: Late and post-glacial history of meromictic Längsee (Austria), in respect to climate change and anthropogenic impact. *Aquatic Sciences 60*, 56–88.

Schneider, H., Höfer, D., Irmler, R., Daut, G. & Mäusbacher, R. 2010: Correlation between climate, man and debris flow events - A palynological approach. *Geomorphology 120*, 48–55.

Schnellmann, M., Anselmetti, F. S., Giardini, D., McKenzie, J. A. & Ward, S. N. 2002: Prehistoric earthquake history revealed by lacustrine slump deposits. *Geology 30*, 1131–1134.

Schultze, E. & Niederreiter, R. 1990: Paläolimnologische Untersuchungen an einem Bohrkern aus dem Profundal des Mondsees (Oberösterreich). *Linzer biologische Beiträge 22*, 213–235.

Schwalb, A. 2003: Lacustrine ostracodes as stable isotope recorders of late-glacial and Holocene environmental dynamics and climate. *Journal of Paleolimnology 29*, 265–351.

Schwander, J., Eicher, U. & Ammann, B. 2000: Oxygen isotopes of lake marl at Gerzensee and Leysin (Switzerland), covering the Younger Dryas and two minor oscillations, and their correlation to the GRIP ice core. *Palaeogeography, Palaeoclimatology, Palaeoecology 159*, 203–214.

Seppä, H., Birks, H. J. B., Giesecke, T., Hammarlund, D., Alenius, T., Antonsson, K., Bjune, A. E., Heikkila, M., MacDonald, G. M., Ojala, A. E. K., Telford, R. J. & Veski, S. 2007: Spatial structure of the 8200 cal yr BP event in northern Europe. *Climate of the Past 3*, 225–236.

Seppä, H., Hammarlund, D. & Antonsson, K. 2005: Low-frequency and high-frequency changes in temperature and effective humidity during the Holocene in south-central Sweden: implications for atmospheric and oceanic forcings of climate. *Climate Dynamics 25*, 285–297.

Serpelloni, E., Anzidei, M., Baldi, P., Casula, G. & Galvani, A. 2005: Crustal velocity and strain-rate fields in Italy and surrounding regions: new results from the analysis of permanent and non-permanent GPS networks. *Geophysical Journal International 161*, 861–880.

Serva, L. 1994: Ground effects in intensity scales. *Terra Nova 6*, 414–416.

Siegenthaler, C., Finger, W., Kelts, K. & Wang, S. 1987: Earthquake and seiche deposits in Lake Lucerne, Switzerland. *Eclogae Geologicae Helvetiae 80*, 241–260.

Siegenthaler, U. & Eicher, U. 1986: Stable oxygen and carbon isotope analyses. *In* Berglund, B. E. (ed.): *Handbook of Holocene Palaeoecology and Palaeohydrology*, 407–422. John Wiley & Sons, Chichester.

Sileo, G., Michetti, A. M., Chunga, K. & Berlusconi, A. 2007: Remarks on the Quaternary tectonics of the Insubria Region (Lombardia, NW Italy, and Ticino, SE Switzerland). *Bollettino della Società Geologica Italiana 126*, 411–425.

Sletten, K., Blikra, L. H., Ballantyne, C. K., Nesje, A. & Dahl, S. O. 2003: Holocene debris flows recognized in a lacustrine sedimentary succession: sedimentology, chronostratigraphy and cause of triggering. *The Holocene 13*, 907–920.

Sodemann, H. & Zubler, E. 2010: Seasonal and inter-annual variability of the moisture sources for Alpine precipitation during 1995–2002. *International Journal of Climatology 30*, 947–961.

Solomon, S., Qin, D., Manning, M., Chen, Z., Marquis, M., Averyt, K. B., Tignor, M. & Miller, H. L. (eds.) 2007: Climate Change 2007: The Physical Science Basis. Contribution of Working Group I to the Fourth Assessment Report of the Intergovernmental Panel on Climate Change. 996 pp. Cambridge University Press, Cambridge.

Spötl, C., Nicolussi, K., Patzelt, G. & Boch, R. 2010: Humid climate during deposition of sapropel 1 in the Mediterranean Sea: Assessing the influence on the Alps. *Global and Planetary Change 71*, 242–248.

Stančikaitė, M., Sinkunas, P., Seiriene, V. & Kisielienė, D. 2008: Patterns and chronology of the Lateglacial environmental development at Pamerkiai and Kašučiai, Lithuania. *Quaternary Science Reviews 27*, 127–147.

Stebich, M., Mingram, J., Han, J. & Liu, J. 2009: Late Pleistocene spread of (cool-)temperate forests in Northeast China and climate changes synchronous with the North Atlantic region. *Global and Planetary Change 65*, 56–70.

Stockmarr, J. 1971: Tablets with spores used in absolute pollen analysis. *Pollen et Spores 13*, 615–621.

Stouffer, R. J., Yin, J., Gregory, J. M., Dixon, K. W., Spelman, M. J., Hurlin, W., Weaver, A. J., Eby, M., Flato, G. M., Hasumi, H., Hu, A., Jungclaus, J. H., Kamenkovich, I. V., Levermann, A., Montoya, M., Murakami, S., Nawrath, S., Oka, A., Peltier, W. R., Robitaille, D. Y., Sokolov, A., Vettoretti, G. & Weber, S. L. 2006: Investigating the Causes of the Response of the Thermohaline Circulation to Past and Future Climate Changes. *Journal of Climate 19*, 1365–1387.

Strasser, M., Anselmetti, F. S., Faeh, D., Giardini, D. & Schnellmann, M. 2006: Magnitudes and source areas of large prehistoric northern Alpine earthquakes revealed by slope failures in lakes. *Geology 34*, 1005–1008.

Stucchi, M., Galadini, F., Rovida, A., Moroni, A., Albini, P., Mirto, C. & Migliavacca, P. 2008: Investigation of pre-1700 earthquakes between the Adda and the middle Adige River basins (Southern Alps). *In* Fréchet, J., Meghraoui, M. & Stucchi, M. (eds.): *Historical Seismology*, 93–129. Springer, Dordrecht.

Stuiver, M., Grootes, P. M. & Braziunas, T. F. 1995: The GISP $\delta^{18}O$ climate record of the past 16,500 years and the role of the sun, ocean and volcanoes. *Quaternary Research 44*, 341–354.

Stuiver, M. & Reimer, P. J. 1993: Extended $^{14}C$ data base and revised Calib 3.0 $^{14}C$ age calibration program. *Radiocarbon 35*, 215–230.

Stuiver, M., Reimer, P. J., Bard, E., Beck, J. W., Burr, G. S., Hughen, K. A., Kromer, B., McCormac, G., van der Plicht, J. & Spurk, M. 1998: INTCAL98 radiocarbon age calibration, 24,000-0 cal BP. *Radiocarbon 40*, 1041–1083.

Stuiver, M., Reimer, P. J. & Reimer, R. W. 2005: Calib 5.0 program and documentation. (http://calib.qub.ac.uk/calib/).

Sturm, M. & Matter, A. 1978: Turbidites and varves in Lake Brienz (Switzerland): deposition of clastic detritus by density currents. *In* Matter, A. & Tucker, M. E. (eds.): *Modern and Ancient Lake Sediments*, Special Publication of the International Association of Sedimentologists 2, 147–168. Blackwell, Oxford.

Subetto, D. A., Wohlfarth, B., Davydova, N. N., Sapelko, T. V., Björkman, L., Solovieva, N., Wastegård, S., Possnert, G. & Khomutova, V. I. 2002: Climate and environment on the Karelian Isthmus, northwestern Russia, 13000-9000 cal. yrs BP. *Boreas 31*, 1–19.

Svensson, A., Andersen, K. K., Bigler, M., Clausen, H. B., Dahl-Jensen, D., Davies, S. M., Johnsen, S. J., Muscheler, R., Rasmussen, S. O., Röthlisberger, R., Peder Steffensen, J. & Vinther, B. M. 2006: The Greenland Ice Core Chronology 2005, 15–42 ka. Part 2: comparison to other records. *Quaternary Science Reviews 25*, 3258–3267.

Swierczynski, T., Lauterbach, S., Dulski, P. & Brauer, A. 2009: Die Sedimentablagerungen des Mondsees (Oberösterreich) als ein Archiv extremer Abflussereignisse der letzten 100 Jahre. *In* Schmidt, R., Matulla, C. & Psenner, R. (eds.): *Klimawandel in Österreich – Die letzten 20.000 Jahre ... und ein Blick voraus*, 115–126. Innsbruck University Press, Innsbruck.

Sywula, T. 1974: Małżoraczki (*Ostracoda*). *Fauna Słodkowodna Polski 24. 315* pp. Państwowe Wydawnictwo Naukowe, Warszawa.

Teller, J. T., Leverington, D. W. & Mann, J. D. 2002: Freshwater outbursts to the oceans from glacial Lake Agassiz and their role in climate change during the last deglaciation. *Quaternary Science Reviews 21*, 879–887.

Thomas, E. R., Wolff, E. C., Mulvaney, R., Steffensen, J. P., Johnsen, S. J., Arrowsmith, C., White, J. W. C., Vaughn, B. & Popp, T. 2007: The 8.2 ka event from Greenland ice cores. *Quaternary Science Reviews 26*, 70–81.

Thompson, R., Battarbee, R. W., O'Sullivan, P. E. & Oldfield, F. 1975: Magnetic susceptibility of lake sediments. *Limnology and Oceanography 20*, 687–698.

Tinner, W., Lotter, A. F., Ammann, B., Conedera, M., Hubschmid, P., van Leeuwen, J. F. N. & Wehrli, M. 2003: Climatic change and contemporaneous land-use phases north and south of the Alps 2300 BC to 800 AD. *Quaternary Science Reviews 22*, 1447–1460.

Turney, C. S. M. 1998: Extraction of rhyolitic component of Vedde Microtephra from minerogenic lake sediments. *Journal of Paleolimnology 19*, 199–206.

Valsecchi, V., Tinner, W., Finsinger, W. & Ammann, B. 2006: Human impact during the Bronze Age on the vegetation at Lago Lucone (northern Italy). *Vegetation History and Archaeobotany 15*, 99–113.

van Geel, B., Buurman, J. & Waterbolk, H. T. 1996: Archaeological and palaeoecological indications of an abrupt climate change in the Netherlands, and evidence for climatological teleconnections around 2650 BP. *Journal of Quaternary Science 11*, 451–460.

van Geel, B., van der Plicht, J., Kilian, M. R., Klaver, E. R., Kouwenberg, J. H. M., Renssen, H., Reynaud-Farrera, I. & Waterbolk, H. T. 1998: The sharp rise of $\Delta\,^{14}C$ ca. 800 cal BC: possible causes, related climatic teleconnections and the impact on human environments. *Radiocarbon 40*, 535–550.

van Husen, D. 1977: Zur Fazies und Stratigraphie der jungpleistozänen Ablagerungen im Trauntal. *Jahrbuch der Geologischen Bundesanstalt Wien 120*, 1–130.

van Husen, D. 1979: Verbreitung, Ursachen und Füllung glazial übertiefter Talabschnitte an Beispielen aus den Ostalpen. *Eiszeitalter und Gegenwart 29*, 9–22.

van Husen, D. 1989: *Blatt 65 - Mondsee.* Geologische Karte der Republik Österreich 1:50 000. Geologische Bundesanstalt, Wien.

van Husen, D. 1997: LGM and late-glacial fluctuations in the Eastern Alps. *Quaternary International 38–39*, 109–118.

van Husen, D. 2004: Quaternary glaciations in Austria. *In* Ehlers, J. & Gibbard, P. L. (eds.): *Quaternary glaciations: extent and chronology, Part 1: Europe*, 1–13. 1st ed. Elsevier, Amsterdam.

Vaughn, B. H., White, J. W. C., Delmotte, M., Trolier, M., Cattani, O. & Stievenard, M. 1998: An automated system for hydrogen isotope analysis of water. *Chemical Geology 152*, 309–319.

Veski, S., Seppä, H. & Ojala, A. E. K. 2004: Cold event at 8200 yr BP recorded in annually laminated lake sediments in eastern Europe. *Geology 32*, 681–684.

Vinther, B. M., Clausen, H. B., Johnsen, S. J., Rasmussen, S. O., Andersen, K. K., Buchardt, S. L., Dahl-Jensen, D., Seierstad, I. K., Siggaard-Andersen, M. L., Steffensen, J. P., Svensson, A., Olsen, J. & Heinemeier, J. 2006: A synchronized dating of three Greenland ice cores throughout the Holocene. *Journal of Geophysical Research 111*, D13102.

von Grafenstein, U. 2002: Oxygen-isotope studies of ostracods from deep lakes. *In* Holmes, J. A. & Chivas, A. R. (eds.): *The ostracoda: applications in Quaternary research*, 249–266. American Geophysical Union, Washington.

von Grafenstein, U., Eicher, U., Erlenkeuser, H., Ruch, P., Schwander, J. & Ammann, B. 2000: Isotope signature of the Younger Dryas and two minor oscillations at Gerzensee (Switzerland): palaeoclimatic and palaeolimnologic interpretation based on bulk and biogenic carbonates. *Palaeogeography, Palaeoclimatology, Palaeoecology 159*, 215–229.

von Grafenstein, U., Erlenkeuser, H., Brauer, A., Jouzel, J. & Johnsen, S. J. 1999a: A mid-European decadal isotope-climate record from 15,500 to 5000 years B.P. *Science 284*, 1654–1657.

von Grafenstein, U., Erlenkeuser, H., Müller, J., Jouzel, J. & Johnsen, S. J. 1998: The cold event 8200 years ago documented in oxygen isotope records of precipitation in Europe and Greenland. *Climate Dynamics 14*, 73–81.

von Grafenstein, U., Erlenkeuser, H., Müller, J., Trimborn, P. & Alefs, J. 1996: A 200 year mid-European air temperature record preserved in lake sediments: An extension of the $\delta^{18}O_P$-air temperature relation into the past. *Geochimica et Cosmochimica Acta 60*, 4025–4036.

von Grafenstein, U., Erlenkeuser, H. & Trimborn, P. 1999b: Oxygen and carbon isotopes in modern fresh-water ostracod valves: assessing vital offsets and autecological effects of interest for palaeoclimate studies. *Palaeogeography Palaeoclimatology Palaeoecology 148*, 133–152.

Vose, R. S., Schmoyer, R. L., Steurer, P. M., Peterson, T. C., Heim, R., Karl, T. R. & Eischeid, J. 1992: The Global Historical Climatology Network: long-term monthly temperature, precipitation, sea level pressure, and station pressure data. ORNL/CDIAC-53, NDP-041. Carbon Dioxide Information Analysis Center, Oak Ridge National Laboratory, Oak Ridge, Tennessee.

Walker, M. J. C. 1995: Climatic changes in Europe during the last glacial/interglacial transition. *Quaternary International 28*, 63–76.

Wanner, H., Beer, J., Bütikofer, J., Crowley, T. J., Cubasch, U., Flückiger, J., Goosse, H., Grosjean, M., Joos, F., Kaplan, J. O., Küttel, M., Müller, S. A., Prentice, I. C., Solomina, O., Stocker, T. F., Tarasov, P., Wagner, M. & Widmann, M. 2008: Mid- to Late Holocene climate change: an overview. *Quaternary Science Reviews 27*, 1791–1828.

Webb III, T., Ruddiman, W. F., Street-Perrott, F. A., Markgraf, V., Kutzbach, J. E., Bartlein, P. J., Wright, H. E., Jr. & Prell, W. L. 1993: Climatic changes during the past 18,000 years: regional syntheses, mechanisms, and causes. *In* Wright, H. E., Kutzbach, J. E., Webb III, T., Ruddiman, W. F., Street-Perrott, F. A. & Bartlein, P. J. (eds.): *Global Climates since the Last Glacial Maximum*, 514–535. University of Minnesota Press, Minneapolis.

Wick, L. 2000: Vegetational response to climatic changes recorded in Swiss Late Glacial lake sediments. *Palaeogeography, Palaeoclimatology, Palaeoecology 159*, 231–250.

Wiersma, A. & Jongma, J. 2010: A role for icebergs in the 8.2 ka climate event. *Climate Dynamics 35*, 535–549.

Wiersma, A. P. & Renssen, H. 2006: Model-data comparison for the 8.2 ka BP event; confirmation of a forcing mechanism by catastrophic drainage of Laurentide lakes. *Quaternary Science Reviews 25*, 63–88.

Wohlfarth, B., Filimonova, L., Bennike, O., Björkman, L., Brunnberg, L., Lavrova, N., Demidov, I. & Possnert, G. 2002: Late-glacial and early Holocene environmental and climatic change at Lake Tambichozero, southeastern Russian Karelia. *Quaternary Research 58*, 261–272.

Wohlfarth, B., Gaillard, M.-J., Haeberli, W. & Kelts, K. 1994: Environment and climate in southwestern Switzerland during the last termination, 15–10 ka BP. *Quaternary Science Reviews 13*, 361–394.

Wohlfarth, B., Lacourse, T., Bennike, O., Subetto, D., Tarasov, P., Demidov, I., Filimonova, L. & Sapelko, T. 2007: Climatic and environmental changes in north-western Russia between 15,000 and 8000 cal yr BP: a review. *Quaternary Science Reviews 26*, 1871–1883.

Wohlfarth, B., Skog, G., Possnert, G. & Holmquist, B. 1998: Pitfalls in the AMS radiocarbon-dating of terrestrial macrofossils. *Journal of Quaternary Science 13*, 137–145.

Wulf, S., Kraml, M., Brauer, A., Keller, J. & Negendank, J. F. W. 2004: Tephrochronology of the 100 ka lacustrine sediment record of Lago Grande di Monticchio (southern Italy). *Quaternary International 122*, 7–30.

Wurth, G., Niggemann, S., Richter, D. K. & Mangini, A. 2004: The Younger Dryas and Holocene climate record of a stalagmite from Hölloch cave (Bavarian Alps, Germany). *Journal of Quaternary Science 19*, 291–298.

Yu, G. E. & Harrison, S. P. 1995: Holocene changes in atmospheric circulation patterns as shown by lake status changes in northern Europe. *Boreas 24*, 260–268.

Yu, S.-Y., Colman, S. M., Lowell, T. V., Milne, G. A., Fisher, T. G., Breckenridge, A., Boyd, M. & Teller, J. T. 2010: Freshwater outburst from Lake Superior as a trigger for the cold event 9300 years ago. *Science 328*, 1262–1266.

Yu, Z. 2007: Rapid response of forested vegetation to multiple climatic oscillations during the last deglaciation in the northeastern United States. *Quaternary Research 67*, 297–303.

Yu, Z., McAndrews, J. H. & Eicher, U. 1997: Middle Holocene dry climate caused by change in atmospheric circulation patterns: Evidence from lake levels and stable isotopes. *Geology 25*, 251–254.

Zanchetta, G., Borghini, A., Fallick, A. E., Bonadonna, F. P. & Leone, G. 2007: Late Quaternary palaeohydrology of Lake Pergusa (Sicily, southern Italy) as inferred by stable isotopes of lacustrine carbonates. *Journal of Paleolimnology 38*, 227–239.

Zarzycki, K., Trzcińska-Tacik, H., Różański, W., Szeląg, Z., Wołek, J. & Korzeniak, U. 2002: *Ecological indicator values of vascular plants of Poland.* 183 pp. W. Szafer Institute of Botany, Polish Academy of Sciences, Cracow.

Zawisza, E. & Szeroczynska, K. 2007: The development history of Wigry Lake as shown by subfossil Cladocera. *Geochronometria 27*, 67–74.

Zhao, C., Yu, Z., Ito, E. & Zhao, Y. 2010: Holocene climate trend, variability, and shift documented by lacustrine stable-isotope record in the northeastern United States. *Quaternary Science Reviews 29*, 1831–1843.

Zillén, L. & Snowball, I. 2009: Complexity of the 8 ka climate event in Sweden recorded by varved lake sediments. *Boreas 38*, 493–503.

# List of publications

## ISI journal papers and book chapters

- N. Andersen, S. Lauterbach, D. L. Danielopol, T. Namiotko, M. Hüls, H. Erlenkeuser, A. Brauer, U. von Grafenstein and DecLakes participants: **Were there overshooting warm temperatures in Central Europe after the abrupt 8.2 ka and 9.1 ka cold events?** *Geology* (to be submitted).
- R. Schmidt, K. Weckström, S. Lauterbach, R. Tessadri and K. Huber: **North Atlantic climate impact on early late glacial climate oscillations in the southeastern Alps inferred from a multi-proxy lake sediment record.** *Journal of Quaternary Science* (accepted pending minor revisions).
- S. Lauterbach, E. Chapron, A. Brauer, M. Hüls, A. Gilli, F. Arnaud, A. Piccin, J. Nomade, M. Desmet, U. von Grafenstein and DecLakes participants: **A sedimentary record of Holocene surface runoff events and earthquake activity from Lake Iseo (Southern Alps, Italy).** *The Holocene* (accepted pending minor revisions).
- S. Lauterbach, A. Brauer, N. Andersen, D. L. Danielopol, P. Dulski, M. Hüls, K. Milecka, T. Namiotko, M. Obremska, U. von Grafenstein and DecLakes participants (2011): **Environmental responses to Lateglacial climatic fluctuations recorded in the sediments of pre-alpine Lake Mondsee (northeastern Alps).** *Journal of Quaternary Science* (in press), DOI: 10.1002/jqs.1448.
- S. Lauterbach, A. Brauer, N. Andersen, D. L. Danielopol, P. Dulski, M. Hüls, K. Milecka, T. Namiotko, B. Plessen, U. von Grafenstein and DecLakes participants (2011): **Multi-proxy evidence for early to mid-Holocene environmental and climatic changes in northeastern Poland.** *Boreas 40*, 57–72, DOI: 10.1111/j.1502-3885.2010.00159.x.
- T. Swierczynski, S. Lauterbach, P. Dulski and A. Brauer (2009): **Die Sedimentablagerungen des Mondsees (Oberösterreich) als ein Archiv extremer Abflussereignisse der letzten 100 Jahre.** *In*: Schmidt, R., Matulla, C., Psenner, R. (Eds.) *Klimawandel in Österreich: Die letzten 20.000 Jahre ... und ein Blick voraus.* Alpine Space 6, 115-126. innsbruck university press, Innsbruck. ISBN 978-3-902571-89-2

## Published conference abstracts

- **EGU General Assembly, 02–07 May 2010, Vienna, Austria**
  T. Swierczynski, S. Lauterbach, P. Dulski, A. Brauer and B. Merz (2010): Extreme runoff events of the last 2000 years reconstructed from varved sediments of Lake Mondsee (Upper Austria). *Geophysical Research Abstracts 12, EGU2010-13209.*

- **AGU Fall Meeting, 14–18 December 2009, San Francisco, USA**
  T. Swierczynski, S. Lauterbach, A. Brauer and B. Merz (2009): A 2000 year flood record from annually laminated sediments of Lake Mondsee (European Alps, Upper Austria). *EOS Transactions 90 (52), NH43A-1281.*

- **BALTEX Conference, 25–28 May 2009, Szczecin, Poland**
  S. Lauterbach, A. Brauer, B. Plessen, P. Dulski, K. Zamelczyk, K. Milecka, T. Namiotko, M. Hüls, N. Andersen, U. von Grafenstein, D. L. Danielopol and DecLakes Participants (2009): Lake Hańcza (northeast Poland) – A new multi-proxy record of Lateglacial and early Holocene climate and environmental change from the Eastern Baltic. *Conference Proceedings, p. 12–13.*

- **EGU General Assembly, 19–24 April 2009, Vienna, Austria**
  T. Swierczynski, S. Lauterbach, P. Dulski, U. Frank, R. Naumann, B. Merz and A. Brauer (2009): A record of historical runoff events in annually laminated sediments of Lake Mondsee (Upper Austria). *Geophysical Research Abstracts 11, EGU2009-5926.*

- **EGU General Assembly, 19–24 April 2009, Vienna, Austria**
  S. Lauterbach, A. Brauer, P. Dulski, G. Schettler, K. Milecka, M. Hüls, N. Andersen, T. Namiotko, D. L. Danielopol, U. von Grafenstein and DecLakes Members (2009): A multi-proxy record of Lateglacial climatic and environmental changes from Lake Mondsee (Upper Austria). *Geophysical Research Abstracts 11, EGU2009-8436-1.*

- **Open workshop "Socio-environmental dynamics over the last 12,000 years: the creation of landscapes", 01–04 April 2009, Kiel, Germany**
  T. Swierczynski, S. Lauterbach and A. Brauer (2009): Flood events in a changing environment – The sedimentological record of Lake Mondsee (Upper Austria). *Conference Proceedings, p. 7.*

- **ESF EuroCLIMATE Final Conference, 29–30 September 2008, Giens, France**
  D. L. Danielopol, Á. Baltanás, N. Andersen, A. Brauer, W. Geiger, H. Erlenkeuser, M. Hüls, S. Lauterbach, T. Namiotko, A. Piccin, M. Pichler, M. Reina, G. Roidmayr and U. von Grafenstein (2008): The usage of the ostracod *Candona candida* (O. F. Müller) as companion to *Candona neglecta* Sars for ecostratigraphy of deep-lake sediments in Europe. *Conference Proceedings, p. 25–26.*

- **ESF EuroCLIMATE Final Conference, 29–30 September 2008, Giens, France**
  M. Hüls, S. Lauterbach, A. Brauer, N. Andersen, M. J. Nadeau, P. M. Grootes and DecLakes Members (2008): Radiocarbon dating of lake sediments from the DecLakes program. *Conference Proceedings, p. 45.*

- **ESF EuroCLIMATE Final Conference, 29–30 September 2008, Giens, France**
  S. Lauterbach, A. Brauer, P. Dulski, N. Andersen, M. Hüls, K. Milecka, J. Nomade, U. von Grafenstein and DecLakes Members (2008): Chronology and sediment microfacies from three DecLakes sediment records (Lake Mondsee, Lake Iseo, Lake Hańcza). *Conference Proceedings, p. 51–52.*

- **ESF EuroCLIMATE Final Conference, 29–30 September 2008, Giens, France**
  K. Milecka, S. Lauterbach, A. Brauer and DecLakes Members (2008): Vegetation succession and environmental changes recorded in sediments of Lake Hańcza". *Conference Proceedings, p. 52–53.*

- **ESF EuroCLIMATE Final Conference, 29–30 September 2008, Giens, France**
  U. von Grafenstein, N. Andersen, Á. Baltanás, A. Brauer, H. Erlenkeuser, D. L. Danielopol, P. A. Danis, W. Geiger, G. Hoffmann, S. Lauterbach, M. Hüls, T. Namiotko, A. Piccin and M. Reina (2008): Quantitative reconstruction of $\delta^{18}O_P$ from ostracode calcite in deep lakes in Europe. *Conference Proceedings, p. 79.*

- **EGU General Assembly, 13–18 April 2008, Vienna, Austria**
  T. Swierczynski, S. Lauterbach, A. Brauer and DecLakes Participants (2008): Detrital layers as a sedimentary record of historical flood events – A case study from Lake Mondsee (Upper Austria). *Geophysical Research Abstracts 10, EGU2008-A-07966.*

- **EGU General Assembly, 13–18 April 2008, Vienna, Austria**
  S. Lauterbach, A. Brauer, P. Dulski, B. Plessen, K. Zamelczyk, K. Milecka, N. Andersen, M. Hüls and DecLakes Participants (2008): Multi-proxy evidence for delayed early Holocene warming in Northeastern Poland from Lake Hańcza sediments. *Geophysical Research Abstracts 10, EGU2008-A-02776.*

- **Geo-Pomerania (Joint Meeting PTG-DGG), 24–26 September 2007, Szczecin, Poland**
  S. Lauterbach, N. Andersen, K. Milecka, T. Namiotko, K. Zamelczyk and A. Brauer (2007): A multi-proxy record of climate change at the Lateglacial / early Holocene transition from Lake Hańcza, Northeastern Poland. *Schriftenreihe der Deutschen Gesellschaft für Geowissenschaften 53, p. 163.*

- **EGU General Assembly, 15–20 April 2007, Vienna, Austria**

  S. Lauterbach, A. Brauer, P. Dulski, J. Nomade and DecLakes Participants (2007): Lateglacial climate changes in a sediment record from Lake Mondsee (Upper Austria). *Geophysical Research Abstracts 9, 07200.*

- **DEKLIM/PAGES Conference "The climate of the next millennia in the perspective of abrupt climate change during the late Pleistocene", 07–10 March 2005, Mainz, Germany**

  A. Brauer, J. Mingram, P. Dulski, S. Lauterbach, S. Opitz, G. Schettler, S. Wulf and Monticchio Working Group (2005): First results from the last interglacial at Lago Grande di Monticchio: varve chronology and microfacies analyses. *Abstracts Volume, p. 47–48.*

- **GeoLeipzig 2004 – "Geowissenschaften sichern Zukunft" (Joint Meeting DGG-GGW), 27 September–01 October 2004, Leipzig, Germany**

  A. Brauer, J. R. M. Allen, U. Frank, S. Lauterbach, J. Mingram, S. Opitz and S. Wulf (2004): Das letzte Interglazial in Süditalien – erste Ergebnisse des neuen Sedimentprofils vom Lago Grande di Monticchio, Süditalien. *Schriftenreihe der Deutschen Geologischen Gesellschaft 34, p. 161.*

# Curriculum vitae

This page contains personal data. It is thus not part of the online publication.

# Erklärung

Hiermit erkläre ich gemäß § 9 Abs. 7 der Promotionsordnung der Mathematisch-Naturwissenschaftlichen Fakultät der Universität Potsdam, dass ich die von mir vorgelegte Dissertation mit dem Titel

***Lateglacial to Holocene climatic and environmental changes in Europe – multi-proxy studies on lake sediments along a transect from northern Italy to northeastern Poland***

selbstständig angefertigt, die benutzten Quellen und Hilfsmittel vollständig angegeben und wörtliche und sinngemäße Zitate als solche gekennzeichnet habe sowie Tabellen, Karten und Abbildungen, die anderen Werken in Wortlaut oder dem Sinn nach entnommen sind, in jedem Einzelfall als Entlehnung kenntlich gemacht habe. Ich erkläre außerdem, dass diese Dissertation noch keiner anderen Fakultät oder Hochschule zur Prüfung vorgelegen hat; dass sie, abgesehen von unten angegebenen Teilpublikationen, noch nicht veröffentlicht worden ist sowie, dass ich eine solche Veröffentlichung vor Abschluss des Promotionsverfahrens nicht vornehmen werde. Die Bestimmungen der Promotionsordnung sind mir bekannt.

## Teilpublikationen

N. Andersen, S. Lauterbach, D. L. Danielopol, T. Namiotko, M. Hüls, H. Erlenkeuser, A. Brauer, U. von Grafenstein and DecLakes participants: **Were there overshooting warm temperatures in Central Europe after the abrupt 8.2 ka and 9.1 ka cold events?** *Geology* (to be submitted).

S. Lauterbach, E. Chapron, A. Brauer, M. Hüls, A. Gilli, F. Arnaud, A. Piccin, J. Nomade, M. Desmet, U. von Grafenstein and DecLakes participants: **A sedimentary record of Holocene surface runoff events and earthquake activity from Lake Iseo (Southern Alps, Italy).** *The Holocene* (accepted pending minor revisions).

S. Lauterbach, A. Brauer, N. Andersen, D. L. Danielopol, P. Dulski, M. Hüls, K. Milecka, T. Namiotko, M. Obremska, U. von Grafenstein and DecLakes participants (2011): **Environmental responses to Lateglacial climatic fluctuations recorded in the sediments of pre-alpine Lake Mondsee (northeastern Alps).** *Journal of Quaternary Science* (in press), DOI: 10.1002/jqs.1448.

S. Lauterbach, A. Brauer, N. Andersen, D. L. Danielopol, P. Dulski, M. Hüls, K. Milecka, T. Namiotko, B. Plessen, U. von Grafenstein and DecLakes participants (2011): **Multi-proxy evidence for early to mid-Holocene environmental and climatic changes in northeastern Poland.** *Boreas 40*, 57–72, DOI: 10.1111/j.1502-3885.2010.00159.x.

Potsdam, den 18.01.2011